

SEWING MACHINE, FABRIC AND THREAD DYNAMICS

by

RYSZARD CHMIELOWIEC

a thesis submitted in accordance
with the requirements for the degree of
Doctor of Philosophy

Being an account of work carried out
under the supervision of

Professor David William Lloyd

Department of Textile Industries

The University of Leeds

March 1993

I do confirm that the work submitted is of my own and that
credit was given where reference has been made to the work
of others.

THESIS

CLASS MARK

T26562

**TO MY MOTHER SATISFACTION...
TO MY WIFE CHRISTINE-MARIE FOR SUPPORT....**

A B S T R A C T .

In recent years, sewing technology has witnessed dramatic increases in machines speeds, new types of materials, new sewing threads and evaluation methods - but the principal type of sewing machine remains the lock-stitch type and this is likely to remain the most common and versatile for the foreseeable future, particularly for sewing woven fabrics.

Sewing machine speed increases lead to a loss of control of the sewing process due largely to an increase of the dynamic forces and consequently to problems such as seam pucker.

In this research computer-based instrumentation and high-speed digital image and signal acquisition systems were developed to study the dynamic effects of the sewing machine, fabric and thread on seam pucker.

Needle thread tension, needle bar pressure/tension, presser-foot pressure and displacement signals were acquired simultaneously by 4 strain-gage/piezo-quartz sensors mounted on a Pfaff-563 machine and results were related to pucker measured by a CCD colour-video camera system integrated with the sewing machine.

A series of experiments conducted on various types of fabrics provided illustrative examples of the characteristics of each signal acquired (distinctive shape, amplitudes-peaks/ valleys locations, duration etc), and also enabled their characteristics to be compared and the interactions among the signals to be studied. For example it was found that the increases in magnitude of the dynamic forces in relation to sewing machine speed increases from 200rpm to 5500rpm were lower than expected (needle thread tension 2.6 fold, presser-foot 1.2 fold and needle penetration force 3.2 fold). A comparison of the needle thread tension for standard woven fabrics and micro-fibre fabrics showed a significant difference in the signal shape, location and amplitudes.

The instrumentation developed is located at the Institute of Textiles and Clothing of the Hong Kong Polytechnic University in Hong Kong.

A C K N O W L E D G E M E N T S .

To begin with I would like to convey my thanks to Dr Stan Galuszynski, formerly of SAWTRI for the initial advice and encouragement given to me in 1986, to pursue our joint interest in the problem of seam pucker by further study of the subject....

My appreciation is also due to the Institute of Textiles and Clothing of Hong Kong Polytechnic, especially to Dr K.K. Chan, the former Head of the Institute, for his understanding and support, as well as to Dr K.W. Yeung, Head of the Institute, for his financial sponsorship and scientific advice. I would like to thank Dr J.I. Curiskis, former Reader, for his involvement in organising the provision of the necessary equipment in the initial stages of the research, Mr Y.L. How for the facilitation of textile testing in the laboratories under his supervision and Mr C.Y. Cheng for his involvement in securing miscellaneous engineering aid during the assembly of the instrumentation. I would also like to thank my good friend Dr C.K. Chan for his continuous encouragement throughout our studies together at Leeds University, Mrs M.Y. Kwong for sharing her FOM data base, and many colleagues within ITC for much sympathetic support.

My especial gratitude is due to my Sponsors, who contributed to this project by providing equipment, materials, technical support and advice; to the G.M.PFAFF AG in Germany especially to Mr E. Marger, the current Director of Pfaff Hongkong for his involvement and generous attitude to the donation of a new sewing machine and to providing technical support throughout all the stages of the development of the instrumentation; to the Rhein-Nadel Machinennadel GmbH in Germany, especially to Mr H. Lange, Vice-President of Research and Development, for securing the range of needles and threads used as well as facilitating useful consultations in Hong Kong and Aachen; to the C & P Computers and Peripherals Ltd in Hong Kong,

especially Mr K.S. Yeung, the Managing Director for the donation of an RGB high-frequency monitor and technical assistance; to TAL Hong Kong Ltd for providing the selected fabrics for testing and Toray Co, for micro-fibre fabrics; to the DSP Development Co.,USA for lending me (at the last stage of writing up) their very useful newest version 3.01B of DADiSP and providing efficient and speedy technical support.

I wish to express my gratitude to Dr J.M.K. MacAlpine for his advice and specialist technical support from the Department of Electrical Engineering, as well as to Dr D.Lane-Smith for his expertise in debugging one of the transducers.

My special thanks are also due to Prof. Dr Wlodzimierz Wiezlak from the Technical University in Lodz for consultations on the interpretation of the RSTM graphical signals distribution.

Last, but not least very special appreciation to the Leeds University Department of Textile Industries, and in particular to Dr G.A.V Leaf and Dr S.C. Harlock for their specialist advice during consultations. I would also like to express my thanks to Mrs V. Whitehead and Mr D. Brook for providing a splendid atmosphere in his laboratory during the time spent at the University.

Finally my especial and most sincere appreciation and gratitude are due to my research supervisor Prof. D.W. Lloyd for his very constructive, creative and friendly form of advice and supervision, which provided invaluable input for carrying out this research and without which it could not have been accomplished.

Without doubt, my wife's help and support throughout the later stages of work in particular, was invaluable and I am very grateful for it.

Ryszard Chmielowiec

CONTENTS

Abstract.....	1
Acknowledgements.....	2
I. Contents.....	4
II. List of Figures.....	9
III. List of Tables.....	13
Chapter 1. INTRODUCTION AND SCOPE OF RESEARCH.	
1.1. Introduction.....	1
1.2. Objectives.....	3
1.3. Scope of research.....	3
1.4. Accomplishments of the research.....	4
Chapter 2. LITERATURE REVIEW.	
2.1. Sewability in clothing manufacture.....	6
2.1.1. The technology of clothing manufacture.....	6
2.1.2. Definitions of sewability.....	7
2.1.3. Early work on sewability.....	8
2.1.4. Sewability evaluation by the assessment of thermal damage.....	10
2.1.5. Needle penetration forces.....	12
2.1.6. The effect of sewing thread on sewability.....	15
2.1.7. Review of sewability testers.....	18
2.1.7.1. Early sewability testing methods.....	19
2.1.7.2. Integrated computer-based sewability measuring systems.....	21
2.1.7.3. The recent development of dynamic integrated measurement systems.....	23
2.1.8. Sewability testing(summary table).....	26
2.2. Pucker literature review.....	33
2.2.1. Definitions of seam pucker.....	34
2.2.2. Seam pucker as a garment defect.....	35
2.2.3. Early attempts to categorise seam pucker...	36
2.2.4. The mechanism of seam pucker in woven fabrics.....	37
2.2.5. Pucker evaluation and prediction methods...	43

2.2.6. Pucker Evaluation Methods(summary table)....	51
---	----

Chapter 3. THE METHODOLOGY AND SYSTEM INSTRUMENTATION DESIGN.

3.1. Introduction.....	60
3.2. Basic design requirements.....	60
3.2.1. Specification requirements for the ETS.....	61
3.2.2. Sewing machine selection	62
3.2.3. Data acquisition hardware.....	69
3.3. The development of the transducers.....	75
3.3.1. The study and search for suitable sensors and associated instruments.....	76
3.3.2. The needle-bar pressure/tension transducer.....	80
3.3.3. The presser-foot force transducer.....	84
3.3.4. Charge amplifiers.....	85
3.3.5. The needle thread tension transducer.....	86
3.3.6. Study of the thread passages.....	89
3.3.7. The calibration of the transducers.....	93
3.4. The RSTM Data acquisition system.....	105
3.4.1. The circuitry of the system.....	106
3.4.2. The DAP software programme of A/D signal.....	108
3.4.3. The DAP operation programme of the acquisition system.....	112
3.4.4. An overview of the RSTM system.....	114
3.4.5. The RSTM Reports.....	124
3.4.6. Maintenance of the system.....	127

Chapter 4. THE DEVELOPMENT OF THE PUCKER EVALUATION SYSTEM.

4.1. Introduction.....	130
4.2. Preliminary investigation into image processing techniques used in other disciplines.....	133
4.3. A preliminary evaluation of the Puckermeter to be used in the comparative evaluation of the new SPMS method.....	139

4.4. The digital image processing hardware and software.....	141
4.4.1. Image processing operations.....	142
4.4.2. The selection of processing hardware.....	147
4.4.3. Illumination of the seam pucker specimen in the SPSM method.....	153
4.5. Seam pucker quantification methods.....	155
4.5.1. The selection of the correlation methods.....	156
4.5.2. Investigation of the influence of fabric colour and pattern on seam pucker image.....	157
4.5.3. Pucker evaluation by means of digital image processing.....	159
4.5.4. The calculation of the seam pucker severity level.....	160
4.5.5. The menus, Area and Line histograms of the SPMS system.....	161
Chapter 5. EXPERIMENTS AND ANALYSIS.....	166
5.1. The structure of the experiments, their range and the test procedures.....	166
5.1.1. RSTM testing on commercial fabrics.....	166
5.1.2. Formulas for calculating the number of tests and the amount of fabric needed.....	168
5.2. The selection of fabrics and sewing threads for the purpose of the experiments.....	172
5.2.1. Testing the selected fabrics.....	172
5.2.2. Test results of the selected sewing threads.....	174
5.3. Experiment Series 1. Identification of single cycles.....	176
5.3.1. The distribution of the sewing thread tension at various speed levels.....	176
5.3.2. The application of the cycle marking method to the signals in the shaft angle domain.....	184

5.4. Experiments Series 2. Effect of increasing speed on the dynamic interaction of the signals using the same fabric type.....	192
5.4.1. The characteristics of the needle penetration force signal.....	192
5.4.2. The effect of the inertia of the needle bar transducer.....	195
5.4.3. The effect of increasing speed on needle penetration force.....	200
5.4.4. The distribution of the needle thread tension with speed increase.....	204
5.4.5. The distribution of the presser-foot pressure and displacement signals with speed increases.....	213
5.5. Experiment Series 3. Dynamic interaction among RSTM signals at the highest speeds.....	220
5.5.1. The characteristic points of the RSTM signals according to the shaft angle domain	221
5.5.2. Peak Analysis of the RSTM signals.....	228
5.6. Experiment Series 4. Seam pucker in micro-fibre fabrics.....	234
5.7. Experiment Series 5. The interaction of the dynamic forces on seam pucker for 15 types of fabrics.....	243
5.7.1. The distribution of the dynamic forces of the NTt and PFp signals in relation to machine speed.....	243
5.7.2. An analysis of the needle bar pressure and withdrawal forces.....	247
5.7.3. The relationship between the maximum values of the dynamic forces of the sewing machine and seam pucker.....	249
 Chapter 6. SUMMARY AND CONCLUSIONS.	
6.1. Summary of findings.....	257
6.2. Conclusions.....	258
6.2.1. The compliance of the sewability	

testing system.....	262
6.2.2. The results of the analysis of individual signals.....	259
6.2.3. Changes in the interactions of the dynamic signals with sewing machine speed.....	262
6.2.4. Some aspects of the correlation of the individual signals.....	265
6.3. Recommendations.....	268
Chapter 7. REFERENCES.....	272
Appendix I. The RSTM-DAP test numerical data file(extract).....	282
Appendix II. RSTM-DAP.C Data Acquisition Programme	282
Appendix IIIa. RSTM-DAP.CODE.SYS file. Coding system and calibration- maintenance procedure.....	285
Appendix IIIb. RSTM-DAP.CFG: System configuration file(extract).....	290
Appendix IV. The technical data of the Kistler force load washer type sensor.....	292
Appendix V. The technical data of the Kistler force sensor.....	293
Appendix VI. The fabrics selected for the experiments.....	294
Appendix VII. An example of the test result of KES-F Bending Test of the micro-fibre fabric.....	297
Appendix VIII. FAST test results of the micro-fibre fabric type Y(example).....	298
Appendix IX. The RSTM and SPMS test results (extract).....	300
Appendix X. The technical data of the QUANTIMET Image Analysis System.....	301
Appendix XI. The SPMS seam pucker quantification programme(extract).....	303
Appendix XII. DT2871 + DT7020 + DT2869 boards.....	304
Appendix XIII. DADiSP Worksheet for X,Y,Z fabrics....	309

II. LIST OF FIGURES.

Chapter 2.

- 2.1.01. Needle penetration forces in quasi-static and dynamic conditions.....14

Chapter 3.

- 3.2.01. Design of the RSTM set-up.....62
- 3.2.02. Back view of the ETS sewing unit.....66
- 3.2.03. Front view of the ETS.....66
- 3.3.01. Transducer calibration curve.....82
- 3.3.02. Schematic section through Washer 9001.....82
- 3.3.03. View of the Force-link 9301A transducer.....84
- 3.3.04. Section through transducer 9301A assembly...85
- 3.3.05. Schematic diagram of thread transducer.....88
- 3.3.06. Schematic diagram of thread passages.....90
- 3.3.07. Three traces of the NTt signal.....91
- 3.3.08. The same signals as above in expanded form...91
- 3.3.09. An example of the filtered NTt signal (1kHz).....92
- 3.3.10. The filtered thread signals acquired at different settings.....92
- 3.3.11. Static calibration of NPF and PFp transducers.....95
- 3.3.12. The Needle and Presser-foot Bar's calibration and presser-foot transducers....97
- 3.3.13. Presser-Foot transducer's calibration response traces.....98
- 3.3.14. The needle thread transducer's static and dynamic calibration.....101
- 3.3.15. Presser-foot displacement transducer's calibration.....103
- 3.4.01. Schematic diagram of the system circuitry...107
- 3.4.02. Flow block-diagram of the DAP program.....114
- 3.4.03. The view of the RSTM set-up.....115
- 3.4.04. Testing in progress.....115
- 3.4.05. The DAP "View Results" menu.....117
- 3.4.06. The view of the DAP window "All Signals"...117

3.4.07. Photo of screen graph with "All Signals" results. Test no. 0027R307.dat.....118

3.4.08. Photo of the screen graph of the all signals results in the expanded version....118

3.4.09. Photo of the single channel NTt signal of test 0027R307.....119

3.4.10. The screen photo of the Presser-Foot displacement(PFd) signal119

3.4.11. The Presser-Foot pressure(PFp) of test no 0027R307.....120

3.4.12. The screen graph of the needle penetration force (NPF) signal.....120

Chapter 4.

4.1.01. Quantimet data of the AATCC:88B Standard...136

4.1.02. AATCC:88B Photographic Standard.....137

4.1.03. The view of the Puckermeter.....140

4.1.04. The specimen clamped between the puckermeter jaws.....140

4.2.01. Diagram of the pucker evaluation set-up.....151

4.2.02. The view of the RSTM/SPMS system set-up....152

4.2.03. The seam pucker frame grabbed image display.....152

4.2.04. Block-diagram of the SPMS hardware.....153

4.4.01. SPMS "View histogram" menu.....163

4.4.02. Fabric image with template window frame....163

4.4.03. Graph of the histogram.....163

4.4.04. Pucker Area template.....164

4.4.05. The Line template.....164

4.4.06. Pucker shade intensity distribution.....164

Chapter 5.

5.3.01. An investigation into the cycle marking method on the NTt signal.....179

5.3.02.	Main points of the NTt signal in the cycle marking method (CMM).....	179
5.3.03.	Designation of the NTt signal peaks and valleys.....	179
5.3.04.	Cycle marking by a Timer2 signal on NTT and NPF signals.....	179
5.3.05.	An example of the correctness of the cycle marking methods.....	183
5.3.06.	Tabulated form of the signals above.....	183
5.3.07.	An example of signal cycle marking by two different methods.....	187
5.3.08.	Procedure of extracting a dummy NPF signal	189
5.3.09.	An example of smoothing the signal by averaging.....	190
5.4.01.	The highest resolution of the single cycle NPF signal at 200 rpm.....	194
5.4.02.	The characteristic points of the NPF signal at 3000 rpm speed.....	194
5.4.03.	The effect of inertia force on the needle penetration signal.....	196
5.4.04.	Extracted NPF signal at various speeds.....	201
5.4.05.	Overplotting of the three extracted NPF signals.....	202
5.4.06.	The needle thread tension (NTt signal) at different speed levels in shaft angle domain.....	205
5.4.07.	NTt signal distribution at 9 speed levels with marked phases of importance	207
5.4.08.	Needle thread tension (NTt signal of the neighbouring cycles) at different speed levels.....	210
5.4.09.	The distribution of all 4 RSTM signals at speeds of 200rpm and 5500rpm.....	211
5.4.10.	The distribution of the PFd and PFp signals at all speed levels.....	216

5.4.11.	The interaction between presser-foot pressure and its displacement at 9 speed levels.....	219
5.5.01.	Dynamic interaction of the 4 RSTM signals at 3000rpm with the phased diagram.....	223
5.5.02.	The FFT Spectrum function applied to the analysis of filtering the NTt signals at 5500rpm.....	231
5.5.03.	Peak Analysis of the dynamic forces.....	232
5.6.01.	The distribution of dynamic forces in micro-fibre fabrics.....	237
5.6.02.	The Peak Analysis of the dynamic forces in micro-fibre fabrics.....	238
5.6.03.	An analysis of the NTt distribution in micro-fibre fabrics and Wool/Polyester standard fabric Q.....	240
5.7.01.	The distribution of the NTt signals for 12 fabric types.....	245
5.7.02.	The distribution of the PFp signals for 12 fabrics.....	245
5.7.03.	The distribution of the NPFp maximum values according to sewing machine speed...	248
5.7.04.	The distribution of the NPFp in the figure above transformed into Y-axis logarithmic scale.....	248
5.7.05.	The results of the Pucker Index for 11 fabrics tested at 7 speed levels.....	250
5.7.06.	The criteria for the decisions on pucker levels (acceptance/rejection).....	252

LIST OF TABLES.

Chapter 2.

- 2.1.01. Sewability testing.....25
 2.2.01. Pucker evaluation methods.....51

Chapter 3.

- 3.4.01. RSTM testing Report.....125

Chapter 5.

- 5.2.01. Woven fabrics selected for experiments.....173
 5.2.02. Sewing threads selected for experiments.....175
 5.3.01. Distance between NTt signal points.....177
 5.3.02. RSTM tests selected for the NPF signal studies....185
 5.3.03. Investigation of the distribution of NPF signals..188
 5.4.01. The variation of the 3 extracted NPF signals
 at 3 speed levels.....203
 5.4.02. The peak values of the NTt signals and their
 location in Phases III(A) and VII(B).....209
 5.5.01. The dynamic interaction of the main RSTM
 signals.....225
 5.5.02. An example of the filtering (on input) of
 the NPF signal.....229
 5.5.03. The correlation of the maximum signal values
 with the sewing machine speed increase.....232
 5.5.04. The change in amplitude of the signal peaks with
 the increase in machine speed.....233
 5.5.05. The maximum increases of the RSTM signals.....233
 5.7.01. Statistical analysis of the pucker index versus
 sewing machine speed for 15 fabric types.....251
 5.7.02. The changes of the RSTM signals' maximum peaks
 in comparison to a values acquired at 200rpm.....253
 5.7.03. Example of correlation between dynamic forces,
 speed and pucker index for fabric Q.....254

Chapter 1. INTRODUCTION AND SCOPE OF RESEARCH.

1.1. Introduction.

In the evolution of this research, it became apparent that the dynamics of the sewing process, under actual processing conditions, needed examination through the development of computer-based instrumentation with high speed data sampling rates.

The initial objective of this project was therefore to develop instrumentation to study the high-speed dynamic effects found in garment assembly operations through measuring the following factors, sewing thread tension, needle penetration forces, presser-foot forces and displacement, and to apply this instrumentation to study the sewability of fabrics as measured by the severity of pucker.

The term sewability relates to "the efficacy of joining two or more layers of fabric material with thread via machine sewing"(1).

Sewability problems are displayed in finished garments in the form of effects such as damage by the needle, thread breakage, seam slippage and seam pucker. The number of problems related to sewability, and their economic severity, has increased with modern trends towards higher speeds, partial and/or full automation, and changes in textile material input (e.g. fabric and sewing threads, new dyes and fabric finishes, together with the use of synthetic fibres in both fabric materials and

sewing threads). These have created many new problems during sewing operations, especially at higher speeds (over 3000 stitches per minute). Such problems become even more important as the apparel industry becomes more automated. To counteract the increased difficulties in processing new materials (from the clothing technology point of view), a new approach by means of a more complex investigation into sewing methods was needed. This however required more advanced, computer-based instrumentation and methodology.

An example of such instrumentation had to be developed and used in this project. The instrumentation principally had to consist of a lock-stitch sewing machine with a range of transducers, able to acquire large amounts of information regarding sewing process dynamics, and was based on the following principles:

1. It had to have increased sampling frequencies for acquiring data, which could not be collected by existing low frequency methods,
2. The number of channels available for simultaneous data acquisition had to be larger than had been previously used,
3. A desk top PC could be used, because the computing power of low cost desk-top machines had grown rapidly and this allowed a large amount of data to be collected and stored.
4. Available scientifically based software could provide increasingly sophisticated methods of mathematical

data manipulation for signals acquisition and analysis. The increased speed of sewing machines had been one of the contributing factors towards the increased difficulties in achieving satisfactory seam performance e.g. puckerless and strong seams.

To investigate the sewing process at higher speeds there was a need:

- to increase sampling frequencies of data collection,
- and to use transducers capable of matching the responses of the higher frequencies.

1.2. Objectives.

Summarising, the objectives of this research were three-fold:

- to develop a robust sewability experimental testing station, containing modern electronic data acquisition instrumentation,
- to widen the body of knowledge in the area of sewing machine, fabric and thread dynamic interactions during high speed sewing, and
- to provide flexible testing facilities for a wide range of investigations and more advanced further research in the Institute of Textiles and Clothing of the Hong Kong Polytechnic University.

1.3. Scope of research.

The research was registered at Leeds University and was supervised by the University, with the experimental part being conducted at, and supported by the Institute of

Textiles and Clothing of the Hong Kong Polytechnic.

The initial concept was of an investigation into the mechanism of seam pucker occurring during the sewing process, directed towards needle, presser-foot and thread forces. However with the rapid progress of research in this field in other centres, e.g. research in the USA(57)in 1988 and later in 1992(58), where high frequency sampling was used in investigating the interaction between fabric and the feeding mechanism of the sewing machine, it became apparent that the programme of research should also involve gaining a deeper insight into the interactions of higher frequency forces and their influence on the sewing process, without filtering them. However the realization of this more advanced concept proved to be a more time consuming and challenging exercise.

1.4. Accomplishments of the research.

In the course of the research the following main aims were accomplished:

1. The testing instrumentation was built, providing the facility to acquire a range of data on the dynamic forces generated during sewing, particularly at the high speeds.
2. A system of integrated data analysis was developed as well as system of data storage and retrieval facilities.
3. An instrumented objective quantification method of pucker measurement was built and was integrated into the sewability testing system (initially only the use of the AATCC pucker grading method was considered, but in the

course of the research it become important to have a computer-based image processing system, matching the technical level of the signal data acquisition system developed in the first stage).

4. A series of experiments was conducted which provided illustrative examples of the interactions of the dynamic forces during the process of sewing, e.g. some findings from experiments:

-the distributions of signals showed that, each fabric type has its own distinctive characteristic of the stitch forming cycle, such as the altitudes of the responses of the dynamic forces in the form of peaks/valleys and their shapes, their location according to the shaft angle revolutions, duration(frequency),etc. For example, it was found that, the distribution of the needle thread tension in micro-fibre fabrics differed significantly from that in standard woven fabrics, which require different pre-settings of the sewing machine.

-the magnitude of the increase of the dynamic forces in relation to sewing machine speed increases(from 200rpm to 5500rpm) was found to be lower than expected and e.g for the needle thread signal it was 2.6 fold, for the presser-foot pressure signal 1.2 fold and for the needle penetration force signal 3.2 fold.

-the correlation analysis of individual dynamic forces with the seam pucker index, ranked their influence as follows: -the needle thread tension, -pressure-foot pressure, and -needle penetration force.

Chapter 2.**LITERATURE REVIEW.****2.1. Sewability in clothing manufacture.**

Clothing manufacturing operations are basically involved with the conversion of initially flat textile materials into a three-dimensional garment, through a number of operations. These start with spreading the fabrics into single and/or multi layer blocks, cutting all layers in the spread simultaneously, and then sewing, fusing and pressing to convert the components into garments. In order to do this, a fabric has to be converted into a three-dimensional, smooth, unbuckled shape through a very complex production process with a large number of operations, the majority of which are sewing operations in which fabric sewability is becoming of the utmost importance.

Considerable work has been done in the last 50 years in the broad area of fabric sewability, and some of the more important developments in the methods and instrumentation of sewability testing are tabulated in chronological order and evaluated below.

2.1.1. The technology of clothing manufacture.

The technology of clothing manufacture is very complex, but the methods of assembling cut fabric pieces still depend (in the majority of cases) on the old concept of joining fabrics by sewing. The principal type of

sewing machine remains the lock-stitch, which is most widely used and is likely to remain the most common and versatile machine for the foreseeable future, particularly for sewing woven fabrics.

The pressure from industry for higher productivity has been matched in recent years by considerable increases in sewing speeds. Apart from increases in speed, new types of textile materials and new finer sewing threads have also been developed, which have required finer sewing needles and improved control of the sewing process. These developments have not been without their associated problems during the course of clothing manufacturing, e.g. achieving puckerless seams at higher sewing speeds required finding the appropriate combination of needle, thread and sewing parameters. In each case the solution of such problems required an understanding of commercial sewing related to seam characteristics and properties such as seam strength, extension, damage, and appearance.

2.1.2. Definitions of sewability.

The most important knowledge in garment design and production preparation concerns the behaviour of fabrics in the manufacturing process, as this allows for a pre-determination of the parameters of the process. These parameters are commonly called "sewability factors".

Sewability was defined in 1989 by Curiskis(1) as "the efficacy of joining two or more layers of fabric material with thread via machine sewing". Uchiyama(3) defined

sewability as the "ease with which a given fabric can be transformed into the final three-dimensional garment". Adding to this definition words such as 'without causing sewing problems' or 'damage to the product' would explain this term more explicitly. It is also useful to point out that fabric sewability has qualitative as well as quantitative aspects, which should not be excluded in the evaluation of sewability. These aspects are complex and are highlighted by Solinger (2) in his famous handbook.

2.1.3. Early work on sewability

Early contributions towards an understanding of sewing technology came from a paper published by Davies(4) in 1933, which contains results of an investigation into stitches and seams in the course direction in plain, knitted fabrics. Six types of seam were measured with respect to strength, extensibility and thread usage, and the results provided a basis for analysis and subsequent improvement of quality and for a costing of thread usage. This constituted one of the first published examples of sewability, treated as a 'problem in sewing'.

In the paper published in 1939 (5) by the Shirley Institute (one of a series of reports on quality of fabrics, garments and sewing, started in 1936), the causes of seam failure in woven fabrics produced by transverse loading, were for the first time, defined and categorised into breakage of the sewing thread, breakage of the fabric, and slippage of the cloth yarns lying close to and

parallel with the seam. The work of the Shirley Institute was the first example of such systematic research in the world and it continued during and after World War II.

The first work, which although rudimentary, nevertheless partially relates to the topic of this research, was done in 1951 by Scott(6), who analyzed the needle penetration traces generated by a force transducer placed in a machine for sewing sacks (additionally the thermal damage caused by the needle was observed but not quantified). Frederick(7) in 1952 studied the effects of needle damage on seam strength in cotton fabrics and his report implied that all seams failed through fabric breakage caused by needle cuts to the yarn. His work demonstrated the need for a better method of calculating seam effectiveness. In the old method the number of damaged yarns had been counted and their value was taken as characterising sewing efficiency. Frederick's work resulted in an improved seam efficiency formula, the ratio of seam tensile strength : fabric tensile strength, expressed as a percentage.

This allowed more accurate comparisons of seam efficiency at the stage of garment design. Nevertheless, this was still inadequate as the sole measure of fabric sewability, since other investigations had discovered many more factors of importance, such as sewing environment and human factors, which influenced sewing operations.

2.1.4. Sewability evaluation by the assessment of thermal damage.

Investigations into many new problems in sewing, arising from the use of new synthetic fabrics, evolved from the application of basic engineering principles, e.g. measurements of the needle penetration forces and measurement of the heat generated by the needle and its effect on fabric damage in the process of sewing. This type of work led to many innovations in sewing, such as new shapes and coatings of needles, lubrication of threads, the finishing of fabrics and recommendations on the revised setting of sewing machine parameters.

Early research on sewability was characterised by investigations of damage to fabric caused by the needle. After Scott(6) there were several attempts to assess thermal damage. Soldhelm(8) discovered that a wax content in a cotton fabric reduced the needle temperature, as did other lubricants. Frederick and Zabieboylo(9) mounted silver soldered constantan wire in the back groove of the needle at different positions. By using a special pyrometer the needle temperature was measured during sewing and the conclusion was reached that the interior of the needle was hottest and that the heat generated was a function of fibre frictional properties and cloth tightness.

Dorkin and Chamberlain(10,11) studied the effects of increases in machine speed in relation to a set of various factors (the needle, the fabric and thread characteristics, the number of plies). They also measured needle heating using thermocouples, by the insertion of a small

diameter ferrous wire inside the needle eye and by soldering this into the needle groove at different points up to the needle shoulder.

Needle heating became more important when synthetic fabrics were sewn at higher speeds (a trend brought about for productivity reasons). Needle heating (as a result of friction between the needle and fabric) increases with machine speed and can cause melting of the fabric and sewing threads, blocking of the needle eye and consequent thread breakage or even needle failure. Khan(12) studied the behaviour of needle penetration forces in simulated conditions, using an Instron tensile testing instrument, with the aim of identifying needle-fabric interactions leading to heat generation. The penetration and withdrawal forces and energy expended were measured as functions of needle velocity. The needle velocities were, however, 3-4 times lower than in actual sewing conditions. The results obtained for three major variables (the number of layers, the needle diameter and needle finish) confirmed that they affect the magnitude of needle penetration forces and that the relation of the needle piercing force to needle diameter is linear. This was confirmed also with respect to the number of the fabric layers. Howard(13) confirmed the effect of increasing needle diameter in generating more heat. But because the heat detector could not respond to rapid changes in needle temperature, the profile of needle temperature distribution was inaccurate.

As a result of intensive investigations(9,11-13),

other work (14-16) into problems of needle/thread/fabric interactions, many technical improvements were developed including a special needle design, needle coatings, fabric and thread finishes, fabric lubricants and needle cooling methods. For example, Schmetz developed a special needle called "the blued, bulged eye needle". The eye of this needle was enlarged, which reduced the contact time with the fabric during the passage of the needle through the fabric layers. All the above mentioned research results contributed greatly to the body of knowledge on sewability of knitted and woven fabrics.

2.1.5. Needle penetration forces.

At this stage research results from needle penetration experiments were incomplete, as the velocity of the sewing needle had not been fully investigated and therefore results differed. The approaches to the problems that had been investigated were of an empirical character and showed the limitations caused by research conditions.

Nowak(17) did very informative work and carried out one of the most important single pieces of research thus far, when he analyzed the characteristics of the needle penetration process in quasi-static and dynamic form in real, not simulated, conditions, in contrast to previous researchers. His results showed that needle penetration forces are of the same character under quasi-static and dynamic conditions, but the magnitudes are four times higher in dynamic conditions (Fig. 2.1.01). Unfortunately

the maximum sewing machine speed of 3000 rpm was only in the middle range of the speeds used by researchers today. Also the character of the needle penetration force curves was affected by the low resolution of oscillograph copy film, despite the relatively high frequency response of the tensometric sensors in the needle bar and throat plate (652Hz and 1332Hz, respectively). Figure 2.1.01 shows the similarity of the common points on both curves, except for points 2,4 and 6. This difference can be attributed to the differences in linear velocity of the needle in the two cases. From these experiments it was obvious that quasi-static conditions were not suitable for the evaluation of needle penetration forces, and could only be used for qualitative assessment.

Leeming and Munden(18) studied the factors affecting needle penetration forces in knitted fabrics and designed the "L&M Sewability Tester", which has also been used for woven fabrics. Details of the tester are included in Table 2.1.01.

Nestler and Arnold(19) contributed to knowledge on sewability by investigating the relationship of needle penetration forces and thermal damage in a lock-stitch sewing machine. The structure of fabric and its resistance to needle piercing was widely discussed by Gersak and Knez(20) and Galuszynski(21). However the results obtained showed a good correlation only between the needle type and fabric mass and surface finish, but no definite correlation with the speed of the sewing machine.

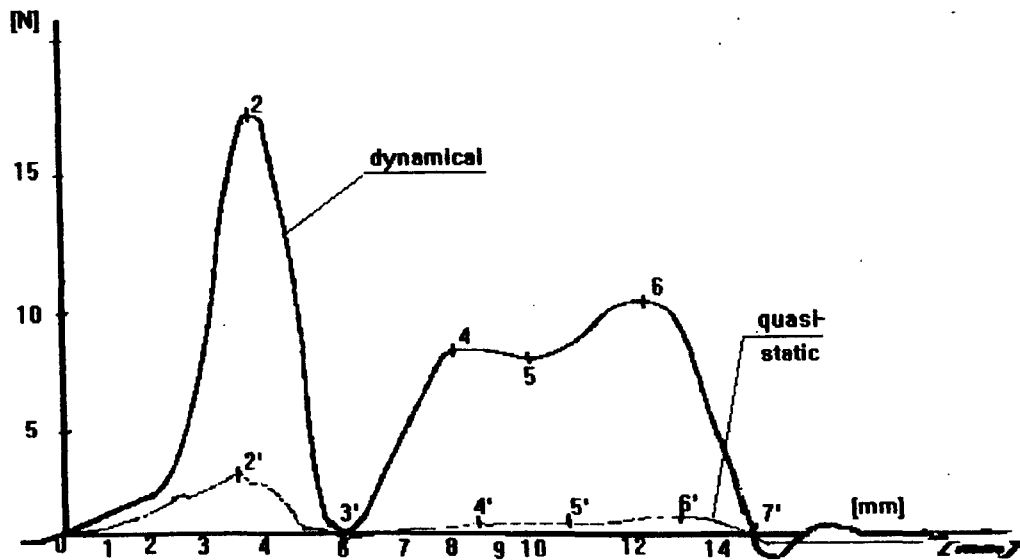


Fig. 2.1.01. Needle Penetration Forces in quasistatic and dynamic conditions.

[Source: R.Nowak, (17)]

Stylios(22) investigated the influence of dynamic forces on fabric damage by measuring their magnitudes for every stitch cycle on purpose built instrumentation on an overlock machine (details are described in Table 2.1.01). Needle penetration forces were measured and the sewing damage to various type of knitted fabrics was recorded by a special camera and quantified in relation to needle peak forces. The details of the instrumentation are provided later in the section and in Table 2.1.01. The possibility of relating the quantified needle penetration forces to simultaneously observed damage (in real time) was very innovative and showed the future direction for wider analysis of other factors affecting sewability. It also

influenced this research, principally through its concept of simultaneous data acquisition of other signals besides that of the needle penetration force.

2.1.6. The effect of sewing thread on sewability.

This field has been widely investigated in many countries, due to increasing problems faced by the clothing industry such as rapid growth in the variety of fabrics developed, in response to the changing demands of the fashion market as well as the need to provide more suitable sewing threads to match them Jones(23). Kolesnikow, Pankowa and Alexeev(24) in 1952 published their research on sewing thread tension variations during the sewing process, which they linked to the number of resistance points from thread guides which cause an increase in thread tension. The results of their work, although in a rudimentary form, were among the first published, and stimulated intensive research in academia and also by the thread and needle manufacturing sectors over the following decades.

In general, although the characteristics of current sewing threads are adequate, their technical properties still require improvement to match more demanding process requirements more closely. The physical and mechanical properties by which the quality of thread should be judged include breaking strength, elongation at break, variation of physical and mechanical properties, and twist stability (thread liveliness). However these parameters still do

not mirror the conditions of sewing thread behaviour during the process of sewing. During sewing, a thread is subjected to a multitude of frequent changes of tensile forces(25-28), which are destructive and reduce thread strength in lock-stitch machines by 30% and more (27,29). This reduction in seam strength requires stronger threads, which are consequently more expensive (30). A weakened thread is also prone to break, which consequently leads to stoppages of the sewing machine. Wiezlak and Siejka(31) reported the results of an analysis of time wastage due to thread breakages. The total production time wasted in a lock-stitch sewing machine amounts to 1%. The result suggests the importance of the selection of adequate sewing conditions, where sewing threads will be less subjected to damaging tensile stresses and strains.

Past research into sewing threads has been concentrated in two main directions:

- defining the proper parameters correlated with thread breakage (25,27-41) and
- quantification of forces to which thread is subjected, their causes and their distribution during stitch formation (26-27,37,42-53).

Some of the above research is discussed below as it is closely related to this project, particularly in the form of instrumentation and the results obtained.

The experiments performed by Tomanec and Sramek(26), Nowak and Wiezlak(27), Gersak and Knez(29), Deery(48) and Ferreira(51), are among the researches worthy of mention

which focused on measuring thread tension and defining its magnitude during the sewing process. Tomanec and Sramek(26), working on the lock-stitch machine discovered that a relationship exists between the stress in the thread and the load on the plate tensioner of the sewing machine. Nowak and Wiezlak(27) measured the distribution of dynamic stresses of the sewing threads on two lock-stitch sewing machines and found that maximum values were at speeds of 500-1000 rpm and 800-1800 rpm. Also the tension decreased with the increase of the sewing speed, which was later confirmed by Deery(48). They concluded however, that the maximum value of the dynamic tension was lower than the strength of the threads used. In some circumstances particularly in the unfavourable speed range with maximum thread tensions, a high static tension and the existence of weak places in the thread itself could cause thread breakages. This investigation was limited to two sewing machines, and there is a need for further investigation using newer types of machines.

Gersak and Knez(29) using PC-based instrumentation measured thread strength reduction and dynamic strain and found that these were functions of the following factors:

- the number of passages thread makes over thread guides,
- thread frictional properties,
- thread fineness, and
- the pressure force that the disc tensioner exerts upon the sewing thread.

They also analyzed the loading of the thread and confirmed the strength reduction range measured by the previous researchers(27,28).

Derry(48), found tension was related to factors stemming from the sewing machine design, sewing speed, needle number and the load on the plates of the thread tensioner, and thread characteristics such as fibre type and thread construction. Whilst his experiments were wide and extensive, their practical use is very limited, since the results were qualitative being presented through randomly selected oscilogrammes.

An interesting approach to the simultaneous measurement of the tension of lock-stitch sewing threads needle and bobbin threads, was adopted by Ferriera(51), who measured the peaks of the tension of the threads and studied their effect on the seam balance. The tension was measured at several levels of sewing machine speed and the shape of distribution was analyzed. According to Ferriera, it is important to ensure that any further research on the behaviour of the sewing thread be carried out in relation to other forces in the sewing process and be concentrated on measurement of the sewing thread tension under dynamic conditions, as these are closer to commercial conditions.

2.1.7. Review of sewability testers.

Research on this topic was related to the dynamics of the sewing process (sewing machine, fabric and thread), with particular emphasis on the higher speed range, where

dynamic forces are much greater and more destructive, and very difficult to quantify. The literature on this subject is surveyed below and a summary of testing methods and/or instrumentation used is tabulated in Tables 2.1.01 and 2.2.01. The tables listing the number of organisations or researchers involved are arranged in chronological order, providing an overview of previous developments and the difficulties associated with the development of reliable instrumentation.

2.1.7.1. Early sewability testing methods.

This section relates to methods and or instruments used in measurement of the sewability of (mainly) woven fabrics. which are tabulated chronologically in Table 2.1.01.

The first instrumented machine mentioned in the literature was a bagging machine(6), which had a force transducer mounted on the needle bar. Needle penetration traces were obtained and the damage to the fabric was evaluated. However, no further details about it could be found in any available library collection.

The second work carried out at Quarter Master General in Philadelphia, was related to the method of quantifying seam efficiency(7). The formula of Seam Efficiency:

$$SE[\%] = \frac{\text{Seam Strength}}{\text{Fabric Strength}} \times 100,$$

did not however take into account the sewing conditions. Further research on the sewing conditions resulted in an expansion of the range of investigations of the causes of damage by a needle to the fabric, e.g., due to heat gener-

ation. Some of this work was mentioned in Sections 2.1.2 and 2.1.3.

Early work on sewability was related principally to the following areas:

- the search for a simple method/formula of assessing sewability through, for example, needle heat or seam efficiency, based on a knowledge of a limited number of parameters, mainly for qualitative assessment (3-6,8-13,17-22,25),
- evaluation of separate components of the sewing process, for example, needle penetration force or sewing thread tension, for quantitative purposes (5,17,18,22,24,26-31,34-53).

These measurements were based on the application of commonly available instruments used in the engineering field, which were usually able to collect only a small amount of data and needed time consuming calculations. Despite the above disadvantages, the early work contributed to the body of knowledge on sewability and showed the complexity of the problems facing the industry, particularly in the process of the development of sewability prediction methodology. This however required more advanced techniques and instrumentation, such as fabric objective measurement technology (FOM) and instrumentation of the sewing machine with very sensitive sensors integrated in PC-based equipment. These requirements become pre-requisites for current research into sewability and are reviewed in the next section .

2.1.7.2. Integrated computer-based sewability measuring systems.

Recent developments in measurement instrumentation coincided with the availability of high speed, high precision data acquisition software and hardware labelled as HSD-CBS (High Speed Dynamics-Computer Based System) in Table 2.1.01. As a result, it has become possible to observe and record dynamic changes with a precision in time as fine as 10^{-9} sec. Such measurements can provide invaluable insights into high-speed sewing (speeds above 3000 rpm for a lock-stitch machine) and should help in apparel processing. A more detailed review of recent developments of integrated systems, as a subject very closely related to this research, is included in the next section 2.1.7.3 below.

In the light of recent developments in instrumentation(39,54-57), which enable rapid measurements to be made, the dynamic components of the sewing process participating in stitch formation can now be measured with higher accuracy. The importance of these measurements of the sewing process is that quantification is related to real time, not to simulated conditions (56,57). The present measurements are 'nearly real'. The resolution reaches 10^{-9} sec, and compulsory pauses in blocks of data acquisition are small, so that it is acceptable to call the acquisition of data "continuous", as if it was acquired in real time. With the capability of modern instrumentation, many more factors, besides that of the

needle penetration force described in the previous sections, can be measured simultaneously, leading to a more accurate and precise sewing process analysis.

With increased sampling capabilities many unforeseen factors that arise can be quantified and provide fresh input for (fabric, thread, machine) designers.

The first important computer-based measurements were carried out by the Denkendorf Institute of Technology (56) and reported in 1985. The throat plate of a lock-stitch machine was strain-gauged around the needle hole with a cut off part of the presser-foot preventing interference with the aluminium gauge. The analog input signals were amplified and converted to digital form and analyzed by an Apple IIe micro-computer. The sampling rate was 30 KHz. The programme was written in BASIC and displayed 255 data points in 50 cycles, with 5 data points per cycle only, as force magnitude in stick and/or bar forms versus time. Tests were carried out at a speed of 1000 rpm with and without needle thread to investigate different fabric finishes. This system is worth mentioning as the first known attempt to integrate an instrumented sewing machine with a computer. However, the system exhibited some shortcomings; firstly, instability of the strain gauge, located transversely to the axis of the fabric feed direction; secondly, the 1000 rpm speed level was insufficient to expose the full needle piercing forces; and thirdly, there was no capability to measure withdrawal forces.

2.1.7.3. Recent developments of integrated measurement systems for sewability evaluation in dynamic high speed conditions.

Since one of the important problems in sewability is fabric damage, another very interesting research project by Stylios(22) is worth outlining here (out of the many included in Table 2.1.01). PC-based instrumentation was developed and this time the overlock machine most commonly used for knitted fabrics, was selected (Rimoldi-Orion 627). Instrumentation consisted of a strain-gauged needle (applied successfully for the first time) and a strain-gauged throat-plate (part of the plate was converted to a cantilever, through cuts in the plate itself). The top and underside part of the cantilever contained two piezo-resistive semi-conductor strain gauges. The throat-plate cantilever's natural frequency response was 35 Hz. In the light of current research trends, the frequency response of the transducer was too low, which led to smoothing of the signal and to the risk of some of the higher frequencies of the signal being missed, particularly in an analysis of the interactions of the other kinematic components of the machine. The data acquisition programme was written in the language C. The number of data points was 228 per cycle at 3220 rpm. The author claimed that the system was fully portable and could be used for testing other machines. However, a doubt exists over the reliability of the gauged needle in repetitive measurements for commercial applications. Additionally the needle penetration signal was correlated with a video-camera for the

purpose of monitoring fabric damage. The correlation of the pictures (the needle interaction with the fabric, at the stitch formation zone) with the needle penetration forces was accomplished and this example showed the possibility of monitoring knitted fabric damage in real-time. In view of the tendency to automate garment operations, there is a need to widen the body of knowledge on the interaction between fabric, thread, and sewing machine in an integrated environment, so that such interactions can be predicted and controlled. With the arrival on the market of modern objective fabric testing technology (KES-F, FAST) and high-speed data acquisition boards(58-61), the pre-requisites for these research areas are now available. The most recent research in the USA(57,58), as well as in the UK (59-61) has provided new understanding, such as the level of forces at high frequencies in the machine feeding area, needed for the creation of self controlling automatic lines, where high reliability of process design is an indispensable factor. The trend to higher measurement frequencies in the dynamic environment is continuing.

Further details of research activities in this area by other researchers are provided in tabulated form or will be mentioned in the second part of the literature review on pucker testers.

2.1.8. Sewability Testing
(Literature Review)

Legend:

LST -Lock stitch,
CST -Chain stitch,
OVK -Overlock stitch,
NPF/ -Needle Penetration
NWF /Withdrawal Force,
SST -Seam strength,
FST -Fabric strength,
C/M -Sewing machine,
FDD -Feed Dog displacement,

HSD-CBS -High Speed Dynamics-
Computer Based System,
QE,OE-Quantitative/Objective
Evaluation respectively,
VA -Visual Analysis,
Transducer type:
TPQZ -Piezo Quartz transducer,
TSG -Strain Gauge transducer,
SCSG -Semi-Conductor strain
gauge.

rpm -revolutions per minute,
np -needle penetration,-s,
Rt -Real time,
NFR -Natural frequency
response,
SR -Sampling rate,
PFp -Presser Foot pressure
PFd -Presser Foot displacement
NTt -Needle Thread tension,
BTt -Bobbin Thread tension,

Table 2.1.01.

Ref.no /Publ. year	Tester and/or test method	Max. speed in rpm	Measuring device and/or location.	Equipment	Output	Remarks
6/ 1951	Scott, Singer Institute.	not given	Force transducer on the needle bar.	Bagging machine.	NPF signal traces.	Damage causes
7/ 1952	Q.M.G., Philadelphia, USA.	any speed	Measurement of seam efficiency (SE).	LST C/M and Strength Tester.	Seam effi- ciency [%] = SST:FST	Modified SE method
10/ 1952	Dorkin & Chamberlain Textile Institute, U.K.	low, middle range	Needle heating during sewing.	Insertion of a sensor into needle.	Effects of M/C speed on temp.	Experi- mental research
24/ 1952	Research Clothing Institute in Moscow.	not given	Measurement of NTt. Resistance tension-meters used.	Single needle LST.	Signal traces on OScgraph.	Experi- mental research

12/ 1970	NCSU (USA). Needle/fabric interaction.	static	Simulation of needle penetration.	Instron	NPF signal traces.	Experimental research
17/ 1967- end - 1972	Technical University in Lodz, Poland. a. NTt (static and dynamic). (*) b. NPF (dynamic and quasi-static). Main research aim: to define fabric resistance to needle piercing and thread interaction. Research results published in a series over a few years period.	up to 4700	a. NTt. TSG located between tensioning discs and thread take-up lever device. FR: 182 kHz b. Needle-bar modifi- cation. Bar's lower part replaced by tube with prestrained beam inside and a needle clamp inserted into remaining bar. FR: 852 Hz c. Throat Plate. Two strain gauges between feed-dog slots of the throat plate. One on the top, the other underside. FR: 1333 Hz	LST single needle. Signals recorded on Oscillograph Quasistatic NPF was measured separately on Sadamel dynamometer Needle was static and fabric in a moving tube	Graphical and numerical data. 60 data points per one cycle Comparison between static and dynamical conditions	Two LST C/M were compared during studies. Complex experi- mental research
13/ 1971	Thorrington Needle Research Laboratory, USA. Complex research with a high precision results.	4200	Measure of the needle without thread. Emissivity detector detects changes of the needle temp rise.	Union Spe- cial C/M 63400B.	Various needle fa- ctors as: shapes, finishes and sizes were tested.	Indust- rial research

43/ 1975	J&P Coats Ltd, UK,	static	Two measuring functions: NTtention and PF pressure.	J&P Coats Tension/ Pressure Meter.	NTt in [cN] PFp in [N]	QE + OE Portable device.
46/ 1976	HATRA, U.K. It was claimed, that a fabric mechanical damage can be tested	up to 4250	Measures the sewing needle temp. by means of infrared detector located near the needle point. Needle temperature characterises fabric friction. Require controlled conditions.	HatraSew Sewability Tester. LST or CST sewing machines can be tested.	Needle temp. is converted to NPF. Results in a form of: an index of severance on [0.1-10.0] scale.	Indust- rial applica- tions.
34/ 1977	Kirby Lester Electronics, U.K.	not given	NTt measurement at the LST running C/M.	TA7 Tension Analyser.	Monitoring tension signal peaks.	Indust- rial applica- tions.
18/ 1978	Leeming & Munden, U.K.	100 np	Needle/fabric inter- action simulator. Force transducers.	L & M Sewability Tester.	Mean pene- tration force value as [%] of se-wability.	QE + OE. Indust- rial and commer- cial applica- tions.
40/ 1981	Sandoz Ltd.	4800	NPF measured on throat plate.	LST single needle C/M	Mean NTP of 50 stitches.	QE + OE

49/ 1984	Tokyo University. Faculty of Technology. NTt in vicinity of the rotating hook.	2250	SGT mounted on a cantilever. Studies of thread disengagement from the rotating hook. NFR: 9 kHz	Single needle LST + photo- camera + strobosc. light.	NTt signal traces and hook movement.	QE +OE
56/ 1985	Denkerdorfer Techno- logie-Berichte. Germany. System used for testing fabric finishing.	1000	Measurement of NPF with threaded and unthreaded needle. Throat plate gauged around needle whole. NFR: not provided. SR: 30kHz	Single needle LST machine. A/D to D/A signal con- version.	NPF only without a NWF. NWF=Nbt= Needle Bar tension.	HSD-CBS, QE, OE.
20/ 1985	Gersak, Technical University Maribor, Slovenia. NTt and needle temperature. Later research into NPF.	up to 5000	No details on thread and heat transducers. NPF force measured by PQZ-leaf, placed on one side of a cantilever beam and on the opposite side - a special whole was made for the needle passage. Transducers's FR not given	LST-single needle. Textronix 564 OScope. Cantilever located transversly to the feed- dog slots.	Graphical and numerical data. Thread strength reduction via dynamic loading of the thread	HSD-CBS, QE, OE.

21/ 1985	Galuszynski, SAWRTI. South Africa.	1740	<p>a. NTT: especially gauged(*) cantilever located after the thread take-up device</p> <p>b. PFP: part of the throat plate cut into cantilever with two semi-conductor strain gauges on the top and on the underside.</p> <p>NFR -not provided (*) -semi-conduct.SG.</p>	<p>LST single needle C/M.</p> <p>Signal traces recorded on Oscope.</p>	<p>Quantified NPF traces and graphical results with statistical analysis.</p>	QE + OE
22/ 1988	Stylios, Leeds University, U.K.	5200	<p>-Measurement of NPF via strain-gauging sewing needle itself and the throat plate cantilever. NFR:35 Hz</p> <p>-Evaluation of knitted fabric damage by synchronising video camera with the needle penetration.</p>	<p>Instrumented OVR C/M, was synchronised with NAC high-speed VideoCamera and Stroboscope.</p>	<p>Quantified NPF with statistic. evaluation -provide a base for VA of the fabric damage by the sewing needle.</p>	<p>HSD-CBS, VA, QE, QO Novum: -Portability, -Small size SG mounted directly on the needle!</p>
57/ 1988	Matthews, NCSU, Raleigh, USA.	4300	<p>Measurement of NPF and PFP signals.</p> <p>PQZT inserted into Needle and Presser-Foot bars. NFR -not available for PQZT.</p>	<p>Sewing Dynamometer</p> <p>Instrumented LST C/M, 1-needle.</p>	<p>NPF and PFP signal values and statistical calculations.</p>	<p>HSD-CBS, QE, OE.</p>
<p>Fabric resistance to needle piercing and sewing thread interaction.</p>	<p>Magnified pictures of needle and fabric interaction allow VA of the fabric damage in a real-time.</p>	<p>Quantified force traces measured in real-time.</p>				

51/ 1990	Ferreria, Leeds University. A study of threads' tensions on a lock-stitch sewing machine. Analysis of treads interaction.	up to 4500	Measurement of NTt and Btt. NTt transducer's NFR: 5.8 kHz Btt transducer's NFR: 5.5 kHz	LST single needle C/M Data acquisition via amplification of its A/D signal and processing by PC system.	Graphical and numerical data values with stat. analysis were provided in a form of hard copies.	HSD-CBS, QE + OE Novum: strain-gauged bobbin thread high NFR transducer!
39/ 1990	Catchpole, University of Durham, U.K. Stitch quality monitoring in sewing operations.	wide range	Three thread tensions signals were acquired via strain-gauged cantilevers with a SCSG. NFR:12 kHz SR: 42 kHz /1 channel Continuous monitoring of sewing process.	CST 2thread C\M, instrumented with 3 transducers. Data collected using 68020 based system.	Tension signals profiles were categorised according to frequency spectrum.	HSD-CBS, QE, OE. Missed stitches were detected
54/ 1991	Pfaff GmbH, Germany. System presented at the IMB'1991 on the special exhibition stand: "Pfaff's New Technology corner"	any speed	System of continuing monitoring of NTt. The signal graphical traces acquired on the screen - can be compared simultaneously with an ideal optimum standard. Any deviation adjusted instantly. NFR -not provided.	LST single needle C/M. Signal's data acquired via transient recorder.	NTt signal acquired in real-time is a trace of one or a series of cycles, in a graphical form.	HSD-CBS, QE, OE.

55/ 1991	SATRA, Clothing Technology Centre, U.K. System of monitoring needle thread tension in real time	3000 and 3400	Measurement of NTT. Signal was acquired by the WIRA/M&S and Kirby- Lester sensor. NFR -not provided.	Instrumented two LST 1- needle C/M were used during trials.	STt signal traces presented in a graphical form.	HSD-CBS, QE, OE.
59,60/ 1992	Stylios, Bradford University, U.K. SS in SIE(Sewability Integrated Enviroment).	any speed	A complex sewability evaluation integrated system of monitoring and quantifying several factors as: NTt; NPF; PFp; PFd; FDd; and Pucker evaluation/ prediction method.	LST single needle C/M with a set of transducers acquiring A/D signals Pucker Measuring Apparatus.	Numerical and graphical results with stats assessment	HSD-CBS, QE, OE, DIP, Computer based Expert System.
57,58/ 1988- 1992	Little, Clapp NCSU, Raleigh, USA. Objective measurement of fabric/ machine interaction. Series of experiments with a statistical analysis were conducted.	up to 4600	Monitoring and analysis of dynamical feeding system. PFd and PFp output voltages were simultaneously acquired by a transducers: -PFp via PZQT and -PFd via non-contact variable impedance transducers.	LST single needle C/M Pfaff-483. Two-channel Digital OScope with memory for data storage and transfer via RS-232 IBM PC.	Signals numerical values with stats were processed on DSP software.	HSD-CBS, QE, OE. Novum: FFT signal analysis in spectrum domain!

<p>61/ 1993</p>	<p>Chmielowiec, Leeds University/ Hong Kong Polytechnic.</p> <p>Research into sewing dynamics and digital image processing by the use of RSTM, especially built computer-based multi-purpose instrumentation.</p> <p>RSTM stands for: Richard's Sewability Testing Method.</p>	<p>up to max of 5500rpm</p>	<p>1. RSTM system. Simultaneous measurement of four C/M signals in real time:</p> <p>-NTt in [cN], -PFd in [mm], -PFp in [N], -NPF=NBP&NBt in [N],</p> <p>2. SPMS system. Rapid acquisition of the sewn sample image and via digital image processing (quantification and evaluation)</p>	<p>Instrumented single needle LST Pfaff- 563.</p> <p>RSTM: A/D and D/A signal data acquisition system pro- vides 6 I/O channels: -I: 4 A/D -O: 2 D/A</p> <p>SPMS: RGB image processed via Frame Graber DT 2871 board</p>	<p>RSTM: Numerical values of 4 signals with simultaneous statistical assessment.</p> <p>SPMS: Objective pucker grading. Scale: 0.00-5.00</p>	<p>HSD-CBS, QE, OE, DIP,</p> <p>Novum: -CCD camera in a rapid pucker evaluation</p> <p>-A four signals values provide basis for expert system design.</p>
---------------------	--	-------------------------------------	---	--	--	---

2.2. Pucker literature review.

The problem of puckered seams occurs in most branches of the sewing industry and is accentuated by the recent increase in the amount of man-made fibres used in fabrics. The problem is one of the most recurring and troublesome facing the clothing industry and is frequently a cause of serious economic losses to the producers of garments made from woven as well as knitted fabrics(62).

2.2.1. Definitions of seam pucker.

Recent editions of the Oxford English Dictionary define: "Pucker ~ as the contracting or gathering (of brow, seam, material) into wrinkles, folds, or bulges, intentionally or as a fault e.g. in sewing". Crum in his Shirley Institute 1984 Technical Survey(62) on "Methods of joining fabrics" cites some research work done on seam pucker and also some attempts to define its characteristics. From time to time the marketing sector of the apparel industry tries to market certain types of garments with puckered seams as "fashionable, intrinsic features of design"(63). This recalls the old saying "if you cannot beat your enemy"... Galuszynski(64) in his wide survey on seam pucker (over 50 related publications), used the following definition: "a distortion of the fabric along the seam line, causing a wrinkled appearance". Stylios and Lloyd(65), as well as many other researchers investigating a wide variety of factors directly or indirectly contrib-

uting to seam pucker, suggested an explanation of the mechanism of seam pucker in terms of: "the interaction between the sewing thread and fabric in the stitch, and their relative properties, which in turn control the occurrence or non-occurrence of seam pucker". Zorowski and Patel in 1970(66), whilst investigating thread tension causing pucker, compared fabric layers to double iron sheets. The sewing thread was pulled (under tension), through the stitch holes and after load release the thread contracted, which led to a corrugated surface (simulating a puckered seam). However, the model developed did not take into account fabric limp behaviour and thread irregularity, which they characterised as "an untypical complexity in comparison to mechanical engineering principles". They described seam pucker as "a mechanical instability phenomenon" and did not pursue further investigations.

It should be noted that the above three attempts to define seam pucker did not take into account any environmental factors; the operation of the sewing machine, the operator's skill, the manufacturing technology or end-use/after-care conditions, the latter being very important commercially.

Other missing components were, and still are, being investigated world-wide, with the use of more advanced instrumentation and measurement technology such as computer based hardware and software.

2.2.2. Seam pucker as a garment defect.

"Is there a solution to the problem of seam pucker?". An article published in 1978 by the Coat's Thread Advisory Service stated that "throughout the thirty years that we have been serving the sewing industry, the most recurring problem encountered had been that of seam pucker"(67). The prolonged difficulty in finding a solution on the part of a professional body of world renown in this field, supports the view that seam pucker is a very complex problem.

Stohlman(68), describing the quality control system in the apparel industry in the USA, lists the Classification of Garment Defects used to determine the acceptability of products, which serves as a guide for US Government agencies in awarding state contracts. All defects with respect to appearance and wearability have to be defined according to their degree of severity. Puckered seams are listed in the category of critical defects.

The garment industry as a whole is making considerable efforts to reduce pucker severity by using various tools, attachments and specialised sewing machines to improve seam appearance. These efforts can only be seen through internal and external direct inspections of the final products owing to the lack of trustworthy statistics. Two actions undertaken to evaluate quality in the clothing industry throughout South Africa(30,69) suggested that puckered seams prevail in smaller companies with a limited investment in modern machinery. Their reports suggested that the common complaint of a lack of resources

to improve the quality of garments was not fully justified. Much improvement could in fact be achieved by implementing more stringent quality systems such as those recommended by the American Apparel Manufacturers Association (70), by the British Standards Institution (71) or by improving standards to achieve higher quality and a wider recognition, eg: "Q-Mark"(72), and/or world-wide registration within the ISO:9000:1987 quality standard series. There still remains a very considerable amount of work to be done however, in the fields of research and development in this area.

2.2.3. Early attempts to categorise seam pucker.

A review of some of the more significant pucker measurement and/or prediction methods is included in Table 2.2.01. The table contains 15 topics from as early as 1951 up to the present time.

The work of Dorkin and Chamberlain(74) is the most detailed study reported in this field and is often referred to by other researchers. They identified five origins of seam pucker, which they believed accounted for approximately 90% of the cases which arose. They also highlighted the curious fact that pucker often delays its appearance until the garment concerned has been laundered. Any wetting during heavy rain or an accidental exposure to water may also cause pucker. Their study also recommended investigative and preventive methods (Table 2.2.02), to bring about pucker elimination or at least reduction.

According to them, there were five basic causes of pucker, which were the following:

- differential fabric stretch,
- fabric dimensional instability,
- sewing thread pucker,
- fabric structural jamming, and
- pucker due to mismatched patterns.

Galuszynski in his survey(64) categorised the causes of seam pucker into four groups:

- feeding pucker (created by differential feed between top and bottom fabric layers),
- tension pucker (pucker resulting from tension of sewing thread),
- inherent pucker (pucker resulting from fabric structural jamming),
- shrinkage pucker (pucker created by differential shrinkage of joined fabrics).

In this survey published in 1986, the mechanism of seam pucker, its causes, prevention, identification and evaluation were discussed in terms of the available literature, and have been compiled into a reference guide for industrial use.

2.2.4. Mechanism of seam pucker in woven fabrics.

Some work on this subject, although included in the survey by Galuszynski, is worth further mention in this review as providing a foundation for this research.

According to the work of Dorkin and Chamberlain (74),

the number of seam components that contribute to seam formation can be seen in Fig. 2.2.01.

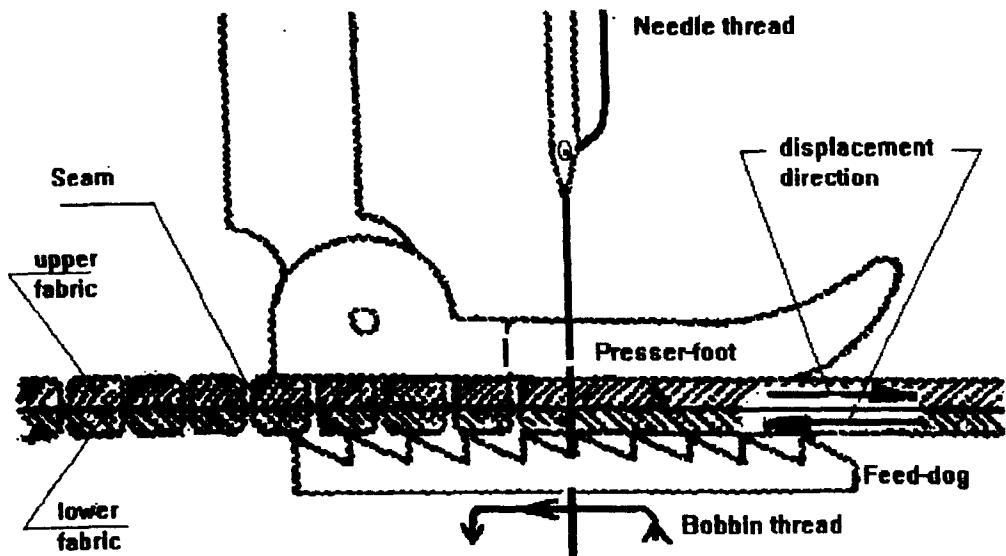


Fig. 2.2.01. Factors involved in seam formation
(From 74).

Galuszynski(64) suggested that when a seam is formed, these components are acted upon by the feed and needle mechanism of the sewing machine, which exerts on each seam component a complex system of frictional forces: advancing forces (acting upon fabric moving forward) and resisting forces (acting in an opposite direction). However, the forces acting on the different components may differ, according to the amount of deformation produced by each component. Consequently, on release after seam formation, as the components start to recover, seam pucker may occur.

The mechanism of seam pucker has been investigated by a number of researchers. The first attempt by Dorkin and Chamberlain(74), looked into the problem of seam elongation and the contraction of seam components. Taylor and Clarke(75) tried to relate the classical wave theory (from engineering mechanics), to the buckling and deformation of fabrics during sewing at a speed of 5000 rpm, which was caused by the presser-foot and the feed-dog. They studied 46 differently finished threads and the sewing of several types of all-cotton fabrics of different weave and weight in various combinations, resulting in several recommendations. Some of these findings were confirmed by Dorkin and Chamberlain; in particular:

- seams sewn in the warp direction pucker more than weft or bias directions; the latter produces the least amount of pucker,
- wash-wear treated fabrics puckered less than untreated ones, but there was no appreciable difference after laundering,
- mercerised threads gave smoother seams than soft-finished ones before laundering; after laundering the seam appearances were similar,
- thinner threads produced less pucker - before and after laundering,
- puckering increases with the number of stitches per unit length,
- some were flat before laundering, whereas french seams only became flat after laundering,

-some of the treated threads used caused pucker during the sewing process, others appeared initially to give smooth seams, but these puckered shortly after removal from the machine.

The above findings seemed to correlate with the existing experience of industry at the time (as described in many technical magazines and reports). The experience gained from such research has allowed industry to reduce seam puckering on an ad hoc basis. However, with the increased number of new fibres and fabrics, industry is still not fully equipped with reliable methods for combating or preferably for predicting its occurrence. Prediction requires a detailed knowledge of 'seam pucker phenomena', as it has been named by Zorowski and Patel(66), who introduced a model in which seam pucker was treated as a mechanical instability phenomenon between the fabric and sewing thread. They considered fabrics as deformable bodies, where the performance of each individual type could be related to the inherent mechanical properties, the geometry and shape of the component, and the load to which it was subjected. However they stated, that this was only one of many types of seam pucker, which they had attempted to investigate.

Inherent seam pucker in woven fabrics was defined as fabric structural jamming caused by insertion of the needle and sewing thread. The first explanation of it was given by Dorkin and Chamberlain(74), who claimed that when the fabric already had a maximum number of yarns per unit

length (or very nearly so), there was no room for the insertion of the sewing thread. To make room for the thread, the fabric had to be extended along the line of the seam. As no extension sideways was possible, the extension along the seam line had to be accommodated by the fabric itself (known as "swelling"), creating a puckered seam. There have been some attempts to predict, by means of equations, when inherent pucker would appear, during the course of sewing parallel to one of the weave yarns. Townsend and Chamberlain(75) introduced the term "Percentage Distortion" (two sewing thread diameters over stitch length) but there was no fabric geometry factor in this formula. Fabric geometry and sewing thread diameter were incorporated in the studies by Taylor and Clarke(76) as a formula for the number of stitches which can be safely sewn in a given construction (25,4 mm minus number of yarns per inch multiplied by yarn diameter and divided by 3 thread diameters).

Fabric structural jamming in terms of yarn, thread diameter, stitch and yarn density was discussed by Schwartz(77). According to his equation, jamming as a cause of seam puckering, would occur when:

$$d_s > \frac{1}{S2} \left(1 - 2 \frac{d}{p}\right) \dots\dots\dots(1)$$

where:

- d_s = sewing thread diameter
- S = number of stitches per length
- d = yarn diameter

p = yarn spacing

For compressible yarns this equation becomes:

$$d_s > \frac{1}{S^2} \left(1 - 2 \frac{dk}{p}\right) \dots\dots\dots (2)$$

where:

k = thread compressibility factor, $0 < k < 1$

Neither the above nor the other(74,76) inherent pucker models deal with sewing in a bias direction, which effectively reduces fabric sett.

Stylios and Lloyd(78) observed experimentally that cutting the stitches on both sides of the fabric always reduced the amount of pucker, even where all other causes of pucker had been, as far as possible, eliminated. This led them to the conclusion that the sewing thread, or some interaction between fabric and thread, played an important part in causing pucker. These observations were expanded by experiments, where relative magnitudes of the range of various properties of threads and fabrics were determined and results were related to the possibilities of pucker occurrence. They stated that an unavoidable tension present in the threads and stitch causes fabric in a stitch to bend and be compressed. In cases where the fabric is compressible, the threads can recover without causing pucker. On the other hand, if a fabric is jammed or nearly jammed, the stiffness of the fabric and thread controls the pucker formation.

Summarising the above conclusions, it might be useful, to list according to Galuszynski(64), a number of factors (stipulated in many investigations as causing or influencing seam pucker occurrence), which fall under the following headings:

- a. fabric: structure, mechanical properties and dimensional instability,
- b. sewing thread: tension, extensibility, relaxation, diameter and shrinkage,
- c. seam: stitch and seam type, stitch length stitch density,
- d. incompatibility of: fabrics, threads,
- e. sewing machine: type, feed, needle, needle/plate assembly and speed of sewing.
- f. environment: setting of sewing machine, skill of the operator, mismatched patterns and after-care.

It is also worth pointing out, that the review in the previous Section 2.1. also contributes towards an explanation of pucker complexity.

2.2.5. Pucker evaluation and prediction methods.

The first information on this subject according to Cram(62) was presented by Scholes in 1951(73), during Shirley Institute lecture No.1907, and details are also included in Table 2.2.01. The evaluation, preventive procedures and recommendations of Dorkin and Chamberlain(74) are contained in Table 2 of their paper. According to

their procedures, one very easy and practical way of identifying pucker type is by cutting a few stitches and:

- if the pucker disappears this means that it was caused by a sewing thread tension,
- if it does not disappear, the cut threads must be removed.

As the threads are removed the pucker should disappear indicating that it was caused by fabric structural jamming due to the presence of the sewing threads. However, there may be cases, where after the removal of the sewing threads the pucker still remains. In such cases it is possible that the needle penetration may have led to the structural jamming of the fabric.

The next method developed in the USA in 1962, is recommended by the Association of Textile Chemists and Colourists(79) and is known as Seam Puckering, Tentative Test Method AATCC-88B:1964T. Over the years, this method has been frequently, although fairly insignificantly, modified. Its procedure relies on a visual assessment of the seam appearance viewed under standard lighting conditions. Test specimen are compared with photographic standards grouped in five grades, where Grade 5 represents a pucker-free seam, and Grade 1 very severe pucker. Due to the inherent subjectivity of this method, it is recommended that a minimum of three judges should average their results. The method is also frequently used by researchers as a comparison with other, newer methods (it has also been employed in this project). Shiloh(80) in 1971,

together with other researchers developed the Sivim Wrinklemeter, an instrument used for evaluating wrinkles in fabrics, and it was later used for assessing pucker. By this method traces of the contours of the fabric along parallel lines, close to a seam line were obtained. The sensor was a tracing needle, which rested lightly on the fabric and followed its undulations as fabric passed underneath it on a moving plate. The trace signals were amplified and recorded electronically. Measurements of the height and slope of the undulations were thus obtained and converted to index-severity values. It was claimed that the Wrinklemeter method correlated very well with the AATCC method.

Rosenblad-Wallin and Cednäs(82,83) introduced the term "Limit of Contraction" (LOC) to define a fabric length before visible puckering of fabric is observed. They found that the coefficient of friction, bending stiffness and mass had an important effect on the magnitude of the LOC (see also Table 2.2.01).

Belser et al(84) designed an instrument, where the magnitude of seam pucker was evaluated quantitatively by an examination of the surface profile of the seam using a photoelectric device (see also Table 2.2.01). The use of light however was to some extent disadvantageous due to the inability of photo-cells to distinguish the intensity of shade from hue colour intensity, particularly with a darker coloured fabric pattern. Bertoldi and Munden(85) experimented with a similar instrument to Belser's, which

they named a Puckermeter (for the purpose of their study the instrument was called the "B&M Puckermeter"). The principal difference between the two instruments was the orientation of the light source and the detector to the seam (for details see Table 2.2.01). It was claimed(62) that this method is superior to the one mentioned in (84), in overcoming problems deriving from coloured fabric patterns, whilst at the same time retaining a capability of a kind akin to that of the human eye.

Another instrument was designed by WIRA as a "Pukka Tester"(86) to facilitate prediction of the amount of differential feed before pucker would occur. The instrument held two fabric strips with a pre-determined difference in extension, so that they could be sewn together to produce a seam with a controlled amount of overfeed. The appearance of the seam indicated whether the overfeed limit had been exceeded. Collins(87) attempted to use the Pukka Tester to measure differential pucker, but the results were inconsistent.

Research in SAWTRI(88) on some aspects of seam pucker resulted in the development of the "SAWTRI Puckermeter" and modification of a Wrinklemeter by its integration with a micro-computer. The design principle of the puckermeter was similar to that of the Pukka Tester, providing for the extension of a sewn fabric strip, clamped between two pairs of jaws located on opposite sides, one of which was moveable, by means of a driving shaft along a scaled platform. The clamped specimens were extended to a

puckerless point and the difference between the initial length and the extended one was converted to a pucker index [P]. The instrument was found to correlate well with the AATCC and Wrinklemeter methods. Evaluation of this instrument was also carried out at Hong Kong Polytechnic(89). The results confirmed Galuszynski's claim of portability and application in non-destructive testing. Also the good reproducibility of the SAWTRI Puckermeter resulted in its application in this research (Chapter4).

Stylios and Lloyd(90) modified the L&M Sewability Tester by adding a tensionless thread feeder to achieve a "mock seam" leaving a loose thread loop on the top of the fabric. Stitching consisted of a series of double-thread loops protruding on the top side of the fabric and possessing all the characteristics of the cut-stitch machine seam. The application of this type of "mock stitch" was justified experimentally and found to possess good reproducibility. The next step in this test was a visual comparison of the specimen with the one produced conventionally. Identification of pucker type by this method was found less troublesome than by the one proposed by Dorkin and Chamberlain. Additionally fabric structural jamming was studied and a set of recommendations proposed (65).

An interesting contribution to pucker prediction methods, by the evaluation of fabric behaviour during production and wear stages, was made through a series of investigations by Sorensen(91,92), who used three seam types in woven cotton and cotton/polyester fabrics. Fabric

properties were tested on KES-F instrumentation and pucker evaluation was performed according to the AATCC-88B:1984 test procedure. A good correlation was found between seam puckering and logarithms of fabric bending, tensile elongation and surface roughness properties.

Similar experiments were carried out in simulated industrial conditions by Lam et al(93). Seam pucker in shirting fabrics was evaluated by a group of 25 experienced technologists/assessors, who were asked to consider the minimum acceptable grade of pucker. Results showed that 60% suggested grade 3 and others considered grades 2, 3-4 and 4 as acceptable limits. This indicated a fundamental difference between the perception of an individual and supported the need for a more objective method than the commonly used AATCC standard to be provided.

A remarkably different approach was adopted by Shimazaki(94), who used photography to study the profile of a seam near the seam line. He analyzed the frequencies of random and periodic sinusoidal waves and compared them with the moulded forms of seam profiles. The conclusions showed that frequencies of waves were affected by the mechanical properties of the fabric and that the unwanted frequencies of the waves of pucker could be reduced by a reduction of stitch density and sewing thread tension.

With the recent availability of new instrumentation and computers with higher processing speeds, new approaches in research have been tried recently in the form of digital image processing or scanning devices using

lasers. Inui and Shibuya(95) designed two pucker evaluation instruments. The first used a scanning laser beam. Pucker was correlated with the position of a beam of light deflected by the fabric specimen. The second apparatus was based on an ultrasonic scanning device. Pucker was correlated by time and the intensity of ultra-sonic wave reflection. The second instrument, it was claimed, could be used to measure "micro-pucker" (pucker of a higher frequency and undulations of a smaller magnitude, usually located near the needle holes). Such a concept would seem to be a rather overengineered invention due to the infrequent occurrence of this type of pucker.

Stylios(59,60) presented during a Conference in Bradford in 1992, a laser pucker measuring device (SPLS), based on a seamed fabric strip travelling under a laser beam, scanned parallel to the seam line. Data of the magnitude of the "pucker undulations" was converted into a numerical pucker index. The advantage of the laser technique was its ability to test in natural light conditions, contrary to the AATCC method and regardless of the colour pattern of the fabric. The weakness of this approach was that laser scanning is a rather slow operation in comparison to the instant image capture by a CCD camera.

The latest contribution comes from Gupta et al(96), who investigated directional variations in fabric properties and seam quality. In garment manufacturing, frequently two plies are joined together with different orientations, as on the shoulder, and often with a con-

stantly changing bias angle, as on the collar. Seams in different combinations were made from five fabric types and were photographed from the front and back under highlights placed at a 15 degree angle, to emphasize seam distortion. These photographs were graded against the AATCC-88B method. Fabric properties were tested on KES-F. Statistical analysis showed that "bending, shear, tensile and surface properties cannot be considered constant properties of a fabric". Even "slight changes in sample orientation can result in significant changes in the physical characteristics of these properties". Furthermore, the research concluded that: "variations in material properties which accompany changes in sample orientation affect seam quality". Each of the five fabrics tested exhibited a wide range of seam distortion, from seam waviness to severe pucker, depending on the orientation of its two plies. The authors advised companies to examine the behavioral properties of fabric both on-and off-grain to avoid future complications.

In summary, it can be said that up to now the methods described, the instrumentation developed and the ways of predicting the occurrence of seam pucker, have been used with varying degrees of success in production or as a basis for practical advice. They do not have the means to provide quick results and cannot be installed on-line as part of the manufacturing process. Nevertheless each experiment and testing method developed has contributed to an increase in the body of knowledge on seam pucker.

2.2.6. Pucker Evaluation Methods (Literature Review)

Legend:

CStd -Commercial standard,
 PA -Practical advice,
 C -Commercial application,
 I -Industrial application,
 CM/NCM-Contact/non-contact
 Measurement,

EXP -Experimental,
 R+D -Research applications,
 PSI -Puckering Severity Index,

QUANTIMET-Quantitative method,
 OBJ. -Objective method,
 SUBJ.-Subjective method,
 LOC -Limit of Contraction,
 ROC -Radius of Contraction,

Table 2.2.01

Publ. year/ Ref.no	Tester and/or test method	Appli- cation type	Measuring device, form of evaluated object and /or its location	Equipment	Output	Remarks
73/ 1951	Shirley Institute. ROC of curved seams. ROC=radian of curvature. Regarded as a first publication related to seam pucker.	PA for C&I	Fabric strip (1m long), seamed in the middle and one side trimmed in width to 25 mm, causes strip to curve. This method replaces direct measurement of seam layers lengths, which is time consuming in practice due to small differences usually involved.	Ruler only	Curvature radius [%]. 20mm radius corresponds to 0.5% of pucker and regarded as acceptable. 90mm =2% as severe pucker.	CM, SUBJ., According to author -method accuracy is sufficient for garment making-up.

74/ 1961	Dorkin and Chamberlain. First and complex work lying down the foundation of pucker phenomenon.	PA for C & I	Test seam 12" long and 3" wide (warp-and-weft wise). The scheme includes a detailed procedures to determine causes of pucker due to: -fabric structural jamming; thread tension changes, -fabric dimensional instability -fabric displacement -mismatched parts.	Require simple testing device and procedure follow up	Preliminary examination and determination of seam pucker causes leads to improvement in quality. Max.limits in [%] were provided.	CM and practical prediction methodology of sewability General scheme for tests of sewability is provided by the authors.
79/ 1962	AATCC Test Method 88B-1964T, last modified in 1984. Most commonly adopted method around the world.	CStd	Visual comparison of specially prepared samples with standard photographs at prescribed lighting conditions in the dark room. Requires 3 opinions to have a mean of three. It is regarded as an unofficial international standard.	Require special testing stand with the prescribed lighting.	Pucker graded according to scale: 1 - 5; (1=severe, 5=least). Precision of 0.1 of a grade.	NCM and SUBJECTIVE method. Relies on human eye and previous experience

84/ 1968	Belser's Method. Light reflectance measurement.	EXP (R+D)	Examination of the fabric sample profile by using collimated light source and photocell detector located to seam plane respectively: -light(90°) and -detection (30°). The sample is placed on the travelling carriage.	Belser apparatus Stadimeter was used to measure curve length.	Ratio of total length of seam curved surface to seam the length. Corrections for color and fabric pattern have to be made.	QUANTIMET. Objective. Results correlate well with AATCC-88B.
80/1971	Shiloh's Method. Earlier, before the pucker - the fabric wrinkles used to be measured.	EXP (R+D) & I	Obtaining traces of the contours of the fabric along lines close to and pararell with the seam. The sensor is a tracing needle which rests very lightly on the fabric and follows the undulations as the fabric passes under-neath on a moving plate.	Sivim Wrinkle- meter.	PSI index, as product of values of height and slope of undulations	QUANTIMET. PSI result correlates well with AATCC-88B

82/ 1974	LOC evaluation. LOC is investigated before puckering occurs.	EXP	LOC measured by thickness test. Decrease in the length of fabric is related to fabric weight and thickness, bending stiffness and frictional properties. Some amount of mechanical pressure was applied to flatten or reduce wrinkles of the seams.	Tests used: thickness test + crease angle test + Dimensional stability test.	Individual results indicate fabric suitability for pucker reduction.	Individual components characteristics should not differ widely.
85/ 1974	Bertoldi's B&M Pucker-meter. Instrument assesses the shadow pattern created by the light falling on the puckered surface.	EXP	Method similar to Belser's except the orientation to the seam plane: -light source(45°) and -photocell detector(90°), Straight line traces of contours indicate that a seam is flat and without pucker. Results unaffected by changes in colour pattern either fabric design.	B&M Pucker-meter.	'Index of Pucker' IP [%] as: a ratio of trace-curve length to the unit length of seam. No special corrections required.	QUANTIMET. Authors claimed that method performance is closely related to human eyes. Comparison with AATCC method not known.

86/ 1979	WIRA, UK. Pukka Tester.	EXP	<p>Instrument designed to facilitate prediction of the amount of differential feed, before seam pucker would occur.</p> <p>The instrument holds two fabric strips with a determined difference in extension, so that they can be sewn together to produce a seam with controlled amount of overfeed.</p>	<p>Pukka Tester.</p> <p>Fabric specimen size: -length: 90 mm, -width: 7 cm.</p>	<p>The appearance of seam after opening and pressing indicates whether the overfeed limit has been exceeded.</p>	<p>Not of very high accuracy.</p> <p>Clamping devices do not keep firmly samples of lengths approx.100 mm.</p>
94/ 1983	<p>Shimazaki, Japan.</p> <p>Studied configuration of seam pucker.</p>	(R+D)	<p>Pucker was imposed on fabric by the use of profiled sino wave forms.</p> <p>The profiles of pucker were measured at certain distance from the plate and the spectral analysis were carried out. Waves frequency is much affected by mechanical properties of the fabric.</p>	Pucker forms/model	Correlation of wave lengths correspond with fabric behaviour.	Pucker consists of random and periodic waves.

22/ 1986- 1988	Stylios, Leeds University (Parts I + II).	EXP	<p>Part I: A range of experiments leading to empirical prediction of the seam pucker were carried out in relation to fabric and sewing thread properties.</p> <p>Modified L+M was used to assess Jamming Pucker.</p>	LST C/M was used to prepare test samples. and	A set of graphs was developed, based on correlation of various properties of: fabric/ thread/ and C/M settings.	QUANTIMET, subjective AATCC method was used in evaluating seam pucker.
88/ 1986	SAWTRI Puckermeter	I & C	<p>Part II: Extension of Part I, via investigation of needle penetration forces interaction leading to fabric damage evaluation.</p> <p>Puckermeter method depends on on extending 2-ply seamed fabric strip sample (clamped between two jaws one of them is movable along seam axis length).</p> <p>Jaws replacement is recorded on the platform ruler at the point of the top fabric wrinkles disappearance.</p>	Instrumented LST sewing machine was used.	Calculation of pucker index P[%].	<p>QUANTIMET</p> <p>A good correlation with the AATCC method was found.</p>
Non-destructive measurement of pucker of garments is possible with.				Puckermeter apparatus as a portable and simple in operation device.	Results in 1.0-5.0 scale, and later converted to: 0.00-7.00 scale.	

88/ 1986	<p>SAWTRI Wrinklemeter</p> <p>Non-destructive measurement of pucker in garments is possible with SAWTRI puckermeter.</p>	I + C	<p>SAWTRI modified wrinklemeter method includes PC-based evaluation of the differences in the amplitudes of peaks and valleys</p> <p>Wrinklemeter is equipped with two sensors as a tracing needles, along seam length.</p>	One sensor placed on the seam line and the second 10mm from seam line	Lengths measured by two sensors lead to calculation of pucker index P, on 0.00-6.50 scale.	A good correlation among two SAWTRI devices and AATCC method was found.
91,92/ 1991/ 1992	<p>DBTI, Denmark. Sorensen's method.</p> <p>Contribution to prediction of fabric behaviour during production and wear.</p>	EXP	<p>Possibility of pucker occurrence are also related to propensities of textile fabrics.</p> <p>Pucker was measured after subjecting samples to a series of various treatments in varied testing conditions and properties changes were compared.</p>	KES-F system employed in fabric testing.	<p>Good correlation between pucker and 3 fabric properties:</p> <ul style="list-style-type: none"> -bending, -surface roughness -tensile elongation 	<p>QUANTITAT, Objective for fabrics only.</p> <p>Subjective AATCC method used in pucker grading.</p>

95/ 1991	Inui and Shibui. Research Institute for Polymers and Textiles Japan. Two (a & b) contactless seam pucker measurement methods.	R+D	a.Laser method: Measures a moderate and severe pucker. b.Ultrasonic method: For a very small pucker. Measurement requires very high precision.	a. Laser displace- ment mea- surement. b. Ultra- sonic image scanner.	a.Pucker is correlated with the position of reflected beam light. b.Pucker is correlated by time and intensity of ultra-sonic wave reflection.	QUANTIMET, objective. a.Sample size same as AATCC method. b.Sample size smaller than laser method, li- mited to near seam line.
59,68 /1992	Stylios, Bradford University. SPLS system as: Seam Pucker Laser System integrated into SIE (Sewability Integrated Environment)	(R+D) & EXP	Measurement of laser beam light reflection magnitude Sample strip of the seamed fabric is lying on the travelling carriage under the laser beam head, which scans path on the one side of a seam and the opposite side is scanned during backward movement.	PC based SPLS apparatus integrated with sewability system	System calculation based on AI principle applied to comparative experiments with the simulation of the human evaluation.	QANTIMET, objective, PC based method. Correlates with AATCC method.

96 /1992	Gupta... [et al], NCSU, Raleigh Research on relationship between material properties, and sewability.	EXP	Samples were cut multi-directionally (12 angles types), paired and sewn on LST M/C. The seam distortion was emphasised by lighting under 15° angle, recorded on photographs and compared with AATCC standards.	Fabrics tested on KES-FB and AATCC-84B method was used.	Seams photographs made from face and back side. Seam Distortion Index.	Subjective pucker testing.
Current re-search /1993	Chmielowiec, Leeds University/ Hong Kong Polytechnic. SPMS stands for: Seam Pucker Measuring System.	(R+D) EXP	Developed on the principle of CDD digital image capture, just beyond the throat plate and via PC based programme. Results of pucker level are rapidly calculated. SPMS system is integrated with RSTM programme measuring dynamical forces in real time. Provision of colour and pattern of fabric weave are build into programme.	RSTM Sewability testing station. Location: HK Poly-technic.	Special algorithm designed to quantify pucker grading. Pucker scale: [1.00-5.00]	QANTIMET, objective, and rapid results. Correlated with AATCC and SAWTRI methods. Archived images can be retrieved from the video tape

Chapter 3. METHODOLOGY AND SYSTEM INSTRUMENTATION.

3.1. Introduction.

The aim of this research was to develop instrumentation to study the high-speed dynamic effects of the sewing machine in garment assembly operations, by means of measuring the sewing thread tension, needle penetration forces and presser-foot forces and displacement. The signals of the aforementioned forces have high-frequency components from various sources, which may impede smooth sewing and subject the components (fabric and thread) of the sewing process to complex, changing forces. This can contribute to excessive buckling of the fabric surface in the seam area and consequently weaken the seam (87). To provide the foundation for such a project it was necessary to design and build special testing facilities in the form of an Experimental Testing Station (ETS), which was renamed later as RSTM after successful trials.

3.2. Basic design requirements.

The principal imperative of the research was the ability to acquire simultaneously the highest possible quantity of data in real time and at high frequencies(97). The signals to be studied were identified as:

- a. Needle Thread Tension (NTt),
- b. Presser-Foot Displacement (PFd),
- c. Presser-Foot* Pressure (PFp), and
- d. Needle Penetration Force (NPF).

*) In practice this force was measured by a transducer inserted into and rigidly linked to the presser-foot bar. To obtain the value of presser-foot pressure, according to the label, division by the measured presser-foot area would be required.

The essential prerequisites of the sensors to be used to measure these variables were sensitivity, robustness, small size and mass, and an ability to be 'built-in' to the sewing machine mechanisms. All four signals were to be acquired at much higher frequency sampling rates than had been used previously. Data acquisition was to be followed by a separate data processing and analysis stage.

3.2.1. The specification for the Experimental Testing Station of Sewability (ETS).

The first step in the design process was the preparation of a general ETS specification, with the main characteristics required for the system. After an initial literature review and a survey of the available hardware components, the "configuration" of the ETS was decided.

At the centre of the ETS was a sewing machine, which was to be instrumented with a set of computer-based electronics, but with minimum modification to the sewing machine itself. It was decided that the main components of the hardware and software of the system should be the latest state of the art acquired from well-known specialised producers, to provide robustness and flexibility for further expansion as stated in the research aims.

The main hardware components were the data acquisition boards and associated control/calibration instruments (digital oscilloscope), amplifiers, an IBM PC-compatible computer and associated printing and plotting peripherals. Fig. 3.2.01 below represents the ETS set-up:

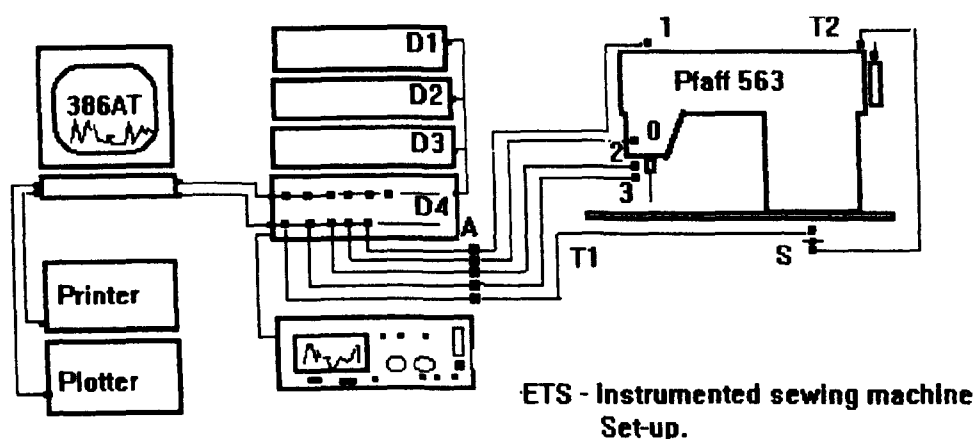


Fig. 3.2.01. Design of RSTM set-up

Legend:

A-signal amplifiers; D1-DT7020 Array Floating Point Processor; D2-DT"Connect"; D3-DT2841-L; D4-DT707 connection board; D5-Digital Oscilloscope; T1-Timer1,time signal; T2-Timer2,time signal; S-Switch between T1 and T2; 0-NTt,needle thread tension signal; 1-PFd, presser-foot displacement signal; 2-PFp,presser-foot pressure; 3-NPF, needle penetration and withdrawal force.

3.2.2. Sewing machine selection.

Extensive market research was carried out into the latest developments in hardware components suitable for further instrumentation of the Pfaff sewing machine. High flexibility and portability features had to be provided

to allow for utilisation of the hardware in other related research areas.

The decision to select a lock-stitch type sewing machine for the research was based on the two following factors:

- recently two research projects had been carried out at Leeds University using an overlock sewing machine (to study knitted fabrics) and therefore it was decided to use another type of machine for this research.

- the lock-stitch sewing machine was the obvious choice, being the most popular for sewing woven fabrics which form the bulk of commercial fabrics.

Some additional practical factors were also influential in the final decision on the selection of the brand and type of machine:

- the need to have a relatively new type of machine which had undergone successful industrial pilot trials and which was to be produced in a long commercial series, so that results would remain relevant after the project had been completed, and

- the requirement for the machine to be manufactured by a well-known producer, who would be willing to provide the necessary maintenance and spare parts, as well as professional expertise during the research itself, by the provision of consultancies, etc.

During the IMB-1988 (International Sewing Machinery Fair

in Cologne), several well known producers were consulted and the German company Pfaff GmbH decided to support the proposed research. Pfaff Hong Kong Industrial Co. also assured Leeds University that it would provide the necessary support for Hong Kong Polytechnic, where the experimental part of the research was to be carried out. Consequently a Pfaff-563 class lock-stitch type sewing machine was donated to the Institute of Textiles and Clothing of Hong Kong Polytechnic and a "Quick-Rotan" digital stop-motor and control system were also provided on a loan-basis for the duration of the research, as well as assistance in precision machining, calibration and maintenance.

3.2.2.1. Machine characteristics.

The Pfaff 563 type sewing machine, is a high-grade, high-speed seamer, with a maximum sewing speed of 5500 stitches per minute. The positive bobbin case opener ensures unhindered passage of the needle thread loop during stitch formation. Stitch type: lock-stitch 301. The maximum stitch length was 3,5 /4,5 mm, depending on settings. Needle sizes for light weight fabrics: Nm 60-80; medium weight: Nm 90-100; needle system 134 was also recommended. Needle-bar stroke: 33 mm. Balance wheel: 65 mm effective diameter. Fabric feeding was modified by a specially designed feeder Fig. 3.2.02. and Fig. 3.2.03.

Other modifications are described later in this chapter. The lifting range of the presser-foot had to be

reduced to 4,8 mm from its original 7 mm (the space being needed for the insertion of the transducer into the presser-foot bar). The machine was described by the manufacturer as: "low noise, vibration-free, running at top speed, having a central fresh oil supply system for sewing hook and needle bar and maintenance free anti-friction bearings. Included also is a fully enclosed gearcase with long-life pad lubrication"(98).

3.2.2.2. Electronic controls.

The "QUICK" digital SYNCHRO type P40S motor was an integral part of the machine. The motor speed recommended for light weight materials was 2800 spm (at 50Hz current). The machine was capable of two-way rotation, reversible, fast adjustable acceleration and brake ramp, rapid treadle response (see Oscilloscope; diagram Fig. 3.2.04). No noise was generated between sewing cycles and the motor was quiet while running. All machine sewing parameters could be reset instantaneously. A non-volatile memory eliminated battery back-up of the stored data.

3.2.2.3. Machine modifications.

There was a need for a number of small mechanical and electrical modifications, for the purposes of the research. The main modifications to the sewing machine are listed below:

Fig.3.2.02-left.
Back view of the
ETS sewing unit.

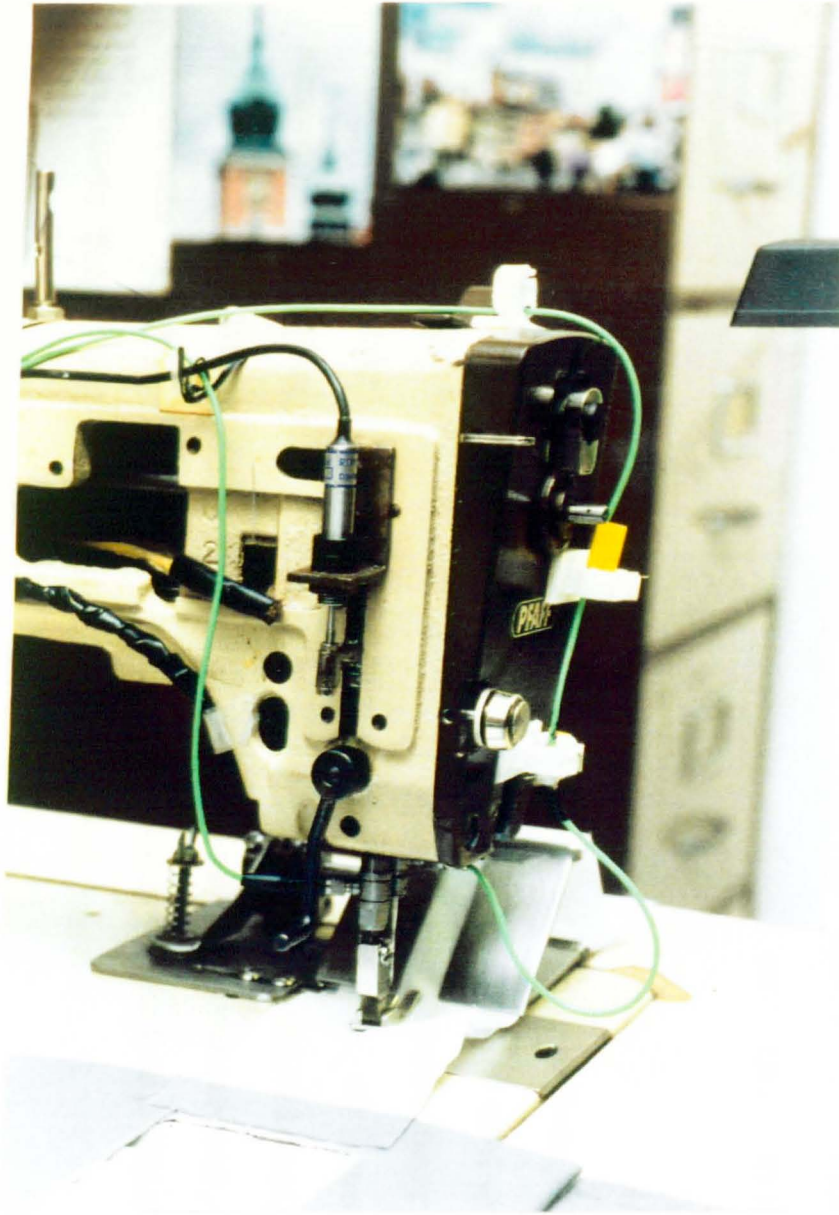
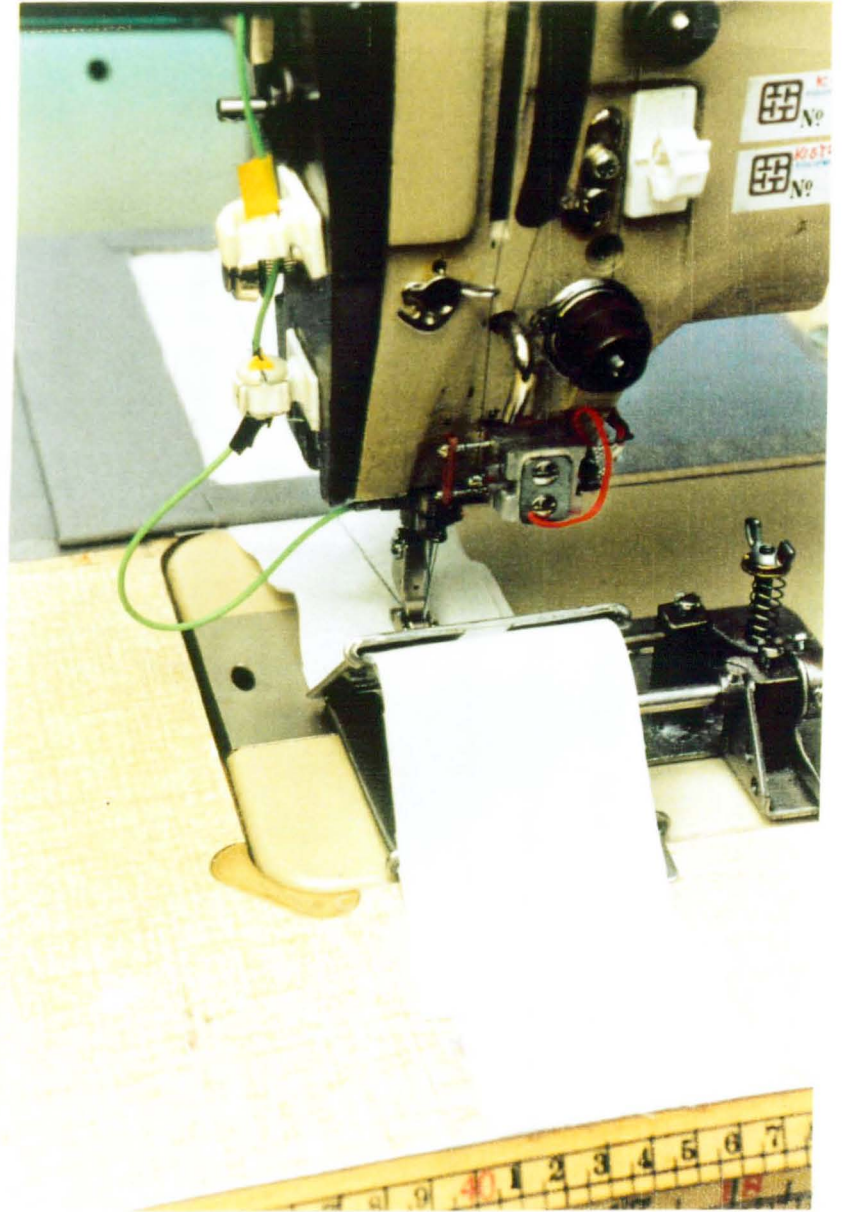


Fig. 3.2.03-on
the right. The
ETS front view.



a. The small mass(3 grams) Kistler washer type sensor(99) was inserted into the needle bar, which became the NPF transducer. This required the re-design of the bottom part of the bar and high-precision machining of the bar itself. After the transformation of the needle-bar into the transducer, the total mass was increased as follows:

-original needle-bar *	23.4200 g,
-modified needle-bar *	26.3021 g,
-difference	2.8821 g,
-increase	12.3 %.

(* including needle).

Apart from the modification of the needle-bar, it was also necessary to cut a slot (10 mm wide and 25 mm high) in a wall of the left cover of the machine head compartment where both needle and presser foot bars were located, (see Fig. 3.2.02 and Fig. 3.2.03) to provide space for the vertical movement of connecting cable of the NPF transducer.

b. The presser-foot bar.

There also was a need to insert a Kistler load-cell transducer/sensor into the presser-foot bar, using precision machining, to accommodate the PFp transducer (see Fig. 3.2.02). Apart from the insertion of the sensor, the presser-foot bar had to have an additional link to the LVDT presser-foot bar displacement transducer, which was located at the back of the sewing machine. This was made from duralumin to reduce total mass.

The changes in mass were as follows:

- original presser-foot bar	21.4362 g,
- modified	32.6232 g,
- LVDT rod	2.1345 g,
- extension bracket	17.0733 g,
- extension total	20.2078 g,
- load-force sensor	12.0000 g,
- original extension bracket	11.8013 g,
- new extension bracket	17.0733 g,
- bracket expanded beam *	5.1720 g,
= Total original mass	35.3720 g,
= New transducer mass	52.8310 g,
= Difference in mass	17.4590 g,

Modification resulted in an increase in mass, due to the load-force sensor mass of 12g and the additional expansion link(*) to the LVDT transducer body.

The chosen Pfaff-563 machine was equipped with a "Quick-Rotan" Stop-Servo Motor with an electronic controlling system. The steering programme, based on digital processing, had 8 function levels with pre-programmed sets of functions, with flexibility options, which could be amended according to process requirements. The system allowed the initialisation of sewing to be pre-set, according to the needle-bar displacement domain. This feature was found extremely useful in the synchronisation of signal timing. Through a direct linkage of the motor control circuit with an input of DT707 connecting board, the Timer1 (T1) signal input allowed the shaft revolution

to be marked. The second amendment was the assembling of a special switch alternately linking the T1 or the T2 timers into the input of DAP acquisition. Simultaneously voltage scaling of T2 was introduced, providing time signal marking adjusted to the amplitude of other signals to ensure clarity of display.

3.2.3. Data acquisition hardware.

3.2.3.1. The computer and peripherals.

Retrospectively the decision to purchase the "EVEREX" AT-386 Personal Computer with a 20 MHz processing speed, 64 K cache memory and 2Mb RAM, which was taken in 1988, seems a modest approach, but at the time it appeared to be among the most powerful personal computers available on the market.

The computer had a sufficient number of free slots to accommodate two additional data acquisition boards, and had 2 parallel and 2 serial ports. This allowed the HPDeskJet 500+ printer and two plotters (the HP2574 6-pen colour plotter and/or Tektronix 100HC 4-pen colour plotter), to be connected, the latter being linked to the Tektronix 2201 digital oscilloscope with a 1Mb memory and 2 channels.

In practice, after the installation of the data acquisition boards, it became apparent that the system was prone to frequent hanging. After investigation it was found that the problem was due to insufficient cooling of the CPU. The DT2020 AP board generated extensive heat,

which required the insertion of a double cooler. Simultaneously the mother board had to be replaced with a higher capacity RAM of 8 Mb. This was beneficial in the later stages of the research during the installation of the image processing hardware. After these modifications, the computer system worked satisfactorily, except for periodic problems with a virus, requiring reformatting of the hard disk.

3.2.3.2. The digital data acquisition DT2841-L board.

Data acquisition boards help to measure real-information represented by analog signals. The analog signals come from sensors or transducers that convert force, length, time, etc into voltage. The electronic sampling of analog signals is called A/D conversion or analog-to-digital conversion. A/D conversion changes analog voltages into digital codes for computer processing and storage. A complimentary process, D/A conversion - digital-to-analog conversion - changes digital data into analog voltages. This permits a computer to drive chart recorders, signal amplifiers, process actuators, and other analog-input devices.

To communicate with a device that is itself digital, many data acquisition boards provide digital I/O (digital input/output) lines. Digital I/O lines can be set for input or output operation in groups called ports; often comprising eight lines.

The principal factors to consider when selecting a signal acquisition board are: input ranges and types, speed, accuracy, auto-calibration, the modularity, analog outputs, clocks, triggers, and counter/timers. Also of importance are data transfer methods (when throughput requirements are ≤ 40 kHz - clone computers may be used), integrity (continuous performance, simultaneous A/D and real-time DSP (digital signal processing)). Software such as example programmes, drivers and tool-kit, subroutine libraries and maintenance support are indispensable items for designing integrated, multi-purpose, tailor-made applications; these are frequently menu-driven.

For high-speed data acquisition, the method of data transfer is as important as the speed of A/D or D/A. For each word transfer, the software must do several time-consuming operations including requesting the bus to perform the transfer, and relinquishing the bus again. Because the CPU is involved in each data transfer the data acquisition board competes with many other devices on the computer. It should be emphasised that high-speed data acquisition is possible without a high-speed host, and even without DMA (Direct Memory Access), but the amount of data that can be acquired is limited to approximately the amount that can be held in one DMA buffer, 32-64K samples. At a speed of 250 kHz, this would limit sampling time to only 131 ms. Beyond about 250 kHz, the basic limitations in the PC AT bus bandwidth become an issue. To go beyond this 250 kHz limit, Data Translation designed DT-Connect,

an interface specification that permits data acquisition boards to plug directly into-and transfer data directly to-and-from a signal processor or memory board. Using dedicated input and output data ports that support 16-bit transfers at up to 10 MHz, DT-Connect can easily handle extremely high-speed data acquisition - up to 750 kHz (DT2841 series boards).

After much consideration it was decided, that the most suitable hardware and software for digital signal processing would be the above described DT2841 series of high-speed analog and digital I/O boards of the Data Translation Co. from USA. In 1988 Data Translation(100) launched the new state-of-art DT2841-L, high speed board for 750 KHz data acquisition and signal processing (DSP) on IBM PC AT and compatibles.

The characteristics of the DT2841-L board are:

-Analog input. As a member of 'DT-Connect', the board plugs directly into a 'DT-Connect' processor board over high speed data input and output ports, not over the slow IBM PC AT bus. This permits A/D throughput to 750 KHz with 4 differential inputs (in our case, sewing thread, presser-foot displacement, presser-foot pressure and needle penetration signals can be inputted). A/D channel and input gain selection are accomplished using a RAM channel-gain list, which is a 16-location RAM. This allows any sequence of channels to be sampled at any available gain, while maintaining the full A/D throughput rate of

the board. It also permits the same channel to be sampled at different gains, or different channels to be sampled at different rates.

-Analog output. The DT2841-L's digital-to-analog subsystem consists of two channels, each with a 12-bit deglitched D/A converter. These can provide either single outputs or dual simultaneous outputs. Analog values can be output at up to 130 KHz per channel from the 'DT-Connect' processor board via the external data ports.

-Additional features. In addition, the DT2841-L board contains 16 lines of digital I/O organised as two 8-line ports. It contains also two pacer clocks, one of which initiates D/A conversions. By using two pacer clocks, analog input and output operations can occur simultaneously, at the same time or at different rates. Each pacer clock operates under programme control, and provides a usable range of about $1,4 \mu\text{s}$ (714 KHz) to 838 ms (1.2Hz). Each clock can operate from an onboard 10 MHz oscillator, or from an external oscillator, operating at any frequency from dc to 10 MHz. Two external triggers, one each for the A/D and D/A sections, can be used to gate the conversion events.

The external oscillator is selected in place of the on board 10MHz oscillator, as the frequency source for either the A/D or D/A pacer clock, or for both. The external oscillator becomes an input to both prescaler and divisor circuits on the board. By adjusting the rate of the external oscillator and the values of the prescale and

divisor circuits, virtually any desired sampling rate can be achieved.

An onboard AC to DC power convertor generates all the required analog supply voltages from the 5.0 volts, provided on IMB PC AT backplane, and provides high noise isolation from the computer systems's power supplies. The external input/output data ports support simultaneous data transfers to and from the 'DT-Connect' processor board in either block mode (up to 65,536 words) or continuous performance mode. Continuous performance is a data sampling method which provides gap-free transfers of large volumes of data from the 'DT-Connect' processor board memory (D/A conversion) or to 'DT-Connect' processor board memory (A/D conversion), without any loss of samples. The DT2841 Series Block Diagram and technical specification may be found in Appendix XII.

3.2.3.3. The Floating-Point Array Processor DT7020 (FPAP).

Real-time Digital Signal Processing (tandem of DT2841-L board with 'DT-Connect') makes it possible to see the results immediately. This tandem provides direct connection to the DT7020 processor. The DT7020 is a general-purpose 32-bit floating-point array processor, that accelerates Digital Signal Processing operations. Working many times faster than the PC AT, the DT7020 can perform a real FFT on 1024 data points in 13.0 ms.

Software support for DT7020 and DT2841-L boards is provided by the MACH™ DSP Subroutine Library (101).

The FPAP can perform 8 million floating-point operations per second (8 Mflops). Floating-point addition, subtraction, and multiplication operations are performed in a single clock cycle. The board provides 4 Mbytes of data memory to store raw data, intermediate results, or processed data values. Data memory is mapped into the hosts's extended memory space, and can also be accessed using "DT Connect" data ports. The DT7020's microcoded programme instructions are stored in 16 Kbytes of SRAM. Dedicated 16-bit ports are used for data transfer to and from the data acquisition board DT2841-L. The data on the technical characteristics of the above boards is included in Appendix XII.

The work of the DT7020 and DT2841-L boards in tandem was problem-free throughout the time of the project experiments.

3.3. The development of the transducers.

The transducers to study the dynamic forces in high speed sewing needed to match the specifications of the available dedicated high speed analogue input boards, which were becoming available for 386-based personal computers. These enabled data sampling rates of up to 250 kHz to be attained. During the course of the research the newest type of board with a sampling rate of 750 kHz became available and it was decided to acquire it, with the aim of fuller utilisation in the years ahead. The availability of such boards makes it possible to study the

dynamic effects of high speed garment sewing and textile processing.

In the case of a sewing machine operating at a speed of 6000 rpm, three channels of data could be sampled with 2500 data points per channel per cycle. Even at 9000 rpm, 1666 data points could be obtained. At the start of the project, the kind of transducer that was needed to record physical data at such a sampling rate did not exist, so the first part of the project was the development and construction of such transducers.

Four types of transducer were identified as essential to the study, and have already been mentioned in part 3.1. of this chapter. They needed to have sensors with frequencies that surpassed the highest required sampling rate, i.e., even of 1 MHz. This implied mechanical sewing elements of very small mass, high stiffness, and small physical size, as well as associated electronics with high cut-off frequencies and high bandwidth. It was apparent that the development of such transducers, even if suitable sensors were found, (they were already being manufactured for a different type of application) was a task which needed careful consideration of the technical and financial constraints involved.

3.3.1. The study and search for suitable sensors and associated instruments.

In the past most sewability testing was conducted using a strain gauge attached to the underside of the

throat plate. These testers generally provided needle penetration forces which could be used for comparative purposes. A clear-cut force trace is difficult to obtain because the throat plate is subjected to additional forces from the presser-foot. Various solutions have been tried to minimise the influence of the presser foot by using e.g. an alternate feeding mechanism (14,17,20,21,22). When such an approach is utilised, the practical value is limited, because of the artificiality of the sewing system under study. The resolution of force acquisition at high speed sewing, such as was attained by previous investigators, was inadequate as it lost detail at speeds over 2000 rpm. Therefore, before embarking on the research for a specific type of sensor, a non-conventional solution was considered first. The most suitable RSTM would be a mobile one, where a full set of transducers together with their associated instrumentation (including a PC), could be located on a special trolley and "connected" to the machine which was to be tested (similar to a portable electro-cardiograph). This required non-contact transducers employing principles such as ultra-sound, electromagnetic fields or laser-beam optical sensing. A preliminary survey was carried out at Hong Kong Polytechnic Engineering Departments and later at Hong Kong Productivity Council's laboratories. There was some optimism, following the discovery of expertise in the Electronic Engineering Department of Hong Kong Polytechnic. The decisive obstacle in the realisation of

this approach however, was the lack of a laser pulsed beam generator, which was expensive to buy and not available for loan. Another option, the application of a laser velocity-transducer set, type 3544 was considered (Bruel&Kjaer). This approach finally had to be abandoned due to the high cost, the limited space close to the needle area, and the velocity frequency range upper limit of 20 kHz.

During this initial consideration, discussions were carried out with the Hong Kong Office of Bruel&Kjaer, the instrumentation manufacturers, about the aforementioned Velocity Laser and also with regard to the application of acceleration transducers for the vibrations and displacement of the presser bar, so as to avoid mounting the transducer onto the vibrating object. The frequency range of up to 5 kHz and difficulties in mounting the acceleration transducer resulted in the abandonment of this option as well. Optical sensors and ultrasound options were not considered, due to the lack of sufficient expertise at Hong Kong Polytechnic.

A very interesting example of a non-conventional type of sensor were the piezo-electric flexible PVDF films provided for an initial trial by the "Pennwalt" Co.(USA). But these were, on the one hand, oversensitive, picking up voice vibrations in the vicinity of the research room, and on the other hand required the development of small sized housing. A Japanese load-cell (pressure/tension) cell filled with gas as a medium of compression-and-

decompression, was found to be of unsuitable size for insertion into the sewing machine bars.

After the above options were rejected, attention was directed to piezo-quartz sensors and strain-gauges which appeared to be less adventurous media. Small size was the first pre-requisite of the search, which resulted in finding a piezo-electric crystal load-cell produced by Kistler. Kistler also produced a range of sensors (washer type) of various dimensions and one was found to be of a suitable size. The washers themselves were sensing devices, but they were additionally built in to a case equipped with mounting ends, and were pre-loaded. These characteristics were the best found thus far, although they required associated expensive charge amplifiers.

The main consideration in assembling the sewing thread transducer was that it should be located as close to the needle as possible. The search focused on Schmid's 3-point roller type tension measuring meters, widely used in checking yarn tension. Initially another solution was considered as a temporary option, the utilisation of a load transducer used in digital scales. This was a 4 semi-conductor self compensating load type transducer, with a frame made from an aluminium-based alloy. It had a threshold of 0.01 N. By mounting it onto a sewing machine the synchronisation of signals was tested during the design of the data acquisition programme. Although it did not work in the higher range of speeds above 1000 rpm, sufficient signal accuracy was obtained

for DAP circuitry testing and for static and semi-static measurements.

Finally, it was decided that the concept of a cantilever type of sewing thread tension transducer was the most appropriate, taking financial circumstances and the time available for the research into consideration.

A presser-foot displacement transducer of the LVDT type was selected as having suitable characteristics for measuring speeds of over 5000 rpm. Additionally, the trace characteristics did not change with vertical displacement, as happened with optical proximity switches in outward and inward movement.

3.3.2. The needle bar pressure/tension transducer.

Quartz load washers are piezoelectric force transducers, which convert a force into an electrical charge. Such force transducers have an inherently high rigidity and a correspondingly high resonant frequency. This allows them to be fitted into measuring components without altering the elastic behaviour of these significantly. An extract from the specification data of the washer type transducer 9001 is presented in Appendix IV. Some terms related to the needle-bar transducer are given below:

- **Threshold;** the smallest change in the measurand -
Threshold; the smallest change in the measurand that will result in a measurable change in transducer output. With piezoelectric transducers, the threshold is limited by the

inherent noise of the transducer and, above all, of the charge amplifier. The value of the measurand indicated, corresponds roughly to 3 times the noise signal of a normal charge amplifier.

- **Resonant frequency**; the resonant frequency included in the specification table is the measured value for the electrically excited load washer, without load and unfitted. In this case the resonant frequency was not measured owing to the following comment made by Kistler: "The natural frequencies quoted in the table of technical data are of only theoretical importance. If a shock wave impinges on the load washer it is measured with a rise time of about $1\mu\text{s}$. If a load washer is fitted into a cylinder of the same diameter for measuring axial force, it can be said without contradiction that the dynamic properties of the measuring object are not affected by fitting the load washer. There is no need, whatever to take the natural frequency of the load washer into consideration" (99).

- **Linearity (ISA)**; the closeness of a calibration curve to a specified straight line. For piezo-electric transducers this straight line is determined as follows (Fig. 3.3.01):

In this example, the curves were distorted in the ordinate direction to make matters clearer. The two parallels were sought, as close together as possible but enclosing the entire calibration curve. In addition the median parallel had to pass through the zero (no force, no output signal).

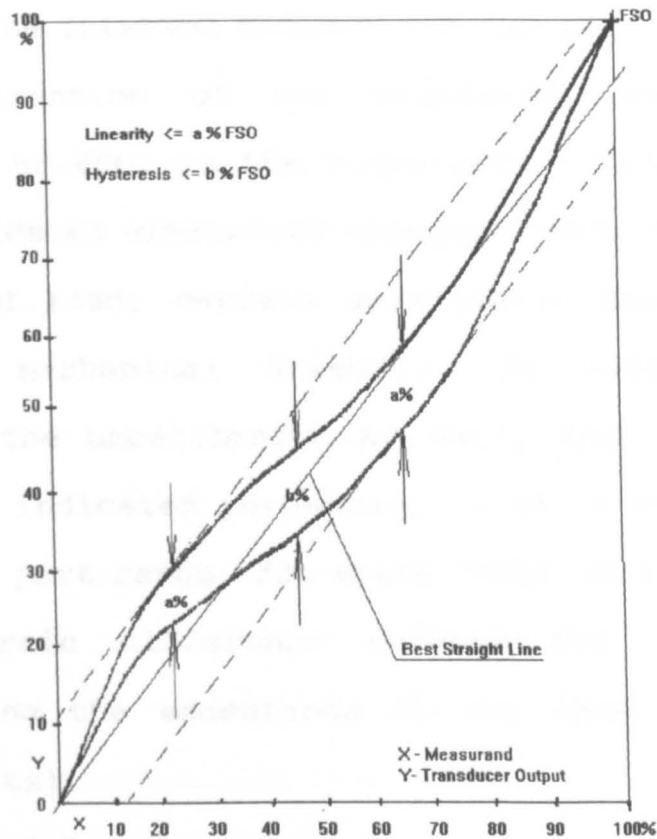


Fig. 3.3.01. Transducer calibration curve.

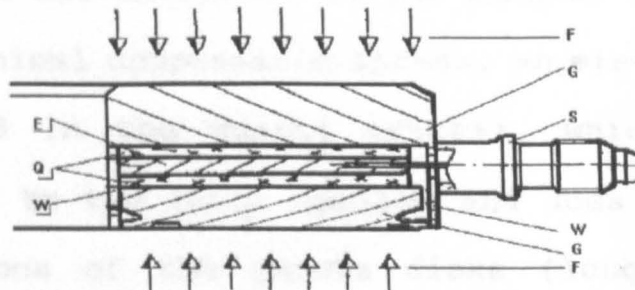


Fig. 3.3.02. Schematic section through quartz and washer sensor 9001 [Q - quartz disk; E - electrode; W - elastic wall; G - housing; S - plug; F - applied force].

The slope of this output signal is the sensitivity of the transducer.

Half the interval between the two parallels (measured in the direction of the ordinate), expressed as a percentage of FSO, is the linearity. Although the quartz itself yields an electrical charge exactly proportional to the applied load, certain unavoidable deviations result from the mechanical assembly. In each part range, including the uncalibrated as well, the linearity stays within the indicated percentage (0.3% in our case) of the particular part range. FSO means "full scale output", i.e. the algebraic difference between the output signals representing the measurands at the upper and the lower range limits).

-Principle of operation:

When a disk of a quartz crystal is compressed it yields an electrical charge. A quartz load washer consists of one or two annular disks of quartz crystal, an electrode and a housing with a plug (see Fig. 3.3.03). The force to be measured must act uniformly on the annular surface. Owing to the mechanical compression stress, an electrical charge is generated in the quartz crystal, which is exactly proportional to the force applied and does not depend on the dimensions of the quartz disks (longitudinal piezoelectric effect). The charge produced is picked up by the electrode and taken to the plug connection. The polarity is arranged so that a compressive force produces a negative charge, which is then converted into positive

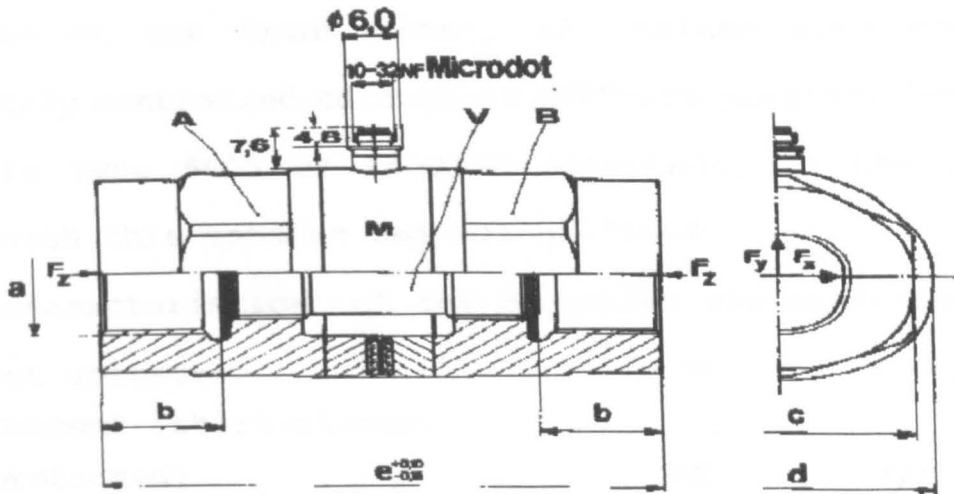
voltage in the charge amplifier. When the load washer is unloaded, a positive charge results. If a negative charge has been generated previously, the under load is dissipated by shorting on the plug. To ensure that the force to be measured is applied uniformly to the angular surface, the mounting surface on the measuring object must be accurately flat, level and rigid. The mounting was carried out with the specialist assistance of Pfaff Hong Kong according to a design provided by the author.

3.3.3. The presser-foot force transducer.

Kistler's quartz force transducer type 9301A, for measuring dynamic and quasistatic tension and compression forces, was mounted into the presser foot bar, with some mechanical modification. This transducer had the previously referred to washer 9001 inserted into a special casing assembly, which was tightly welded to ensure high rigidity (Fig. 3.2.04).

3.3.4. Charge amplifiers:
Fig. 3.3.03. View of the Kistler 9301A Force-Link Transducer; measuring presser-foot force(PFp), before insertion.





3.3.04. Section through the 9301A transducer assembly.

[M -Load Washer; A,B - Nuts; V - Pre-loading bolt;
 $F_{x,y,z}$ - Acting Forces; a,b,c,d,e - Dimensions].

This requirement was necessary in the case of the presser foot, since the presser foot bar was continuously under the highest range of the presser foot bar's spring compression, even when there was no sewing. The technical characteristic is provided in Appendix V. The principles of operation were provided in the part related to the needle-bar transducer.

3.3.4. Charge amplifiers:

Both NPF and PFp transducers required signal amplification by the use of charge amplifiers. Kistler's mains-operated microprocessor controlled one-channel amplifier, type 5011, converted the electrical charge yielded by

piezoelectric transducers into a proportional voltage signal. In addition to the manual setting of the measured values on the front panel, all values also could be remotely controlled through an IEEE-488 parallel interface module Type 5605 or RS-232C interface. In the current research this version was not utilised.

The characteristics of the amplifier are as follows:

Output voltage	V	+/- 10,
-Current (short-circuit protected)	mA	+/- 0...5,
-Impedance	@	10,
-Linearity	% FS	<=+/-0.05,
accuracy to +/-99,9 pC FS	%	<=+/-3,
from +/-100pC FS	%	<=+/-1,
Freq. range -3dB (F.off)	kHz	ca 0-200,
Freq.response err.(F.off)		
to 50 kHz	%	-1...+2,
to 200 kHz	%	-30...+3,
Low-pass filter:		
(Butterwood,2-pol.)[LP],		10Hz-30kHz,
(8 stages:10,30,100,300...,-3dB)		(+/-10%),

3.3.5. The needle thread tension transducer.

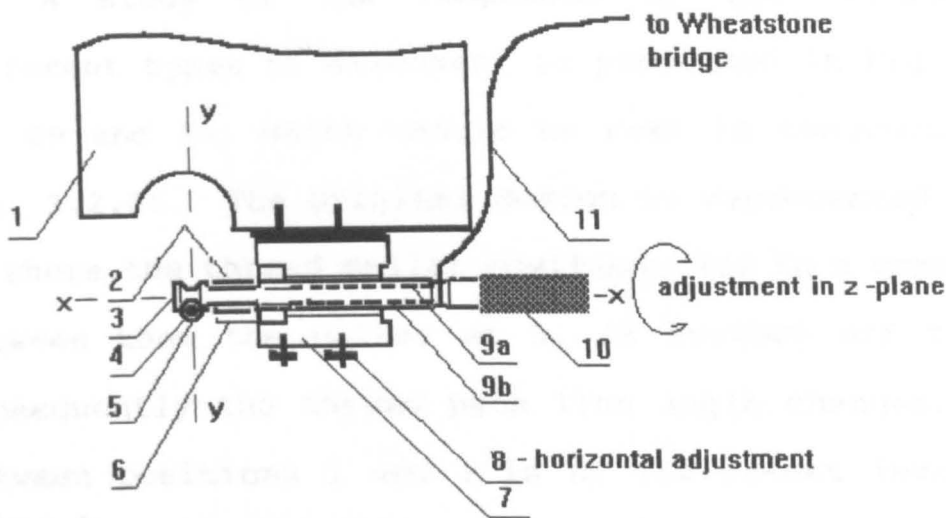
The sewing thread tension transducer was developed through a trial-and-error method. The first version was a load-cell adaptation, made for the sake of testing the DAP (digital data acquisition system) during the compilation of a programme. Experience gained in the first stage, led to the design of a less bulky transducer, consisting of two separate cantilevers working in tandem, assembled in the same housing. Each cantilever was strain-

gauged, using semi-conductor strain-gauges assembled into a Wheatstone bridge.

The cantilevers were made from the alloy material left over from the first transducer. After assembling the transducer the tension traces showed imbalance and oscillation effects. The concept of self compensation of a two-arm transducer was finally found to be the wrong (103,104) approach and was abandoned.

The third approach led also to a type of cantilever, but with one-arm only. It was made from aluminium-tin alloy rod (type 2024; QQ-A-225/6). The strain gauges this time were made by Kyowa Co.(Japan), but were of a general performance type with a foil base.

The main component of the transducer is a cantilever, made in the shape of a one-piece rod, having a profiled head with strain-gauges on one side, and a handle on the other side. The cantilever was firmly clamped between the two jaws of the housing and screwed to the machine body by two screws. Between the transducer and machine, a dense felt washer was placed, isolating the transducer from the vibration of the sewing machine. The effects of the isolation of the vibration, by means of different types of materials for this washer, were tried, and confirmed the reduction in amplitude of the signal noise. Therefore it was decided to select a 4 mm thick, high density felt, as the best option for reducing the vibration of the transducer.



Legend:

- | | | | |
|-------------------|----------------|---------------|------------|
| 1 -m/c body; | 5 -thread bar; | 7 -housing; | 11 -leads. |
| 2 -strain gauges; | 6 -transparent | 8 -screws; | |
| 3 -cantilever; | protective | 9 a,b -wires; | |
| 4 -thread; | shell; | 10 - handle; | |

Fig. 3.3.05. Schematic diagram of the thread transducer.

The size of the head of the transducer was minimised to the point, where a small mass and sufficient rigidity would be provided. The design allowed the adjustment of the transducer in 3 axes (xx, yy and zz). This feature was found to be very useful in the transducer setting stage. See Figs. 3.3.07 and 3.3.08.

-Strain gauge characteristics:

Gauge Factor: $2.08 \pm 0.35\%$; Resistance: $120.4 \pm 0.4\Omega$;
 Gauge length: 2mm grid; Gauge pattern: Uniaxial; Thermal
 Expansion Coefficient [PPM/°C](Aluminium/Tin): 23.4.

3.3.6. Study of the thread passages.

A study of the responses of the transducer to different types of alignment is presented in Fig. 3.3.07, 08, 09 and 10, which should be read in conjunction with Fig. 3.2.06. The original design is represented by Type 1, where the thread puller positions are in a common line. Between them the puller at 3, is further off the line. Consequently the thread path line angle changes. Tension between positions 1 and 3 is at its lowest level during its feeding phase. The angle of the thread path changes between 1a and 1b and cannot be altered, as this is an intrinsic feature of the machine. However some improvement in the thread path line was made (by the machine manufacturer), through taking off a small part of the machine body (in the shape of an oblong groove) and smoothing the change of the direction of its path, before it entered the needle bar guide at position 1a. The above implications were also considered in the assembly of the Ntt transducer, although it was mounted as close as possible to the needle, see Type 2 configuration. The thread passage through the transducer itself was between 3 points; gt (top guide bar), C(transducer cantilever) and gb (bottom bar guide) and is designated as C3Ph (3-point horizontal), where the bending of the strain gauges is in a horizontal plane. A 2-point passage was tried at horizontal and angular positions respectively. For the sake of the completeness of configuration types, the C0Ph was tried.

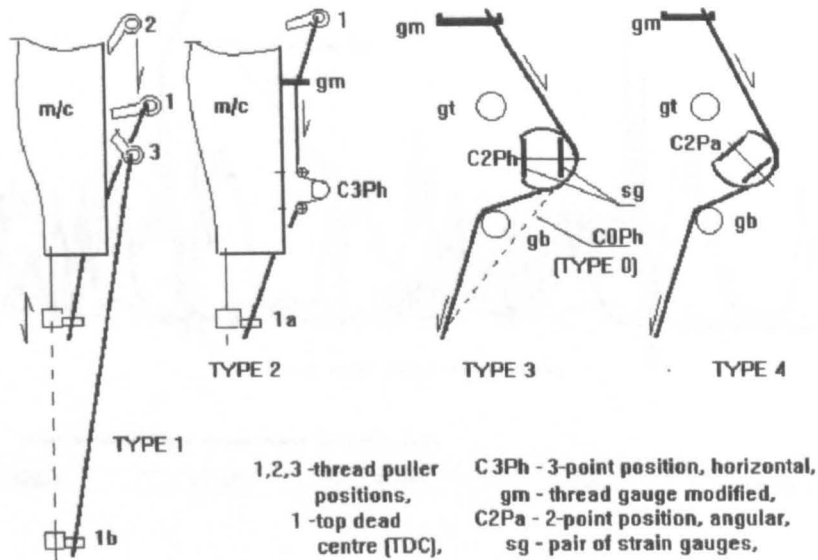


Fig. 3.3.06. Schematic diagram of the thread passages.

[1a,1b-needle thread guide positions(1a -at TDC); (1b -at BDC, the lowest); gm -modified thread guide; gt,gb-transducer's thread guide bars(top and bottom); m/c-sewing machine body].

A comparison with NTt traces is shown in Fig. 3.3.07 as C3Pa (blue), C2Ph (red) and C0Ph (in black). The signals had their own off-sets (acquired separately in the same conditions) and in Fig. 3.3.08, they are expanded for the sake of clarity. A comparison of the signals produces the following conclusions:

- The 3-point transducer's passage applies too big a resistance, and the thread therefore is subjected to an increase of the dynamic forces (of high frequency at high speeds), resulting in thread breaks, at speeds below the

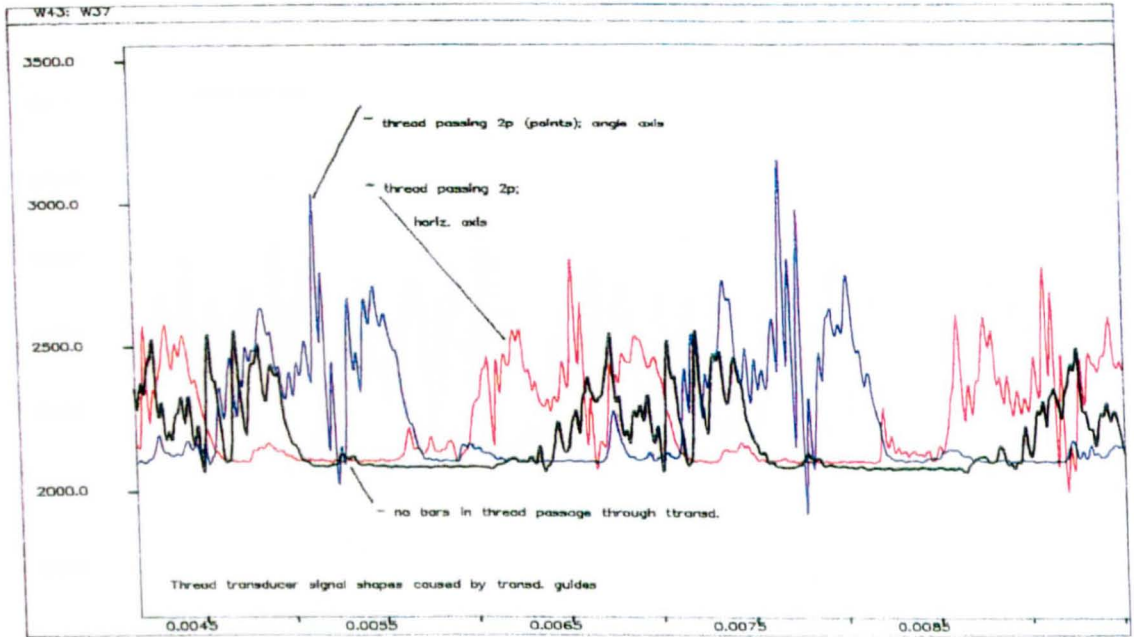


Fig. 3.3.07. Three traces of the NTt signal (blue-at C2Pa; red-at C2Ph; and black-at C0p).

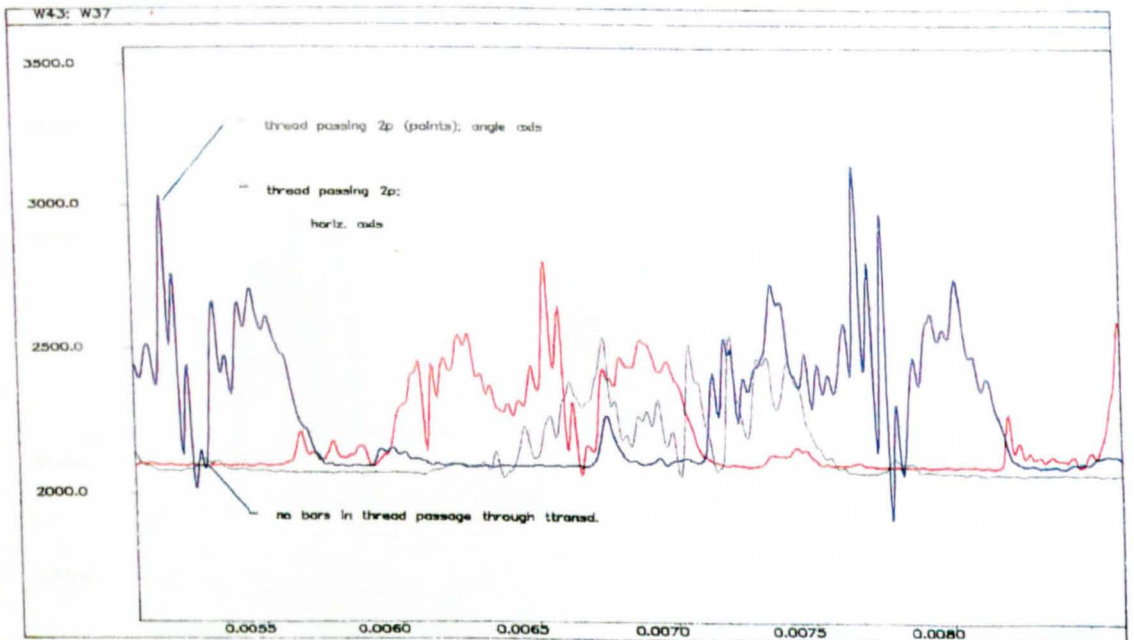


Fig. 3.3.08. The same signals as above in expanded form.

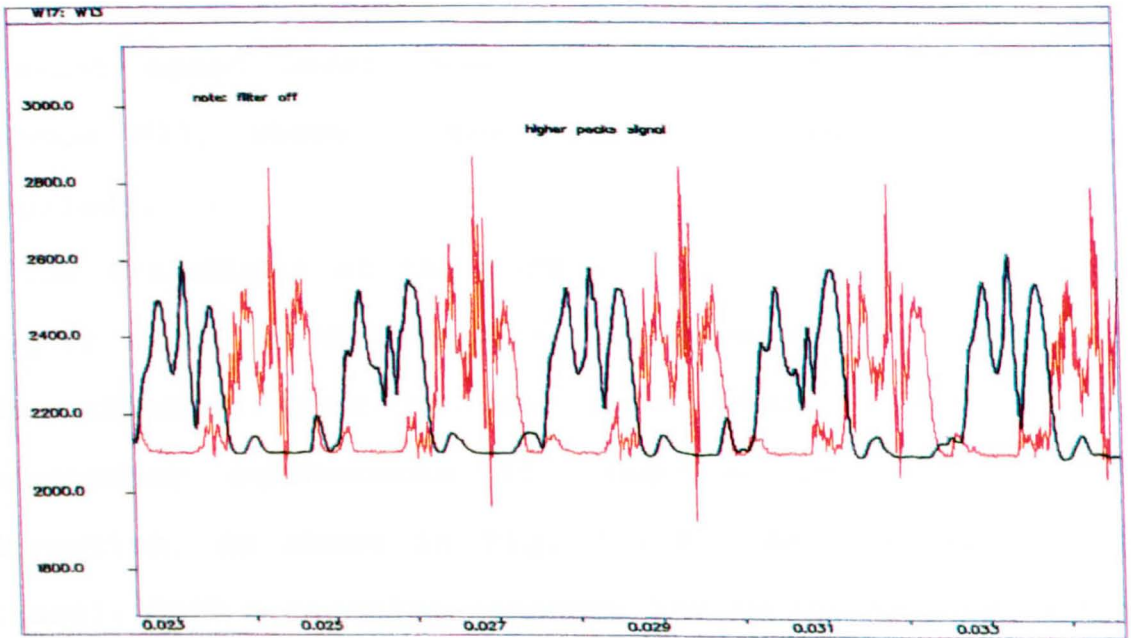


Fig. 3.3.09. Example of the filtered NTT signal (1kHz).

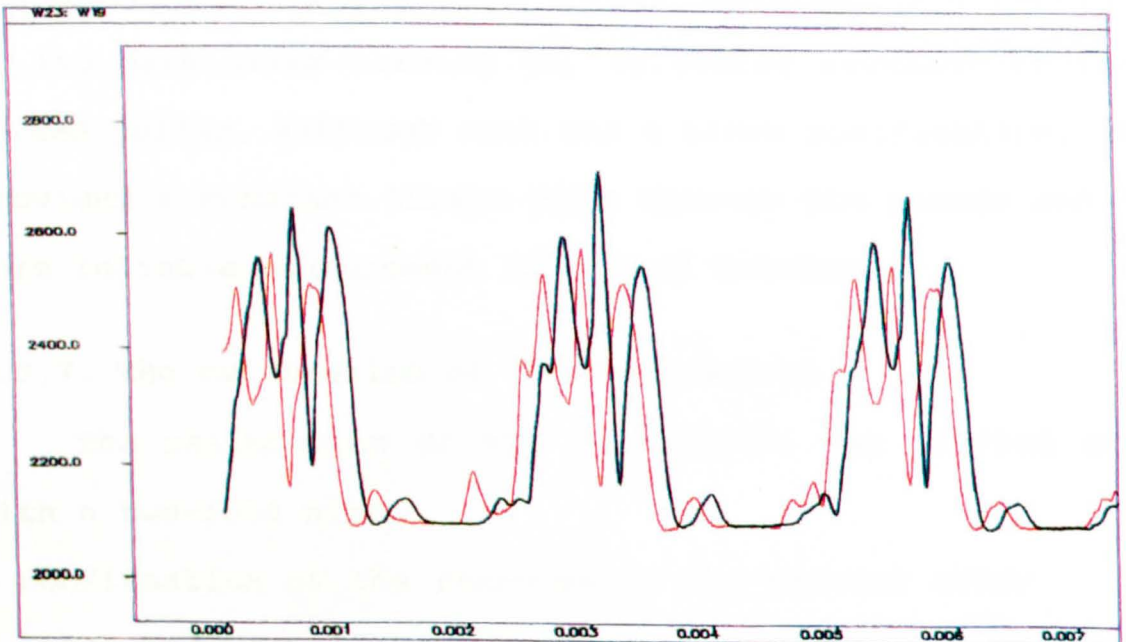


Fig. 3.3.10. The filtered thread signals acquired at different settings (red-at C2Ph; black-at C2Pa).

pre-set speed level (see Fig. 3.3.09 and Fig. 3.3.10, window W23, where 1 kHz filter on signal input was applied).

- The transducer at the C2Pa position is subjected to a higher bending force than in C2Ph, as the force acts at the thinnest part of the cantilever. Therefore the transducer counteracts it, bending in the opposite direction, as shown in Fig, 3.3.07, 08, 09 (red colour trace). Such a negative response led to the abandonment of the Type 4 Set-up.

- For the existing equipment, the transducer had to be set at Type 3 (C2Ph), as a permanent position.

To assure a constant angle of the thread path between gm and cantilever(C2Ph) - the thread guide gm (Fig. 3.3.06) was modified, to prevent the thread changing the direction of its path after leaving gm, following movement of the thread puller. Although this was a minor modification, it provided a constant thread path through the sensor and a more reliable measurement of thread tension.

3.3.7. The calibration of the transducers.

The calibration of the transducers was carried out with a two-fold aim:

- confirmation of the response of the sensors after they had been assembled into transducers,
- converting the transducer signals into meaningful units for the parameters to be measured.

The selection of calibration methods was based on the

specifics of the design and the available instrumentation.

The description of the calibration methods developed in the system design is presented for the piezo-quartz, strain-gauged and LVDT transducers.

3.3.7.1 The needle and presser-foot bar transducers.

After the Kistler sensors had been assembled into bar-transducers (needle-and-presser-foot bars), they underwent calibration to confirm their response. The calibration of both was carried-out by the use of the Dead-Weight ranging from 1g to 9.3 kg. Both bars were in situ in the sewing machine. Before calibration, their holder-clamps were loosened to provide movement with minimum friction. Special brackets (of 300 g weight) were constructed for the weights above 1000g. For calibration below this range, weights had to be attached directly to the bottom parts of the presser-bar and to the needle eye respectively. The sensors were connected by their connecting cables to the digital oscilloscope by means of a charge amplifier.

The 2201 Tek digital storage oscilloscope was used in the static calibration. It had dual vertical input channels with a DC-to-20 MHz analog bandwidth and a DC-to-5 MHz digital bandwidth. The vertical channels were calibrated by deflection factors from 5 mV to 5 V per division at full bandwidth. The variable VOLTS/DIV gain control, increased the vertical deflection factor up to 2,5 times the VOLTS/Div setting.

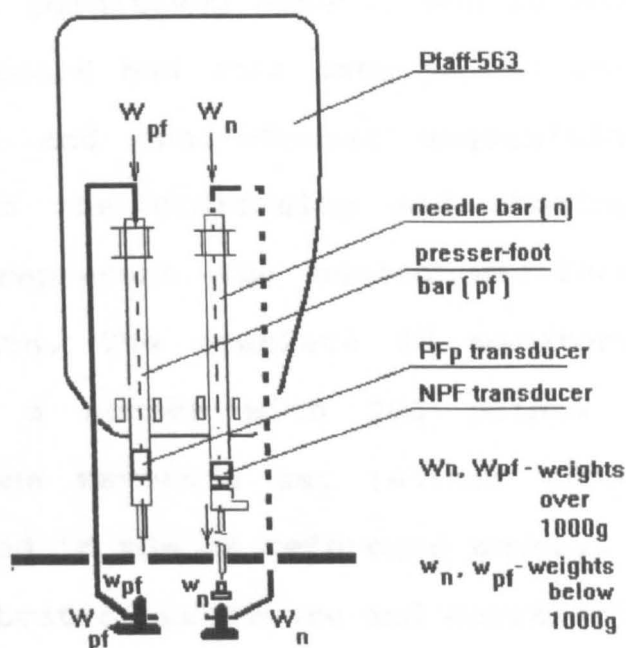


Fig. 3.3.11. Static calibration of NPF and PFp transducers.

The vertical channel display modes were CH1 and CH2 for each one separately, and for both together (in this mode CH1 and CH2 were digitised simultaneously). In horizontal, non-store mode, the deflection system had calibrated sweep speeds from 0.5 s to 0.1 microsec per div. At sweep speeds of 20 microsec to 50 milisecc per division, the digitised display was updated as a full RECORD, where all the waveform data points were replaced at once when the acquisition of signals was triggered. At STORE mode sweep speeds of 10 milisecc to 0.5 sec and 0 % pretrigger, the display was updated in SCAN mode. In SCAN mode, the wave

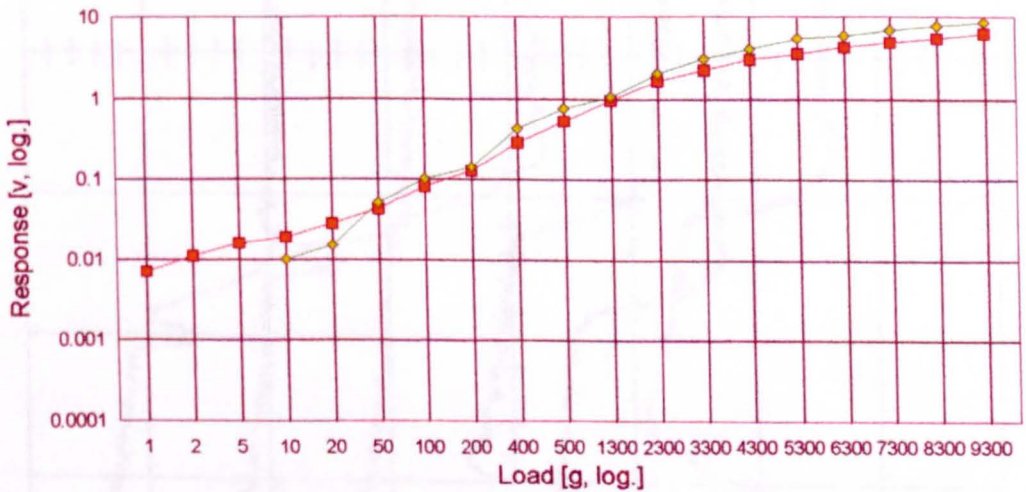
form was continuously digitised and displayed, overwriting the previous, acquisition from left to right. The storage sampling rate, (digitised speed), was 10 MHz per second. A wave form record had 2048 data points per channel for single-channel and dual-channel acquisitions. Waveform acquisition is the digitising and storing of digital values that represent the analog waveform applied to vertical inputs. The complete 2K waveform record was displayed on a screen with 200 points per division resolution. One waveform set (either channel or both) could be stored in the 4K reference memory.

The calibration procedure and correlation graphs are presented in Fig. 3.3.11 and Fig. 3.3.12. In the Figure 3.3.11 - the brackets are drawn as a thick line, to which the loads W_n and W_{pf} are attached. The top part of the bracket lies on the top of a bar. The load W_n or W_{pf} compresses the bar and the transducer responds releasing a charge which is converted by a charge amplifier to a positive voltage which is amplified in the oscilloscope. The signal responses are plotted on the oscilloscope plotter and were averaged using 20 readings for each load measured. Two methods were used, a slow sampling speed of 0.3-0.5 sec per Oscilloscope (Oscope) division (Fig. 3.2.13), and 0.1 msec per division for small loads. The weights below 1000g were attached by very thin wire to the holes of the presser-foot and to the needle eye respectively.

Fig. 3.3.12. The Needle and Presser-foot Bar's calibration. Inset Fig. 3.3.12a: X,Y graph of the average Y's-values.

A	B	C	D	E	F	G	H	I
1	Grams	Volts	Volts	[A v. B] - Needle Bar Transducer Calibration:				
2	1	0.007	0	Regression Output:				
3	2	0.011	0	Constant	0.037733			
4	5	0.016	0	Std Err of Y Est	0.05822			
5	10	0.019	0.01	R Squared	0.999313			
6	20	0.028	0.015	No. of Observations	19			
7	50	0.042	0.05	Degrees of Freedom	17			
8	100	0.08	0.1					
9	200	0.126	0.138	X Coefficient(s)	0.00067			
10	400	0.28	0.42	Std Err of Coef.	4.3E-06			
11	500	0.52	0.75					
12	1300	0.95	1.05	[A v. C] - Presser-Foot Transducer Calibration:				
13	2300	1.65	2.05	Regression Output:				
14	3300	2.25	3.08	Constant	0.016369			
15	4300	3	4.05	Std Err of Y Est	0.158627			
16	5300	3.55	5.51	R Squared	0.997439			
17	6300	4.3	6	No. of Observations	19			
18	7300	4.9	6.97	Degrees of Freedom	17			
19	8300	5.5	7.76					
20	9300	6.3	8.6	X Coefficient(s)	0.000944			
21				Std Err of Coef.	0.000012			
22								
23								
24								
25								
26								

Fig 3.3.12a. Needle Bar and Presser-Foot Transducers Response Static Calibration



Dead -Weight method
 Red=Needle Bar and Green=Presser-Foot Bar transducers

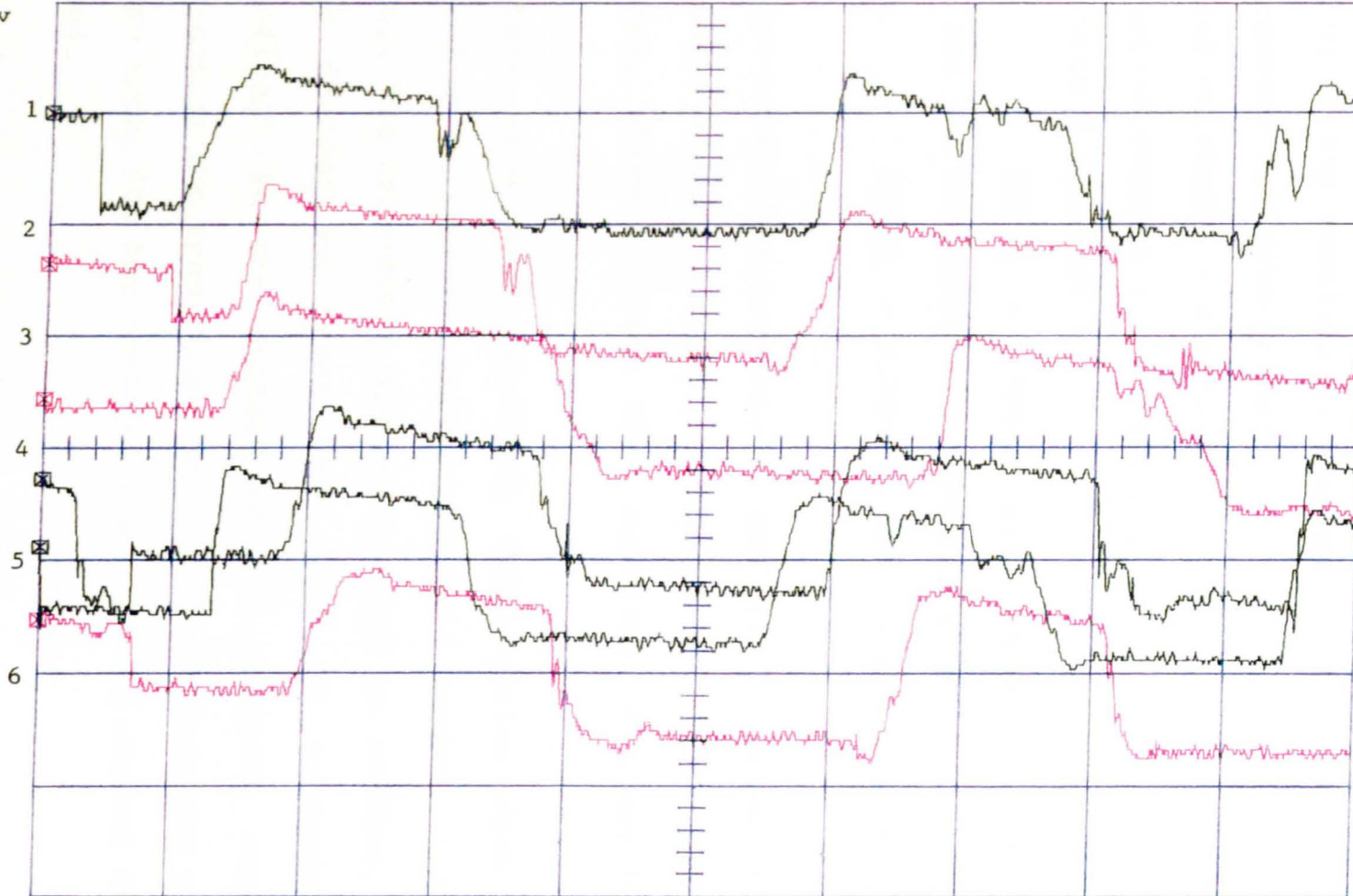
Equations:					
1.[A v. B] - Load v. Voltage (Needle Bar Transducer):	$Y_n = 0.00067 X + 0.037733$				
2.[A v. C] - Load v. Voltage (Presser-Foot Transducer):	$Y_{pf} = 0.000944 X + 0.016369$				

Pfaff 563

PRESSER FOOT TRANSDUCER'S RESPONSE
Calibration (50g load)

- filter off
- channel 2
- long
- Scale :
S=1:00E

0.1V/div



0.5 sec/div

AVE 0.104 Volt

Fig. 3.3.13. Presser-foot transducer's calibration response traces.

The results of the calibration responses of the transducer to Load are presented in the Worksheet Fig. 3.3.12 inset as Fig. 3.3.12a and the presser-foot response traces in Fig. 3.3.13 on a separate page.

According to the statistical analysis in Figs 3.3.12 the least squares analysis gives:

$$Y(n) = 0.00067X + 0.037733 \dots\dots\dots[1]$$

$$Y(pf) = 0.000944X + 0.016369 \dots\dots\dots[2]$$

- with R Squared:

$$RS(n) = 0.999313 \text{ and } RS(pf) = 0.997439,$$

- and the Std Error of X Coefficient:

$$SE(n) = 4.3E-06 \text{ and } E(pf) = 1.2E-07,$$

where:

$Y(n)$ =needle bar regression and $Y(pf)$ =presser-foot.

The signals of both transducers conform with their voltage responses, which is seen when plotting on logarithmic scales.

There were some practical difficulties with the presser-foot calibration using very small weights (1,2 and 5 grams). The transducer did not respond to loading, and it was decided to treat this lack of response as insignificant in the context of the specific working conditions of the transducer, which was continuously under pressure from its bar spring (from a few to several dozen Newtons).

3.3.7.2. The static and dynamic calibration of the thread transducer.

A schematic diagram of the transducer is presented in Fig. 3.3.05. Because the computer was arranged to capture data only when the sewing machine was running, a two-stage calibration process was required. In the first, static stage, the thread tension transducer was calibrated using deadweights attached to a strong, low extensibility sewing thread threaded through the normal thread path. The weights, in the range 1-198 cN, were attached to the thread under the machine table. The tension readings were recorded as transducer output voltages on oscilloscope.

In the second, dynamic stage, the sewing machine was operated at different speeds across the full range of speeds. Data values (dp) acquired by the A/D converter were calibrated against oscilloscope readings taken at the same time. These were used in turn to calibrate the A/D readings directly into cN, using the static calibration obtained previously. The same sewing machine settings, fabric and sewing thread were used throughout the whole process. At each stage, the calibration relationship were calculated from the averages of 10 readings using the DADiSP(V3.0) Linreg2 software. The results shown in Fig. 3.3.14, windows W3, W9 and W15.

Before the calibration of the transducer, the thread tensioning device had to be calibrated using the J&P Coats tensionmeter, which underwent its own separate calibration/control.

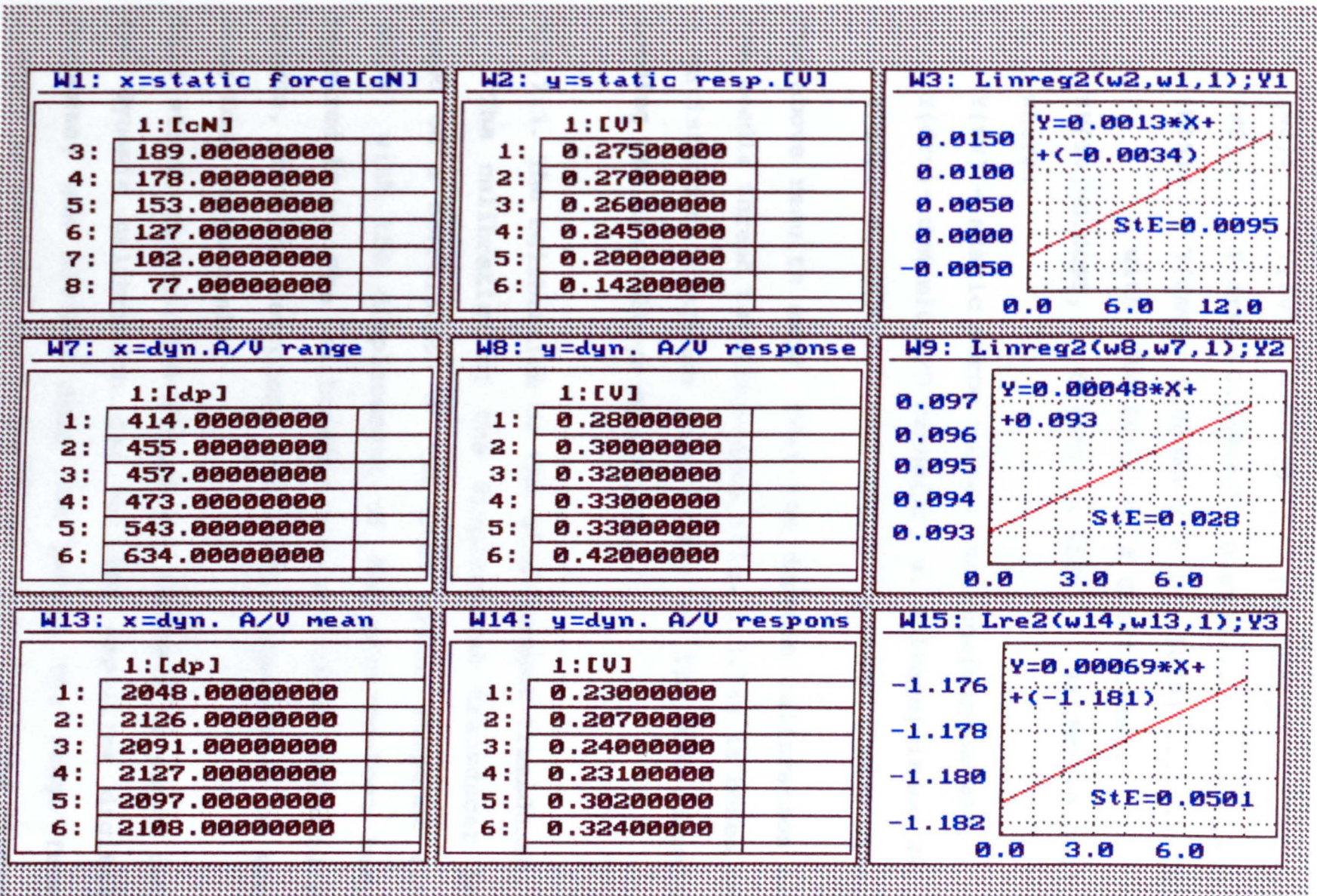


Fig. 3.3.14. The Needle Thread transducer's static and dynamic calibration (at speed levels 1-9).

The regression equations for the calibration in terms of force versus voltage are:

$$(W3): \quad Y(fv) = 0.00130 \quad X + (-0.0034) \dots \dots \dots [3]$$

$$(W9): \quad Y(drv) = 0.00048 \quad X + 0.0930 \dots \dots \dots [4]$$

$$(W15): \quad Y(dmv) = 0.00069 \quad X + (-1.1810) \dots \dots \dots [5]$$

with Std Error of X Coefficient:

$$SE(1v) = 0.0095, \quad SE(drv) = 0.0280, \quad SE(dmv) = 0.0501,$$

where:

$Y(fv)$ - static force versus voltage (window W3),

$Y(drv)$ - dynamic A/D range (dr) v. voltage (window W9),

$Y(dmv)$ - dynamic A/D mean (dm) v. voltage (window W15),

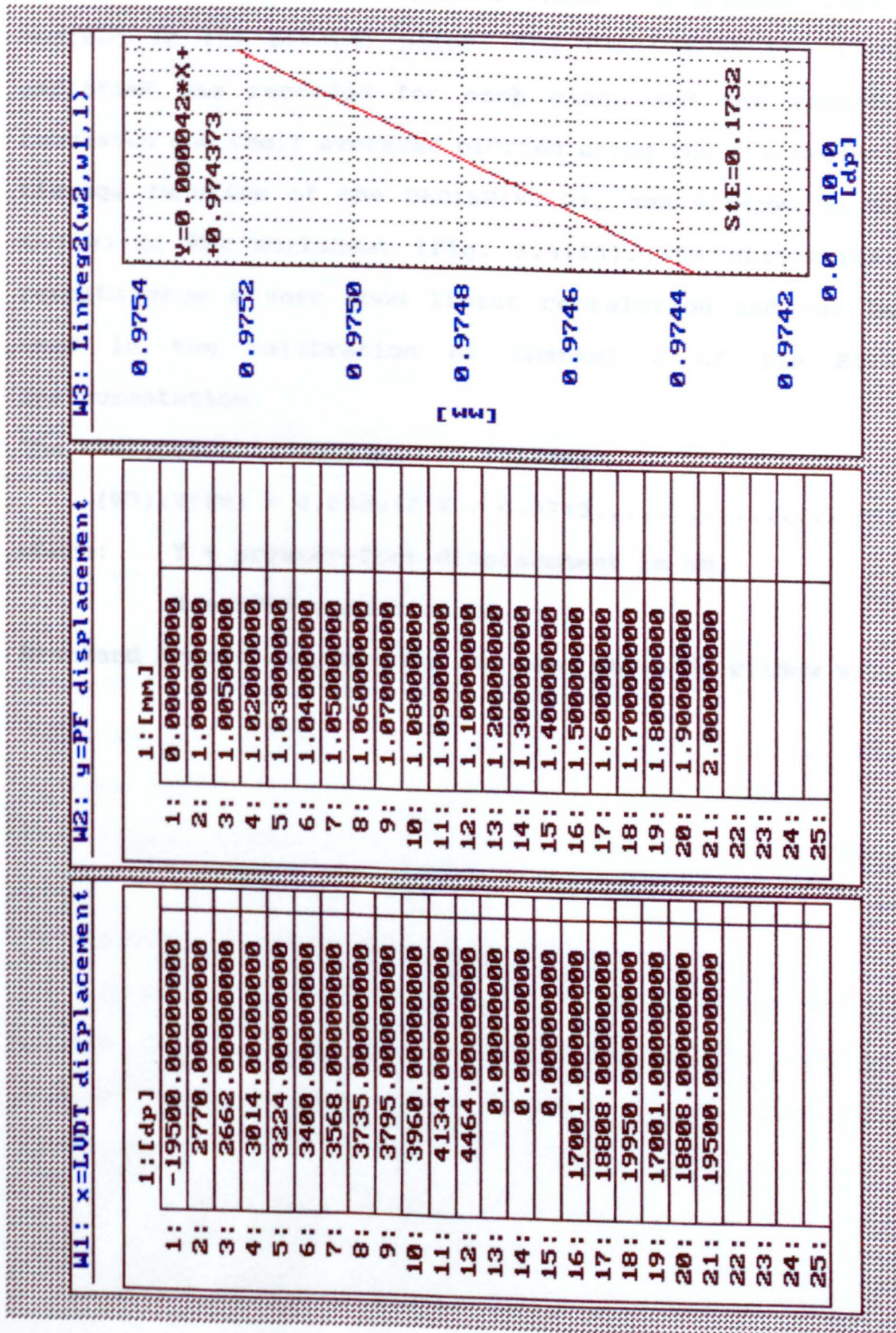
The above results show that the dynamic calibration of the needle thread tension signal (Fig. 3.3.14) is based on a satisfactory response correlation of the A/D signals loading and its voltage equivalents.

3.3.7.3. The calibration of the displacement transducer.

The calibration of the displacement transducer is based on a correlation of the LVDT signal response (in volts) with the displacement of the presser-foot bar, measured in mm. The calibration was carried out using slip gauges, from the Metrology Calibration Laboratory of the Hong Kong Polytechnic.

This static calibration (there was no need to carry out the dynamic calibration due to LVDT amplifier digital response) was divided into two parts, the range from 1.005-1.09 mm, and the range from: 1.0-2.0 mm (the gauges 1.2 mm; 1.3 mm and 1.4 mm were not available).

Fig. 3.3.15. Presser-foot displacement transducer's calibration.



A special metal bridge (a beam of size 12x5x50 mm) with a very smooth surface was placed under the presser foot, centred at its pivotal point. The reading of the LVDT amplifier was recorded for each gauge and the results tabulated and their averages plotted using the statistical Linreg2 function of the DADiSP(V3.0), see windows W1,W2 and W3 of the Worksheet (Fig. 3.3.15). The statistical results show a very good linear correlation and can be used in the calibration of channel 2 of the RSTM instrumentation.

The regression formula was as follows:

$$(W3):Y(fv) = 0.000042 X + 0.9743.....[6]$$

where: Y = presser-foot displacement in mm,

X = LVDT output in dp,

Standard Error: StE=0.1732 (is also shown in window W3).

3.4. The RSTM data acquisition system.

A system of acquiring analog signals in real time depends on the selected hardware and adequate sensing devices, matching the application needs. After acquiring the above components and having the object to be investigated instrumented properly, the next step is the development of a specialised program usually based on a compilation of commercial software and library subroutines. This way of development can be very complicated and is not speedy, requiring thorough testing. Subroutine libraries frequently lack the flexibility required by different applications, and sometimes in the final trials a particular subroutine may have to be abandoned. This risk can be reduced by selecting matched software and hardware from reliable manufacturers who provide rapid technical support. In this project Data Translation hardware and software were chosen as they proved to be the most suitable for the purpose of the research.

In this chapter the design, assembly and experimental trials in the development of the sewability testing station, are outlined and supported by illustrative examples.

3.4.1. The circuitry of the system.

The experimental testing station set-up was shown in section 3.2.1 of this chapter. The components of the acquisition system are shown in Fig. 3.4.01. The block-schematic diagram of the system circuitry outlines the main processing paths from the analog input into the four acquisition channels (ch0, ch1, ch2 and ch3), for processing of the NTt, PFd, PFp and NPF signals respectively. The technical characteristics of the main boards were presented in section 3.2.3. More detailed block-diagrams of the data acquisition paths are included in Appendix XII. The DT2841-L signal acquisition board is equipped with only 4 A/D input ports and 2 D/A output ports. The purpose made switches S1 and S2 connect time signals Timer1 and Timer2 as shown. The switches allow connection of Timer1 or Timer2 into different channels as needed. The switches were located on the main connecting DT707 board. The Screw Terminal Panel on the connecting board accommodates most user connections of the DT2841 Series. Screw connections are labelled for analog input connection, digital I/O lines, and external trigger input. In addition, blank circuit pads are provided for user supplied shunts to accommodate 0 to 20mA current inputs, although they were not used in the RSTM design. The above panel contains an attached one meter long flat ribbon cable, which plugs directly into the DT2841-L board's connector slot.

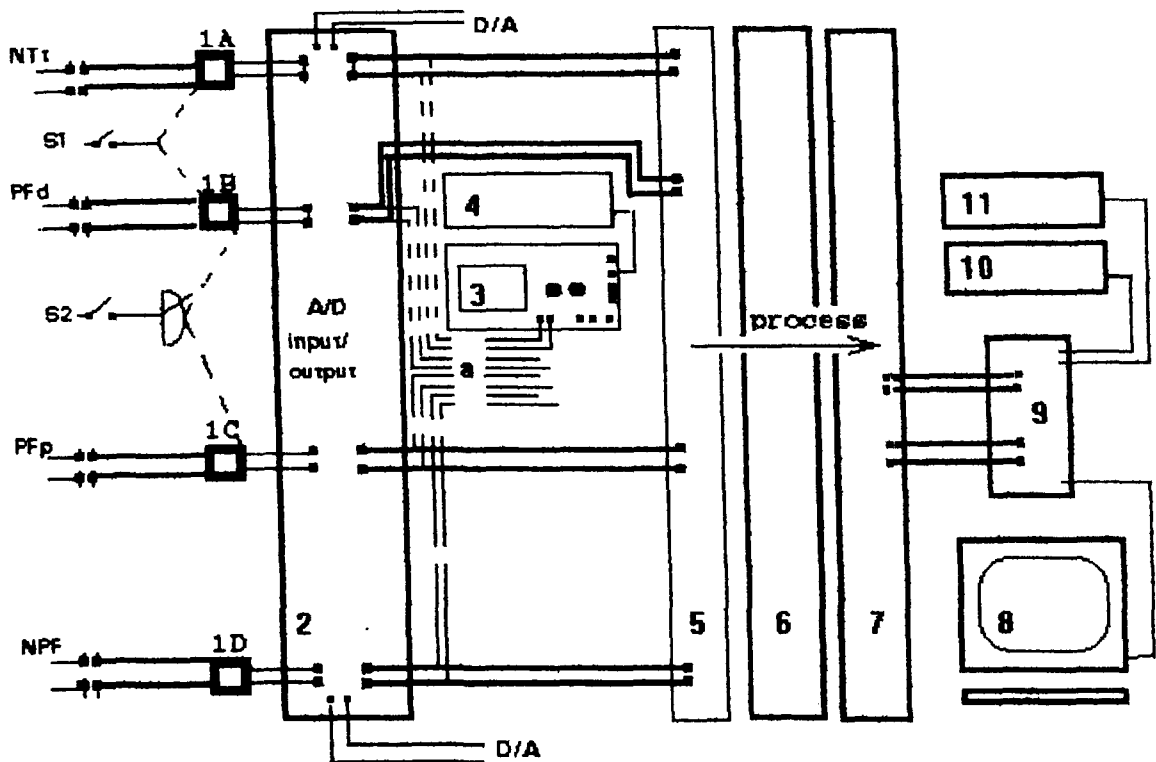


Fig. 3.4.01. Schematic diagram of the circuitry of the system.

[Legend: NTt, PFd, PFp, NPF—the RSTM analog signals; S1—QR's square wave clock signal switch; S2—proximity switch time signal; a—connecting panel; A/D and D/A input/output ports; 1A, 1B, 1C, 1D—signal amplifiers; 2—DT707 connecting board; 3—Oscope; 4—Oscope plotter; 5—DT Connect; 6—DT2841-L board; 7—DT7020 FPAP board; 8—PC/VGA monitor; 9—CPU AT/386; 10—printer and 11—plotter].

The role of the Oscilloscope is an auxiliary one. It was used for signal recognition, calibration and analysis during the development of the system with input/output signals connected through or without the connecting panel marked as "a" on the diagram. However, due to the need for

future maintenance and recalibration, its role is indispensable.

The two D/A output channels were not used in the RSTM set-up, although they were reserved for possible future expansion of the RSTM, should further research allow the self-adjustment of two parameters of machine settings. Sewing thread tension and presser-foot pressure would be the most probable choices for the self-adjustment. Feedback would come from the expert system built-into the RSTM and the Seam Pucker Measurement System (SPMS). The following amplifiers were used:

- channel 0: the dynamical DMA Kyowa amplifier. The maximum bandwidth of the signal was 5kHz. It also had a zero-balance feature built into it, as well as a signal input filter (4-point scale, from 30Hz to 1kHz).

- channel 1: the RDP type 505 amplifier, of max frequency of 300Hz.

- channels 2 and 3: Kistler charge amplifiers with a filtering range from 30Hz to 30kHz. The technical details were included in the previous Section 3.2.5.

The description of the other boards was provided in Section 3.2.3.

3.4.2. DAP software programme of A/D signal.

The aims of the RSTM design detailed in the specification requirements (section 3.4.2.2 below), required the programme to have the flexibility to:

- be used in routine testing for comparing fabric and

thread with respect to their sewability, with filtering of the signals where needed to provide clear traces and statistical results only (see Fig. 3.4.05 and

- to provide a wide range of signal manipulation, mathematical and statistical analysis utilities.

3.4.2.1. Hardware and software requirements for DAP.

In addition to the above hardware, building the DAP (Data Acquisition Programme) required the following software:

- MACH digital signal processing, DSP Subroutine Library SP0605. The library of subroutines was PC/AT and PC-DOS compatible,

- MACH SP0604 Vector subroutine library, supporting array processing with the DT7020 Floating-Point Array Processor (FPAP) connected to a DT-Connect,

- Microsoft, Programming C Language version 5.1.

- DOS 3.3.

The DT7020 FPAP configuration file APCONFIG.DAT contained the following parameters needed to run the program.

```
-apbase    c00000
-apport    250
-timeout   30
-mload     \DT7020\APJUMP.APB
-mload     \DT7020\APMICI.APB
-vload     \DT7020\CONTROLI.VIB
```

The DT2841-L required a DT707 connected to the user interface. Differential input was accomplished on the

DT707 by installing eight 10 kilohm resistors at specified locations.

The DEVICE driver MACH41.SYS was configured as follows using MSETUP.EXE:

```

-board name:          -DT2841-L
-board address:       -2E0
-interrupt level:     -7
-A/D channels:        -4
-channel configuration: differential
-encoding:            -TWO's COMPLIMENT
-polarity:            -BIPOLAR
-sign extension:      -NO SIGN EXTENDED

```

All jumpered selectable parameters were jumpered according to this configuration.

3.4.2.2. The characteristics required by DAP software.

The main purpose of the acquisition system was to acquire the signals coming from the four transducers of the sewing machine. The hardware and software characteristics of DAP software have already been described in the previous sections of this chapter. Other programme characteristics were specified in the RSTM design and are outlined below:

- a. The DAP had to be menu-driven, allowing the staff and other researchers from the Polytechnic to utilise the RSTM.
- b. The DAP had to be linked to other software (in the C Language environment), including the following:
 - MACH SP0604 and SP0605 libraries,
 - Microsoft C Compiler Version 5.1,

- MS DOS 3.3,
- Graphics C,
- Data Translation testing and calibration programmes for the control and maintenance of the boards,
- control software for the hard disk,

c. the file structure had to have the capability of being edited by the main software editors.

d. a mouse had to be installed,

e. the data files coding system (see section 3.4.5.4) and structure, had to provide and be able to store the following principal and auxiliary information:

- the test result reports in a descriptive and graphical form,
- the test results from the testing of fabric and sewing thread properties,
- the parameters of the sewing process,
- the maintenance and calibration procedures,
- the storage of subsequent maintenance and calibration controls,

f. the capability of retrieving and converting past tests into the current DAP configuration. This feature was important owing to changes in configuration files caused by modifications or re-calibrations in the course of the operation of the system. This feature was especially useful in comparing tests carried out under different conditions,

g. the retrieval capabilities had to make it possible for

the test results to be subjected to further analysis such as:

- statistical analysis, Fourier Transforms, Peak Analysis,
- stretching, compressing and overplotting the signals,
- signals recall : all signals, a complete single or part of it (in graph or table form), with the relevant data.

f. The programme had to have back-up facilities, a storage system for archive files and a security (password) system. The above set of requirements was included in the RSTM specification and provided the foundation for the development of the project.

3.4.3. The programme of the DAP operation system.

The programme acquires up to 640K data samples from the four channels of a DT2841-L board. The samples are stored in a large array on board the DT7020. When a specified amount of data has been transferred, a large array of A/D values is sorted by channel and scaled to calibrated values.

The programme compiler command [include] defines input/output (I/O) operations in the initial stage, and the command [define] selects constants [NOLOOP], [BURST_MODE] or/and [CONT_MODE], as well as the clock signal [CLOCK_OL] 'Burst mode'. The length of the input and output buffer constants is defined by macros [IBLEN],

[OBLLEN] and [VBUSSIZ]. The FPAP DT7020's double buffered asynchronous I/O memory is confined to one 64K sample block (256K bytes of RAM) onboard the FPAP, owing to the limitation imposed by the system microcode that:

[2*(input buffer length + output buffer length), had to be less than 64K. If this limit is exceeded, input and output buffers will overlap. To prevent this, the [define BUFF_FULL] command is used to flag a buffer full condition. This signal allows the number of 64K data blocks transferred to the FPAP by the DT2841 to be counted. In the next stage of the program, data types and global variable declarations are defined for use in [READ_CONF]. A number of further macros are defined during the next stage of the operation of the DAP.

It is also worth noting the possibility of linking the other analytical software DADiSP (data acquisition and signal processing) to this programme by means of filling the special reference header, which is permanently attached to numerical four-column data, 8192 rows long, and can be used in Programme V (see Fig. 3.4.02). The subsequent series of data acquisition operations cannot be described in detail owing to their length. The full DAP C. programme capacity is 76kB. More details are given in Appendix II. Finally, the RSTM system's flexibility should be emphasised, as it provides many useful post data acquisition facilities.

Figures given in this section provide an illustration of the system menus and of the RSTM set-up.

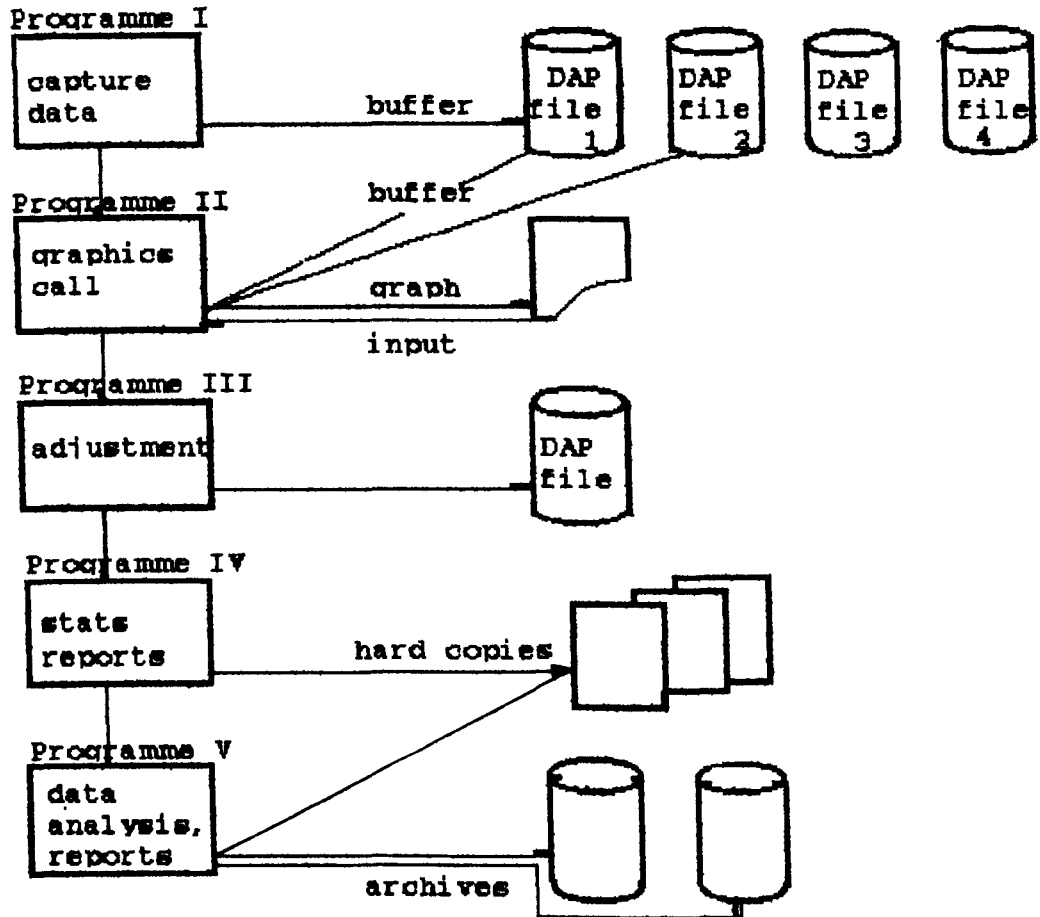


Fig. 3.4.02. Flow block diagram of the DAP program.

3.4.4. An overview of the RSTM system.

As has already been mentioned, the ETS was renamed the RSTM. Therefore in the next chapters the designation of tests will start with RSTM preceding the test code eg. RSTM/0027R307, as is presented in Figs. 3.4.7-12.



Fig. 3.4.03. The view of the RSTM setup.
(The description of the numbered equipment is in the text).

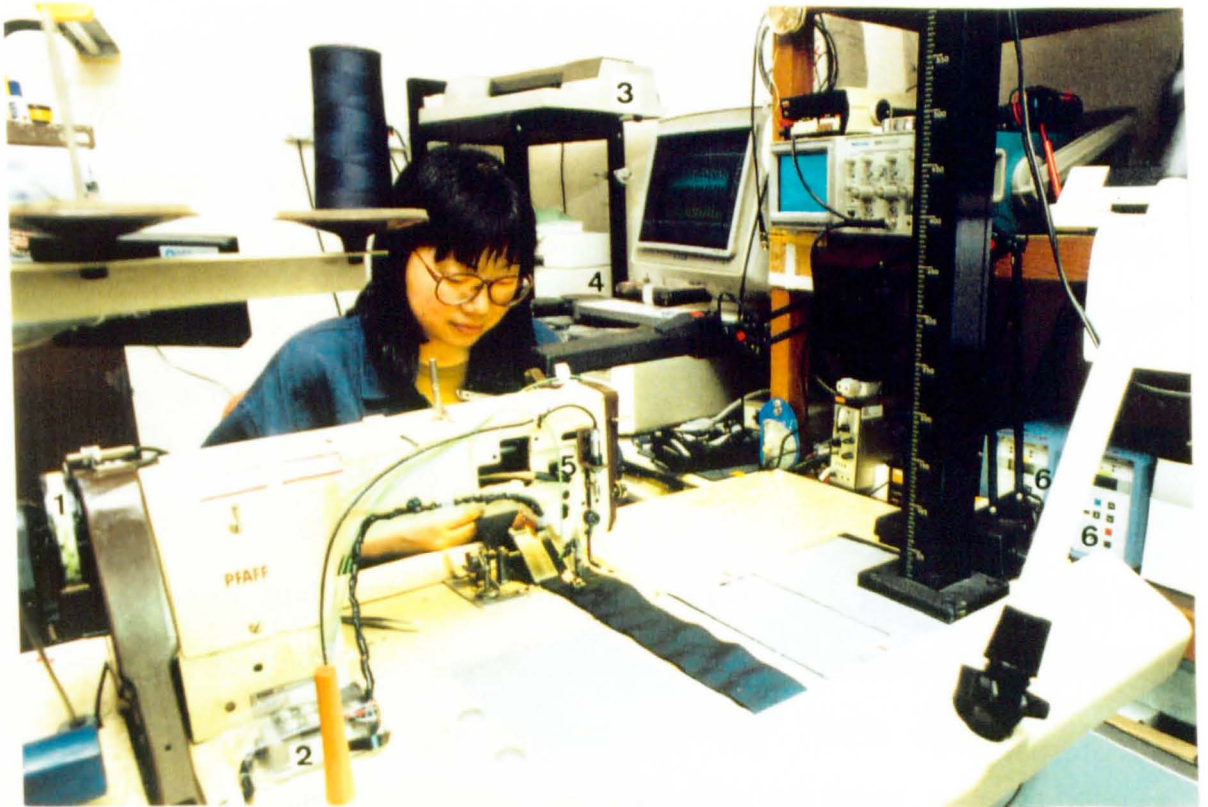


Fig. 3.4.04. Testing in progress...

Fig. 3.4.03 shows a general view of the system. The photograph was taken at location where experiments were conducted. Artificial light and airconditioning were provided. In the centre is an instrumented lock-stitch Pfaff-563 sewing machine. The item marked number 1 is the CPU unit of the Everex PC/AT-386, where the hard boards of the data acquisition are inserted. Item 2 is the VGA monitor of the PC/AT 386, item 3 the digital oscilloscope. Items 4-6 are amplifiers A1,A2,A3 and A4; item 7 is a special fabric feeding device with the ability to apply pressure to the bottom layer of the fabric and consequently to increase the friction of the bottom layer against the machine table, this slows down the advancement of the bottom layer, minimising pucker. The feeder also has a calibrated spring and adjustable metal flap, which slides on the surface of the fabric layer. The NTT transducer is item 8 in the picture and item 9 is the Quick-Rotan Control Box. The last item, marked 10 on the picture, is the Timer2 proximity-switch device. Fig. 3.4.04 shows a technician testing fabric seam performance according to RSTM procedure. The items are marked as follows: (1) Timer2, (2) NTT transducer's Kyowa Bridge; (3)plotter, and (4) printer. On the back side of the machine the PFD LVDT type transducer (5) is linked to the presser-foot bar by means of a special bracket. Kistler's charge amplifiers are marked as (6). The fabric is fed through the fabric feeder marked (7) in Fig. 3.4.03 above.

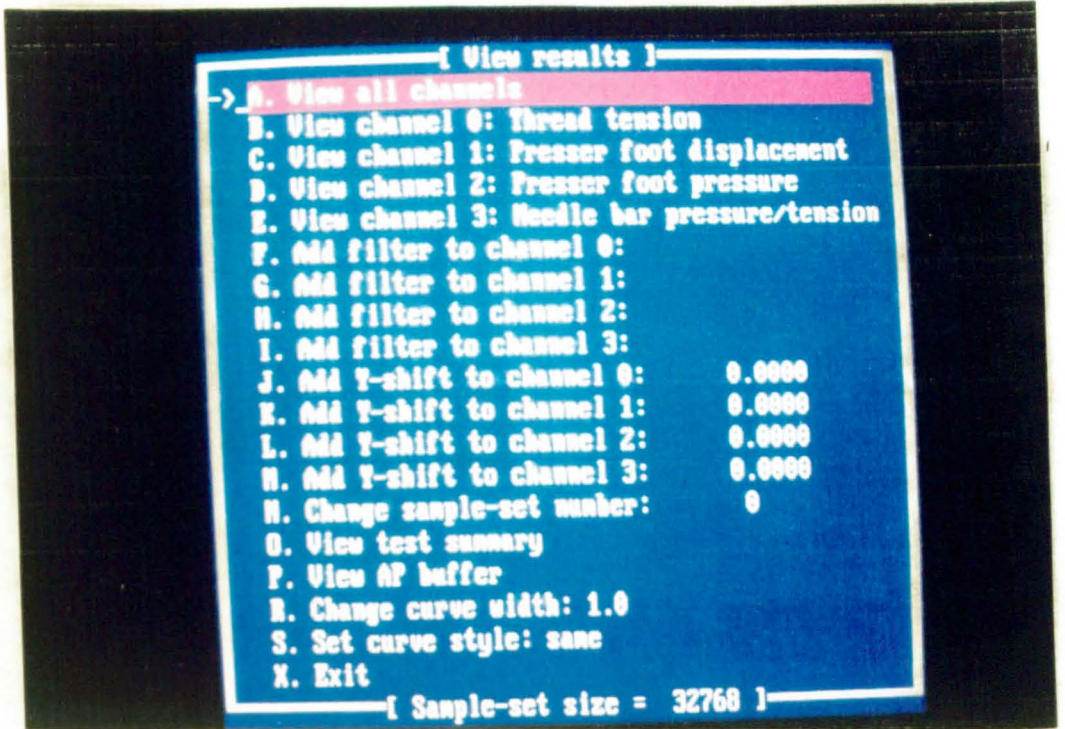


Fig. 3.4.05. The DAP "View results" menu.

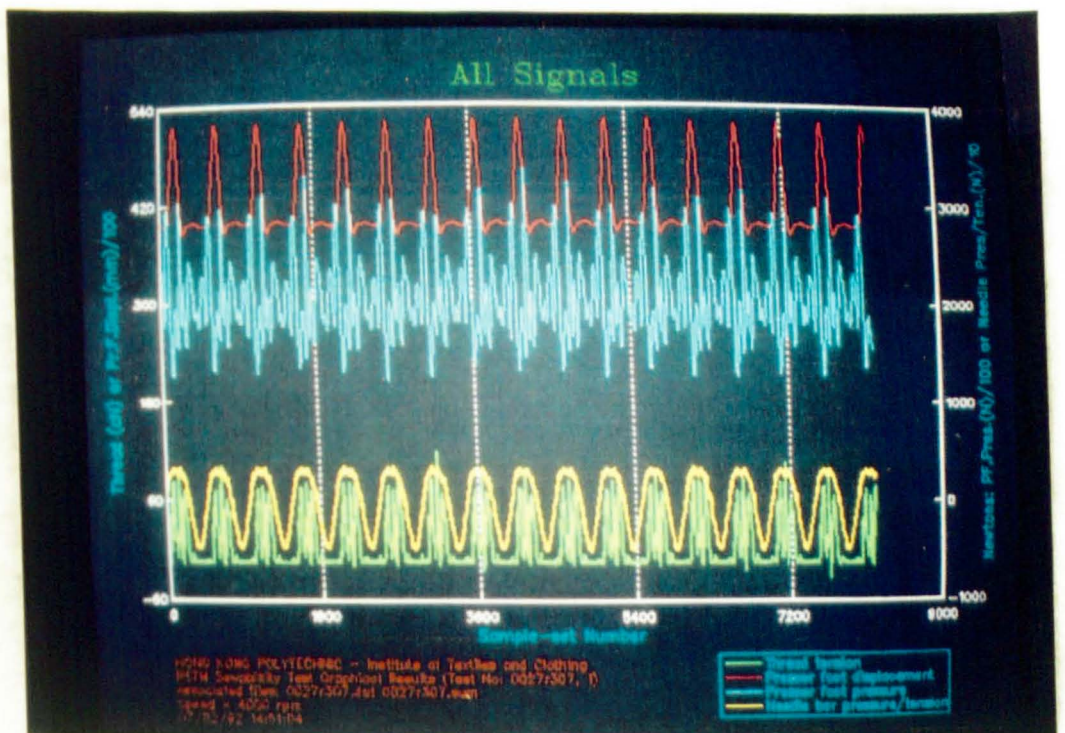


Fig. 3.4.06. The view of the DAP window "All signals".

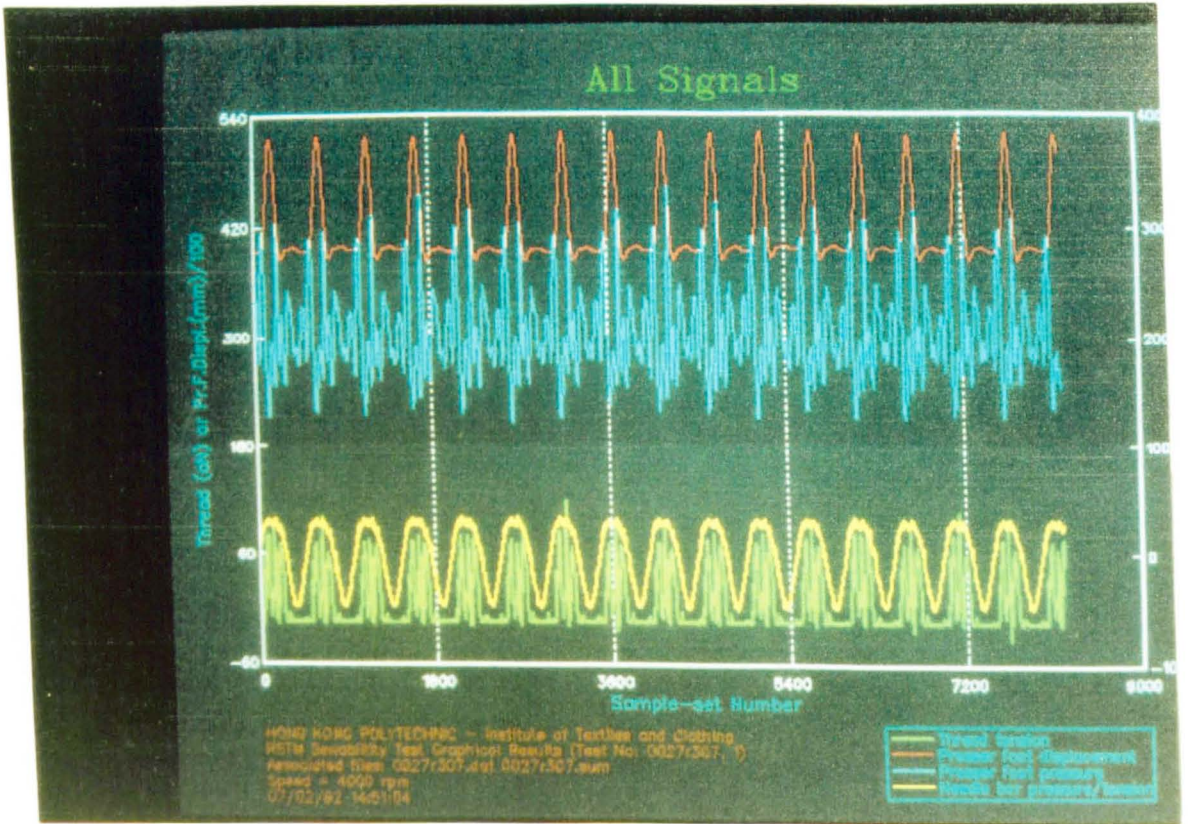
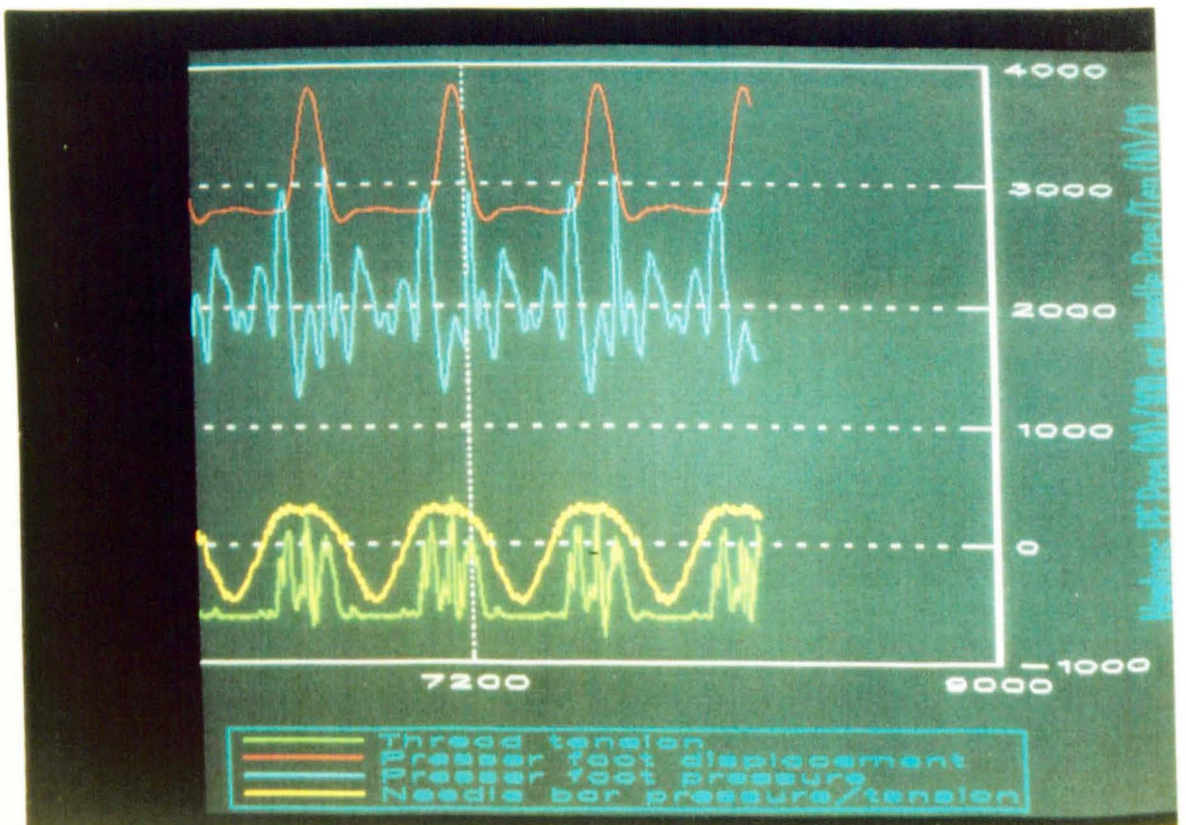


Fig. 3.4.07. Photo of the screen graph with "All signals" results of the test no 0027R307.dat.

Fig. 3.4.08. Photo of the screen graph of the all signals results in the expanded version.



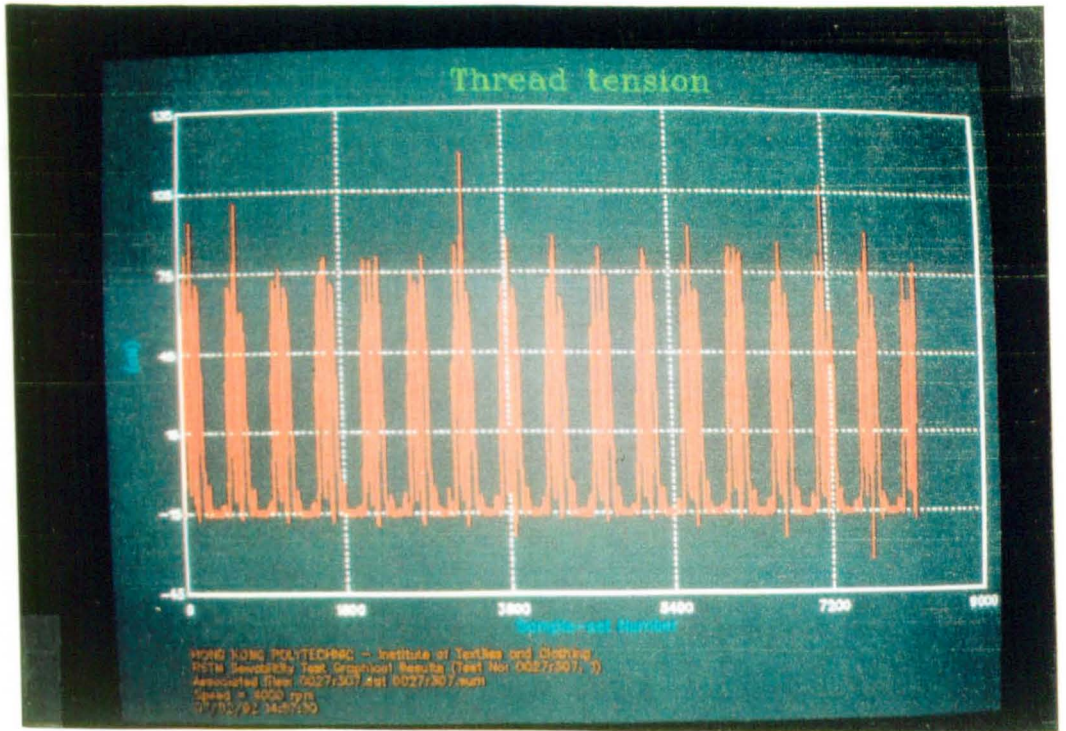


Fig.3.4.09. Photo of a single channel NTt signal of the test 0027R307.

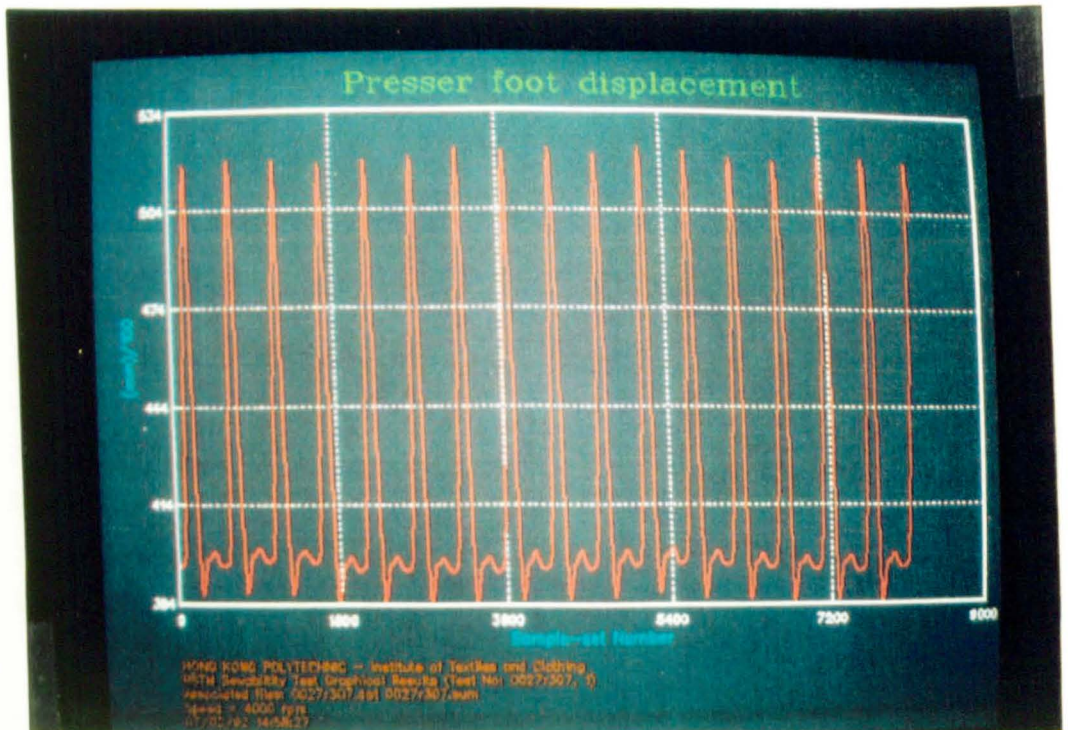


Fig. 3.4.10. Screen photo of the Presser-foot displacement(PFd) signal.

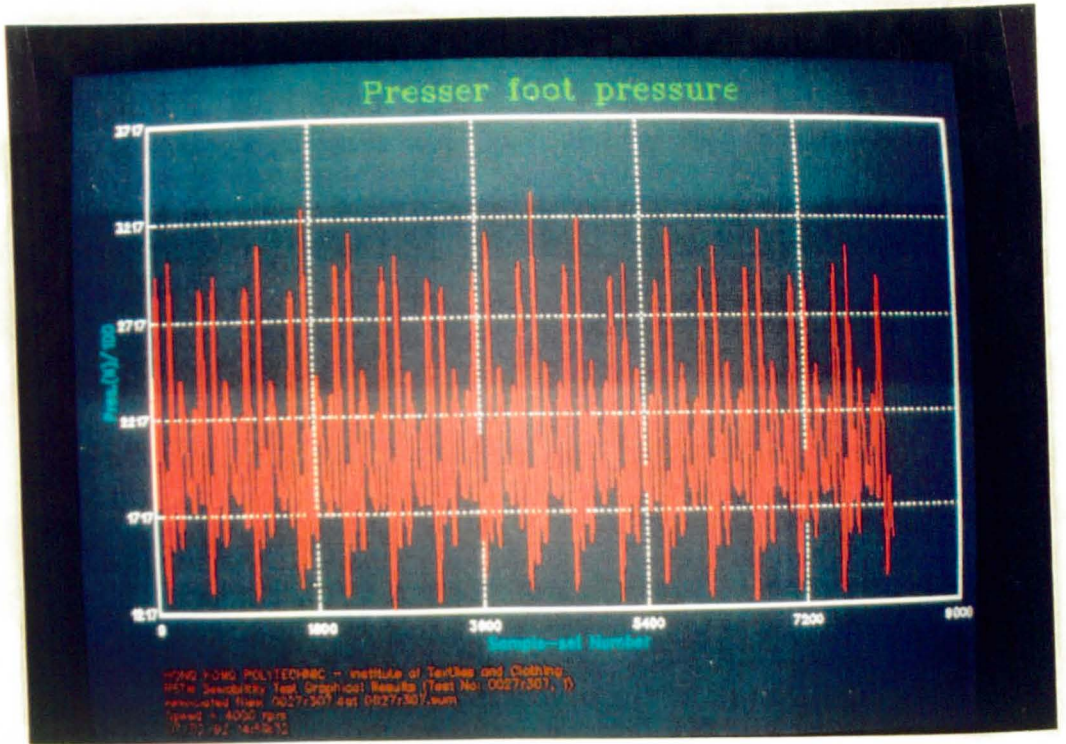


Fig. 3.4.11. The presser-foot pressure(PFp) signal of the test no 0027R307.

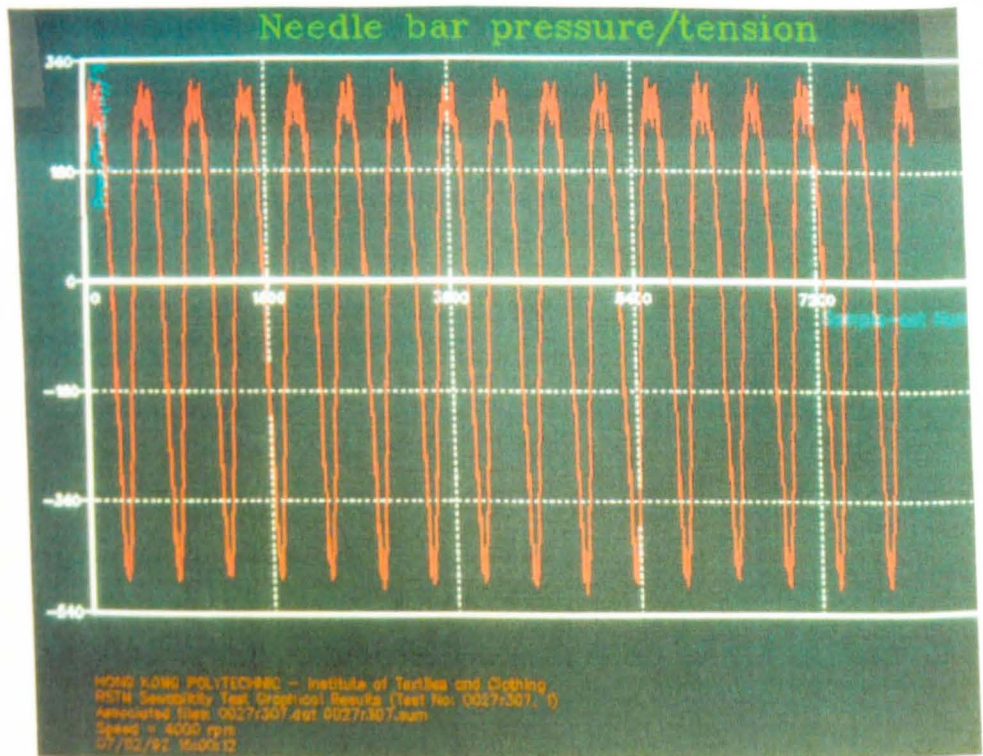


Fig. 3.4 12. The screen graph of the needle penetration force(NPF) signal of the test no 0027R307.dat.

3.4.4.1. DAP capabilities and menus.

The second RSTM/DAP "View Results" menu (Fig. 3.4.04) includes 20 features of the system available for post-acquisition data manipulation. In the bottom part of the menu a useful control feature can be seen "Sample-set size", which confirms the volume of data contained in the acquisition buffers. The acceptable value is 32K. This example, with an extract of the data stored in the buffer, is contained in Appendix I. An important feature also is the ability to view the AP buffer ASCII numerical data (such as the 4-column table, preceded by the DADiSP reference header), which is shown in Appendix I. Single rows of data can be called-up, which is useful for comparing the intersections of the signals. The shifting and filtering functions of the signals (Window; F-M below) widen the range of capabilities of the RSTM system analysis.

The DAP opening menu contains the following features:

- "A. Sewing station setup:
- B. Sewing machine & digital motor settings:
- C. Strain-amplifier settings:
- D. LVDT-amplifier settings:
- E. Charge-amplifier 1 setting:
- F. Charge-amplifier 2 settings:
- G. Presser-foot displacement:
- H. Seam pucker:
- I. View characteristic file:
- J. Save template:
- K. Load template:
- X. EXIT)".

The DAP sub-menu 1: "A. Save all,
B. Save summary,
C. Save data,
D. Print summary,
E. Exit".

The DAP sub-menu 2:
"A. Design digital filter,
B. Select video and
plotter drivers,
C. Set plotter pen's colour,
D. Exit".

The Graphical version of the RSTM report is presented in Fig. 3.4.06. The "All Signals" screen graph is a frame of X and double Y axis, divided into 5 columns and 5 rows. The vertical axis represents 9000 data points (dp) with up to 2000 dp per channel (1000 dp/volt; 5 V is max input of DT2841 board). During acquisition of signal data the buffer is filled from the top to bottom and the graph from left to right. Signals are sampled in the form of a large array, which is then separated by channel in the following sequence starting at (addr_vbuff):

ch0 ch1 ch2 ch3 ch0 ch1 ch2 ch3 ch0...ch0 ch1 ch2...,

The right Y-axis shows the NPF (needle) and PFp (presser foot) forces calibrated in Newtons. The left Y-axis shows NTt (thread tension) PFd (presser foot displacement) in [mm] (see RSTM-DAP.CFG file Appendix IIIa). The legend template contains the name of the institution, the name of the test, the test code name, associated codes of files and the date of testing. The box in the bottom right

allows the signals to be distinguished by colour. The full length of the signal is 8192 data points along the X-axis. The signals may overlap and therefore the colour differentiation is a very useful feature. The RSTM hard copy report can be provided in colour as well as in black and white.

3.4.4.2 The RSTM file coding system.

The requirements of the system had to match the computer-based processing of information and the file name had to be of 8-digits and contain the optimum amount of easily recognisable information on the test characteristics. The file name length of 8 digits is also compatible with other processing software such as Lotus 123, Version R3.1; SPSSPC, Advanced Statistics, Ver.4.0; DADiSP, Ver.2.0B and subsequent versions DAP_RSTM; Statistical package MATLAB; and SP. For example:

/ Q 1 7 3 3 4 0 9 would be an acceptable file name,

where:

- digit1 =fabric type,
- digit2 =experiment type,
- digit3 =stitch density scale,
- digit4 =presser-foot pressure,
- digit5 =types of sewing thread,
- digit6 =thread tension,
- digit8 = sewing speed in rpm.

Note:

Each of the above digits allows the value of a particular parameter to be specified. Details are described in Appendix III. Should the parameters be outside the range

of this eight digit coding system, they could be described in words, for example in the DAP pre-setting comments in the Header.

3.4.5. The RSTM Reports.

In the requirements of the RSTM specification, the system was to provide hard copies of the test results. This requirement was accomplished by designing the reporting function as follows:

- graphical results, plotted in black and white or in colour hard copies, in the form described in the previous section,
 - descriptive reports, where the test settings and tested parameters were included with their statistical evaluation, see example in Table 3.4.01.
- An example of the buffer data is presented in Appendix I.

A report could immediately be printed or plotted as hard copy, left in a hard disk, or stored on a floppy diskette as an archive file. The retrieval capability (the past configuration files of the system could be used for data retrieval) allowed the previously tested data to be investigated and it could be analyzed simultaneously with new data. A RSTM full report, could include five copies of the graphs (an "all signals" graph plus a "single signal" (graphical version)). As can be seen below, the written part of an RSTM testing report consists of two parts: Part I, test settings and Part II, the test results.

Table 3.4.01. RSTM Testing Report. Example. (Page1)

**"HONG KONG POLYTECHNIC INSTITUTE OF TEXTILES AND
CLOTHING
RSTM SEWABILITY TESTING RESULTS
PART I: TEST SETUP
Test number (XXXXXX): Q1743509**

A. Sewing station setup.

Trial Number (1-10): 4
 Date: 09/29/92 User name: Agnes Kwok
 Test details:
 Number of fabric plies (1-10): 2
 - Fabric type of ply #1: q
 - Fabric type of ply #2: q
 Thread types: 1 *1 means needle & bobbin
 -top type: 3 are of the same type,
 -bottom type: 3
 Needle type: 0* * 0 means Rhein-Nadel,
 size 100
 Throat plate type: t t " experimental
 unit,
 Feed dog type: f f " "
 Presser foot type: p p " "

B. Sewing machine & digital motor settings.

(Based on the lock-stitch single-needle sewing machine Pfaff 563). Test developed in 1991 and modified by* in 30 of September 1992. (* Author)
 Speed [rpm]: 5500
 Stitch density [stitches/10cm]:7
 (32 stitches/10cm)
 Seam type (A/B/Manual): A *QR's
 settings
 - Number of pre-set stitches: 30
 - Needle position [Program code]: 345 *QR's
 settings

C. Strain-amplifier settings :

Thread tension signal NTT.
 Range [x100 $\mu\epsilon$]: 1
 Cutoff frequency [Hz]: f
 *(filter off)
 Thread angle scale (1/2/3): 2
 *(C2Ph)

D. LVDT-amplifier settings:

Presser-foot signal Pfp.
 High set point: 19500.00
 Low set point: -19500.00

E + F. Charge amplifiers' settings (in original copy).

G. Data acquisition settings.

Sampling rate [Hz]: 183333
 Number of 16k sample-sets: 2
 Total number of samples: 131072

PART II: DYNAMICAL RESULTS**1. Statistical results:****a. Thread tension:**

- maximum [cN]: 212.54
 - minimum [cN]: -18.01
 - mean [cN]: 33.11
 - standard deviation: 28.41
 - coefficient of variation [%]: 85.79

b. Presser foot displacement:

- maximum [mm]: 3.98
 - minimum [mm]: 2.33
 - rise [mm]: 1.65
 - standard deviation: 0.44
 - coefficient of variation [%]: 4.64

c. Presser foot pressure:

- maximum [N]: 40.95
 - minimum [N]: 4.23
 - mean [N]: 20.24
 - standard deviation: 8.20
 - coefficient of variation [%]: 40.51

d. Needle bar pressure:

- maximum [N]: 64.70
 - mean [N]: 41.68
 - standard deviation: 17.98
 - coefficient of variation [%]: 43.14

e. Needle bar tension:

- maximum [N]: 108.60 *(withdrawal + transducer
 - mean [N]: 56.69 wire bending forces),
 - standard deviation: 30.76
 - coefficient of variation [%]: 54.25

J. Seam pucker.

a. Seam pucker index (SPMS method°): 3.07

3.4.6. Maintenance of the system.

The system, when in operation for more than an initial 40 hours, has to be checked according to the procedures outlined in the Maintenance Manual written by the author and are included in Appendix IIIb.

The RSTM system as a whole depends basically on the reliability of the transducers. Although the instrumentation of the machine consists of many components, which are of the highest quality, the possibility of the transducer becoming "out of control" due to an operational fault or fatigue cannot be entirely excluded. It is therefore worth examining certain factors which could contribute towards such a malfunctioning. In an extreme case of a sewing speed of 5500rpm, the needle also makes an equivalent number of reciprocal movements with a stroke of 35 mm and the same number of reciprocal cycles are attributed to the needle transducer. The Total length of the path of the transducer is $3.5 \text{ cm} \times 5500 \text{ rpm} = 19\,250 \text{ cm}$ or 19.25 m per minute, with 5500 reversals of direction at the TDC and BDC points. This means that it has to acquire 8192 data points (from 16.3 cycles) during 0.18sec of acquisition time, without any acceleration and deceleration time included, with a precision of measurement expected to be in the order of 10^{-6} . Therefore steps should be taken to control the consistency of the transducer output by controlling the state of the circuit connectors, as potential causes of fatigue contributing to operational breakdown. These factors should be taken into consideration in the maintenance procedures. Moreover the serious effect of fatigue can be lessened when testing conditions are not of long, continuous runs and the needle bar is kept at the BDC during non-operation periods, when

the cable loop is at its lowest bending moment. The weakest point of the needle bar transducer is the transducer connecting cable, at the point of its insertion into the plug (there is no solid contact at the wire end). The oscillation (not always in-plane with the needle bar vertical movement), is very difficult to control. The forces on the cable (generated by the needle bar movement) can be minimised by means of a special configuration of the cable loop, though the optimum shape is difficult to obtain. Spiralling the cable into a series of loops is one of the options. However, it was decided to form the connecting cable into a single half-loop to keep its shape stable, so that the least amount of bending occurred at the transducer and two cable holders mounted on the machine body. This cable loop shown from two sides in Fig. 3.3.02 (front of the machine) and Fig. 3.3.03 (back of the machine,) caused the cable at the transducer to break on three occasions, necessitating replacement and re-calibration. Therefore, to prevent this from happening again, an extremely light (0.2g) flexible rubber sleeve, was mounted on the end of the connecting cable and inserted into the transducer's socket collar. This stiffened the part of the cable which was most subjected to bending. It may also be pointed out that a specific feature of the cable loop is that its shape affects the measured value of the needle bar penetration force, particularly during the upward movement of the transducer. The cable(wire) loop is compressed, which results in a

greater value of the withdrawal forces (tension) than that of the needle penetration forces. This will be more clearly seen in the later parts of the analysis of needle penetration forces.

This information may help to give an insight into the complexity of the problems related to the dynamic working conditions of transducers and their maintenance.

The presser-foot transducer does not suffer such extreme oscillations due to its smaller movement during sensing, and consequently, was proved more reliable. Its maintenance is described in Appendix IIIb and the calibration details were shown in Section 3.3.3 of this chapter.

The maintenance procedure of the thread transducer should include an analysis of the signal traces in the filtered and non-filtered mode. During the mounting of the transducer the signal showed an unexpected form of interference, whose source was difficult and time-consuming to locate. It was found that the screening of the wires of the transducer strain gauges was insufficient and that the interference came from the QR sewing machine motor. This was not anticipated as it was claimed that the motor had been fully screened. Therefore attention should be paid to this matter during maintenance.

Periodic calibration of the LVDT transducer should be carried out according to the instructions of the manufacturer and procedures described in Section 3.3.7.2.

Chapter 4. THE DEVELOPMENT OF THE PUCKER EVALUATION SYSTEM.

Since one of the underlying purposes of studying sewing machine dynamics is the reduction or elimination of seam pucker, it was decided to link the RSTM system to objective measurement of seam pucker severity. This would enable pucker severity to be related directly to sewing conditions. Therefore, an attempt was made in this project to develop an instrumented system able to evaluate pucker severity objectively.

4.1. Introduction.

Pucker as a "mechanical instability phenomenon" and as a "fabric garment defect" has already been described in the literature review. A considerable amount of work has already been done on the mechanisms of seam pucker, as well as on methods to prevent it. Hope for finding a speedy solution to the problem of pucker elimination or its reduction, through the design of fabrics without a tendency to pucker, arose when a series of studies started on the link between pucker occurrence and the evaluation of the physical-mechanical properties of fabrics, through the use of the recently developed Fabric Objective Measurement Technology-see Postle(105).

In garment processing sewing operations play the most important part. During this process there are many complex interactions between the sewing components, which if optimised, can lead to an optimum seam, and consequently

to an acceptable quality of garments with a puckerless appearance and greater durability.

The increased processing speed of sewing machines and the range of new fabrics available, increases the importance of the new methods of pucker prevention through the modification of the presser-foot(106). Examples of these are: the feeding of fabric layers by the needle itself, a method of "slowing down the bottom layer of the fabric" (before the needle) and finally a means for pulling the sewn fabrics by a pair of rolls installed beyond the stitch formation zone (54,64). All these factors have contributed greatly to improvements in seam quality. However, they are only auxiliary techniques, applied by the clothing manufacturers themselves or the sewing machine producers.

Parallel work has continued on designing the properties of fabrics to perform satisfactorily in the garment making-up and wear stages. Pucker is a complex mechanical phenomenon, which has been investigated theoretically and empirically to provide methods for predicting and preventing pucker occurrence at the stage of fabric design. It has become possible to broaden the data base of fabrics and to collect a great deal of information on fabric performance throughout the preassembly and assembly stages of garment manufacture. Cooperation between fabric makers and garment producers has brought new insights into the complexity of fabric assembly technology(107). The Experiments by Kawabata et

al(108,109) have led to the use of "snake diagrammes" to help to eliminate the occurrence of pucker in commercial garment making. Dealing with pucker problems by empirical methods also requires new approaches towards pucker evaluation. Causes of pucker and methods of prevention have been investigated by many researchers (reviewed in Chapter 2). The work by Dingra and Postle (110) and their attempt to grade the pucker in the 3-dimensional armhole of a jacket, using a 2-dimensional photographic AATCC standard (during an investigation into fabric overfeed) was the first experiment of its type, and confirmed the need for more objective methods of pucker evaluation. Amirbayat and MacLaren Miller(111) who tried an interesting approach to quantify seam pucker by applying 'compression energy balance theory' and the research by Kwong(112) into quantification of the fabric overfeed in the 3-dimensional parts of a garment, are examples of new approaches to seam pucker.

With such a substantial amount of accumulated knowledge on seam pucker, the need for improvements in pucker measurement and prediction methods have become an important issue in the textile and clothing industries, highlighted particularly in the Japanese MITI complete automation project(113) and in the European R+D industrial technologies development programme(114).

4.2. A preliminary investigation into image processing techniques used in other disciplines.

The initial proposal for the improvement of pucker evaluation was to use a viewing cabinet similar to that used in the evaluation of fabric pilling and snagging(115). The installation of Cannon's first still picture digital camera inside a viewing cabinet was considered as a means of seam specimen image capture. According to the proposal, AATCC:88B photographic standards would be digitised to form a reference standard stored with the SPMS programme (Seam Pucker Measurement System). After acquiring the tested specimen image into the SPMS standardised window, the next step, the grading decision, would be made against the standard grades by comparing the tested specimen window to the standards. This approach was aimed at eliminating the need for a special dark testing room.

This approach however had to be abandoned because the black and white picture from the camera was of insufficient resolution (below 100,000 pixels¹) and the coloured images were distorted. The proposal was evaluated critically and was found to be only an intermediate stage on the image processing development path and it became apparent that other more advanced proposals would have to be tried (117).

¹ Pixel - the fundamental picture element of digital image. Also, the coordinate used for defining the horizontal location of a pixel in a image(116).

Attention then focused on trying simple, existing image capture software, to acquire an image of sufficient quality. A series of experimental trials was conducted at the Hong Kong Productivity Council Optical Laboratory, on the image processing programme, used for the evaluation of the surface quality of metal products. It was found that, in B&W, there would be no problem in acquiring a video image. The difficulty lay, however, in the set-up of the system, which required special lighting of the specimen to resolve the effects of the fabric pattern and the intensity of the colour type in a B&W image.

The next SPMS experimental trials were conducted at the Hong Kong Polytechnic Applied Physics Laboratory, where the QUANTIMET 520 Image Analysis System was used (117). The system hardware consisted of a CCD colour camera, a set of microscopes, a RGB monitor and a PC IBM/XTS VGA unit. The system's image analysis electronics were in the form of an image frame grabber, an A/D convertor, image storage memory card, and a 16/32 bit 68000 type micro-processor and a series of DIP (Digital Image Processing) utilities (see Appendix XII for detailed description).

The AATCC:88B standard photographs were digitised and displayed in a grey-shade window. Each image was processed digitally to determine an overall intensity level for the window. The intensity level (scale 0-darkest level and 63, the brightest) data were plotted on a graph and presented against each AATCC grade (see Worksheet Fig.

4.1.01). The bottom part of the Worksheet explains how the standard specimens (standard original photographs) were located on the platform of the Quantimet image capture unit. The platform was too small to digitise a full-size photograph, therefore the specimen was divided into 3 parts and the areas B and C were also evaluated. Fig. 4.1.01a shows the intensity of the shaded area of each pucker grade (see Fig. 4.1.02; copy of the original standard). The shape of curve A of the main area, shows the intensity at level 4, as lower than at puckerless grade 5; This may be due to the non-uniform lighting of the original pucker standards or of the standard photographs. Nevertheless this experiment, showed a relationship between the pucker grades and the level of intensity. It made possible the assumption that a new method could be based on the intensity pattern obtained from the Photographic Standards of AATCC:88B.

The next SPMS experimental series of tests, using a quickly assembled temporary set-up, were carried out at the Laboratory of the Computing Studies Department of the Hong Kong Polytechnic. DT "Video Tutor" software was used together with a colour TV Camera of a resolution of 320,000 pixels. Examples of these tests are shown in Appendix XI as histograms of AATCC:88B Standard shade intensity. The room lights were a mixture of fluorescent bulbs of different design. The testing conditions were as follows: the light intensity 1500 lux, angle of illumination 5 degrees (horizontal), camera distance from

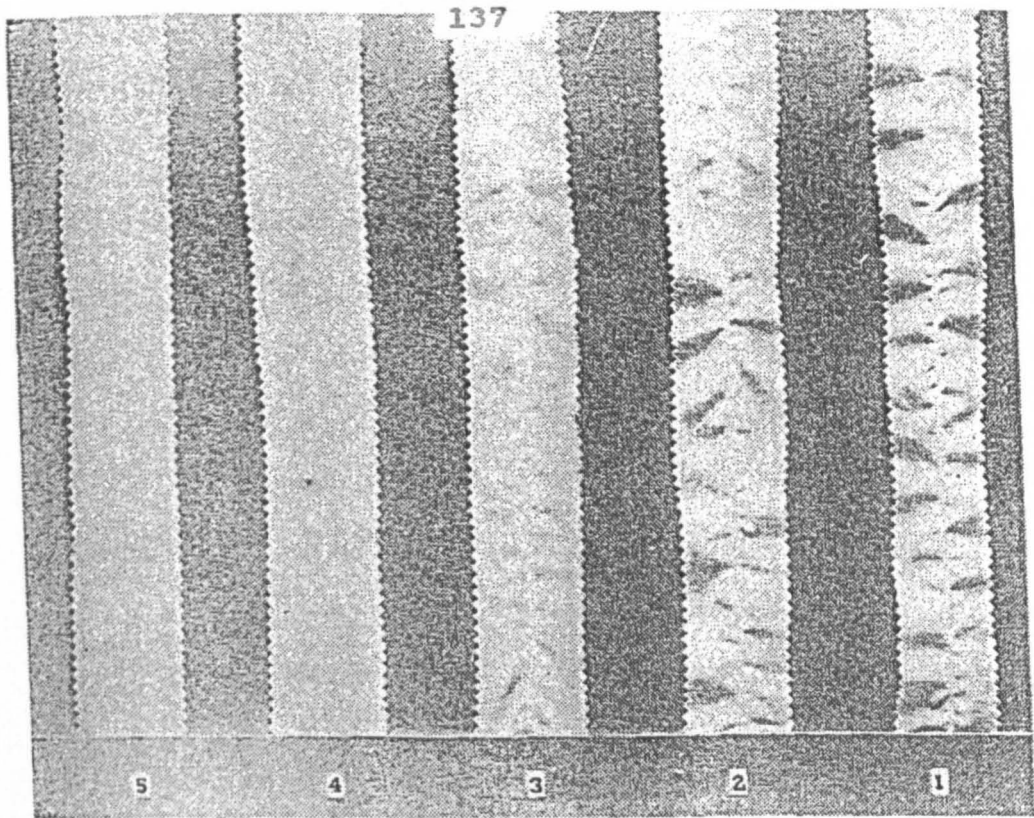


FIG. 1
PHOTOGRAPHIC COMPARATIVE RATINGS FOR SINGLE
SEAMS.

(The pictures shown here should not be used as standards.)

Fig. 4.1.02. Photographic Standard of the seam pucker
from AATCC Technical Manual.

the specimen 50 cm and specimen size 4x35 cm (the same specimen size as was used in the other preliminary study of the Puckermeter(89)).

This, still preliminary, test was extended to find the optimum conditions for the future layout of the testing system, using fabric specimens(118). Various conditions were tried such as:

- variation of the angle of illumination to accentuate the shaded areas of the pucker waves,
- various lengths of specimens,

- variation in the distance of the light source from the object,
- different locations of the camera (distance and angle),
- variations of pucker viewing area size and form (Area method and/or Line method),
- influence of the colour of the thread of the stitch on the image intensity,
- influence of the fabric pattern and colour on seam pucker image.

The results were analysed and the following conclusions were drawn from the tests:

- the mean of intensity level standard deviation and the mean of the coefficient of variation across the specimen were found to be effective in distinguishing the grade levels of the Photographic Standards of the AATCC:88B method, but the latter value is recommended as more discriminating,
- the angle of lighting affected the coefficient of variation(CV%), especially the severe pucker grades. The coefficient of variation of pucker grade 1 changed from 18 to 73 when the angle of lighting changed from 0 to 90 degrees. However for the samples of grade 5, the CV% had changed only from 4 to 9,
- the increases in light intensity caused the CV% rise; the contrast of pixels intensity increased as well,
- decreases of specimen lengths and widths caused an

increase in CV%, because the number of pixels also changed,

- only slight changes in CV% were noted when the camera location was changed,
- fabric pattern and particularly colour types influenced the CV% values; this will be described separately.

4.3. A preliminary evaluation of the Puckermeter to be used in the comparative evaluation of the new SPMS method.

The Puckermeter developed at SAWTRI underwent efficiency trials at Hong Kong Polytechnic (89). The details of its design were included in Table 2.2.01 in Chapter 2. Views of the Puckermeter are presented in Figs. 4.1.03 and 4.1.04. The concept of non-destructive testing used in the Puckermeter procedure also applied in the above study. Several types of fabrics were tested. During specimen preparation pucker was purposely induced. The swatches of fabrics used can be found in cell A of the Table in Appendix VI.

The trials were conducted in two stages: firstly, evaluation by the use of the AATCC:88B method and secondly, with a Puckermeter (because whilst the specimen being stretched between the jaws of the Puckermeter yarn distortion was expected to occur).

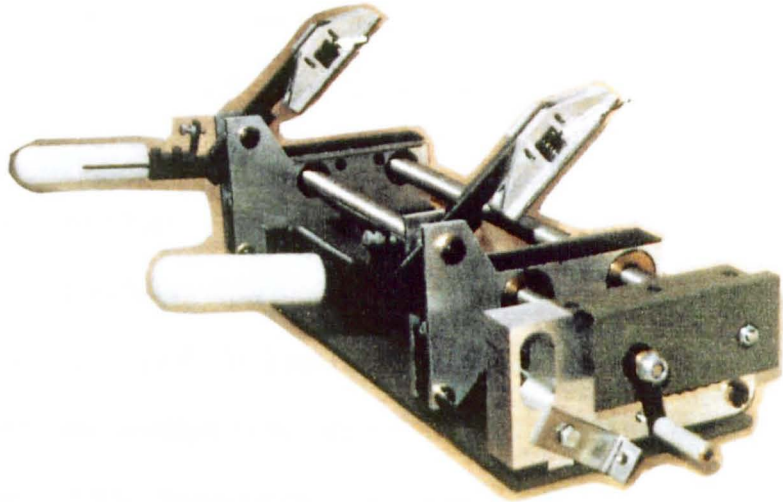
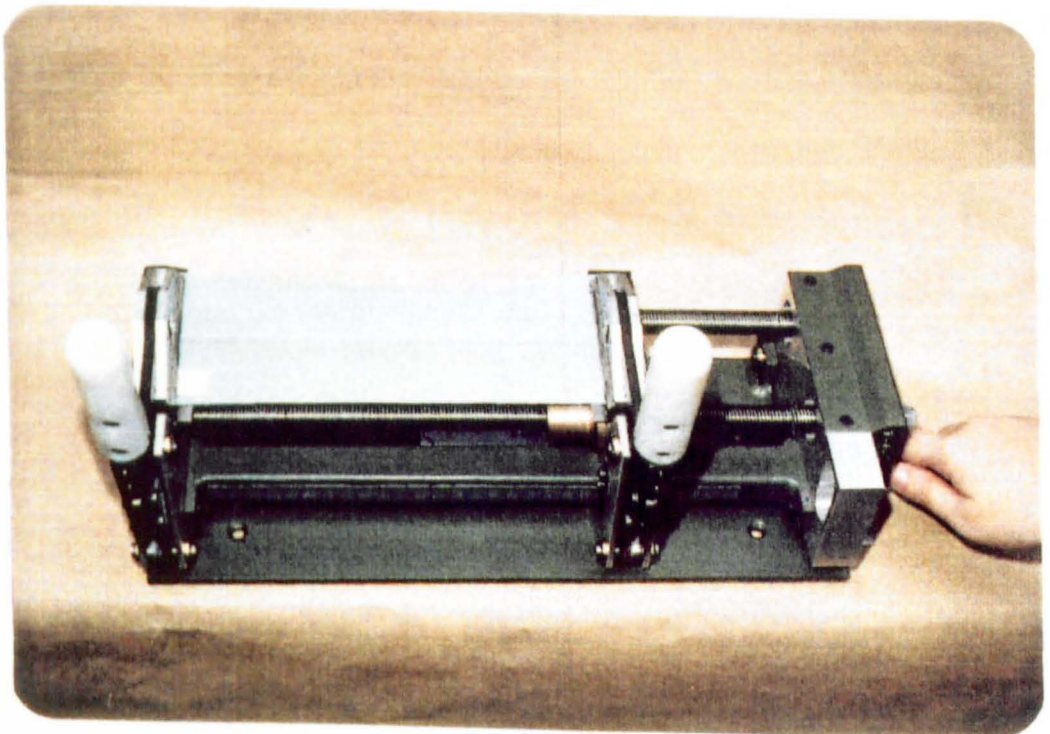


Fig. 4.1.3. The view of the Puckermeter used in the experiments.

Fig. 4.1.04. The specimen clamped between the puckermeter jaws.



Over 100 specimen were evaluated and the regression equation [1] was found as:

$$Y = 5.16 - 1.03X - 0.2X^2 \dots\dots\dots[1]$$

where:

X - pucker grade by the AATCC 88B method,

Y - pucker index P, measured by Puckermeter,

The correlation coefficient was calculated as 0.86. The good correlation suggested that the SAWTRI Puckermeter was suitable for this research (along with the AATCC method) and could be used in a comparative evaluation of the new Seam Pucker Measuring System (SPMS).

4.4. The digital image processing hardware and software.

The decision to integrate the image processing sub-system into the RSTM system was based on the concept of including fabric sewability evaluation (in the form of a Seam Pucker Index) calculated by the image processing software programme (SPMS) with the other measured parameters of sewing. To achieve this aim a versatile hardware from a reputable supplier was required. The main parts of the hardware required were:

- Frame Grabber,
- An Image Acquisition Board and
- An Image Display Monitor.

Image processing boards help to analyze visual information represented by standard or non-standard video signals. The video signals come from a standard video camera, scanner, etc. The electronic sampling of video signals is called

image acquisition, and is performed by a device called a frame grabber, which can also store and display the images. Image acquisition converts an image into an array of data points, which can be stored digitally, processed and enhanced, and subsequently displayed on a video monitor.

4.4.1. Image processing operations.

"Image processing is a general term applied to a range of operations, which alter frame data to extract more meaningful information"(119). These processing techniques allow images to be enhanced in a number of ways that:

- allow the image contrast to be corrected,
- combine two images,
- emphasize or de-emphasize details,
- highlight edges,
- rotate images, and so on.

Image processing operations can be divided into two broad categories, those which are performed on individual pixels (Pixel Point Processing), and those which are performed on groups of pixels (Pixel Group Processing). Pixel Point Processing divides further into operations performed on a single image, or on two or more images.

"Single Image Point Processing alters each pixel value in a single frame individually, and is used to enhance the image contrast. The multiplication operation causes each pixel value in the image to be multiplied by

a constant. This increases the contrast of an image uniformly, and can be used to brighten a dark image. Multiplication is sometimes called 'histogram stretching'. When applied to the entire image, whose picture values are uniformly low, multiplication can extend the values to fill the entire range. An additional operation of division, causes pixel values to be divided by a constant. This reduces the contrast of an image, and can be used to darken a bright or washed-out image"(120).

"There is also an offset operation, in which each pixel value in the frame is increased or decreased by a constant value. Offsetting does not alter the resolution of a image. Rather it uniformly brightens or darkens the image, so that the features of the image can be seen more clearly. The offset operation is often called a 'histogram slide': the difference between the lowest and the highest intensity value is not changed (as it would be if a multiplication had been used), but the range of intensities is shifted to become brighter or darker"(120).

"Dual Image Pixel Point Operations are used to combine two images. The additional operation combines pixel values of one frame with corresponding pixel values of a second. This has the effect of combining two images - superimposing one on the other - and can be used to apply overlays or to combine live images with animation. The subtraction operation, conversely, reduces all pixel values in a frame by the corresponding picture values in another"(120). Substraction shows the differences between

two frames, and can be used to detect product variation in automated inspection work, moving objects and also to evaluate seam pucker, as is the aim of this project.

More advanced image processing techniques include FFT(Fast Fourier Transform), and a range of geometric processing operations. FFTs convert image data from the spatial domain to the frequency domain. This permits extremely precise high pass, low-pass, or band pass filtering operations: it allows any frequency to be discreetly added or removed or every frequency value within a specified range to be eliminated. Geometric operations include high quality zooming, image rotation, and image warping(120,121).

Apart from this basic information on image processing the following terms extracted from the hardware Supplier's Technical Notes are directly relevant to the SPMS system(122), as:

"- Video Input: the inputs and outputs of frame grabbers are basically compatible with any of a number of video standards; the most popular are the PAL and NTSC systems (mains frequency 50 and 60Hz respectively. Standard video signals are actually complex wave forms and contain information about the brightness of each region of display, along with timing pulses, which indicate the end of each display line (horizontal sync) and the end of each display frame(vertical sync). The vertical and horizontal sync signals associated with the video input are used to control the timing on the frame grabber. Because frame

grabbers acquire images in real time, that is, in the 1/30 second RS-170(60Hz monochrome signals)allowed for each video frame, special video-speed A/D converters must be used. The RS-170 allows 52.59 μ s for each line in the image to be sampled. This is called the active line time. In this time a 512 by 512 frame grabber, for example , must convert 512 pixels or perform 512 A/D conversions.

- **Resolution:** the number of picture elements or pixels, which make up a digitized frame determines the 'spacial resolution' of the signal-the amount of detail, with which shapes in the image are represented. Spatial resolution of digitized frames is expressed as a matrix: the number of pixels(columns) per line by the number of lines(rows) into which the image is divided. Typical spatial resolutions are 512 pixels by 480 lines, or 640 pixels by 480 lines. Brightness resolution has to do with how accurately a particular digital pixel value represents the brightness or colour of the corresponding location in the original video signal. In a monochrome signal, it is the number of shades of grey, which can be represented; in a colour image, it is the number of different colours that can be represented. Brightness resolution is determined by the resolution of the A/D converter or converters, that perform the image acquisition. An 8-bit converter is said to have an 8-bit grey scale, and this divides the total signal voltage range, or the intensity spectrum ranging from total black to total white, into 256 values ($2^8=256$), sometimes called 256 shades of grey. Colour frame grabbers

use three A/D converters to simultaneously sample the Red, Green and Blue components (RGB) of the colour signal. For colour frame grabbers, brightness resolution is determined by the sum of all converter resolutions-24bits, where 8-bit converters are used (24 bits corresponds to 16,777,216 different colours). Sometimes the spatial resolution and brightness resolution of a frame grabber are specified jointly, as: '640 x 480 x 8'. This translates into 640 pixels per line by 480 lines of spatial resolution with 8 bits of brightness resolution for each pixel.

-Aspect Ratio: the ratio of the horizontal dimension to the vertical dimension of the image. This is important with graphics standards.

-Memory: Frame-Store Memory stores an entire frame's data. Since the acquisition hardware converts pixels one at time, the buffer also serves as a repository that accumulates a complete frame pixel by pixel. Frame data can be analysed later, processed and displayed. Image files are large (256 Kbytes or more for monochrome; 768 Kbytes for 24-bit colour, and have the ability to store multiple frames onboard for real-time processing or display.

-Image Display: most frame grabbers contain circuitry which converts the digital pixel data back into an RS-170 or CCIR-compatible signal for display. This allows the stored or processed image to be viewed so that processing or acquisition can be checked on a separate analog RGB monitor.

-Colour Image Processing: to facilitate the processing of colour images the hardware has to have a converter between the RGB colour space and HSI (hue, saturation, intensity) data"(122).

The latter is a more natural way of describing colour than traditional RGB. "HSI components convey important information directly: hue is the colour itself (blue, yellow, purple); saturation: is the depth of colour (pink, red); and intensity: is overall brightness or darkness"(122). HSI saves processing time because for most applications there is a need to examine one component - RGB almost always requires all three to be examined. For example, to check the colour of a plain one-colour fabric the hue value should be examined. To check saturation, examine the value to separate pale blue from deep blue. Since the intensity value corresponds to the monochrome version of an image there is a possibility of using it with any of the dozens of monochrome-only processing algorithms(123,124).

4.4.2. The selection of processing hardware.

Since hardware for the RSTM system had already been purchased from Data Translation Co., it was decided to purchase the image processing equipment from the same company as well. As the fabrics were in a large variety of colours the purchase of a monochrome board would not have been adequate. It was decided to acquire a colour processing board, which could be used in other

applications as well. The image processing required a frame grabber for video inputs and a processor board. Both units had to be connected by an open interface specification, which was a DT-Connect configuration, already described in Chapter 3.

The acquisition board always initiates data transfer cycles; the processor board responds in accordance with the acquisition board's signals. There are two data paths for transferring signals or image data. Each data path has an IN port and an OUT port. The rate at which data is transferred between the boards varies from less than 1Hz to 10MHz (different boards have different bandwidth). Typically, with an analog I/O (input/output) acquisition board, the data transfer is asynchronous and equal to the sampling rate, usually ranging between 1Hz and 1MHz. In this case the sampling rate is determined by the user application program. The following components were selected:

- DT2871 (HSI) Frame Grabber from Data Translation,
- DT2869 Video Decoder/Encoder,
- Sony TR55 CDD video camera and
- Mitsubishi RGB high-resolution 19 V" monitor,
- DT7020 Floating Point Array Processor, already installed with RSTM.

4.4.2.1. An overview of the DT2871 Frame Grabber board.

The DT2871 is an(HSI) Colour frame grabber for IBM PC AT compatibles. Using real-time RGB/HSI capability, it can

capture an image from an RGB device and process it in the HSI colour space, using the compatible DT-Connect processor and Aurora subroutine library. Images are acquired as 512 x 512 frames with 24-bit colour resolution. The DT2871 can also convert back to RGB from HSI in real time for image display on an analog RGB monitor (in this project the analog "Mitsubishi" monitor). It can store 1 frame plus overlay onboard. Video input: 1 RGB, RS-170/RS-330(512x480x8) or CCIR(512x512x8).

Images acquired by the "Sony" CCD camera (type TR75 of 380,000 pixels effective resolution) are stored and displayed as 512 X 512 frames using as many as 16.7 million colours (24-bit). The DT2871 contains enough onboard memory (1Mbyte) to store a full colour image, with an additional memory for black and white text graphics overlay. The board also has a DT2869 Video Decoder/Encoder included in the system, so as to convert CCD Sony camera images into RS-170 frame grabber input/output. Appendix XII contains more technical data on this board including a block diagram of data transfer.

4.4.2.2. The technical data of the RGB Monitor.

The R.G.B. 19 V" high-resolution colour display monitor, Model C-3920 series was manufactured by Mitsubishi Electric Co. Scanning frequency: vertical; 40-70Hz; horizontal; 15,5-23,5 KHz. Maximum effective screen size: 350mm (W) x 265mm (H). Video amplifier frequency

response: +3dB or better between 50Hz-50Mz. Linearity: >7%. Raster distortion better than 2.5% of raster height.

4.4.2.3. The architecture of the SPMS system.

The components of the SPMS system were selected by their technical specifications. The next step in the design of the system was the assembly stage, during which the board had to be tested to confirm that it conformed with the other parts of the RSTM system. The AT-386 Everex PC mother board had to be exchanged for the more powerful 8Mb RAM memory needed to perform the image and signal processing operations.

The system set-up was redesigned so, that three evaluation methods could be used with the same layout. The set-up schematic diagram is shown in the Fig. 4.2.01. The architecture of the SPMS system hardware architecture is presented in a schematic diagram, Fig. 4.2.04. The seam pucker image captured by the frame grabber is displayed on the RGB monitor (the top one in Fig. 4.2.02). The template (covered by the matt-grey fabric) framed area is the image window (size 20cm x 6cm), to be subjected to pucker evaluation, Fig. 4.2.03.

The arrangements of the three evaluation methods which were carried out in the comparative evaluation of the SPMS system are marked. Method 1 was by means of visual control of the SPMS result and its equivalent grade on the ATTCC scale. Method 2 was an evaluation of the AATCC photographic standards and of the samples placed on

the vertical plane of the special board with the adjusted top 2-bulb lamp.

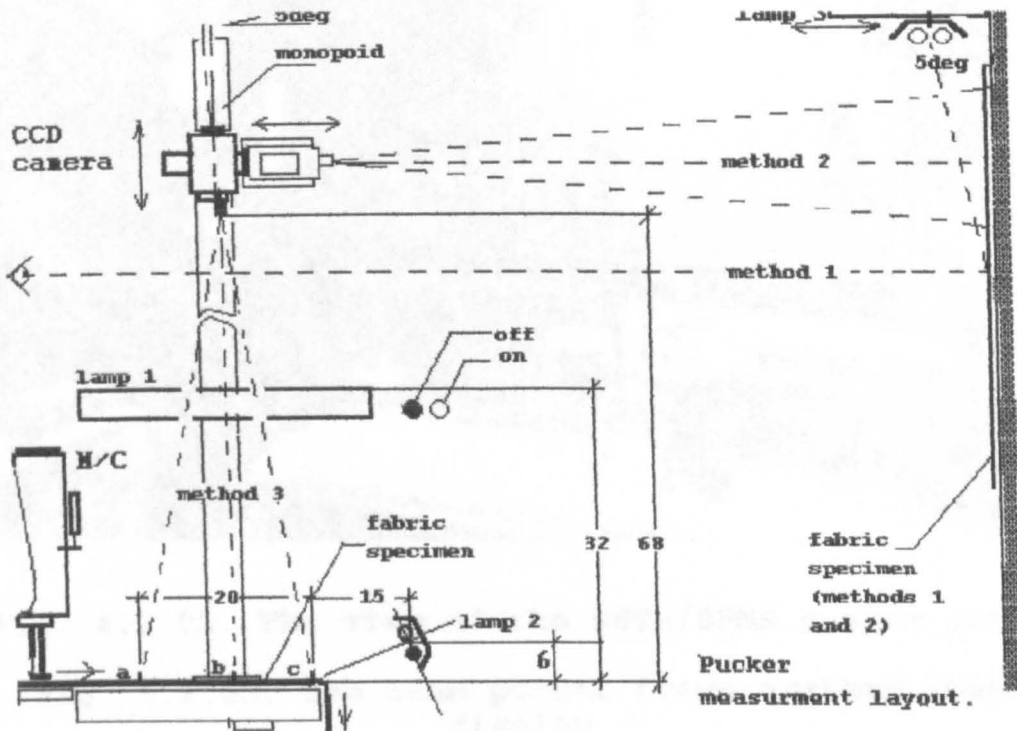


Fig. 4.2.01. Diagram of the pucker evaluation setup.

Method 2 led to a redesign of the setup and the location of the monopod on the machine table, which became the setup for Method 3. In the first version of Method 2 the monopod had been mounted on a special trolley between the machine and the wall board. In the second version the specimen, camera, lights were oriented to give a vertical positioning of the camera, which was found to be not only more convenient for the operator, but also allowed for a easier manipulation of the specimen and camera.

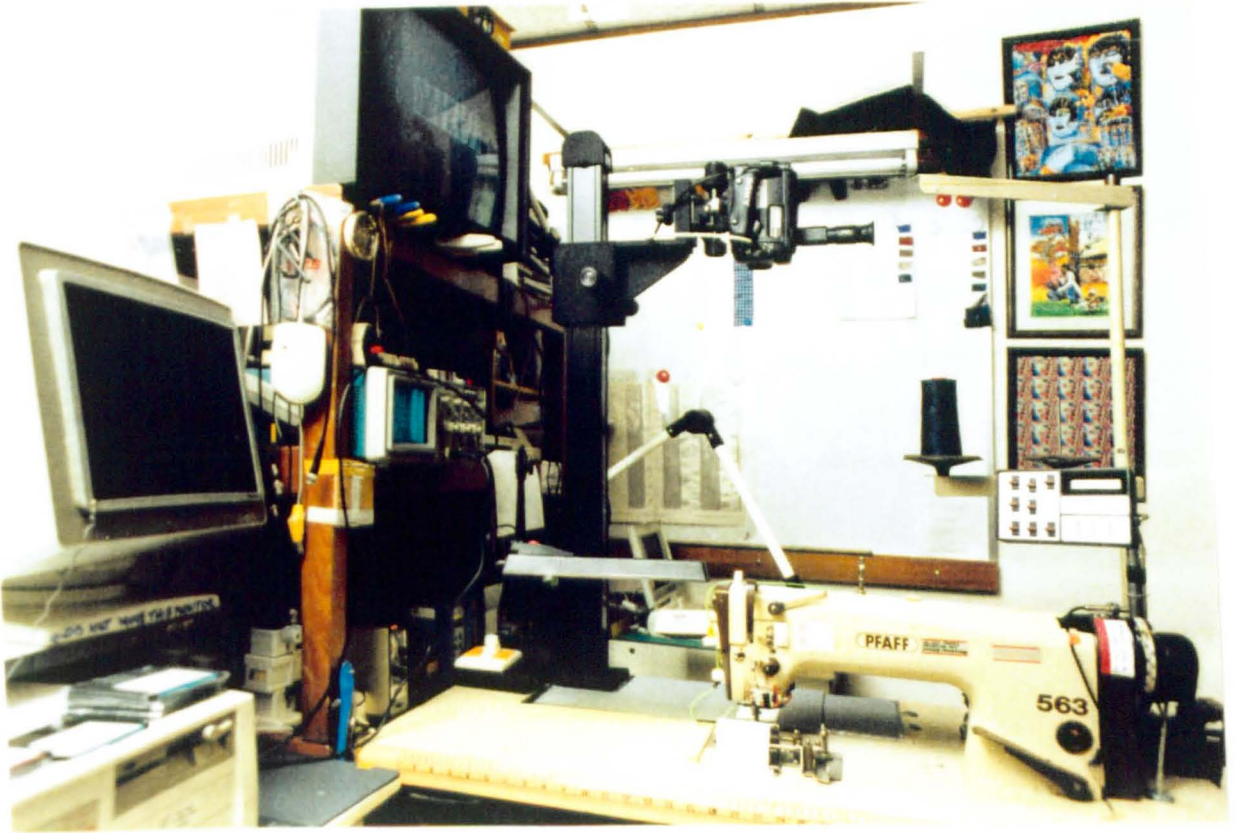
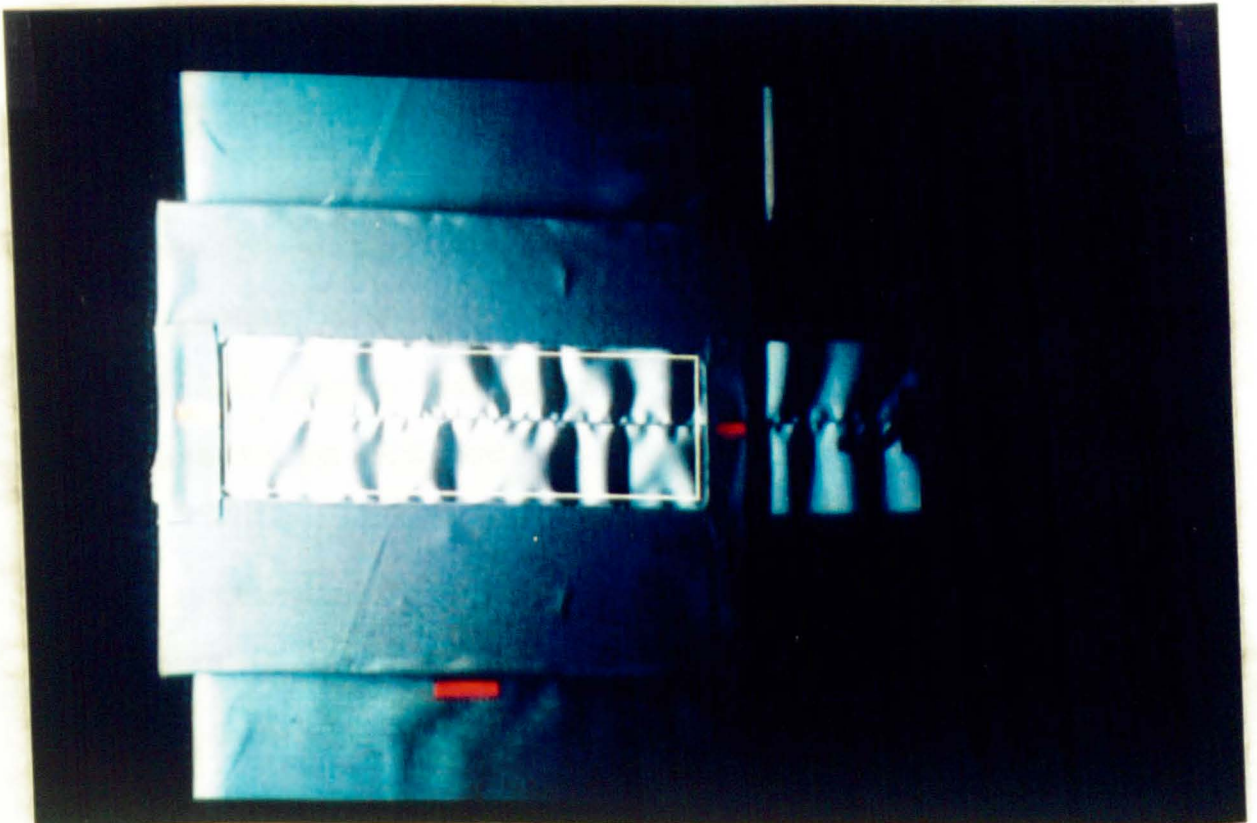


Fig. 4.2.02. The view of the RSTM/SPMS system setup.

Fig. 4.2.03. The seam pucker frame grabbed image display.



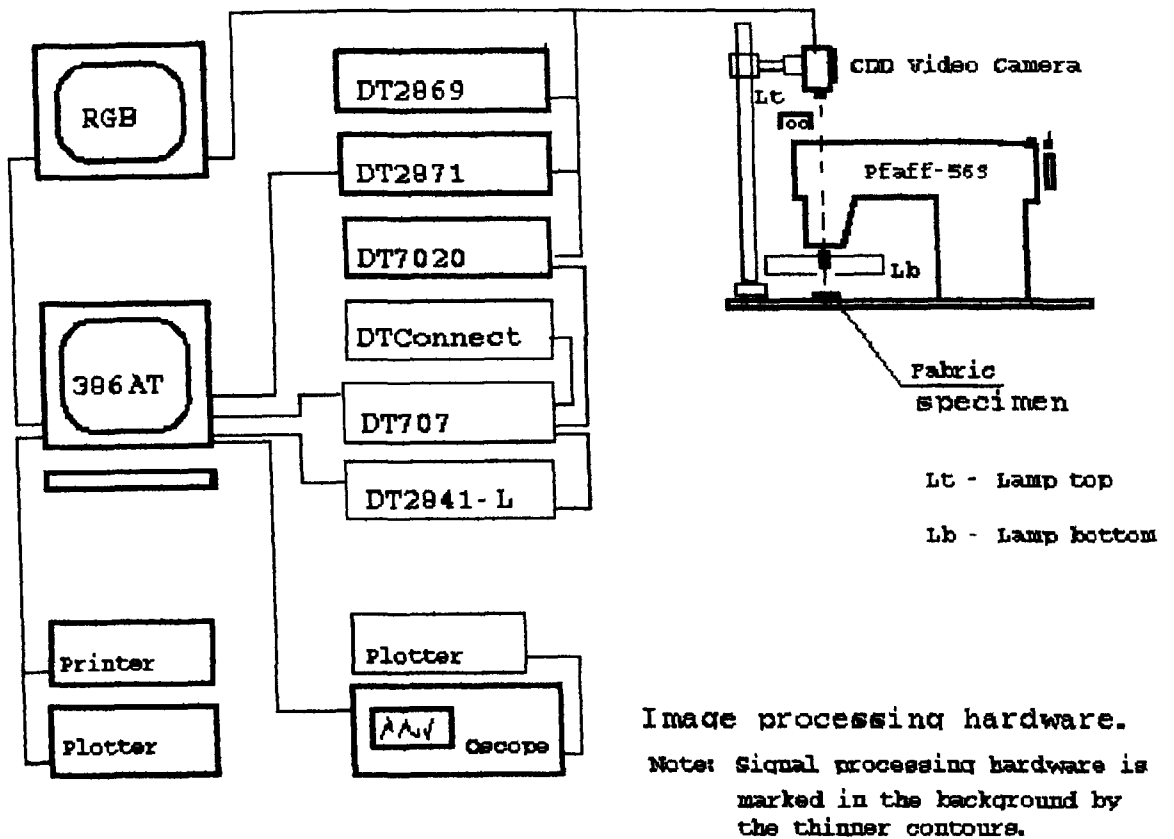


Fig. 4.2.04. Block-diagram of the SPMS hardware.

The seam image was captured when part of the specimen was still under the presser-foot (Fig.4.2.03). This was beneficial during repetitive testing as the settings did not have to be altered.

4.4.3. Illumination of the seam pucker specimen in the SPMS method.

The quality of the seam pucker image captured by means of a photographic or a video camera depends (apart from the quality of the hardware and software) on the

following additional factors, which were also studied:

- the use of a suitably dark testing room,
- the orientation of the specimen in relation to the camera and the illumination method used, and
- the type, pattern and colour of the fabric.

The darkness of the testing room was an important factor in assuring the proper contrast of the object. It was found that by reduction of the light intensity of the testing room the quality of the image on the screen improved. The only light left in the room (apart from the necessary illumination) was the screen of the system monitor.

The orientation of the object was found to have an influence on the coefficient of intensity variation. In the evolution of the investigation of the optimum illumination, described above, a number of trials were conducted to find the optimum orientation of the specimen illumination. In order to achieve the greatest differentiation in the shade intensity, different combinations of single or dual fluorescent bulbs were tried. The optimum illumination (Method 3) was finally established by adjusting the orientation of the lights as shown in the layout in Fig.4.2.01. The top lamp (Lamp1) had to be installed to reduce "camera confusion" (the intensity of the shaded areas of puckered fabric was confused with the colour intensity level of the grey scale).

The pattern of the fabric had a smaller effect on the image quality than the intensity of the colour brightness. In the case of the dark coloured fabrics, a single side light was insufficient and as a result of this the pucker grading results showed an unacceptable level of pucker, although this was not discernible through evaluation with the naked eye. The intensity of illumination was checked by using the Sanwa Luxmeter LX 3010. The readings were carried out at three points for Method 3 (Lamp1 was switched off) and were as follows: point a=700 lux; b=900 lux and c=1300 lux (closest to the side lamp), Fig.4.2.01. These values were accepted as "calibration points" in case the illumination required to be reset. The detailed procedure of operation of the SPMS programme will be described later.

4.5. Seam pucker quantification methods.

To find the relationship between the Photographic Standard AATCC-88B pucker grades and intensity and the pucker severity of fabric specimen and intensity, Least Square Correlation Coefficients(CC) of a single variable regression (from the software STATPAK) were calculated.

The following types of fit were considered:

- Linear : $Y = A + BX,$
- Exponential : $Y = A \times e^{BX},$
- Logarithmic : $Y = A + B \times \text{Log}(X),$
- Power Law : $Y + X^B,$

where:

CC - Correlation Coefficient,
 X - Coefficient of Variation,
 Y - Seam Pucker Grade,

4.5.1. The selection of the correlation methods.

The equation that fitted the data best Correlation Coefficient was selected and for the Standard Photograph they were:

-Linear: $Y = 6.079 + (-0.227 * X); \dots\dots\dots[1]$

CC=0.9880

-Exponential: $Y = 8.998 * \text{EXP}((-9.144\text{E}-2)*X),$

CC=0.9895

-Logarithmic: $Y = 10.361 + (-2.948)*X),$

CC=0.9976

-Power Law: $Y = 44.919*X^ + (-1.141),$

CC=0.9601

Thereafter six fabric types were tested and correlation equations calculated. The samples of fabrics selected had been made with a range of pucker levels and specimens which had pucker levels corresponding to standard grades(as closely as possible). All four types of regression were calculated for each type of fabric. The results of correlations showed that the Linear and Logarithmic regression equations fitted best. This demonstrated the possibility of quantifying the relationship between all five pucker grades. Linear regression was selected as more straight-forward and easier to use.

4.5.2. Investigation of the effects of fabric colour and pattern on the seam pucker image.

The relationship between fabric colour and pattern on shade intensity caused by an irregularity of the fabric surface (e.g. fabric creasing) has been investigated by other researchers(125,126).

In this research the Coefficients of Variation (CV%) of plain fabric(before sewing) were measured and are listed with each fabric type equation (for comparison of colour influence):

a.Pucker Standard (AATCC-88B):

$$\text{Linear: } Y = 6.079 + (-0.227*X) \dots\dots\dots [1]$$

b.The linear regression for the six tested fabrics types (of different colour):

-A	$Y = 6.378 + (-0.122*X)$ CV%: 12.6783,
-B	$Y = 7.581 + (-0.153*X)$ CV%: 14.8363,
-C	$Y = 11.523 + (-0.226*X)$ CV%: 30.0471,
-D	$Y = 6.3993 + (-0.615*X)$ CV%: 13.3472,
-E	$Y = 6.4274 + (-0.135*X)$ CV%: 13.3472,
-F	$Y = 6.4302 + (-0.158*X)$ CV%: 12.95,

From the above equations it can be seen, that great variations exist in the values of the Constant; from

6.378(White) to 11.523(Navy). For example for the Pucker Standard the value of Constant was 6.079 (relatively "Whitish"), while the fabric type C had its Constant of 11.523. This fact confirms, that different fabrics have different initial CV's. This difference in their initial values will result in difference in Constant of the equation. Therefore, the CV% of plain fabric should be measured before fabric is sewn and compared with its sewn equivalent. Also the coefficients of variation of the fabrics suggest some relationship with the equation's constants. Using the Least Square method the following relationship between the constants of the equations and coefficients of variation of the fabrics before sewing was found to be as follows:

$$Y = 2.5369 + 0.2991*X, \dots\dots\dots[2]$$

where:

X = CV for the unsewn specimen,

Y = Value of Constant in the previously
derived equation,

In the final form the equation to measure sewn fabric specimen is:

$$Y = I + (-0.227*X) \dots\dots\dots[1]$$

$$I = 2.5369 + 0.2991*CV \dots\dots\dots[2]$$

or:

$$Y = 2.5369 - 0.227 *X - 0.2991*CV \dots\dots\dots[3]$$

where:

Y = Seam Pucker value,

X = Coefficient of Variation of sewn fabric,

I = Constant Value for equation [1], and
CV= Coefficient of Variation of the
fabric before sewing.

During the course of further investigation the influence of fabric pattern was evaluated by measuring CV% (before and after sewing) on several samples and comparing the difference between equation calculated and equation derived [3]. Due to small differences between both results the equation [3] was used in calculating the pucker severity level in the SPMS method.

Additionally a satisfactory correlation between the SPMS and the Puckermeter methods was confirmed by Wei(125), where the correlation coefficients for different fabric types were in the range from 0.81 to 0.97. The use of the contrast and matched threads in seaming did not cause any significant differences (white thread CC=0.8351 and contrast colour CC=0.8103; and on fabrics with Checked pattern CC's were 0.9315 and 0.9371 and Striped pattern 0.9710 and 0.9284 respectively.

4.5.3. Pucker evaluation method by means of digital image processing.

The main advantages of pucker evaluation by the use of digital image processing techniques should be not only objectivity, but also repeatability and the possibility of the retrieval of the stored images. In the case of the

SPMS system a second archival copy of the original image could be stored on video tape.

The repeatability by means of the CV of the Pucker Index (Coefficient of Variation as a measure of consistency of measurement on the same specimen) was checked at random, for several fabrics and in the same testing conditions. The following results were recorded:

- CV[%] of the Pucker Index measurements taken at 1 minute intervals for the different fabrics were, e.g.: 2.02(fabric B), 2.9(C), 1.63(D), 0.90(E), 2.69(E). The highest was 3.1%(R),
- the value of the Pucker Index(PI) measured initially on one fabric was 2.18 and after 5 minutes it was 2.09(Q),
- after 4 hours PI was 2.2.

Therefore, the system characteristics comply with the requirements set at the SPMS design stage, of providing an PC-based, objective system of pucker evaluation.

4.5.4. The calculation of seam pucker severity level.

With the hardware and software assembled and tested, the next step in the development of the SPMS system was the adaptation of the Data Translation digital image software "Aurora" library subroutines into the short processing programme for seam pucker calculation. This was based on the equation derived from experiments in the previous sections. The programme written by Wei(125) consisted of the following seven steps:

- a- defining the window area of the image to be calculated,
- b- deciding whether to use a single image or two images captured for subtraction,
- c- capturing and storing the images,
- d- subtraction of the images and calculation of the pucker grade,
- e- defining and displaying the Area histogram ,
- f- defining and displaying the Line histogram,
- g- saving the histograms, and Image in a buffer for later retrieval.

The SPMS Window is shown in Fig. 4.2.03 in Section 4.2. The special masking template is seen, although it was no longer used in the programme, since the special path for the passage of the specimen in view of the camera was sufficiently marked by the matt-grey fabric (preventing the reflection of noise; see also Fig. 4.2.02).

To facilitate further future research on image analysis, it was decided to adopt a Line Method in addition to the Area Method to enable the different pucker configurations to be seen at varying locations and distances in relation to the seam line.

4.5.5. The menus, Area and Line Histograms of the SPMS system.

The SPMS system Set-up is shown in Fig. 4.2.01 (marked as Method 3) and a general view is presented in

Fig. 4.2.02. The RSTM hardware components are also shown in the form of a block-diagram, Fig. 4.2.04.

The "View histogram" menu window of the SPMS software program, with the statistical results of the area intensity of the particular fabric is shown in Fig. 4.4.01. The magnified image of the same fabric is presented together with the SPMS standard size template, in Fig.4.4.02. The bottom Figure 4.4.03 shows the histogram graphically, where the Y axis represents the intensity level and the X axis is the window length designated in pixels.

The histogram shape shows high values on the left-hand side and their reduction towards the right i.e., darker shade. This asymmetry of shape is attributed to the uneven illumination of the specimen as the light is placed on the right side, as shown in Fig. 4.2.01. Similar asymmetry can also be seen on the original photographic standard of the AATCC method (brighter top part of the standard specimens) - see Fig. 4.2.02.

Figures 4.4.04 to 4.4.06 show in order: a lower magnification of the fabric; the middle photo (Fig.4.4.05) shows the Line template as close as possible to the seam line, whilst not overlaying the seam itself; and the bottom picture shows the distribution of pucker shade intensity, which also mirrors the configuration of the waves of the seam pucker. The shape of this histogram is unlike the one in Fig. 4.4.03, although both relate to the same fabric.

Fig.
4.4.01.



Fig.
4.4.02.

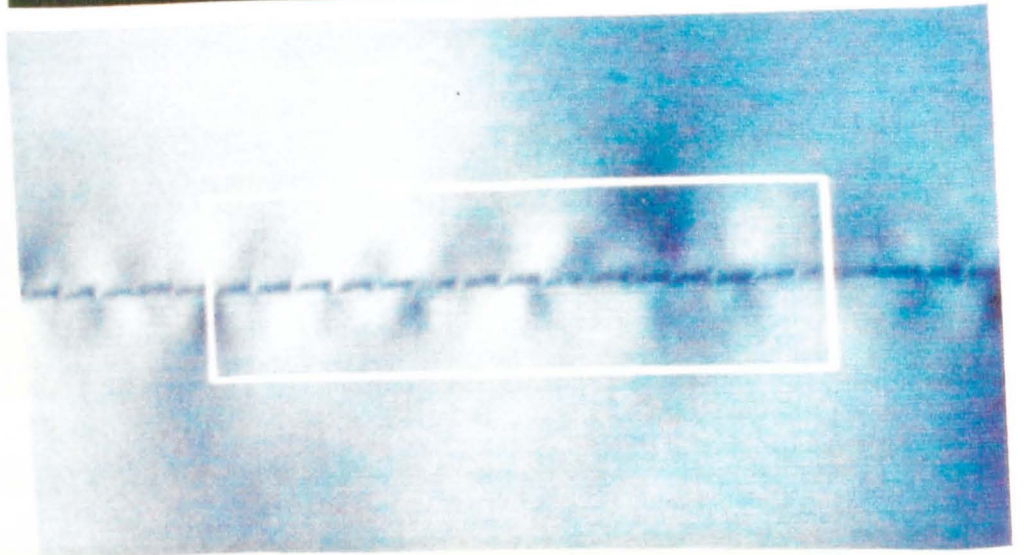
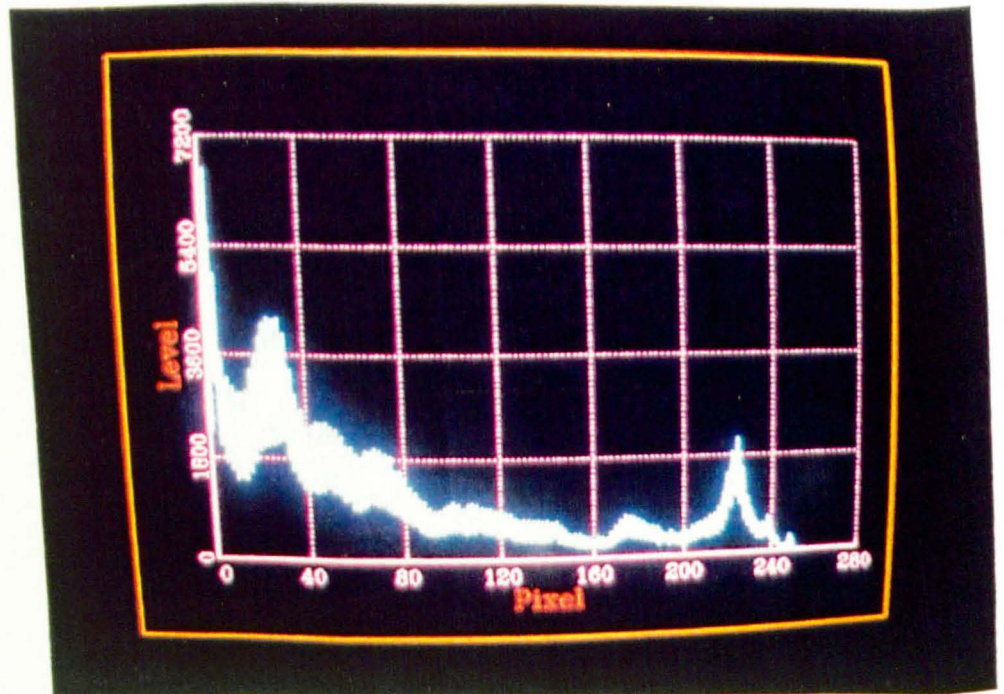


Fig.
4.4.03.



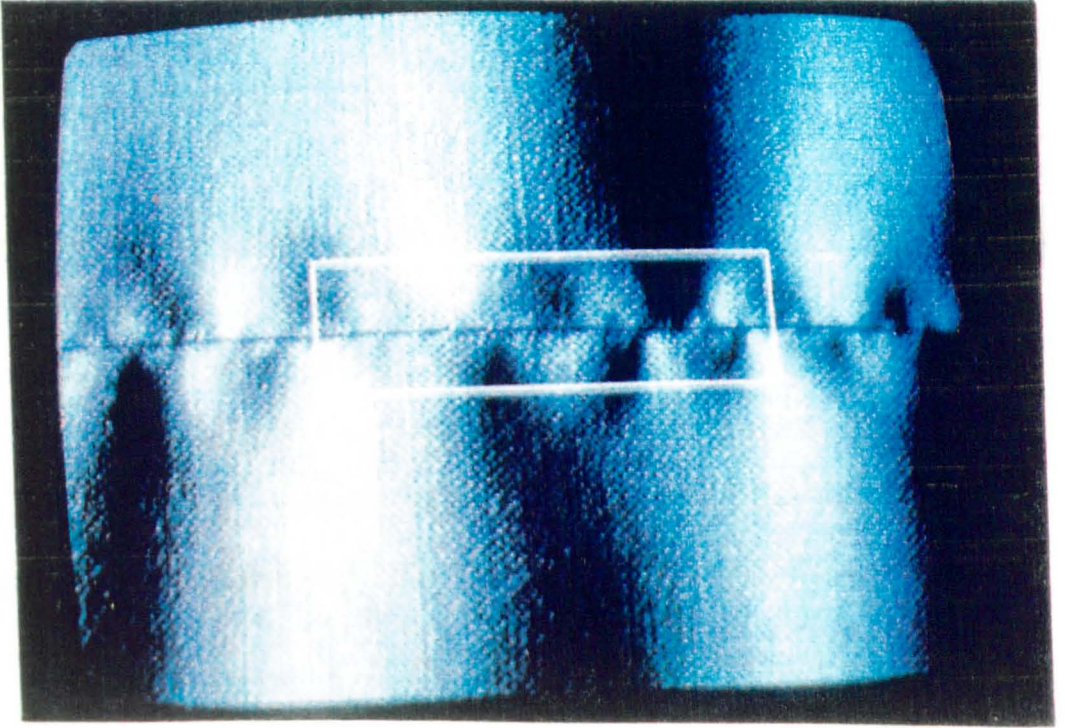


Fig. 4.4.04. The Pucker Area template.

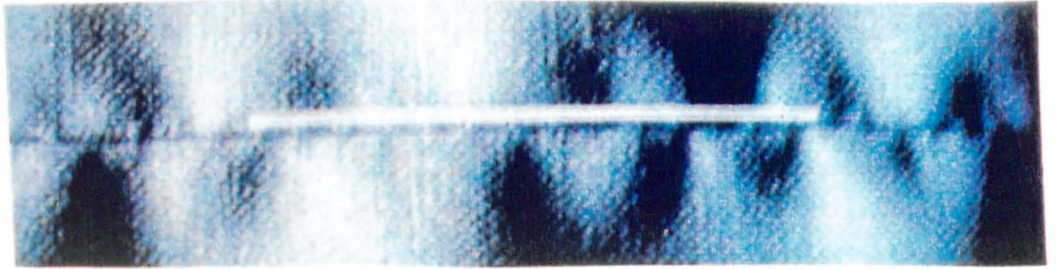
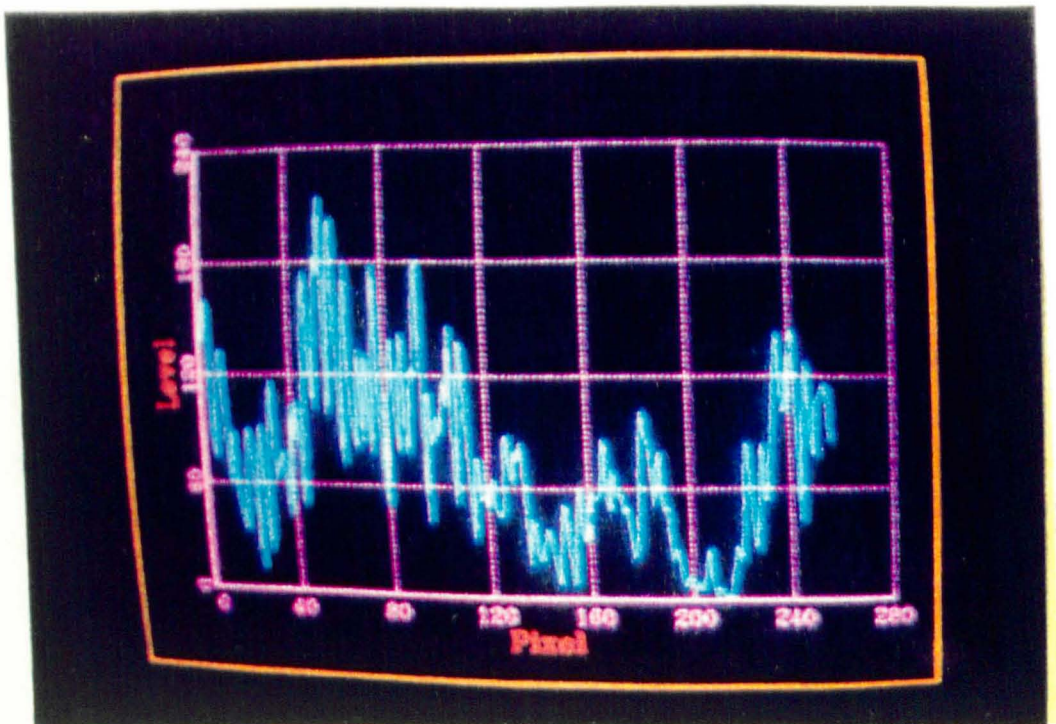


Fig. 4.4.05. The Pucker Line template.

Fig. 4.4.06. The pucker shade frequency distribution.



This can be attributed to a difference in the distance of the template from the illumination source. The work carried out at the Hong Kong Polytechnic(125) on the method of quantifying the other AATCC visual evaluation method (for fabric wrinkling) showed similar problems of the asymmetric shape of the histograms acquired.

Chapter 5. EXPERIMENTS AND ANALYSIS.

In this chapter several series of experiments on the dynamic interactions of the sewing machine and selected fabrics and sewing threads will be described, using the instrumentation developed in the project. The experiments were carried out with the following aims:

- to demonstrate the capability of the signal and image data acquisition systems,
- to measure forces generated during high speed sewing,
- to enable the dynamic interaction between thread and fabric, and its effect on seam pucker, to be studied, and
- to enable other measures for the further modification and expansion of the system to be developed.

5.1. The structure of the experiments, their range and the test procedures.

Initially, the basic intention was to include as broad a range of fabrics to be tested as possible, so that the Hong Kong Polytechnic FOM Data Base could be extended by including sewability test results. Unfortunately the large volume of fabric that this would have required was not available for testing, so it was decided to use a range of post-production remnants, ranging in length from 2.5-5.0m. These constraints required careful planning of the range and structure of the tests.

5.1.1. RSTM testing on commercial fabrics.

The aim was to select fabrics associated with quality problems encountered by a local apparel processing

unit. These were mainly woven, light-weight fabrics, known to be prone to puckering at the seams. Fabrics were selected from the production remnants at a local apparel producer (TAL Co. HK Ltd), who had shown interest in the research results, which it was hoped might lead to improvement in future pre-production operational methods. Increasing quantities of micro-fibres were becoming available for a wide range of apparel products and the industry itself was beginning to experiment with sewing micro-fibres. The Japanese "Toray" Co, through their local office in Hong Kong, was contacted and they provided three new types of recently developed products, which expanded the sample range of fabrics. Sewing threads and needles were provided by another sponsor, the German needle manufacturer "Rhein-Nadel" GmbH, and the local thread manufacturer ("Gunzental Threads" HK Ltd).

To convert the aims of the research into a range of experiments, the following key factors were considered in planning the structure and number of tests on the RSTM and SPMS systems:

- fabric and sewing thread types; ,
- sewing machine settings range(speed, stitch density, presser-foot pressure, needle thread tension);
- and types of needle, presser-foot and throat plate.

These factors had to be balanced to take into account the quantity of fabrics available for the experiments. The fabrics were cut into long strips, 7 cm wide. The total lengths of the fabric strips were measured and the

structure of possible tests evaluated. The following rule was applied: the higher the machine speed, the longer the fabric specimen required, to permit the acceleration and deceleration of the sewing machine. The stitch density and machine speed were used as test variables. Because the research objective was to investigate the dynamics of higher-speed sewing, an average specimen length of 70cm was calculated for the of amount of fabric needed.

An additional factor of some significance was the need to synchronise the fabric feeding with the moment when data began to be acquired once a stable sewing speed had been achieved. This need to handle the fabric and simultaneously control the timing of the start of data acquisition, required some preliminary familiarisation with the equipment and procedures, to ensure that sufficient data could be acquired before the fabric ran out. This problem inspired the design of the "Fabric Feeder" (Fig.3.2.03), which provided fabric guidance and allowed tension adjustment of the sewn fabric layers.

5.1.2. Formulas for calculating the number of tests and fabric needed.

The objective of the structure of the range of tests was to ensure coverage of a broad range of fabric types, sewing threads and sewing machine settings, to match conditions experienced in an industrial environment.

5.1.2.1. The optimum range of a complete set of tests for each variable.

It was decided to calculate first the amount of fabric that would be needed for testing one fabric type, using the following conditions:

3 thread types, 6 needle types, 9 speeds, 4 thread tensions, 2 types of throat plates, 4 presser-foot pressures and 4 levels of stitch density.

The number of tests for 1 fabric type and one speed level only is given by:

3 threads x 6 needles x 4 types of thread tension x 4 presser-foot pressure range x 2 types of presser foot x 2 throat plate types x 4 stitch densities x 1 speed = 4608 tests.

Each single test required the following minimum number of stitches to be preset, to enable the operator to acquire a sufficient quantity of input data to fill the system acquisition buffer with the same amount of cycles in a shorter acquisition time, due to the increase of the speed of the machine, as in a longer time.

-lowest speed range: 50 stitches,

-highest speed range: 255 stitches.

An average stitch density rate was 32 stitches per 10cm. The required minimum specimen length had to be 20 cm, as 50 stitches only could be preset on the machine. Therefore the minimum length of the specimen = 20cm of fabric strip + 10 cm (ends allowance) = 30 cm. For 255 stitches (density of 32 spc), the max length of the specimen =

79.6cm = 80cm + 10cm (ends allowance) = 90cm. Thus 30-90 cm was the estimated specimen length range.

The majority of selected fabrics were 140 cm wide, so the amount of fabric needed could be calculated as follows:

-an average single tested specimen length would be 70cm long,

-one type of fabric to be tested under each set of conditions would require 4608 tests per speed giving $4608 \times 0.70 \text{ m} = 3225.6 \text{ m}$ of fabric.

-a full 140 cm wide fabric provided $140\text{cm} : 7\text{cm} = 20$ specimens (seven cm wide and one meter long).

After subtracting the selvage area of 14 cm from each side the number of specimens reduces to 16.

Therefore the total fabric length = 3225.6 divided by 16 = 201.6m = approximately 200 m of each fabric type per sewing machine speed.

These calculations resulted in the following conclusions:

- a. To carry out a full set of RSTM tests at one speed, 200m of each fabric type was needed.
- b. The full range of 9 speed levels required $9 \times 200\text{m} = 1800$ running meters of each fabric.
- c. The total length of the 20 types of fabrics selected would amount to 36,000 meters.
- d. Such large quantities of fabric were impractical.

5.1.2.2. The reduced testing programme.

A comprehensive testing programme was found to be

uneconomical and impractical, so an achievable testing programme was calculated from the actual quantities of fabric available. Since the main research objective was an investigation of the dynamic forces affecting puckering (which is more significant at higher speeds) it was decided to concentrate the tests on higher sewing speeds.

The final structure of the testing programme was as follows:

a. Fabric type:

-woollen and blended fabrics:	10 fabrics and 38 tests,
-cotton and blends	5 fabrics and 44 tests,
-synthetic fabrics:	5 fabrics and 45 tests,
-micro-fibre fabrics:	3 fabrics and 9 tests,
Total:	23 fabrics and 136 tests,

b. Speed category (9 levels):

-low speed 200,500,1000 [rpm]:	49 tests,
-middle range: 1500,2000,3000 [rpm]:	58 tests,
-high speed range: 5000,5500 [rpm]:	*29 tests,
(*16 fabrics were tested at the highest speeds),	

c. Sewing thread category:

-thread types used	3,
-thread tension levels	3,

d. Needle type category:

-needle types used	2,
-no needle (testing inertia) **,	
(**28 separate tests, no fabric consumed),	

e. Presser-foot pressure category:

-presser-foot pressure levels	3,
-------------------------------	----

d. Stitch density category :

-stitch density levels used 3,

The above tests were to be single trial tests, with the data recorded and stored by the RSTM system on floppy disks. The volume of one set of data would be in the region of 400Kb. The records could be retrieved and presented on a monitor screen in graphical form (signals versus time/angle), as well as in the form of 4 columns of data points (precision 10^{-6}), each column being 8192 rows long. Results could be output as hard copy, consisting of a printed graphical and written report with details of the test settings, as well as a statistical analysis if required.

5.2. The selection of fabrics and sewing threads for the purpose of the experiments.

The decision on fabric selection was based on the following criteria:

- fabrics should have an inherent tendency to pucker,
- should have a history of poor performance in garment production (problem fabrics),
- should have general characteristics allowing them to be grouped together under e.g. composition, weight, finish, application etc.

5.2.1. Testing the selected fabrics.

Basically, for research purposes the specification of the fabrics selected should be known. But this was

difficult to secure, as it was some period since they had been processed.

The selected fabrics (listed in Table 5.2.01) were subjected to testing on KES-F and micro-fibre fabrics on FAST. The results are in Appendices VII and VIII, respectively.

Table 5.2.01

Woven fabrics selected for experiments.

Fabric code	Fabric type	Composition	Mass g/m ²	Remarks
A	Not used in RSTM	5 types in pucker test	See Appx.	Prelimin. testing
B	Suiting (plain)	Wool 45% Polyester 60%	138.6	Cream
C	Suiting (plain)	Wool 100%	173.7	Light Grey
D	Suiting (plain)	Wool 100%	173.7	Light Brown
F	Suiting (plain)	Wool 100%	249.1	Blue Grey
G	Suiting (twill)	Wool 35% Polyester 65%	202.8	Grey with strips
H	Suiting (plain)	Wool 45% Polyester 45%	166.1	Used only in SPMS
I	Suiting (twill)	Wool 100%	236.6	Brown
J	Suiting (twill)	Wool 100%	231.2	Dark Grey
K	Poplin (plain)	Cotton 55% Polyester 45%	108.5	Pink pale
L	Poplin (plain)	Cotton 100%	112.6	White
M	Poplin (plain)	Cotton 100%	107.0	Light Blue pale
N	Poplin (plain)	Cotton 30% Polyester 70%	104.5	Light Blue pale

O	Poplin (plain)	Cotton	100%	112.6	White
P	Oxford (pica)	Cotton	100%	171.8	Pink
Q	Suiting tropic	Wool Polyester	35% 65%	191.2	Grey.Fabric Standard
R	Suiting tropic	Wool Polyester	35% 65%	192.0	Navy.Fabric Standard
S	Lining	Acetate	100%	52.3	Oxford Blue
T	Lining	Polyester	100%	52.3	Olive
U	Lining	Polyester	100%	52.3	Maroon
V	Lining	Acetate	100%	95.7	Navy Blue
W	Lining	Acetate	100%	94.6	Dark Beige
X	Satin, Art.5200	Polyester	100%	160.0	MF, Oxford Blue, WR
Y	Twill, Art.JN23B	Nylon Polyester	30% 70%	129.0	MF, Beige, WR
Z	Taffeta, Art.L5W	Polyester	100%	144.0	Microfibre(MF) Green, WR

Note: Fabrics Q and R were called fabric "standards", and were used for basic experimentation related to the design, development and final evaluation of the system.

5.2.2. The test results of the selected sewing threads.

The threads for this work were provided by Rhein-Nadel GmbH in Germany and Gunzental Ltd (a local HK thread manufacturer). Tests were carried out at the Gunzental Laboratory in Hong Kong, where standard test methods were employed. The properties measured were:

- strength, tenacity and elongation, tested on an Uster Tensorapid CRE tester at 5000 mm/min , according to BS1932,

-twist according to BS2085, on a Shirley Twist tester; and

-thread count tested according to BS2010.

Table 5.2.02 below contains the test results of the sewing thread testing.

Table 5.2.02.
Sewing threads selected for experiments.
100P=100%polyester(S=spun); E.=elongation at..;

Characteristics and properties	No 1	No 2	No 3	No 4	No 5
Manufact.code	N569	N216	3655	3566	Rasant
Colour	White	White	Navy	Navy	Navy
Composition [%]	100SP	100SP	100SP	100SP	100P
Ticket No	36	120	120	100	75
Number of plies	3	2	2	2	2
Count [dtex]	nm	338	338	274	336
Strength [cN]	nm	980	1060	1080	1870
Tenacity[cN/tex]	nm	32.32	39.68	36.93	45.96
-cv [%]	nm	8.20	1.48	7.55	1.31
-95%(c.l.range)	nm	0.24	0.24	1.15	-
E. at break [%]	nm	15.0	20.7	13.8	21.5
E. at 400g [%]	nm	7.3	7.2	3.5	5.4
Twist [tpm]	nm	837	1163	818	669

Note: -"nm" means no measurement.

-for the purpose of the study, the above threads were denoted in the file name as a fifth-digit, according to the RSTM sewability coding system. See Appendix IIIa.

5.3. Experiment Series 1. Identification of single cycles.

As the digital acquisition processing system (RSTM_DAP) did not have any provision for a fifth signal to mark the start/end of a single cycle in a series, it was necessary to overcome this major disadvantage by analysis of the interaction of the RSTM signals. The time signal had to be acquired on one of the 4 existing A/D input channels and to be correlated with identifiable stable points on the traces of other signals, so that single cycles could be extracted from the series.

5.3.1. The distribution of the sewing thread tension at various speed levels.

The following tests were carried out on the standard fabric (test parameters are coded in the file name, according to the coding system, described in Section 3.4.4.2):

a. at the same 5th level of the thread tensioner scale: Tests RSTM/Q1743501-9.DAT and QI7400X1-9.DAT (18 tests). Thread tension level¹ pre-settings are highlighted in bold. Bold zero (6th digit) means, that there was no thread; only a test of inertia force),

b. other adjustment level eg: Q1723301-9.DAT(9 tests). In this case on the 3rd level of the thread tensioner adjustment.

¹ In the file coding system(see Appendix IIIb) the thread tension adjustment level is the 6-th digit. For example levels 5 and 3 correspond to 726 cN and 516 cN respectively. These values were established during static calibration of the thread tensioner, by use of the COAT's tensionmeter(43).

5.3.1.1. Establishing the end points of the signal.

In this experiment the single cycles of three RSTM tests were analysed with the aim of finding a specific, most stable point on one of the main signals, according to which the ends of the single cycle could be marked. The NTt signal was found to be adequate for this purpose.

The following series were acquired at the highest speed level 9: "Timer", 0001A119 and 0002A119. These tests had their thread signals acquired using a 1KHz filter on input. Figures 5.3.01-04 show the analysis of the four series of "Timer" tests (NPF, NTt, Timer1 and Timer2 signals) in window W7 and the magnification of the above signals in the other windows. Table 5.3.01 shows the location points (a-d) of 7 single cycles of the NTt signal marked in dp (system acquisition data points).

Table 5.3.01

Distance between a,b,c,d points [dp] on a NTt signal in 7 cycles.

cycle/ point no	c1	c2	c3	c4	c5	c6	c7
a	395	913	1416	1918	2424	2932	2925
b	411	919	1420	1922	2427	2938	2935
c	418	925	1427	1929	2434	2943	2943
d	433	939	1441	1943	2448	2956	2956
d-b	22	20	21	21	21	18	21
b-a	16	6	4	4	3	6	11

The distance d-b showed consistence approximately 20-21 data points from the TDC (Top Dead Centre) of the needle bar vertical displacement traces.

Also the other cycles were measured and the distance was found as follows:

C7=19; C8=20; C9=20; C10=21; C11=21; C12=21; C13=22;
C14=20; C15=21; C16=22; C17=21; C18=22 and C19=22.

The details of this investigation are presented in Figures 5.3.01-04 on DADiSP Worksheet. In window W7 of the Worksheet, the two timer signals Timer1 and Timer2 are visible. Timer1 is a square-wave signal coming from the QR-stop motor of the sewing machine. The Timer2 signal is generated by a magnetic proximity switch, installed in the vicinity of the sewing machine wheel. It marks every single cycle of the machine shaft revolution at the needle bar TDC. The width of the marked signal is 7 points out of the 500 points of the whole cycle. These signals were found very useful in identifying the start and the end of the cycle on the main traces of the signals.

It is important to note, that the Timer1 signal has a cycle initialisation point at the "moment when the needle enters the fabric"(123). This point is set subjectively by the technician as the beginning of the machine control programme. This subjectivity is sufficient for commercial sewing, but for the purpose of this study a second timer had to be developed, marking the TDC/BDC points of the needle bar movement. According to the Timer1 signal, this initialisation point (g) marked in Fig. 5.3.04 is on average 90 points after point (b).

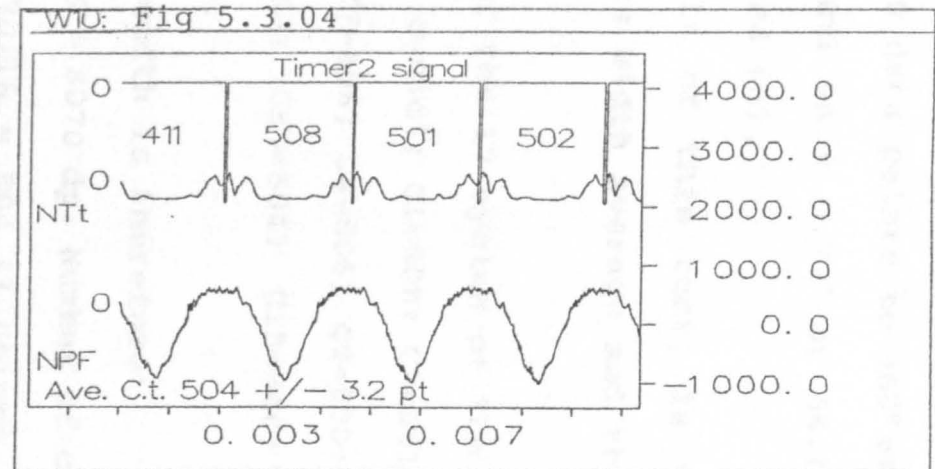
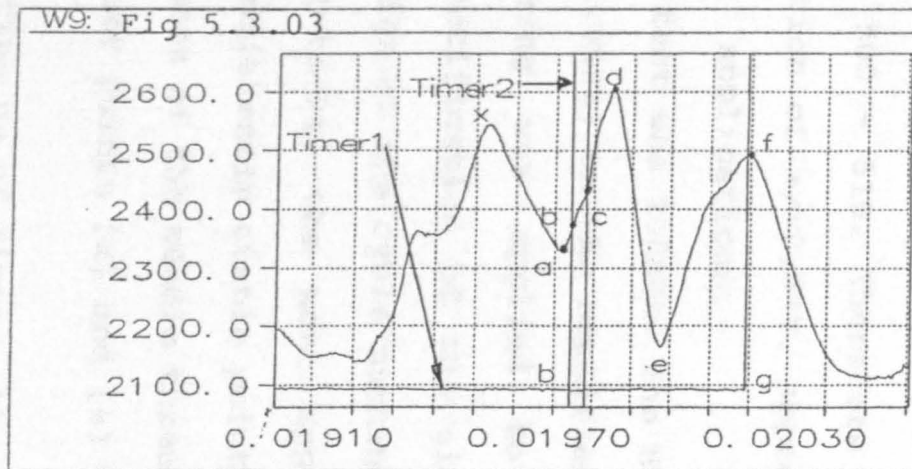
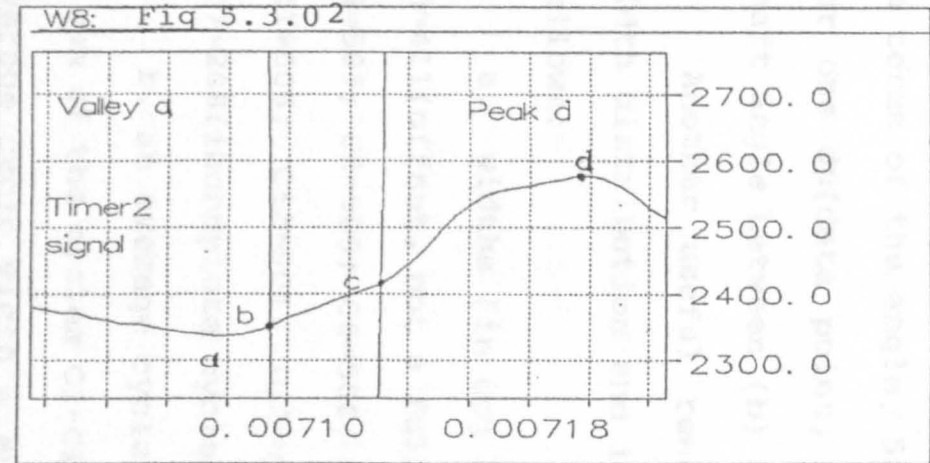
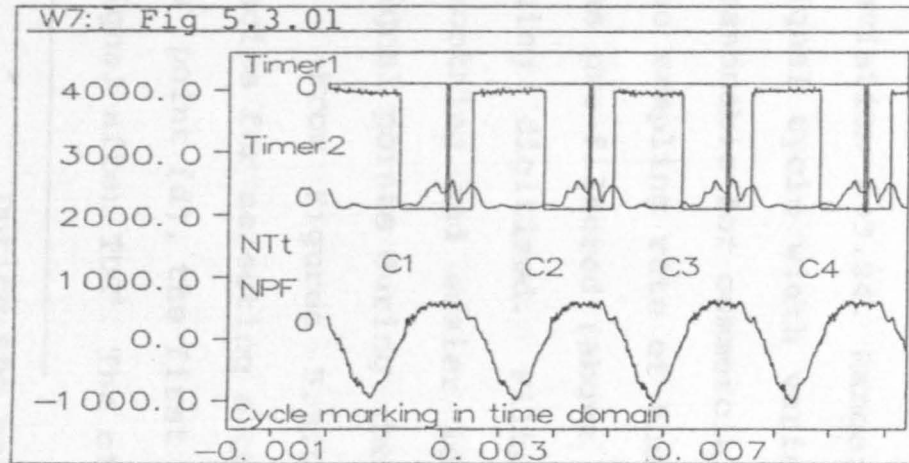


Fig. 5.3.01-04. An investigation into cycle marking method on NTt.

In terms of the angle, 500 data points to 360° means 0.72° per one dp(data point) and $90 \times 0.72^\circ$ or 64.8° for the shaft angle between (b) and (g).

Another useful result of this test, is the cycle width distribution and its width average and they are as follows:

a. widths [in dp] of the 17 cycles of the series:
 C0=411(offset, not a full cycle); C1=508; C2=501; C3=502;
 C4=505; C5=506; C6=508; C7=508; C8=506; C9=500; C10=501;
 C11=506; C12=504; C13=510; C14=504; C15=500; C16=501;
 C17=208(incomplete cycle).

b. an average cycle width is therefore:

A sum of the cycles C1-C16 = 8070 dp. Number of cycles 16.
 Average cycle width = $8070/16 = 504.37$ points. Standard deviation $\delta=3.24$. Range: 500 - 510. Therefore the max. signal cycle width variation of $\pm 0.64\%$, appears quite reasonable for commercial applications.

The sampling rate of the test was 200kHz. The NTt signal was pre-filtered (above 1.0kHz) on the amplifier, before being digitised. Filtering was applied to provide smoothing and easier identification of the significant signal points during design of the cycle marking method.

From Figures 5.3.01-to-04, the most appropriate choice for selecting a consistently stable point seems to be point (d), the first peak of the needle thread tension signal after TDC². The other points (x) and (a) were also

² During the setting up of Timer2, the TDC point was analysed and it was found to be approximately 5-7 points wide and rather flat in shape, without any

examined, but their angular distance from TDC was found to vary more than that of point (d).

The next step, was an investigation made during the second RSTM test 0001A119, which was carried out on the same fabric type and with the same machine setting. The speed range was again at the highest level of 5500 rpm. The objective of the experiment was two-fold, to correlate two similar series of thread tension, and to find out how the signals from individual cycles correlated with a full series of 16 cycles, assuming that the cycles were of the same length. After manually marking all the cycles of the full series the average cycle length was found to be 505.6dp with st.dev.=2.9dp. Two single cycles (500 points wide) were extracted from their own series and overplotted. Although a small difference in their amplitudes existed, nevertheless this was negligible (Fig. 5.3.05), where both single-cycle signals NTt1 (Test "Timer") and NTt2 (test 0001A119) were indistinguishable. The difference can be found in tabulated form (Fig. 5.2.06) in columns C.1 and C.2 respectively. Column C.3 contains data values of the Timer2 signal and column C.4 was added to show the NTt1 signal's neighbouring cycles. These three signals look as if they are overlaid and seem to form one continuous solid line.

distinguishable peak.

5.3.1.2. Checking the cycle marking procedure.

The above described cycle marking procedure was applied to the data of the two following RSTM tests and can be seen in Figure 5.3.01-04:

a. First test: RSTM 0001A119*:

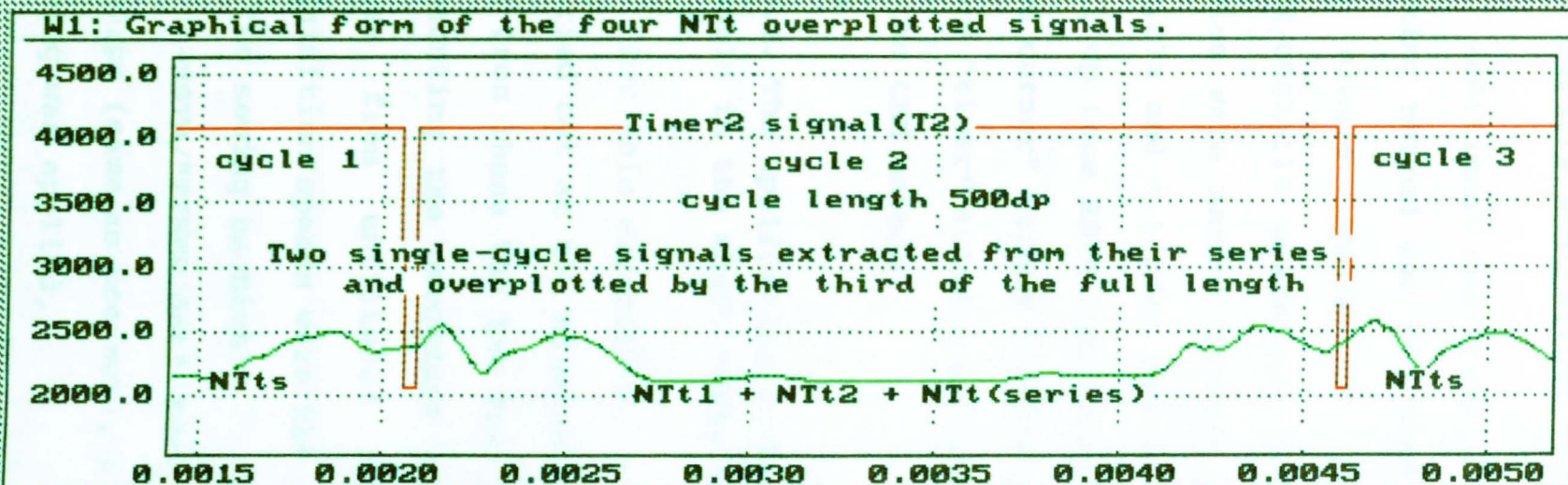
Fabric Q and sewing thread type 3 were used, with a stitch density of 32 stitches per 10 cm, presser foot pressure no 3, thread tension level 3, needle size 100, speed level 9 (5500 rpm). The cycle width was set in both tests as 500 dp. The NTt signal had been filtered on input (1KHz). This frequency level resulted in smoother and clearer signal characteristics, making the location of a "real peak" of the signal easier.

b. Second test: RSTM 0009A009*³:

The needle and thread were removed to test the vibration and inertia of the machine at the pre-set speed of 5500 rpm. The other parameters were exactly the same.

The procedure for peak location was followed. The two signals (NTt and NPF) for each test were overplotted in the same WS(Worksheet) window. The two crossed-hairs were manually manipulated and used alternately to locate consecutive d-peaks. The locations of the peaks were recorded and the 20 point distance was subtracted. The cycle width was then calculated. The start and end cycles which were marked had widths of 439 and 168 data points respectively. The full cycle widths are presented below:

³ *These two tests were acquired before the file coding system was fully developed and therefore their parameters are specially provided.



W2: The above four NTt signals in a tabulated form.

	1:5500/500/thr1	2:5449/500/thr1	3:5500/500/thr1	4:5500/500/thr1
1:	2368.00000000	2373.00000000	4095.00000000	2404.00000000
2:	2369.00000000	2379.00000000	4095.00000000	2396.00000000
3:	2368.00000000	2376.00000000	4095.00000000	2391.00000000
4:	2368.00000000	2378.00000000	4095.00000000	2383.00000000
5:	2368.00000000	2379.00000000	4095.00000000	2375.00000000
6:	2369.00000000	2380.00000000	4095.00000000	2363.00000000
7:	2368.00000000	2384.00000000	4095.00000000	2356.00000000
8:	2374.00000000	2394.00000000	4095.00000000	2343.00000000
9:	2380.00000000	2409.00000000	4095.00000000	2335.00000000
10:	2390.00000000	2431.00000000	4095.00000000	2324.00000000
11:	2405.00000000	2456.00000000	4095.00000000	2315.00000000

Fig.5.3.05-06. An example of the correctness of cycle marking methods in overplotting four signals.

C1: (d1-20)-d0=943-20=923-419=504; C2: 508; C3: 508; C4: 508; C5: 504; C6: 501; C7: 505; C8: 508; C9: 508; C10: 504; C11: 504; C12: 501; C13: 506; C14: 505; C15: =505;

Summary statistics: cycle mean length: 505.3,
Std.Dev.: 2.4,

Additional confirmation of the accuracy of the cycle marking method was provided by comparing the marking of the single cycles of the thread signals on the RSTM/0002A119 graphical traces, where five consecutive cycles were marked according to both methods (see Fig. 5.3.07a and 5.3.07b) and showed a "graphical difference" of 1 dp (one RSTM data point only). The DADiSp "crossed-line cursor" method (method 2) was, and is used in cases, where "timer" signals are acquired and it is indispensable in the CMM method.

5.3.2. The application of the cycle marking method to the signals in the shaft angle domain.

For this experiment, a total of six RSTM tests were carried out at the highest speed level(see Table 3.3.02) and from these the two following tests were selected for presenting the procedure of extracting the inertia and noise from unfiltered NPF signals, because their acquisition speeds were the closest to the pre-set speeds of the sewing machine:

-RSTM/"TIMER.dat" test. Fabric Q. Speed level was 5500rpm (same as pre-set), a "full load" type of specimen sewing was applied,

-RSTM/"0008A009.dat" ("Inertia" test). The test was "run" on fabric Q and its acquisition speed was closest to the preset speed (in its range of testing parameters). An "Inertia" test means that no needle was used and consequently there were no threads.

The test data of RSTM/"TIMER.dat" was acquired at the same speed as the preset, permitting direct comparison between the two tests.

Table 5.3.02.

RSTM tests selected for the NPF signal studies.

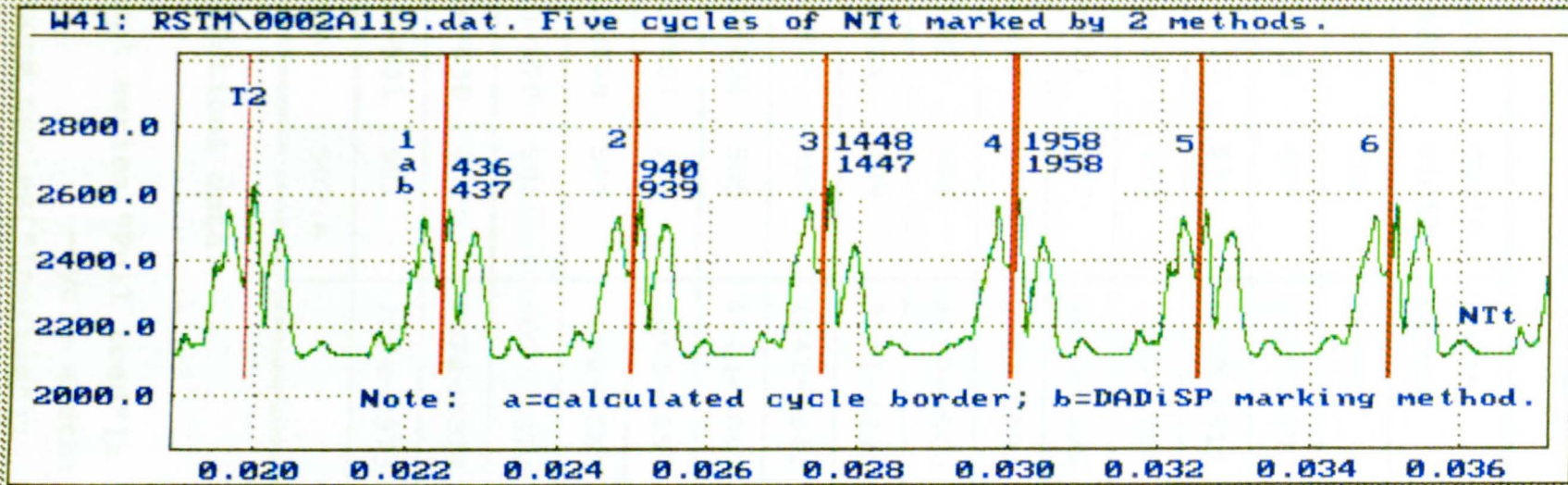
WSheet window	Test number	Speed in rpm	Ch.0 S.type	Ch.2 S.type	Ch.3 S.type
W1-W4	02A119 f.load	5485	1K/s2	T2	640 -1030
W9-W12	03A119 f.load	5486	1K/s2	T2	630 -1039
W17-W20	05A119 f.load	5485	1K/s2	CCM method	627 -1030
W25-W28 *select	08A009 inert.	5565	filter off	T2 on Ch.3	N.A.
W33-W36	01A119 f.load	5449	1K/s2	T2	633 -1037
W41-W46 *select	TIMER	5500	1K/s2	T2	632 -1026

Legend: DADiSP Worksheet with windows(W1,W2,...W100); Ch.0,2 and 3 - DAP channels No.0(NTt),2(PFp)and 3(NPF), into which time marking signals (T2=Timer2 or T1=Timer1) can be connected, by temporarily switching off one of four DAP main signals; Inert.-"inertia", when there is no needle inserted, as opposed to a "f.load" (full load) with needle and threads used; 1K/s2 -1kHz filter and thread transducer's amplifier sensitivity scale level (1-8). CMM -cycle marking method described in Section 5.3.1.1.

The DAP data acquisition software recorded data points as functions of time. Due to irregular cycle widths in a series (they differ +/-10dp out of 500dp per one cycle), any analysis of the distribution of the signal required transformation to a common variable, which in this case was the needle displacement expressed in terms of shaft angle.

In the case of the RSTM hardware this task was not straightforward. The obstacle was the lack of a 5th channel, described earlier. In the analysis of a single cycle of the 8192 dp long series the following procedure was applied:

- a. overlapping a NPF signal with a timer signal,
- b. marking the offsets on both ends according to the TDC points of the timer signal,
- c. removing the offsets, by extracting the remaining series of the full cycles (see Fig. 5.3.08.W5),
- d. marking the individual cycles (as in Table 5.3.03), breaking the series into single cycles, and placing them in separate windows,
- e. adding all the widths of the single cycles widths and finding the cycle mean width (Fig. 5.3.08.W8, time domain),
- f. converting the cycle length (X-axis) to a 360° angular length and removing the "tail" (the end part of a series exceeding 500 data points or 360 degrees, which usually exists, because cycles are of an unequal width).



W49: The tabulated form of the two above signals (NTt and Timer2).

	1:5485/500/thr1	2:5485/500/thr1		
430:	2343.00000000	4095.00000000		
431:	2343.00000000	4095.00000000		
432:	2347.00000000	4095.00000000		
433:	2350.00000000	4095.00000000		
434:	2353.00000000	4095.00000000		
435:	2358.00000000	4095.00000000		
436:	2362.00000000	2048.00000000		
437:	2366.00000000	2049.00000000		
438:	2368.00000000	2048.00000000		
439:	2370.00000000	2049.00000000		
440:	2370.00000000	2049.00000000		

Fig. 5.3.07. An example of signal cycle marking by two different methods.

Table 5.3.03. Investigation of the NPF signal distribution.

Legend: WSheet-DADiSP Worksheet cycle windows (C1-W17);
First 3 Col. =TIMER series; Col. 4-6=0008A009 series.

WSheet window	Cycle width	Cycle range	WSheet window	Cycle width	Cycle range
C1-W17	509	1-509	C1-W33	507	1-507
C2-W18	499	510-1009	C2-W34	503	508-1010
C3-W19	501	1010-1511	C3-W35	500	1011-1511
C4-W20	505	1512-2017	C4-W36	502	1512-2014
C5-W21	507	2018-2525	C5-W37	508	2015-2523
C6-W22	508	2526-3034	C6-W38	507	2524-3031
C7-W23	505	3035-3540	C7-W39	504	3032-3536
C8-W24	499	3541-4040	C8-W40	502	3537-4039
C9-W25	500	4041-4541	C9-W41	500	4040-4540
C10-W26	505	4542-5047	C10-W42	503	4541-5044
C11-W27	501	5048-5559	C11-W43	508	5045-5553
C12-W28	509	5560-6069	C12-W44	504	5554-6059
C13-W29	503	6070-7573	C13-W45	502	6060-6562
C14-W30	499	7574-7073	C14-W46	501	6563-7064
C15-W31	501	7074-7575	C15-W47	503	7065-7562
Mean	503.6			503.6	

Statistical data:

-First series("Full load"):

-cycle width: Mean 503.6; Std.dev.=2.7;

-Second series("Inertia"):

-cycle width: Mean 503.6; Std.dev.=3.6;

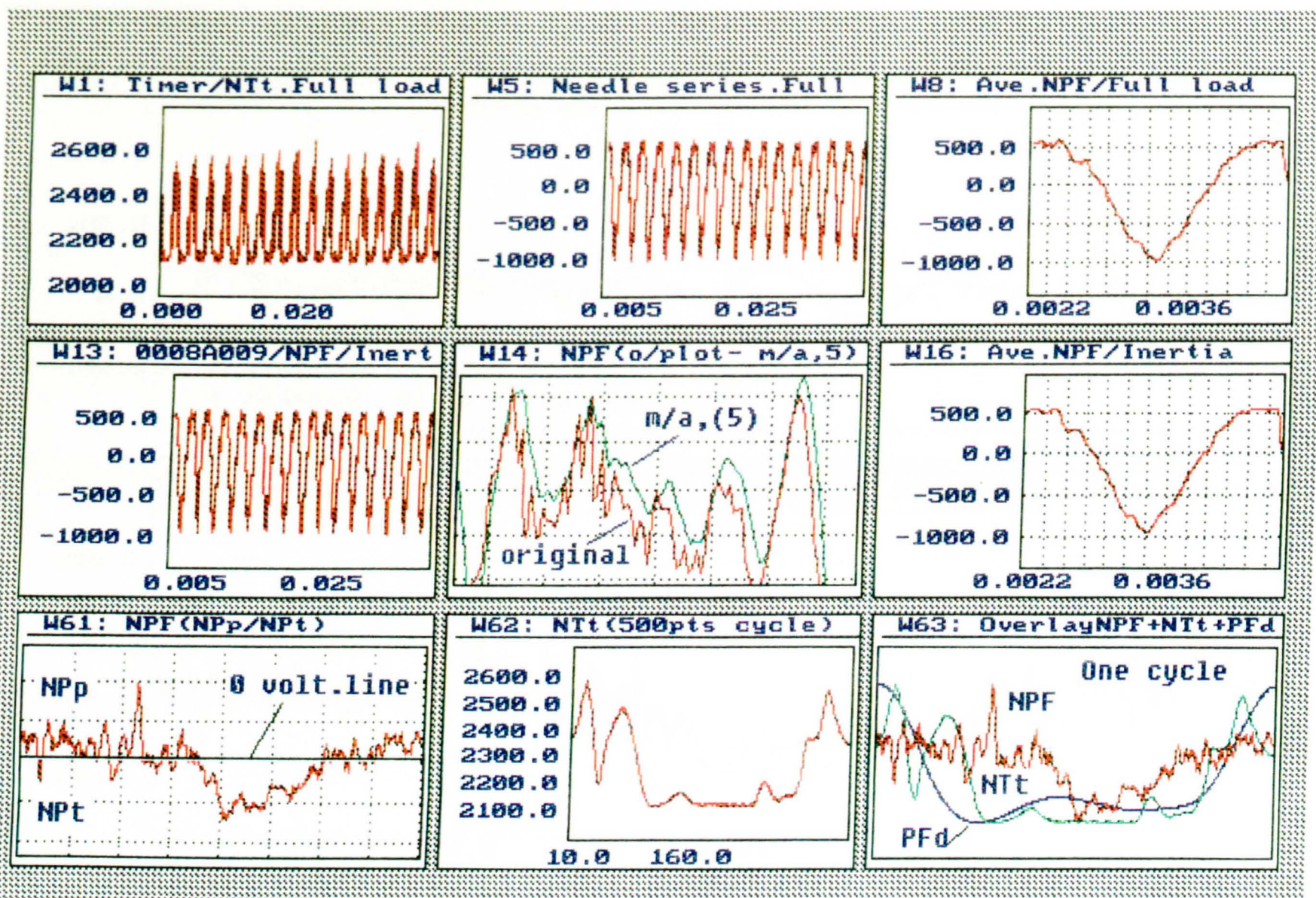


Fig. 5.3.08. The procedure of extracting NPF signal and converting it from time to shaft angle domain (example).

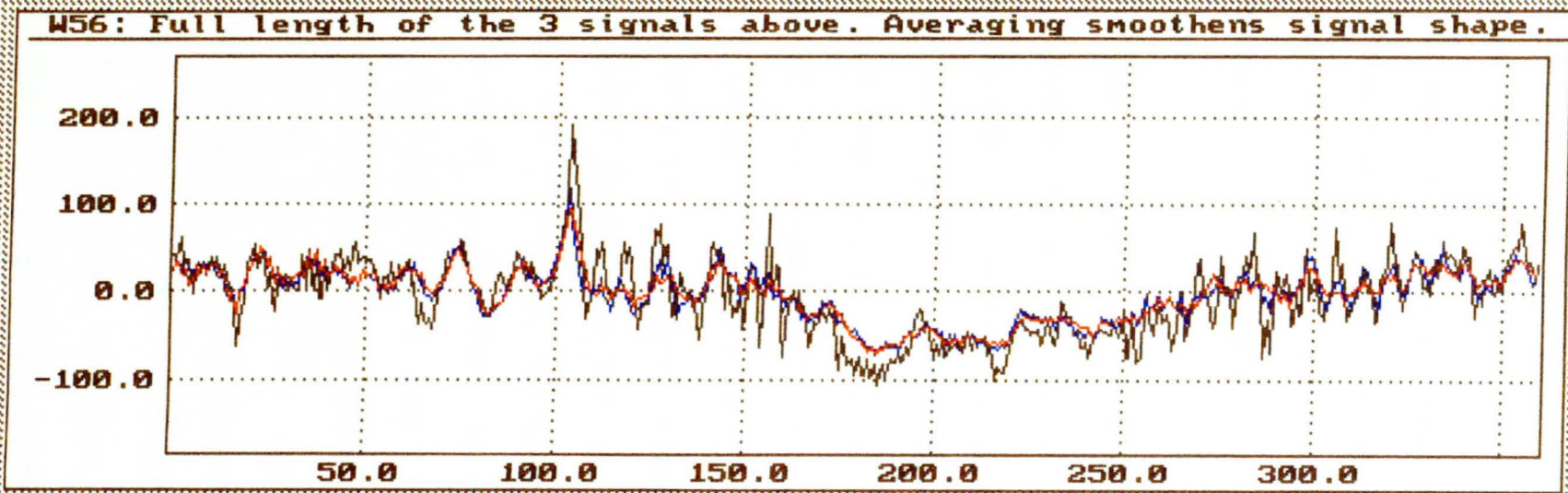
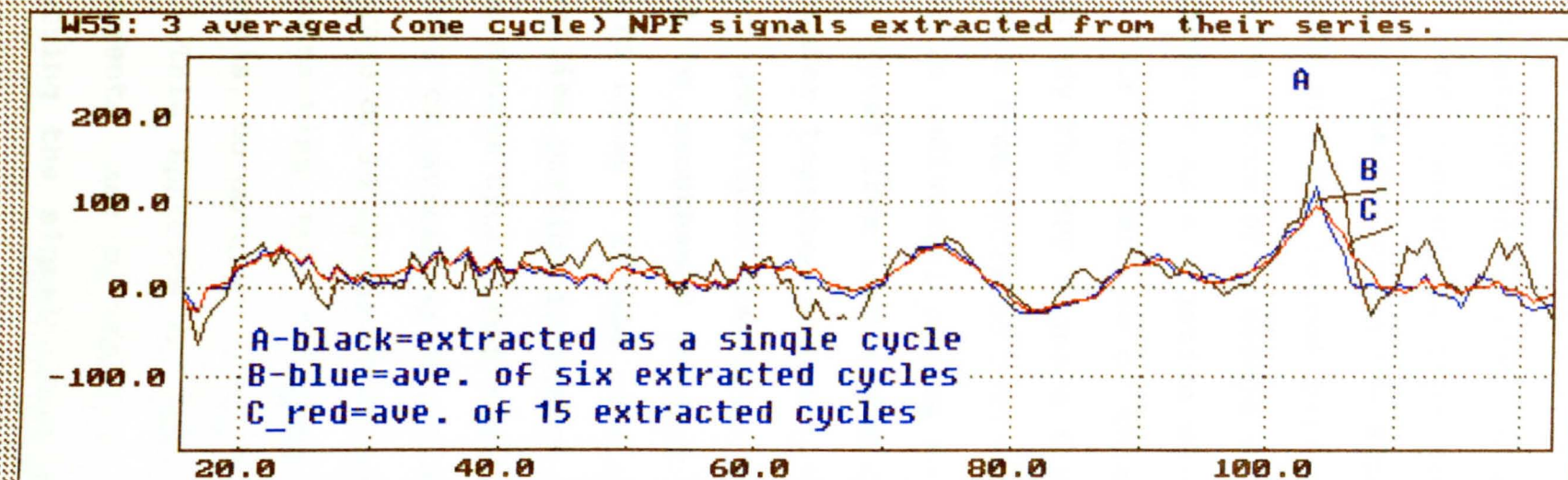


Fig. 5.3.09. An example of smoothing the signal by averaging it from the longer series.

The same steps as above were also applied to the "Inertia signal" (RSTM/008A009, see W13). The resultant NPF signal in W61 window of Fig.5.3.08, is the signal resulting from a subtraction of the two averaged 1-cycle signals (W8-W16) and converting them to an angular x-axis. The top part of the W61 shows the NPP (needle penetration pressure force) and the bottom part is a NPT (needle penetration tension force or a needle withdrawal force, marked by the transducer as a negative voltage).

For the purpose of this study, it will be necessary to study the NPF signals for features that are genuinely present from cycle to cycle and to ignore features present only in individual cycles as a result of random noise. If the traces from individual cycles are averaged by adding a number together and dividing by the number of cycles, real, persistent features will remain and random noise will be smoothed towards an average of zero. Figure 5.3.09 shows 3 traces over one cycle in window W56 and a magnified portion in window W55. Here curve A, in black, is a single cycle, not averaged. Curve B, in blue, is the result of averaging 3 cycles and curve C, in red, the average of 16 cycles. Each of these curves was obtained by subtracting the "inertia" signals from "full load" signals, to obtain the needle penetration force alone.

This approach of smoothing, derived from physical arguments, may be compared with the signal obtained by plotting the signal after applying a five-point moving average method of smoothing. The result is plotted in

Figure 5.3.08(W14). It is clear that the method introduces a displacement along the time axis and distorts the shape of the signal.

5.4. Experiment Series 2. Effect of increasing speed on the dynamic interaction of the signals using the same fabric type.

The purpose of this series of experiments was to investigate the effect of increasing speed on the measured signals. In this series of experiments, the same type of fabric was used for comparability.

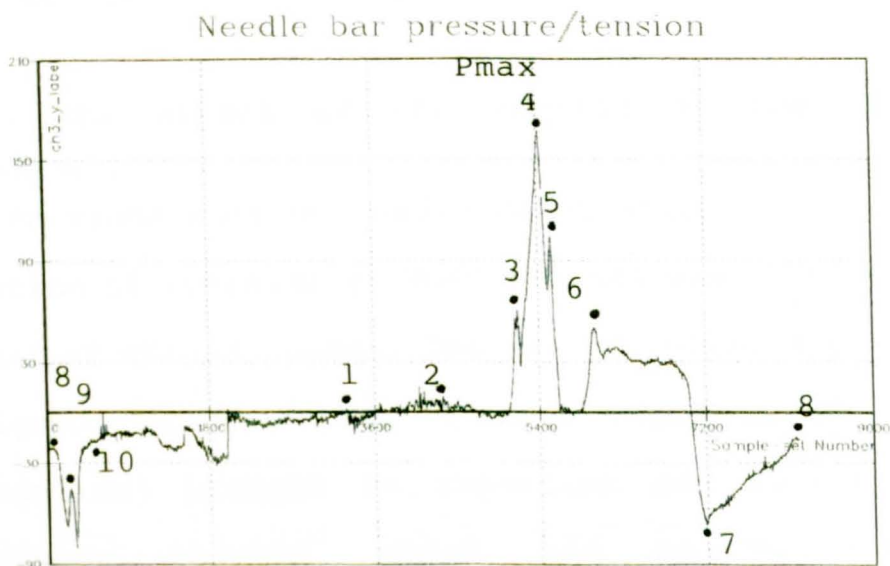
5.4.1. The characteristics of the needle penetration force signal.

At first sight, the shape of the NPF signal with inertia subtracted, looks considerably different from the forms presented by other researchers. The difference comes from the very high signal resolution provided by the RSTM system, allowing a range of higher frequency dynamic forces to be included, which could have been smoothed out in previous research. The highest number of data points per cycle was acquired at the speed of 200 rpm (Fig.5.3.10). Instead of a routine 500 dp per cycle, the acquisition was preset to the max 8192 data points, to be acquired for one cycle only, by tapping QR's initialization button once (it is seen in the beginning of the graph, where the signal trace between p8-p10 is rather different from that on p7-p8). The speed was in the range of 180-200 rpm (180 rpm is the slowest speed level which can be preset on the Pfaff-563).

In this experiment, the NPF signal contained the highest number of data points per cycle reported so far. The very high resolution provided a precise detailed shape of the needle penetration force consisting of NPFp (pressure shown by a positive voltage above the zero voltage line) and NPFT (tension, i.e., needle withdrawal force, below the zero line, represented by negative voltage). The characteristic points represented in Fig. 5.4.01 are as follows:

- 1-needle at the TDC position starting to move down;
- 2-QR's initialisation point, 3-needle point enters the fabric; 4-needle eye enters the fabric, which results in the maximum pressure peak(Pmax); 5-scarf penetration; 6-frictional forces on the shank of the needle; 7-needle at the lowest position; 8-scarf withdrawal; 9-eye withdrawal; 10-point withdrawal.

- The characteristic points of Fig. 5.4.02 describe the signal(yellow) of the needle penetration force which is derived from the NPF "full load"(red) by subtracting the NPF "Inertia signal"(blue). The cycles are marked by two time signals, Timer2(black) and Timer1(not shown). Total cycle width is 480 dp. The Timer1 signal marks QR's programme initialisation points (i). The (i) in the middle cycle is marked as point 2. The beginning of the cycle is marked as point 1 (when the needle starts leaving the TDC in a downward direction); points 3,4 and 5 are the same as in the figure above. Point 6 marks the start of frictional forces exerted on the needle shank.

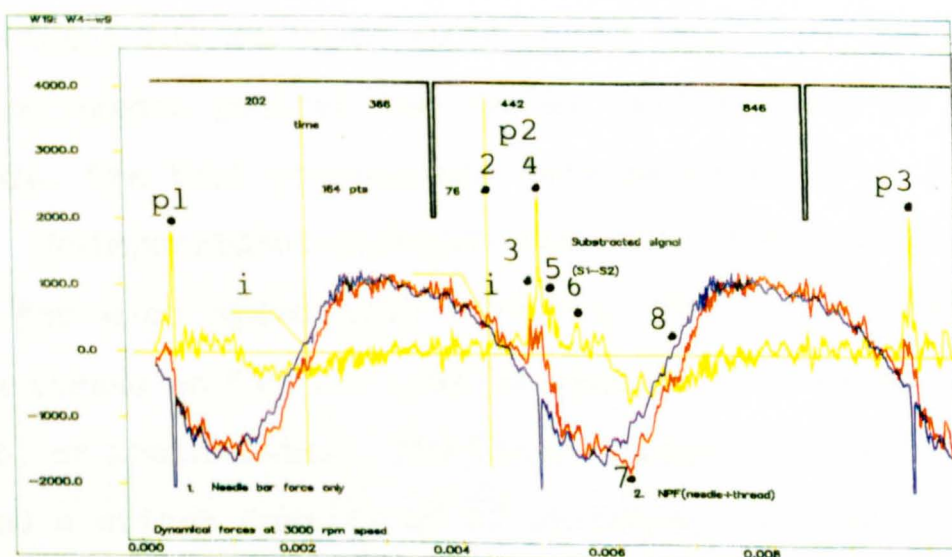


HONG KONG POLYTECHNIC - Institute of Textiles and Clothing
 RSTM Sewability Test Graphical Results (Test No. 302/31/1/30/30, 0)
 Associated files:
 Speed = 3000 rpm *
 05/26/92 16:28:03

* actual acquisition was at 200 rpm.

Fig. 5.4.01. The highest resolution of the single cycle NPF signal at 200 rpm.

Fig. 5.4.02. The characteristic points of the NPF signal at 3000 rpm speed.



Point 7 is the lowest NPF signal position. At point 8, the needle point left the fabric. Points 1 and 3 represent the peaks of the neighbouring cycles.

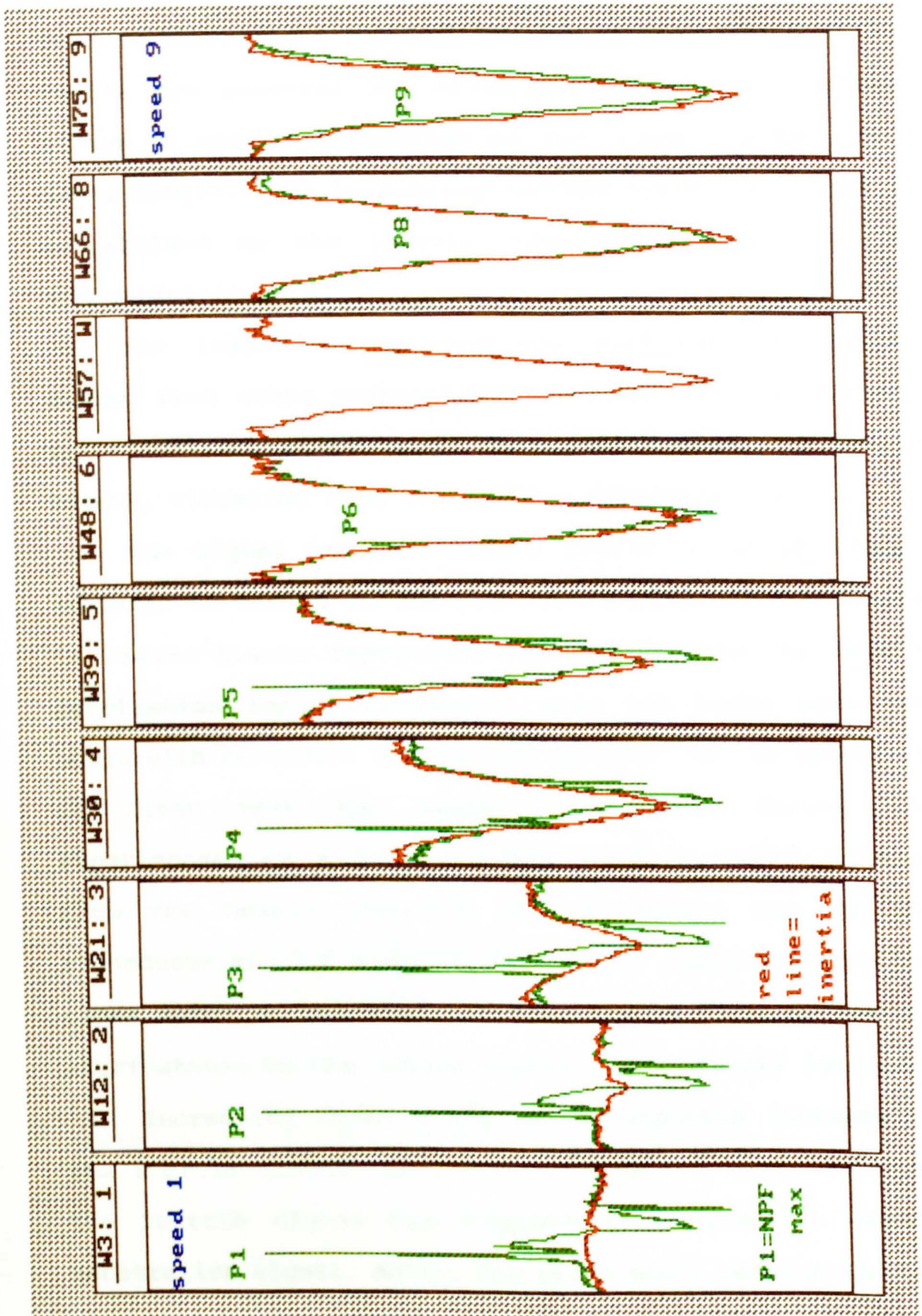
5.4.2. The effect of the inertia of the needle bar transducer.

Previous work on needle penetration forces, with the exception of research in NCSU (57,58) was carried out with the use of strain gauges. The use of piezo-quartz sensors (designed for measuring dynamic impulses of very high frequencies) brought an important new factor, that of transducer inertia, which had to be taken into consideration in the design of the system. The transducers (in the case of the RSTM) are inserted into the needle bar and presser-foot bar respectively. Their responses to the dynamic forces include an inertia component, which changes with the sewing machine speed. Examples of signal traces are shown in Fig. 5.4.01 and Fig. 5.4.02. The current experiment was designed to show the traces of the signals of the needle penetration forces (NPF signal) at various speeds. The test presettings were as follows:

-RSTM/0021Q301-0029Q309.dat. Nine tests were carried out for each speed level. Fabric "Q" (2-ply) was used, with thread no "3"(120 spun/polyester) and needle code "0" (100, of Rhein-Nadel). The thread tension was set at level 3 and a stitch density of 32 stitches/10cm was selected.

The 9-window WSheet Fig.5.4.03 contains the NPF signals together with the effects of the inertia of the system.

Fig. 5.4.03. The effect of inertia force on the needle penetration signal. NPF signal (green colour); Inertia force signal (red colour).



The NPF signal trace acquired at 200 rpm machine speed (green line) is similar to the signal shown in Fig. 5.4.01. The maximum peak of the signal is a point of the needle eye penetration through the fabric and appears always at the same location of the signal in the shaft angle domain. With increasing machine speed, this peak is overwhelmed by the inertia force, which is close to sinusoidal in form.

The jagged places show the existence of changes coming from other components, friction with the thread, frictional forces due to the needle penetrating the fabric layers, vibration from the machine mechanism, etc.

The signal in W3 is of a single cycle of 500dp, compared to 8192dp in the previous example. The red line in Figure 5.4.03 represents the signal from the needle penetration force transducers when the tests were run again with no needle (or thread) present. At low speed, it is clear that the needle penetration forces are superimposed on a low amplitude inertia signal arising from the masses attached to the needle bar by the transducer sensing element. It is also apparent, from the close match of the signals, that the additional inertia attributable to the needle itself can be safely ignored.

Increasing speed produces the expected increase in the inertia signal, until, by a speed of about 3000rpm, the inertia signal has completely swamped the needle penetration signal. Again, the close match between the two signals suggests that the inertia of the needle itself can

be neglected. The inertia signal is omitted from window W57 (4000rpm) due to a corrupted diskette on which the missing data were recorded.

Subtraction of the inertia signal from the full load signal permits the needle penetration force itself to be extracted from the data.

This interpretation of the RSTM data and its meaningful signal analysis (with the use of DADiSP software capability) is based on the following assumptions:

-firstly, that single components of the stitch formation process are specified,

-secondly, that the possibility of signal manipulation during the process of analysis is left open.

The following components(C) are involved in stitch formation:

- 8-influence from other factors(vibration of the machine itself, etc),
- 7-needle bar transducer system,
- 6-needle bar,
- 5-presser-foot,
- 4-feed-dog mechanism,
- 3-fabric(-s),
- 2-needle,
- 1-threads.

-RSTM signals (S) acquired by the DAP programme:

$$S1=C_8+C_7+C_6+C_5+C_4+C_3+C_2+C_1,$$

$$S2=C_8+C_7+C_6+C_5+C_4+C_3+C_2,$$

$$S3=C_8+C_7+C_6+C_5+C_4+C_3,$$

$$S4=C_8+C_7+C_6,$$

$$S5=C_8+C_7+C_6+C_2,$$

-NPF signals calculated(extracted):

$$\text{-Signal EPNFA} = S1-S4=C_5+C_4+C_3+C_2+C_1,$$

$$\text{-Signal ENPFB} = S1-S3=C_2+C_1,$$

$$\text{-Signal ENPFC} = S2-S3=C_2,$$

$$\text{-Signal ENPFD} = S2-S5=C_5+C_4+C_3,$$

-where:

the signal name ENPF(A,B,C,D) stands for the extracted needle penetration force A,B,C,D and contains the following components:

-ENPFA-components included in the NPF, during stitch formation, after extracting inertia + other noise,

-ENPFB-components left - the needle + thread,

-ENPFC-component left - the needle itself,

-ENPFD-component of the inertia of the needle-bar system in the NPF signal. In theory, it can lead to the calculation of the pure needle penetration forces for analysis of the needle behaviour.

However, in practice, this can contribute to an increase in the errors already present in the original data (the acquired data contains a small variation in the machine speeds and also Pfaff's QR electronic control system did not precisely mark the widths of cycles at higher speeds). The method of single cycle initial extraction from the acquired series of 15-17 cycles (by denoting, extracting offsets and single cycles, and approximating them) could have compounded this initial error during further analysis. Therefore in this research, further manipulations of the NPF single cycle signals were limited to the first subtraction, e.g. S1-S4 or S1-S3.

5.4.3. The effect of increasing speed on needle penetration force.

The signals shown in Figure 5.4.04 are the result of subtracting the inertia signals from the full load signals, shown in Figure 5.4.03. The signal in window W61 is missing as the inertia trace was unavailable for this machine speed.

Examination of the traces shows that the peaks corresponding to the needle point and needle eye entering the fabric are almost unaffected by the increasing machine speed.

The broad peak, corresponding to frictional forces on the shank of the needle, increases in amplitude at the needle eye penetration point at the highest speeds. The NPF of one layer of carbon paper shows that P_{max} at the Ne point has a wide bold peak (W7) or a split one as in the window W52 of Fig. 5.4.05 and in the needle shank area the extracted signals show some similarity with small peaks (see also Table 5.4.01). This is to be expected, as dynamic frictional forces increase rapidly with the increasing speed between the frictional elements. Similarly, the peaks of the withdrawal force increase in amplitude with the increasing machine speed. This is for the same reason, as withdrawal forces are caused largely by friction between the needle and the fabric.

The frictional forces will be caused partly by the needle thread, which suffers frictional drag from the needle and from the fabric.

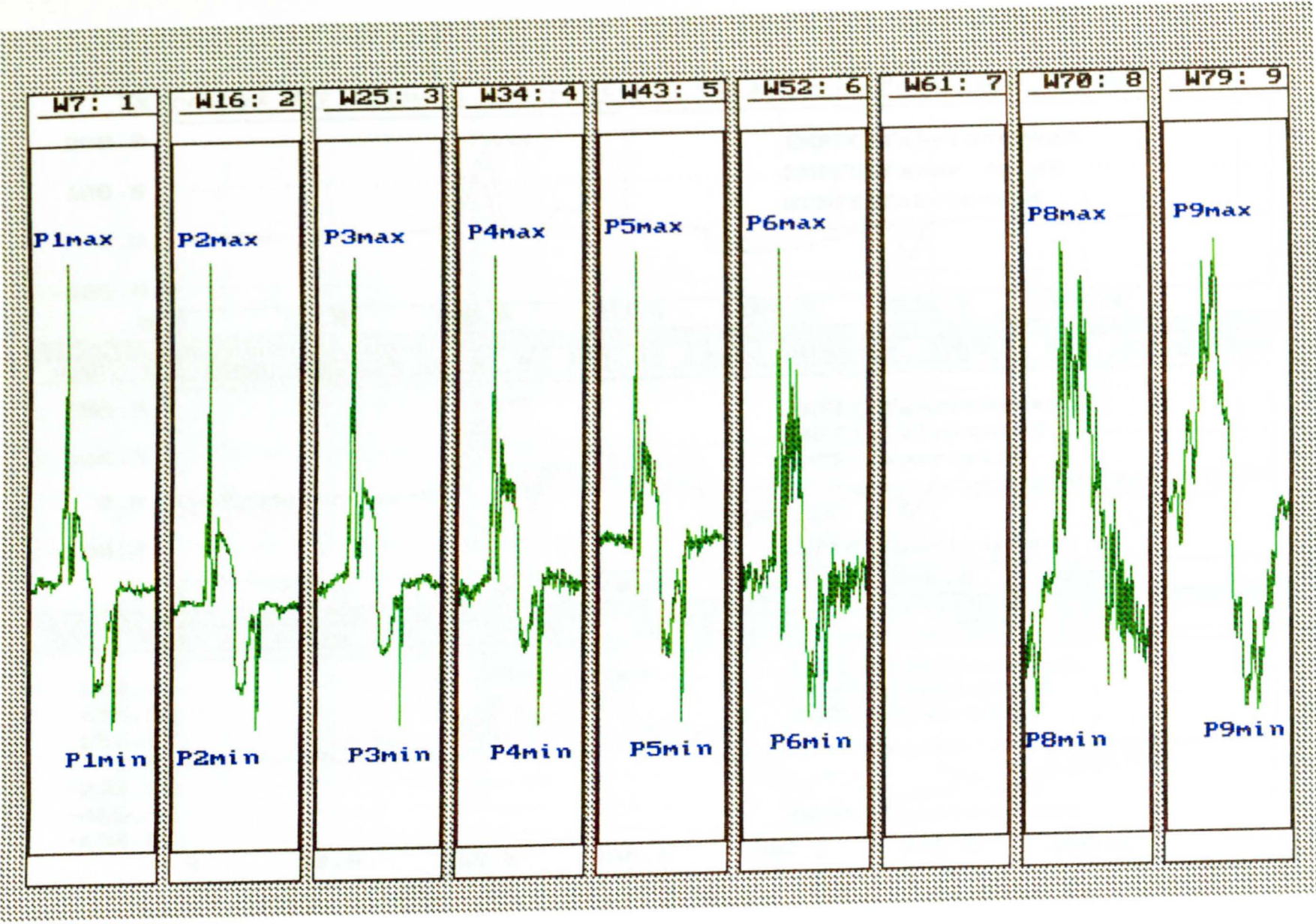


Fig. 5.4.04. Extracted NPF signal at various speeds.

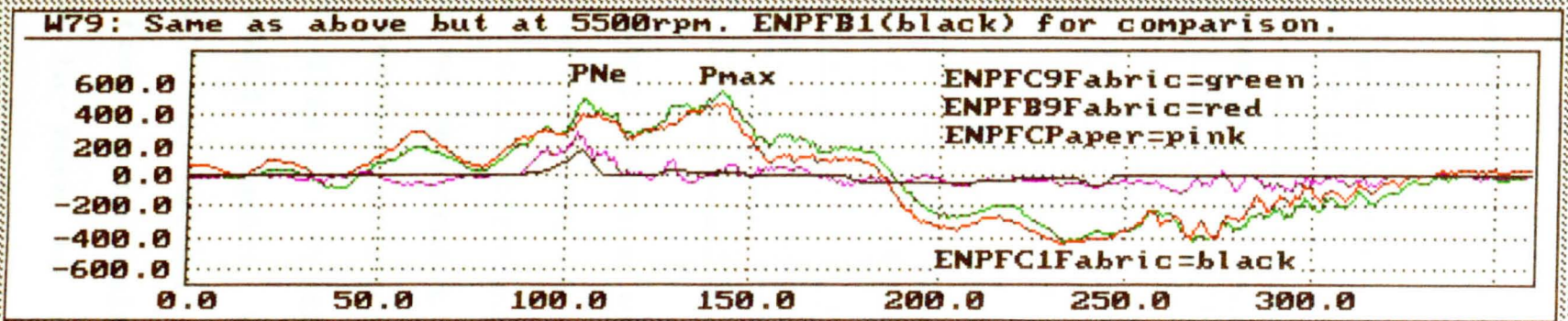
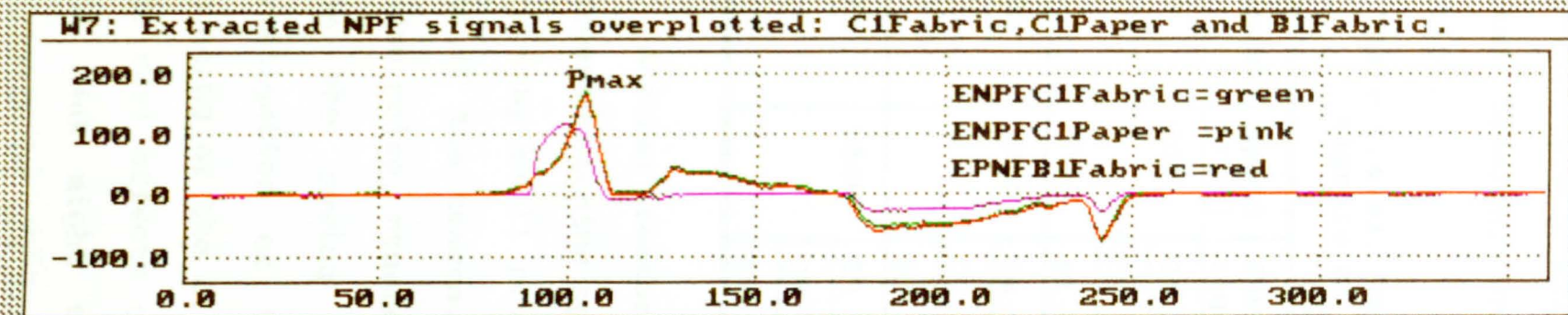


Fig. 5.4.05. Overplotting of the three extracted NPF signals for the fabric and paper at 3 speed levels. (Yaxis=[dp]; Xaxis=shaft angle[degrees]).

These frictional forces will increase with the sewing machine speed. The frictional forces between the needle and the thread will depend partly also on the needle thread tension, which will be discussed in the next section.

**Table 5.4.01. The variation of the 3 extracted NPF signals at 3 speed levels. Pmax in dp.
(See also Fig.5.4.05).**

Window	Speed [rpm]	ENPF signal	Pmax (at Ne)	Pmax (at Ns; shank)	% Pmax Ns:Ne
W7	200	C1 Fabric	169.8	48.3	28.4
		C1 Paper	118.8	3.0	2.5
		B1 Fabric	165.0	43.6	26.4
W52	3000	C6 Fabric	158.7	102.5	64.5
		C6 Paper	155.7	109.4	70.2
		B6 Fabric	150.9	67.6	44.4
W79	5500	C9 Fabric	497.2	545.7	109.8
		C9 Paper	293.5	118.5	40.3
		B9 Fabric	383.8	471.7	122.9

Another feature of the signals that appears with increased machine speed is the increasing amplitude of the very many small peaks, or spikes, that occur throughout most of the traces. Some of these may be the result of random noise, others of vibrations and resonances arising from the sewing machine mechanism itself. Further investigation of these components would require the averaging of the signals from many individual cycles, so that real effects could be separated from random noise. Each peak might then be attributed in turn to the operation of particular parts of the sewing machine.

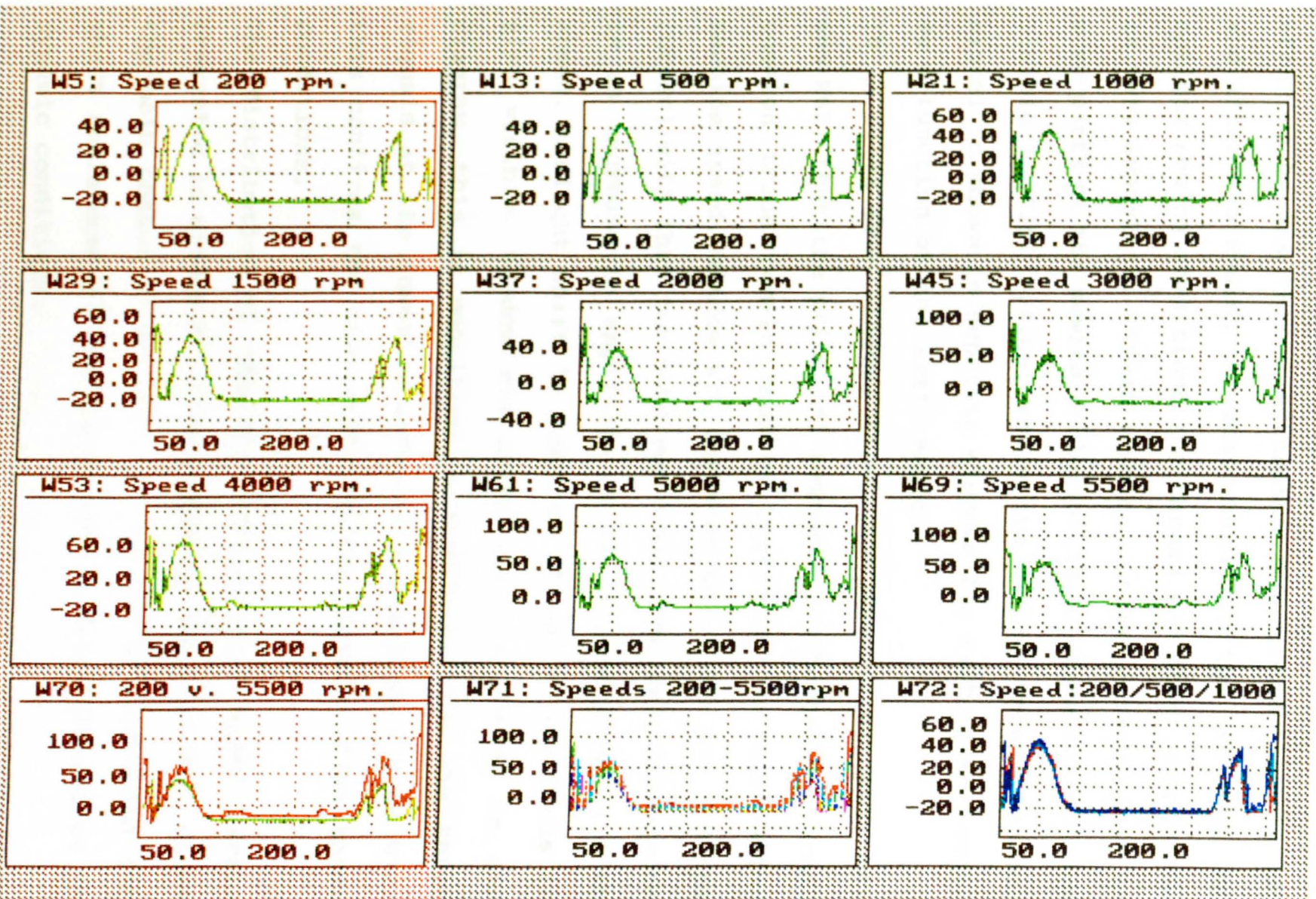
In principle, this might permit the re-design of individual components, such as cams, to give smoother operation at high speeds. Such a study is beyond the scope of the present work.

A comparison between the needle penetration force signals is shown also in Figure 5.4.05, in which signals obtained at different speeds are overplotted. Some of the new peaks occurring at the highest speeds in the parts of the signals caused by friction, appear to shift their location with respect to needle position. This effect would require considerable additional explanation for confirmation and for its causes(if real) to be determined.

5.4.4. The distribution of the needle thread tension with speed increases.

The tensile strength of a sewing thread after sewing is of significant importance to the final seam strength. During the formation of a stitch, the sewing thread undergoes a series of tugs as it is pulled backwards and forwards through the needle(29,49,51,58,128) and also is subjected to many frictional forces on its way from the thread feeding cone(guide bars, tensioning devices, friction of one thread against another, friction from bobbin case etc). Research on the amount of strength lost shows that this loss amounts to up to 50% of the original value, before sewing(27,29).

Fig. 5.4.06. The needle thread tension (NTT signal) at different speed levels in shaft angle domain.



Dynamic changes, particularly at higher speeds, may also cause another problem in a seam; its appearance may be affected by the thread extension and contraction during and after the sewing process. Therefore the setting of optimum sewing conditions for thread and other components is very important. Thread tension changes considerably in some parts of the sewing cycle(127,128). These changes are visible in Fig. 5.4.06, where the sewing thread tension signal is shown in separate windows for each speed level, as a function of the shaft angle.

It is clear from windows W5,W13,W21,W29,W37,W45,W53, W61 and W69, that the principal features of the needle thread tension trace remain broadly unaffected by increasing machine speed. Window W70 compares the trace for 200 rpm (green) with that for 5500 rpm (red). The main difference is an increase in amplitude of the thread tension with speed. A slight shift in position of one of the peaks is also visible. Window W71 plots all the traces on one diagram, this is magnified in Figure 5.4.07. The three signals at the lowest speeds are plotted in window W72; this confirms the similarity of the signals under these conditions.

The distribution of the NTt signals at 9 speed levels presented in window W71 (the window of Fig. 5.4.07), shows the main phases (I to VII) of the stitch formation (in shaft angle domain) and the thread tension variations in dynamic conditions.

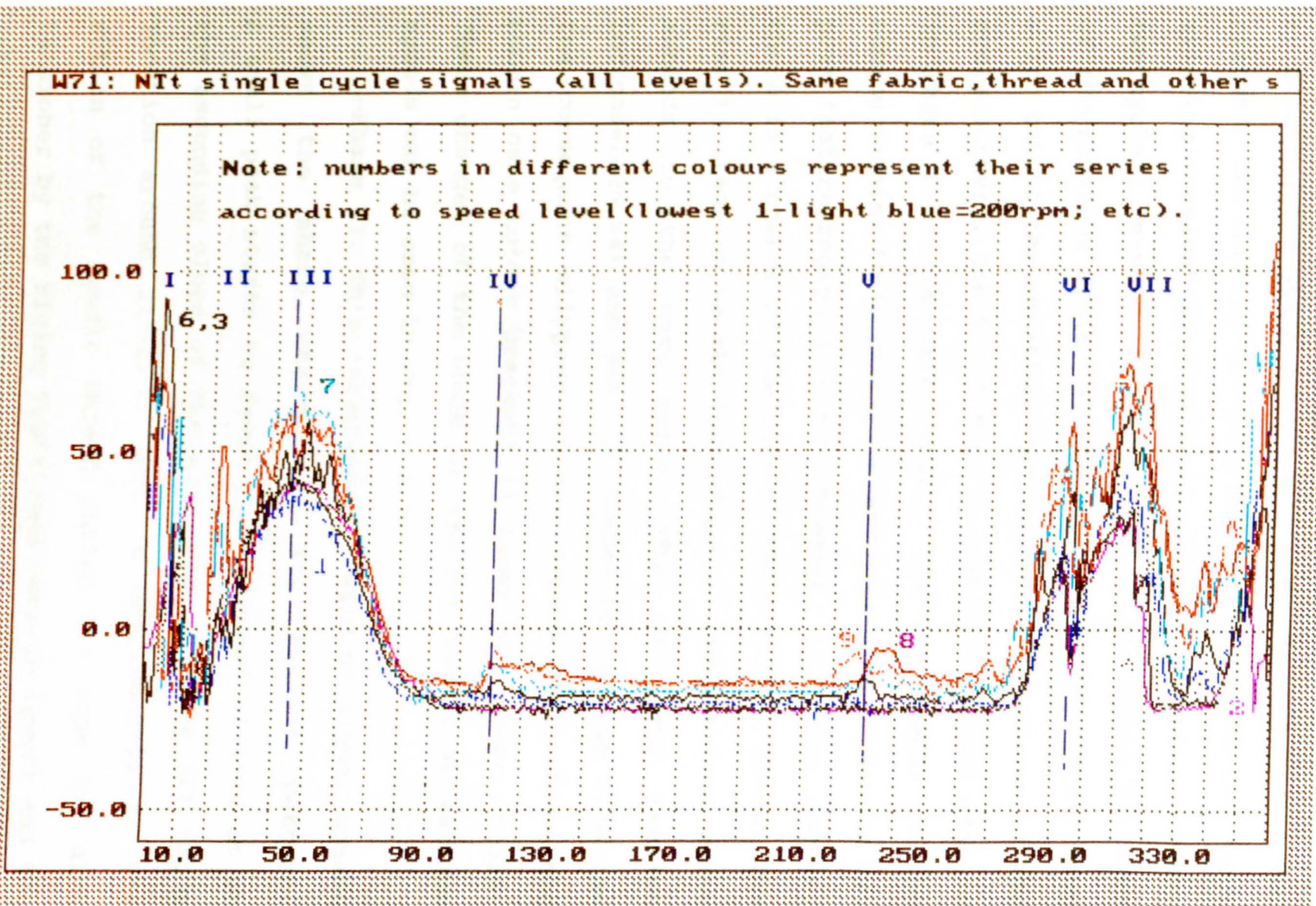


Fig. 5.4.07. Needle thread signal distribution at 9 speed levels with a marked phases of importance.

-Phase I. First multipeak between 0° (end of the TDC's 7degree-wide plateau)- 15° (valley after the first peak). By choosing the start of the cycle as the end of the TDC plateau, the usually two-part multipeak (called the "hook slipping tension" by Kamata et al(49)) is split between two cycles, leaving the first peak in the Phase VII area of the previous cycle. During this phase the thread loop slips out of the rotating hook section jib (almost at the cycle border). See W1 of Fig. 5.4.08. The second peak is in Phase I of the next cycle. For low speeds of the sewing machine it is characterised as a clear, smooth two peak feature(region 11° - 13°). However, at higher speeds, there is a change of the signal shape in this phase. The rise in tension in the last phase of the previous cycle extends to the next cycle. This multipeak tension increase(W25,w41 and W65) is caused by the Tup rise and the consequent slippage of the thread loop (from the bobbin case holder bracket) is lower at lower speeds. These changes of the shape of the Ntt signal at various speeds can be seen in Fig. 5.4.08.

-Phase II. This intermediate phase at higher speeds shows the sharp changes in the tension pattern. A small peak starts to develop at a speed of 1500rpm on the ascending slope of the wide peak of Phase III (at a location around 21° - 23°). This is attributable to the action of the needle thread pulled out from the disk tensioner by the rising Tup(thread take-up lever) and the action of the Cs, which supplies thread to absorb the

rising thread tension during upward movement of the Tup (visible in Figs. 5.4.06 and 5.4.08).

-Phase III. The peak tension varies according to the speed level. The peak values of the NTt signal of Phase VII(B) become higher earlier (at level 6*) than the NTt of Phase III(A) which reached its maximum at level 9. All the speeds from level 6 upwards are marked by an asterix. The dynamic conditions increase the "hook slipping tension" (49,51,128) of the needle thread (thread slipping from the case holder position bracket first and from the jib of the rotating hook after).

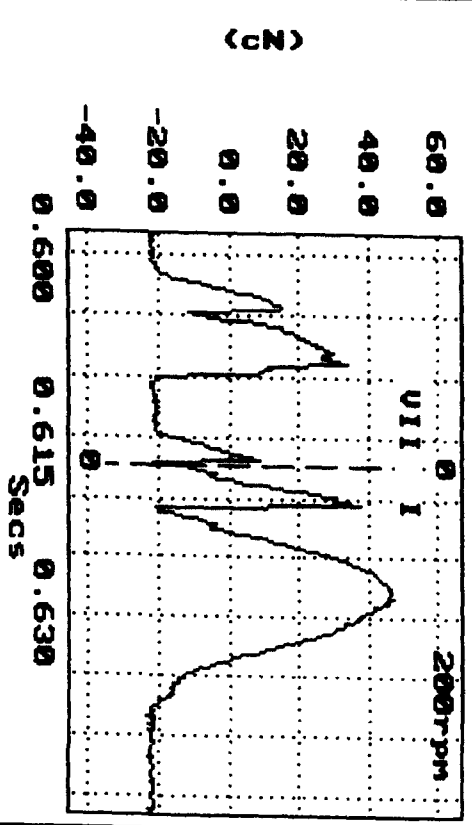
It is also noticeable in window W71 (Fig. 5.4.08), that the Phase III peak with its increase in altitude (with the speed of the machine) also becomes jagged into several sharp shallow subpeaks. This is due to the combined effect of the disk tensioner, Tup and its Cs actions. This tightening of the thread tension occurs at the moment, when the presser-foot loses contact with the feed-dog (bounce at 20°-68° horizontal, see W33 window of Fig. 5.4.09) during the transport of the fabric by the feed dog towards the end of the stitch formation zone.

Table 5.4.02. The peak values of the NTt signals and their location in Phases III(A) and VII(B).

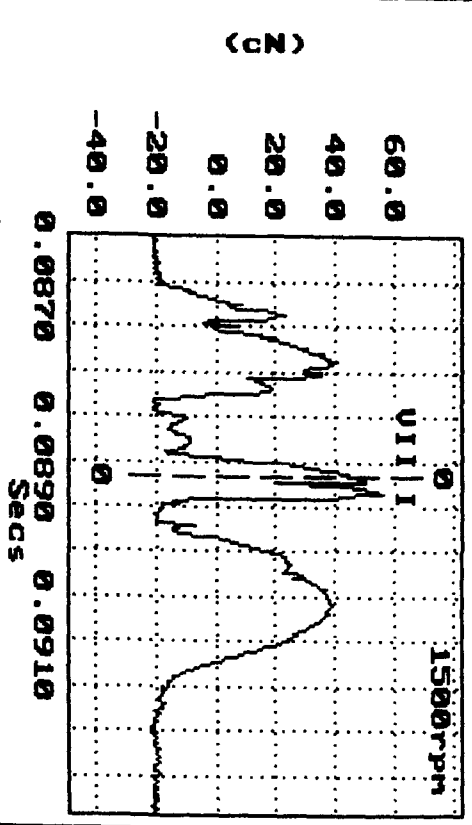
Level	1	2	3	4	5	6	7	8	9
NTt,A, [cN]	40.3	41.3	45.8	42.9	39.2	57.7	66.2	62.2	57.4 *
shaft,A angle[°]	48.2	48.9	49.6	48.9	48.2	50.4	46.0	46.1	48.2
NTt,B [cN]	12.7	34.5	51.9	52.5	55.6	72.1 *	78.1 *	97.7 *	107.1 *
shaft,B angle[°]	353	357	358	358	359	357	357	357	357

Fig. 5.4.08. Needle thread tension (NTt signal of the neighbouring cycles) at different speed levels.

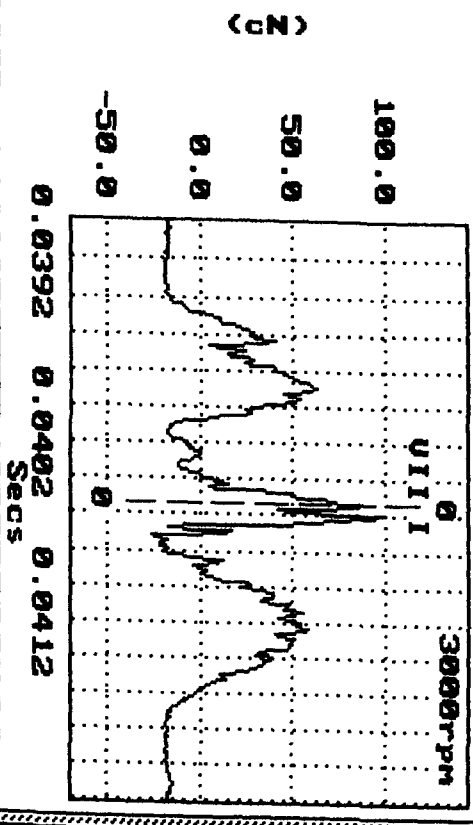
M1: 1.1.THREAD_TENSION



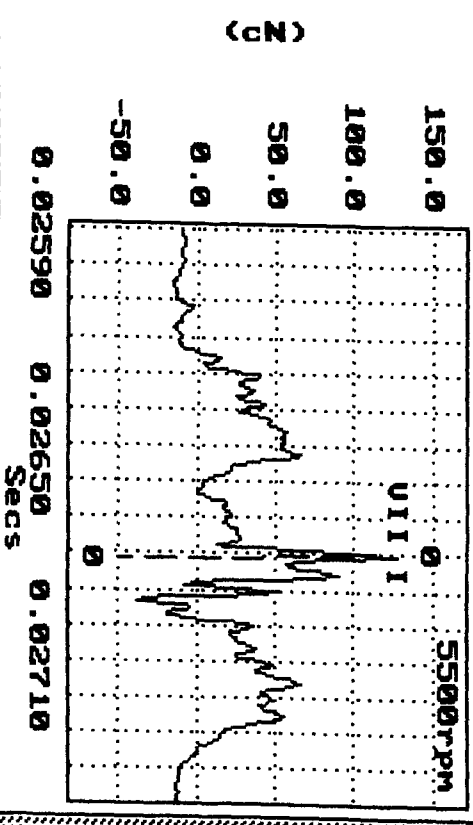
M25: 4.1.THREAD_TENSION



M41: 6.1.THREAD_TENSION



M65: 9.1.THREAD_TENSION



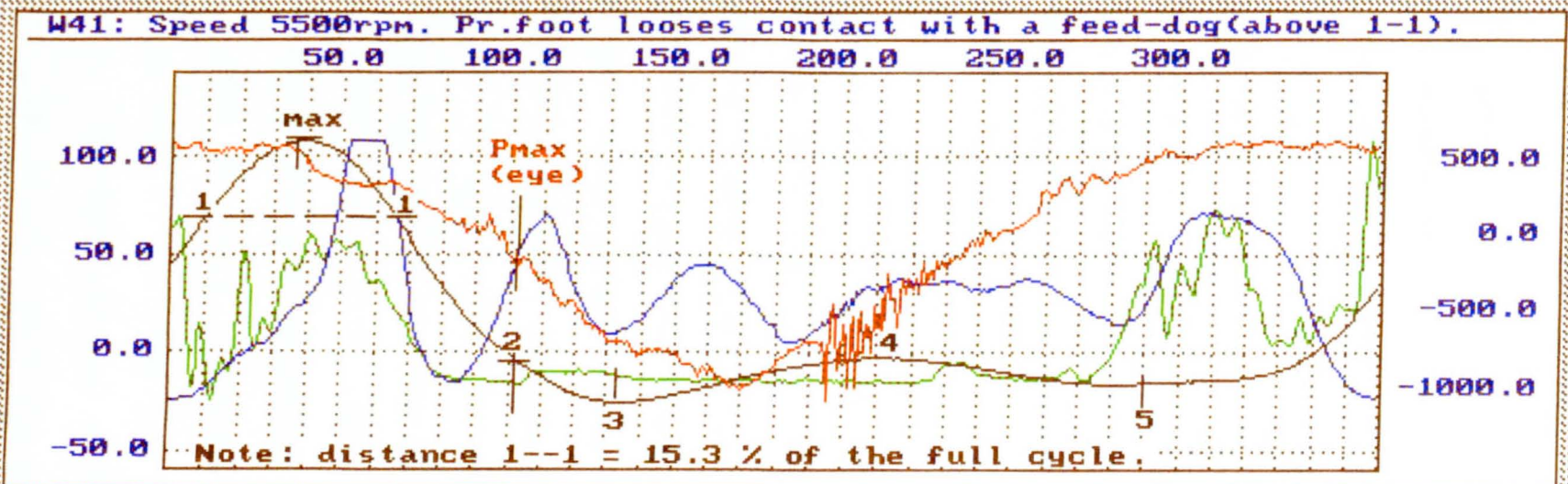
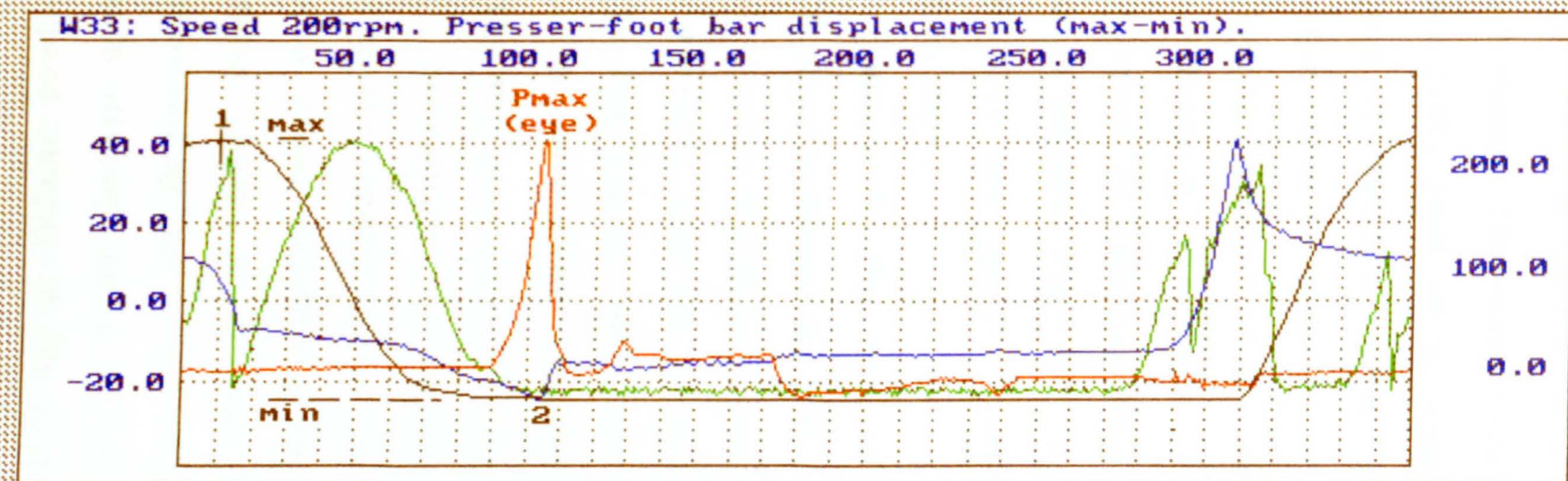


Fig. 5.4.09. The distribution of all 4 RSTM signals at speeds of 200rpm and 5500rpm.

-Phase IV. A slight increase of the needle thread tension after the needle eye has entered the fabrics is visible in the needle thread trace acquired at 3000rpm, which changes its shape from a triangular peak to a 20°-30° wide, flat, peak at 5500rpm(see window W71). This is an effect of the tightening of the thread by the Cs. The maximum value in this phase, is only 15,5% of the highest "slipping tension" of the thread in Phase VI.

-Phase V. This peak also appears for the first time at a speed of 3000rpm. The location of this 20°-25° wide peak is between 220°-250° of the shaft angle. The rotating hook hits the needle thread and carries it around the bobbin case.

-Phase VI. The characteristic feature of this phase is a disengagement of the needle from the loop forming action below the throat plate level. The needle eye leaves the fabrics, the Tup rises from its lowest position and pulls the thread. The thread loop ends move around the rotating hook bobbin case holder, resulting in an increase of the NTt(peak at 295°). The fabric starts moving forward.

-Phase VII. Tension is generated during the Tup rise. The needle thread loop slips out (at around 315°) from the bobbin case, resulting in a drop in thread tension. Between peaks of phases VII and I, the tension is controlled by the compensating spring. Both peaks are not always divided by a valley, as is observed in window W1(speed 200rpm) of Fig. 5.4.10, and which cannot be seen at higher speeds.

5.4.5. The distribution of the presser-foot pressure and displacement signals with speed increases.

During stitch formation the fabric layers are sandwiched between the presser-foot from the top (which applies a considerable pressure on the fabric) and the throat plate or feed dog on the underside. The transportation of the fabric by the feed dog is only possible, when an adequate pressure caused by the presser-foot bar's spring is applied. The lack of an adequate level of pressure may cause negative effects during stitch formation and result in e.g. buckling of the fabric along the seam line (seam pucker). Some aspects of a model of seam pucker mechanism caused by the drop-feed system (pressure-foot bar mechanism) such as the effect of the pressure-foot force on the system of frictional (retarding/advancing) forces caused by the advance movement of fabric layers (due to feed dog movement), have already been considered(130).

For the satisfactory passage of the needle (dynamic penetration) through the fabric layers, the following optimum sewing machine kinetic conditions have to be attained(49,128,130):

- a.the NTt has to be at a minimum(128),
- b.the presser-foot should be at its lowest position,
- c.the timing of the rotating hooks of the bobbin has to be synchronised with the needle movement(49).

To check if the above conditions existed the following tests were made:

-9 tests on fabric Q in a full range of speeds were carried out (RSTM/0021Q301-9.DAT). Their pre-settings have already been described on page 198.

The following parts of the Pfaff-563 lock-stitch machine were used in this experiment: presser-foot spring-hinged type (code number 8152A), feed-dog (code number 059382), throat plate (code 91-06929) and needle hole diameter of 2mm.

The two sets of 4-signals (derived from the acquired data) were overplotted and are presented in DADiSP Worksheet form in Fig. 5.4.09 (W33 - the lowest and W41 - the highest speeds). Additionally, the two especially magnified single cycle signals, each at nine speed levels (for comparison of the signal variation) are shown in WS26(PFp) and WS28(PFd) of Fig. 5.4.10.

Figure 5.4.09 (window W33), shows all four RSTM signals acquired at a speed of 200rpm. The NTt signal is shown as a green line, the PFd is seen in black colour, the blue line represents the PFp and the NPF is shown in red. The distance marked max-min on the presser-foot signal(black colour) is an actual rise of the presser-foot bar. In window WS41 all four signals were acquired at the maximum machine speed of 5500rpm. The feed-dog loses contact with the presser-foot during the 1-1 distance(bounce of the presser-foot), which amounts to 15.3% of the full cycle of the shaft revolution. Some explanation is called for with respect to window W41. The NPP signal's max peak(located at approximately 56°

horizontal) is cut off, because it exceeded the top limit of the bandwidth allocated by the DAP programme. This was corrected by changing the scale of charge amplifiers. The NPF signal (red) in W28 shows some aberration between 185°-242° horizontal. This was found to be a malfunction of the needle bar transducer (a weakening of the transducer's wire in the vicinity of the sensor). The above malfunction was overcome by replacing the wire and inserting its end into a special very light rubber sleeve. For the purpose of this demonstration this part of the signal trace should be ignored.

The presser-foot bar displacement shows a tendency to rise and moves the signal peak (P_{max}) rightwards, closer to the NPF peak (P_{max}) and creates a Valley (V_{min}) within 90°-130°. Bounce starts from around 3000rpm. This departure of the $P_{F_{dmax}}$ from a location in the region of 10° (at 200rpm) to 35° (at 5500rpm) coincided with a 83% rise of the bar. During the bounce of the presser-foot, contact with the feed dog is lost and the sewing thread pulls through the disks of the tensioner. The Top lever completes its upward stroke drawing the slack thread through the uncontrolled fabrics (which contributes to pucker) to set the stitch, which was already suspected by previous researchers (103,130). The effect of inertia on both the PFp and PFd signals was analyzed in the context of the speed increase at all 9 levels of speed. Each of the above signals were overplotted and are presented separately in W26 and W28 respectively, in Worksheet Fig. 5.4.10.

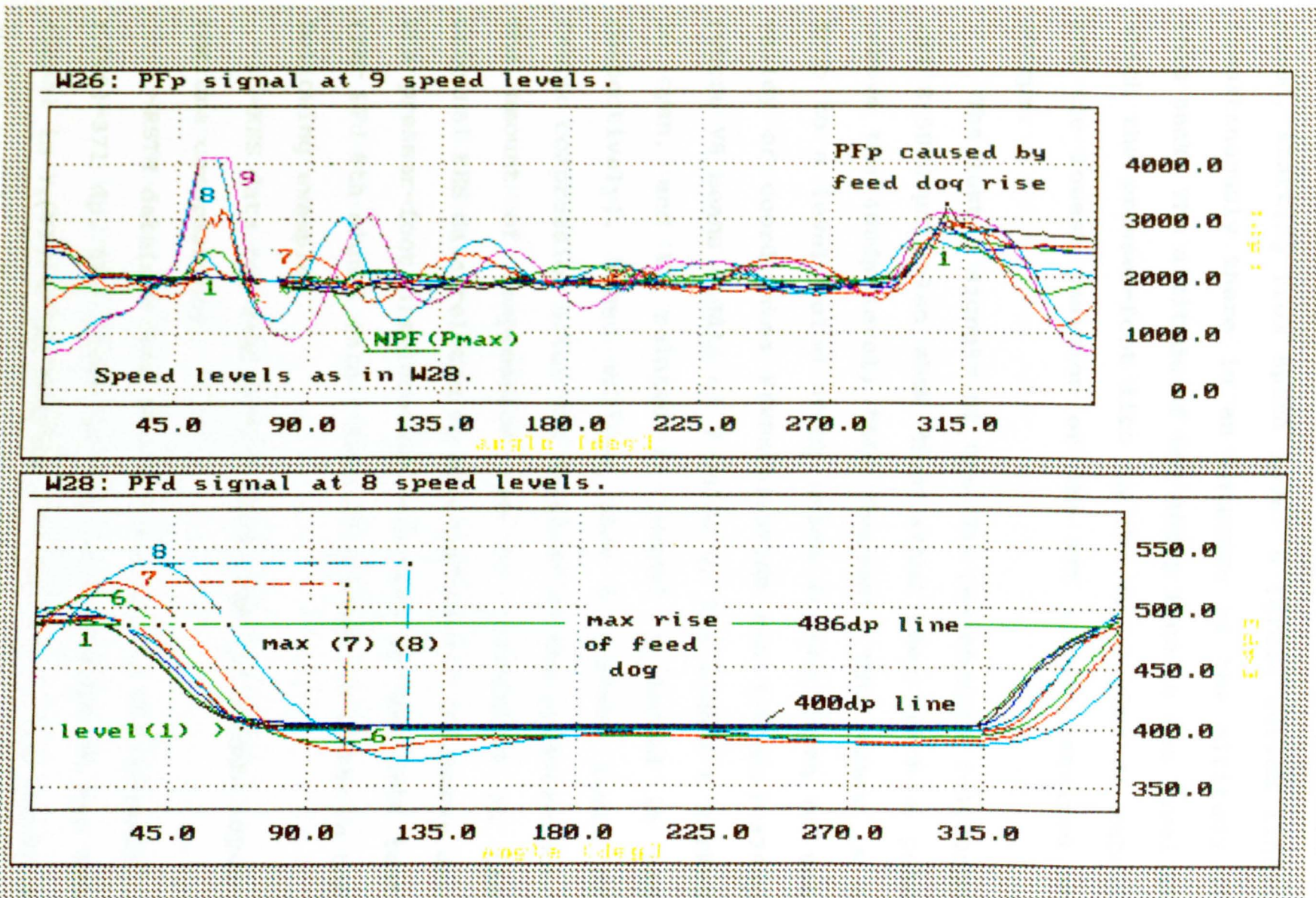


Fig. 5.4.10. Distribution of the PFd and PFp signals at all speed levels. Y-axis=[N]; X-axis=angle[deg].

The bottom window shows the highest peak of the displacement signal moving rightwards with an increase in speed, starting from speed level 6 (green curved line). Simultaneously there is an increase of the altitude of this peak. The altitude of the 400dp line is the level at which the presser-foot lies on the two layers of fabric and the lowest position of the NTt signal acquired at 200rpm.

The last 3 signals of the Pfd (6-3000rpm; 7-4000rpm and 8-5000rpm) also show that after they reach a peak (above the 400dp level) they "bounce". Then there is a drop to a level below 400dp which is the depth of the valley of coordinates $Y(V8min)=371dp$ and $Y(V7min)=379dp$ (where V8 means middle of Y value of the signal 8 marked in cyan, and V7 relates to signal 7 marked in red respectively). These valleys show a certain level of fabric compression after the "bounce" of the presser-foot. The amount of compression can be calculated on the original KES data related to measured fabric thickness and the presser-foot displacement recorded in the RSTM test (for Pfd 8th signal data). Such an attempt is shown in the following example:

-KES data for fabric "Q": $T_0=1.28mm$ for double layers (before compression),

-RSTM data(see W28 of Fig. 5.4.10) of Pfd signal: .
 $Y_1(V8)=371 dp$. The level of the presser-foot of the Pfd signal is $Y_2(V1)=400dp$ (marked 400 dp line, relating to a 200rpm speed) and the Pfd at the start of the presser-foot

bounce $Y_3(V8)=486dp$ (marked 486dp line). It is assumed that the fabric is under no pressure and is 1.28 mm thick(T_0).

-Therefore the fabric thickness when under the presser-foot is as follows: $Y_3-Y_1=486-371=115dp$; $Y_3-Y_2=486-400=86dp$; $Y_2-Y_1=400-371=29dp$. According to the NPF calibration $115dp=1.15mm$. Fabric thickness in an uncompressed state was found to be 1.28mm. Difference $1.25mm-1.15mm=0.13mm$, which is the fabric thickness at Valley min(location $X=121.7^\circ$). Finally, the fabric was compressed approximately 90% at a speed of 5000rpm. At 200rpm the compression value was 66,4%.

The other interesting point is the horizontal forward displacement of the PFd signal in a rightward direction, towards the maximum peak of the NPF. With the sewing machine speed increase this value amounts to 7.8% of the cycle (signal 8 in W28, Fig. 5.4.10, marked in a cyan colour). This is accompanied by a PFp signal valley also moving forward (windows W49 and W50 of Fig. 5.4.11). In such circumstances the conditions for the smooth penetration of the needle at its highest penetration value (at NPF max called also Pmax; marked in all windows by an a-a dashed purple line) are amended. The needle enters the fabric when the presser-foot pressure is relatively high. In these constrained conditions, the NPF has to increase and the needle thread is subjected to sharp pulling (higher frictional forces during the "tensioning phase") at the end of the stitch formation zone (see green signal

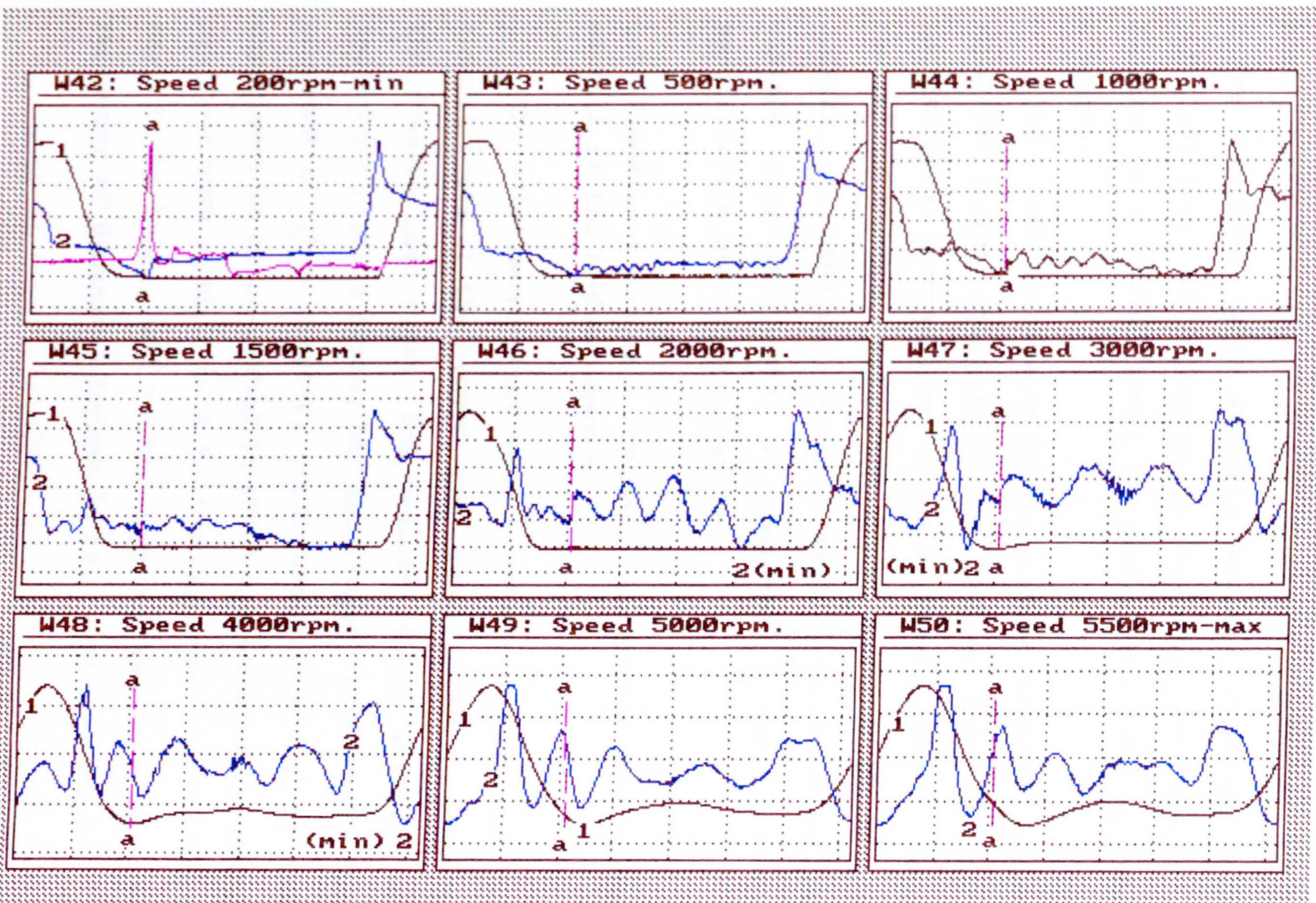


Fig. 5.4.11. The interaction between presser-foot pressure and its displacement at 9 speed levels.

in W41 of Fig. 5.4.10). The signal of the "tensioning peak" in the vicinity of $X=50^\circ$ shows this multipeak with a few sub-peaks. Such unstable sewing conditions will certainly exert an influence on the final seam quality, leading to a higher level of pucker and reduced seam strength.

The 9 test results on fabric Q, test RSTM/Q1733401-9 show the pucker index reduction (pucker increase with machine speed increase) as follows: 5.0(no pucker at speed 200rpm), 5.0, 5.0, 5.0, 4.89, 5.0, 4.77, 4.41, 2.32, 2.39(at speed 5500rpm). The last two figures are below the minimum acceptance index 3, included in many garment manufacturing specifications(132).

5.5. Experiment Series 3. Dynamic interaction among RSTM signals at the highest speeds.

The experiments that were carried out consisted of several tests at the highest and lowest speeds to compare the changes that arose. The results of the analysis of individual signals during the experiments in the previous sections of this chapter, contributed directly to the experiment to be described in which the interaction among all four RSTM signals will be investigated. The findings may, it is hoped, add to the body of knowledge on the behaviour of dynamical forces in the sewing process.

5.5.1. The characteristic points of the RSTM signals according to the shaft angle domain.

In the previous experiments data from tests RSTM/0021Q301-9, RSTM/TIMER2 and RSTM/0008A009 were used. However, for the purpose of this experiment it was decided to run a new series of tests, in which the NPF signal would be extracted by subtracting from the full load signal(S1) the signal(S4), acquired by running the tests (without the needle, fabric and presser-foot) at the same speeds. This new signal was named ENPFA1-9(extracted NPF signal acquired at speed levels 1,2,...9). In the previous experiments the NPF signals were calculated by subtracting from the full load signal (S1) the (S3)signal, acquired without a needle, but with the fabric underneath the presser-foot (version 3 of the classification code for the 2nd digit). It was assumed that these test parameters were closer to the real NPF signal, although in the previous tests the inertia of the needle was also negligible, as seen in Fig. 5.4.03, section 5.4.2.

As was described earlier, the test designation consisted of an 8-digit string, where each number was a coded equivalent of test pre-settings eg. digits 7=needle size and digit 8=speed level. The following 18 RSTM tests were carried out:

- R1753301.dat to R1753309.dat(9 tests) on standard fabric "R"(equivalent of fabric "Q"),
- R4750001.dat to R4750009.dat(9 tests). No fabric, no thread, no needle and no presser-foot were used.

After the test data had been acquired into the DADiSP environment, the data was plotted, the boundaries of cycles were established, and the ENPF signals were extracted and converted to shaft angle domain.

All four RSTM signals were overplotted in single windows, separately for each speed level. However, for the purpose of this section only the 4 RSTM signals (acquired at 3000rpm) are presented in Fig. 5.5.01, due to space limitation. The description of the characteristic points of the signal is included in Table 5.5.01. In window W19 the four signals are overlaid (this overlaying function leads only to horizontal synchronisation of the signal points). The altitudes of the signals correspond only to the two Y-axis scales of the windows. The vertical values of the next signals are not presented, although these can be read from a cross-hair movement inside the DADiSP environment window.

Additionally the horizontal bars of the phased diagram were inserted into bottom window W20, in order to relate these traces to the movement of the components of the machine (at work or idle) such as the needle bar mechanism, needle thread take-up device, and the feed-dog fabric transporting mechanism. The start and end of each phase is denoted by n_0, n_1, \dots, n_4 , and so on. For easier comparison of the points of the traces, the three needle signals are separately presented in the bottom window.

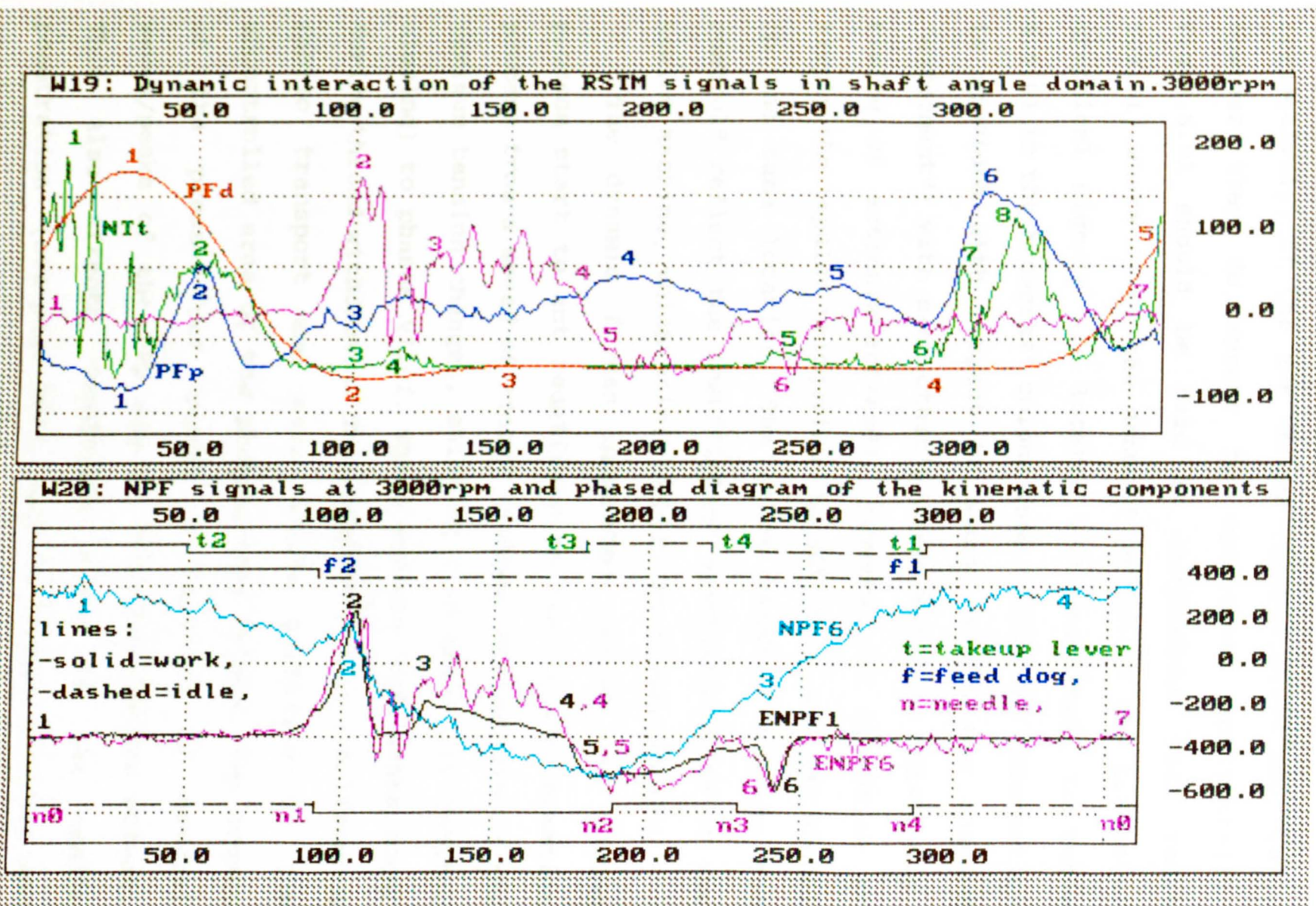


Fig. 5.5.01. Dynamic interaction of the 4 RSTM signals at 3000rpm with the phased diagram of the machine.

Due to the precision specifics of the software, some signal points do not match exactly (eg. peaks 2,3,3 respectively) of the NPF traces (purple,black and cyan), however they do appear to correspond horizontally. Fig.5.5.01 should be read in conjunction with Table 5.5.01, where 43 of the denoted points of the traces of graphical signals are located and described. In Table 5.5.01 in the "remarks" column some additional information is provided with respect to signal compliance (marked "agreement") with each other's characteristic points e.g. timing of action(start/end), reversal of direction or simply the impulse triggering the action of another signal in the same location. The other remarks such as "no control" reflect the insufficient synchronisation of the sewing machine, which mainly occurs at higher speeds.

The dynamic forces generated during the sewing process start to act negatively on the stitch formation process from a speed of around 3000rpm. The pattern of the maximum tension changes, shifting from phase III (stitch closing) to phases VII-I, where several high peaks occur during thread withdrawal. This happens during simultaneous fabric transport and also occurs partially in the uncontrolled area of the presser-foot bounce. The bounce of the presser-foot causes a build-up of several waves/peaks of the PFP signal, the post-bounce effect. This also affects conditions a,b,c of the needle penetration (see-page 197), such as higher pressure and displacement of the presser-foot at the Ne point.

Table 5.5.01. Analysis of the dynamic interaction of the main RSTM signals at 3000rpm.

Legend:

a=NTt signal(green); b=PFd signal(red); c=PFp signal(blue); d=NPF signal(cyan); e=ENPF6 signal(purple); f=ENPF6 signal (black)-acquired at 200 rpm; Tup=Take-up device of the sewing machine; Cs=Compensating spring of the Thread Tensioner; FD=feed dog; Ne=needle eye; TDC and BDC=the needle bar Top/Bottom Dead Centres; i-initialization point of the "Quick Rotan"(QR) sewing machine electronic control system.

This table gives a reference of the distribution of graphical signals (Fig.5.5.01). The characteristic points of the horizontal bars of the phased diagram(W20) are described below this table. See also Figs 5.4.08, 09 and 11.

No	Signal points				Addit.		Locat.	Signal action/interaction in the shaft angle or time domain	Remarks
	a	b	c	d	e	f	X[°]		
1	1						3-28	Tup moves up. Loop slips out of the rotating hook section jib (1st sub-peak) and from the bobbin case holder bracket(2nd sub-peak).	Phases I+II multipeak1
2		1					26	Presser-foot bar at the highest position. Contact with feed dog lost between 0°-40°. See window W28 of Fig. 5.4.11.	Bounce! No control.
3			1				27	PFp at the lowest level. Needle goes down. PFd+PFp>	agreement
4				i			89	Start of the QR's cycle. Marked by Timer1 signal. Needle point about to enter the fabric.	
5					1		91	Needle point enters the fabric.	
6						1	0.0	Start of the ENPF1 signal(at 200rpm) according to the shaft angle domain.	see-bottom window
7	2						45	Tup pulls the needle thread through the disk tensioner and the FD moves the fabric pulling both threads. Tup at the highest.	Phase III, multipeak2.
8		2					105	PFd-displacement lowest point(valley). PFd+ENPF6+EPNF1+NTt>	agreement
9			2				50	On its descent the presser-foot "hits" the FD (PFp at its max).	No control.
10				2			105	Ne penetrates the fabric.	NPF max!
11					2		102.2 105.1 107.9	All NPF signal peaks are very close: -first ENPF split peak(needle eye enters), -scarf enters, -second ENPF split peak(scarf penetrates),	see W20! all in agreement wih ENPF1
12						2	105	ENPF1 signal (shown in W20 for orientation).	

13	3					105	NTt at its minimum (at the Ne penetration point!).	agreement!
14		3				140	Presser-foot returns from the valley. Decompression of the fabric.	
15			3			105	PFp at the NPF maximum peak (Pmax).	
16				3		240	Ne leaves the fabric. NPF6+NTt+ENPF6+ENPF1>	agreement!
17					3	115- -162	Result of fabric frictional forces.	ENPF(6&1) multippeak
18					3	115- -162	ENPF1 signal(200rpm). Result of the action of frictional forces smoother than those of the ENPF6(3000rpm) signal.	agreement
19	4					116	Tension caused by thread tensioner compensation spring Cs impulse (at 116°). ENPF6 small peak>	agreement
20		4				290	PFd signal at the point of the start of the feed-dog rise.	agreement
21			4			180	PFp 2nd wave peak.	
22				4		320	NPF signal's 2nd main peak(colour-cyan).	see bottom window
23					4	170	End of the action of the frictional forces on the needle shoulder.	agreement
24					4	170	Action of the frictional forces on the needle shoulder. Point of inertia change.	agreement
25	5					240	Rotating hook "hits" the needle thread loop.	agreement
26		5				360	PFd at feed-dog highest position. Beginning of the needle TDC.	agreement
7			5			258	The 3rd peak of PFp signal.	
28				5		180	NPF(with an inertia) at the needle BDC.	
29					5	180	Inertia force change in the needle bar.	needle withdraws
30					5	180	Lowest position of the needle in the cycle.	BDC!
31	6					290	Needle left the fabric and NTt increases. Feed dog starts to rise to feed the fabric.	agreement
32		-				-	-	-
33			6			304	4th peak of the PFp signal caused by the rise of the FD. Start of the fabric feeding.	agreement all speeds
34				-		-	-	-

35					6		242	ENPF6 signal shows small increase of the withdrawal force caused by rotating hook. ENPF6+NTt>	agreement
36						6	242	as above. In agreement with the Nft p.5.	agreement
37	7							Takeup spring moves forward increasing NTt.	
38		-					-	-	-
39			-				-	-	-
40				-			-	-	-
41					7		360	ENPF6 lowest at the begining of the TDC!	agreement
42						-	-	-	-
43	8						320	Cs starts supplying the thread to absorb the tension increase.	

Characteristic points of the phased diagram's horizontal bars are denoted as follows:

-Needle (n):

- n0 = (0°) = TDC (Top Dead Centre),
- n1 = needle enters the top fabric layer (start of the working cycle),
- n2 = BDC (Bottom Dead Centre),
- n2-n3 = needle thread loop making,
- n4 = needle leaves the fabric (end of the working cycle),

-Take-up (Tup):

- t1-t2 = needle withdrawal from the bobbin case,
- t1 = start of the working cycle (lowest Tup position),
- t2 = final point of the closing of the stitch (highest Tup position),
- n2-n3 = needle thread supply for the needle moving towards BDC,
- n3-n4 = additional needle thread supply (resulting from thread tensioner construction limitation. The excess of the needle thread removed by the compensating spring (Cs),

-Feed-dog (FD) transport:

- f1-f2 = fabric transport during idle needle movement.

At the highest speeds (5000-5500rpm, see Fig. 5.4.08) the thread remains under strong pulses of tension for a longer period, which leads to a reduction of thread strength.

Furthermore, in the above tests all the signals were acquired without filtering on input, to show the real conditions of the signals, with the existence of some sub-peaks (represented by jagged parts of continuous traces, particularly visible on the red coloured ENPF6 and NPF6 traces in W20).

Finally, the combination of dynamic negative conditions influences the conditions of optimum seam formation and leads to a lower seam quality such as pucker and weakening of the seam.

5.5.2. Peak Analysis of the RSTM signals.

The FFT Spectrum signal transformation was used in the next experiment with the S1's NPF signals unfiltered and filtered (30kHz filter on input). Results show that there is a difference in the frequency band range in bands 0Hz; 400Hz; and 800Hz (which can be seen from Table 5.5.02) and which is mainly due to filtering. Table 5.5.02 shows that the applied filter of 30KHz (on input) did not show the existence of any of the higher frequencies, except these below 1% of the Ymax value, which were assumed to be a high frequency noise (the sewing machine shaft generates basic frequencies of 90Hz at a speed of 5500rpm).

Table 5.5.02. An example of the filtering (on input) of the NPF signal.

Description	Filter on[30kHz]		Filter off		Remarks
	x[Hz]	y[dp]	x[Hz]	y[dp]	
Window	W40		W58		above 800Hz only a noise around 4000Hz can be seen
Test No/speed	"Timer2"5500rpm		"0008A009"5565rpm		
-Band 1	x=0Hz	y=2dp	x=0Hz	y=14dp	
-Band 2	x=393Hz	y=697dp	x=400Hz	y=732dp	
-Band 3	x=787Hz	y=161dp	x=800Hz	y=162dp	

In addition to the above experiment on the NPF signal, a second test of filtering was applied to the NTT signal. A special 1kHz filter(built-in the dynamic amplifier) was used for input, for the purpose of the estimation of the cut-off frequencies. Fig. 5.5.02 provides a graphical analysis, in which the FFT Spectrum function was used again. From window W38 it can be seen that the filter cuts-off the marked values of the peaks by 9.5%(for peak b) and 4.3%(for peak c). This corresponds to changes in frequencies at 400Hz and 1200Hz respectively. Bands 4 and 5 (both red in W46) have respective values above those of their unfiltered equivalents (4 and 5 in green). This can be attributed to the difference in the sewing machine speed (during acquisition) and to specifics of the dynamic conditions of Phase II of the thread tension signal.

The next step in the analysis of the maximum peaks of the RSTM signals was a compilation of the max peaks of the series acquired at the highest speed level 9(5500rpm). It was considered that this approach might be useful in the evaluation of the part played by the increase of dynamic forces with sewing machine speed.

In Fig. 5.5.03 the PFp signal shows a sudden drop at level 6 (3000rpm). A similar pattern prevailed among 16 fabrics (out of 21 tested) which had a mass above 100g/m². No connection was found in relation to seam pucker nor with the other results of the main RSTM signals.

However, the approach was found to be useful also in incorporating the maximum data of the peaks from other series acquired at all speed levels and in tabulating them together in Fig. 5.5.03 in a graphical form. In the same figure the Pucker Index(PI) values of the above tests are inserted and the relationship of all signals (regression data) is additionally tabulated in Table 5.5.03.

It was assumed in the hypothesis of this research, that there would be an almost linear increase of dynamic forces with sewing machine speed increases. However, the tabulated results show that the linear relationship existed only between the displacement of the presser-foot(PFd) and sewing machine speed. This relates also to the Pucker Index(PI), except for the highest speeds.

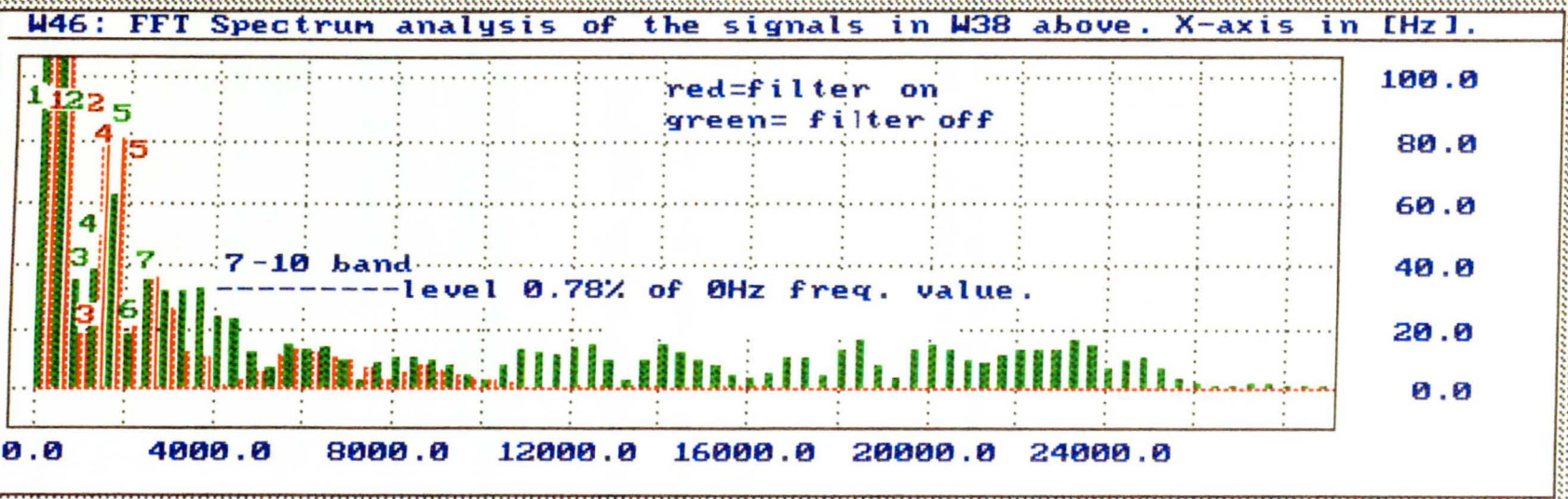
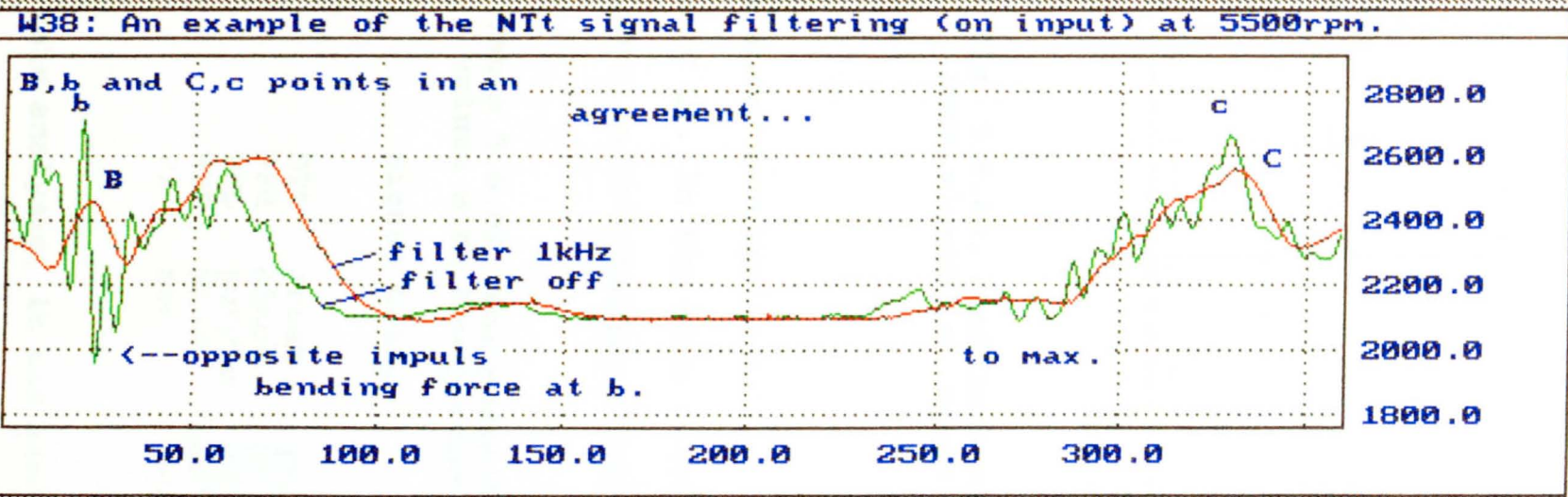


Fig. 5.5.02. The FFT Spectrum function applied to the analysis of filtering the Nrt signals at 5500rpm.

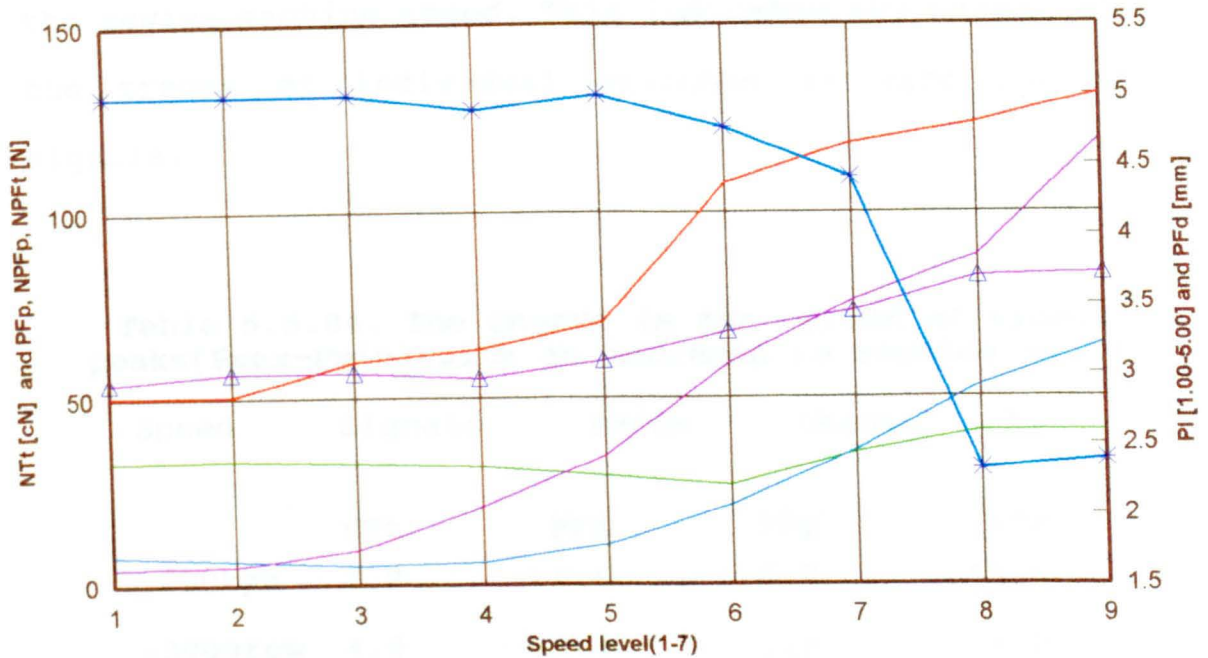


Fig. 5.5.03. Peak Analysis of the dynamic forces. RSTM signals v. Speed level v. Pucker Index.

The above results relate to one type of fabric (standard fabric Q). In the next sections there will be an attempt to confirm this tendency for an expanded range of fabrics.

Table 5.5.03. The correlation of the maximum signal values with the sewing machine speed increase.

Signal	Colour	Fit equation (lin. regression)	St.Err.
NTt	green	$y=11.76X + 38.82$	10.09
PFd	black	$y= 0.107X + 0.81$	0.12
PFp	purple	$y= 0.90X + 30.19$	4.34
NPFt	blue	$y= 4.27X + 15.10$	10.83
PI	red	$y=-0.33X + 5.62$	0.71

In this analysis, it was also found that the difference in the spread of peak values between Pmax-Pmin peaks (in a series of 15 cycles) tended to widen with the increase of

the sewing machine speed. This indicates the uniqueness of the traces of individual stitches in each series of signals.

Table 5.5.04. The change in the spread of signal peaks ($P_{max}-P_{min}$) with an increase in machine speed.

Speed	Signals	range	change	[%]
	NTt	PFd	PFp	NPF
-200rpm	1.2	1.6	6.0	13.5
-3000rpm	4.0	1.0	1.6	9.0
-5500rpm	21.0	2.5	15.8	8.3

Finally, the values of the peaks in tests carried out at the lowest and the highest speeds were also tabulated and their magnitudes were found to increase as follows:

Table 5.5.05. The maximum increases of the RSTM signals.

Signal	Unit	200rpm	5500rpm	%	Remarks
NTt	[cN]	47.0	126.0	2.6	*one phase
PFd	[mm]	4.9	5.9	1.2	max rise
PFp	[N]	32.5	40.9	1.2	inert.includ.
NPF	[N]	22.4	62.0	2.7	inert.includ.
ENPFC	[N]	1.7	5.45	3.2	inert.exclud.

*This value is a nominal value of the series.

The NTt signal has two characteristic maximums (the first in Phase III and the second in Phase I/II, as was presented in Fig. 5.4.07. In Phase III there is an increase of the NTt P_{max} 1.4 fold and at Phase I approximately 9.9 times,

which requires paying closer attention to the sewing needle, thread and sewing machine designs.

The level of needle penetration force increases is also in an approximate agreement (4 and 5,3 fold) with the research results of other researchers(17,19).

5.6. Seam pucker in micro-fibre fabrics.

The characteristics of micro-fibre fabrics are given in Table 5.2.01, and their properties are in Appendices VII(KESF-F) and VIII(FAST).

The fabrics, marked as X,Y and Z, were subjected to the following RSTM tests at speed levels 1,6 and 8(last digits of the file name) corresponding to 200, 3000, and 5000 rpm respectively. The other parameters of the MF (micro-fibre fabrics) tests are also coded according to the coding system described in Section 4.4.4.3 and Appendix IIIa:

- X1533391,6 and 8. Stitch density level 5(40 stitches per 10cm); sewing thread Nm 120, and needle No. 90 (last digit),
- Y1533391,6 and 8, and
- Z1733391,6 and 8 with stitch density level 7 (32 stitches per 10 cm).

The stitch density test parameter of fabric Z was lower (32 stitches per 10cm) than that of the X and Y fabrics. The other parameters were the same in each test. The amount of fabric available for these experiments was limited, so that only 9 tests, could be carried out.

The test results for the above fabrics are shown in the DADiSP Worksheet Fig 5.6.01, where all four signals are overlaid to show their distribution as a function of the shaft angle. The needle eye Ne1 point was marked on the especially inserted traces of the NPF1 signal (cyan colour) in W32, W41, W50 (speed 200rpm) and W59, W68 and W77 (speed 5000rpm) to show that the locations of the peak forces are in agreement at all three speed levels. The colour designations for the RSTM signals are NTF (green), PFD (black), PFP (blue) and NPF (red).

Although the designation of the X and Y axis for the four overlaid RSTM signals is not shown (due to space limitation), their corresponding names are denoted for X-axis as speed [rpm] in shaft angle domain and for Y-left axis as tension or displacement [cN and/or mm] and for Y-right axis as a relevant force in [dp and/or N respectively].

The NPF1 signal in Fig. 5.6.01 (at the lowest speed, when inertia influence is negligible) shows a characteristic shape at all 3 speed levels (points 1-4 marked in a red colour). At point 1 the frictional forces started acting on the shank of the needle and at point 2 the needle shoulder started to penetrate the fabric. At point 3 there is a change in the inertia force of the needle bar. Point 4 shows the maximum withdrawal force NPFt (the negative voltage value). The shape of the signal for MF fabric X (of mass 160g/m²) is different from the signal acquired for the standard fabric Q (of

wool/polyester, with a mass of 192g/m²). The needle (Nm 90) penetration of the fabric of thinner fibres produced a different set of frictional forces (compare the relevant valleys between points 1-2-3 of Figs 5.4.01 and 5.6.01).

Distribution of the dynamic signals of the MF fabrics follows the general trend of an increase of dynamic forces with machine speed. However, the individual RSTM signals show certain difference in altitude and location along the shaft angular movement.

Although the distribution of the dynamic signals of the MF fabrics confirms the general trend of an increase of dynamic forces, however, the individual RSTM signals show certain difference in altitude and location along the shaft angular movement. Therefore an additional Peak Analysis was very useful (see Fig. 5.6.02). In the Worksheet Fig. 5.6.02 the relevant maximum values of the peaks (at 3 speed levels) were tabulated and plotted as XY function in 8 windows. Exceptionally, the relevant values of the NTt signals had to be presented in two more windows. The NTtmax is presented in W13, its Phase III peak value in W58 and Phase VII in W67.

However, although the data acquired at only 3 speed levels (out of 9) is too limited to enable fuller conclusions to be drawn, it is hoped that it may nevertheless enable some important features of dynamic signals in relation to seam pucker to be highlighted (see PI results in W76), which will be pursued further in the next section.

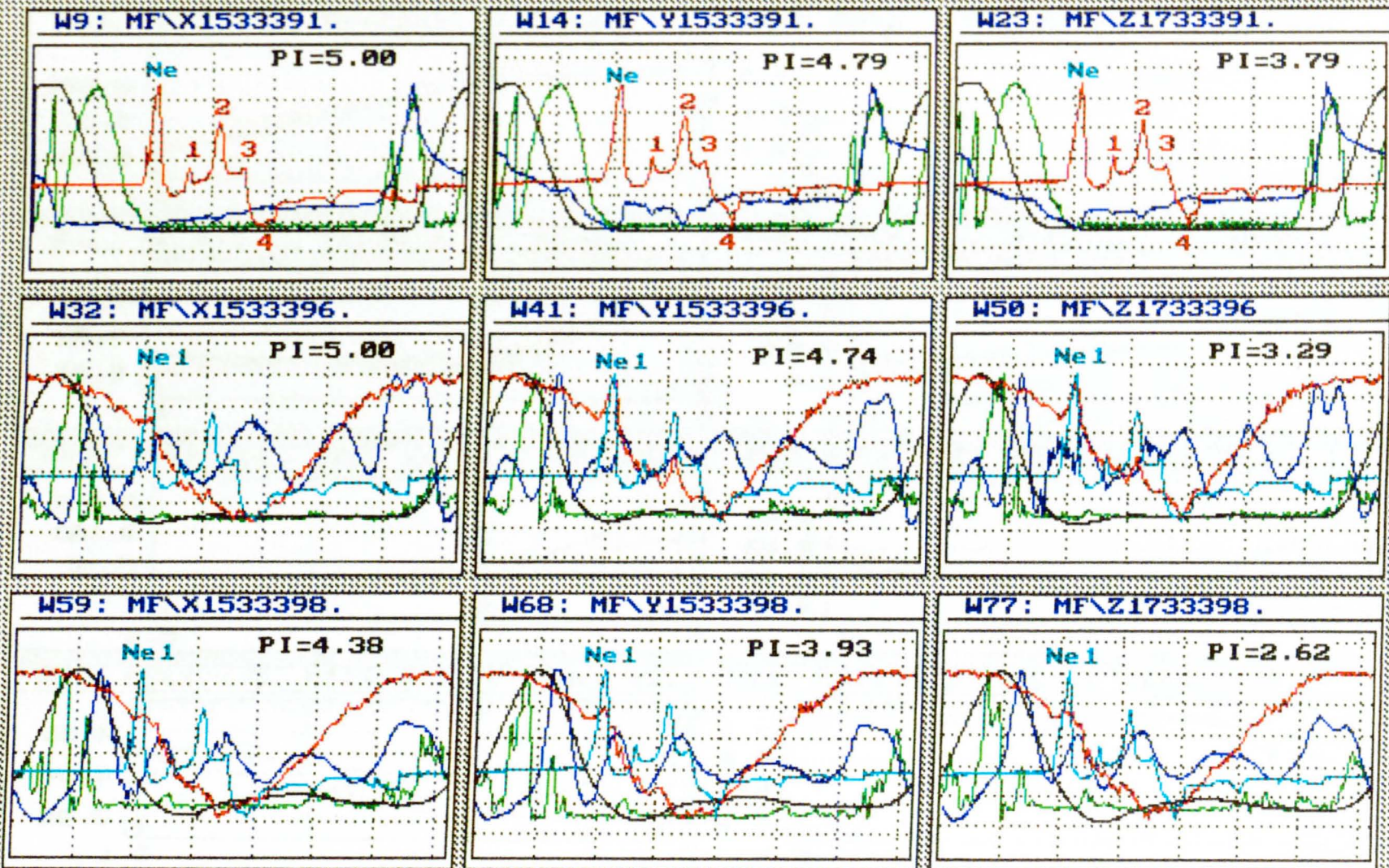


Fig. 5.6.01. The distribution of dynamic forces in micro-fibre fabrics (types X,Y,Z) in relation to Speed (Levels 1,6,8) and to the Pucker Index (PI).

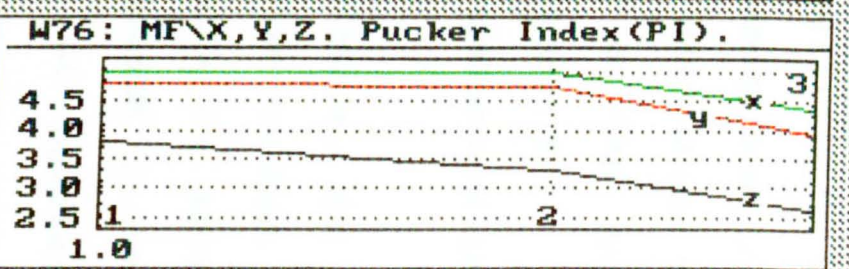
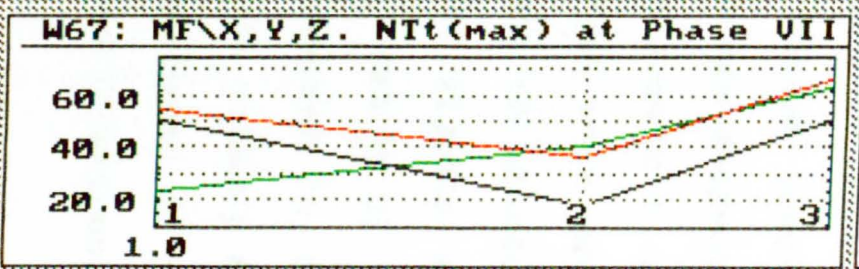
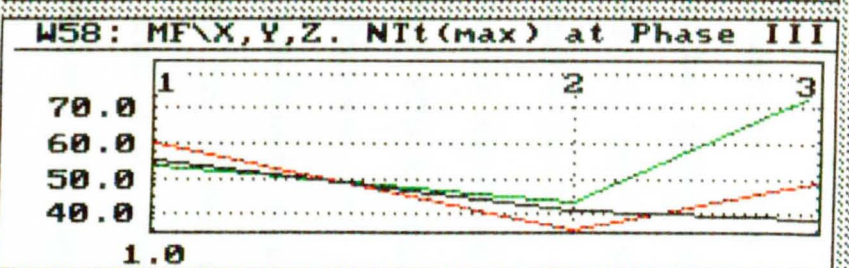
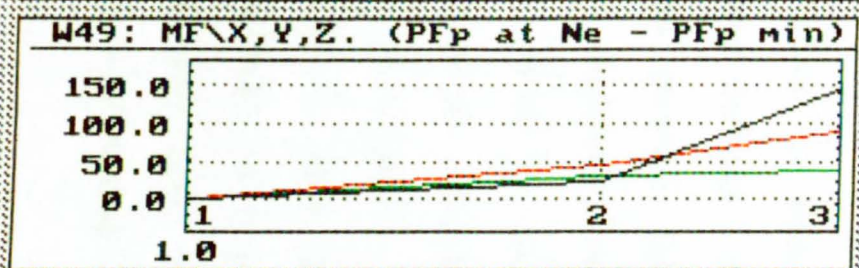
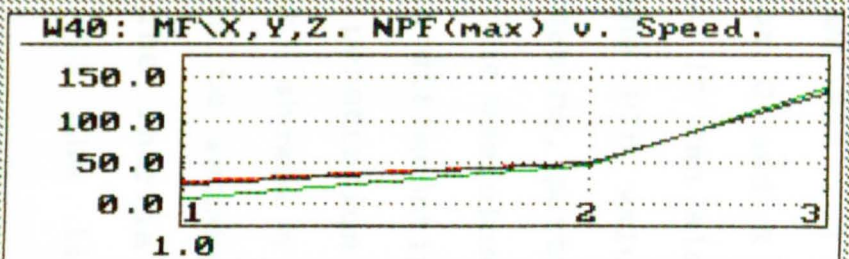
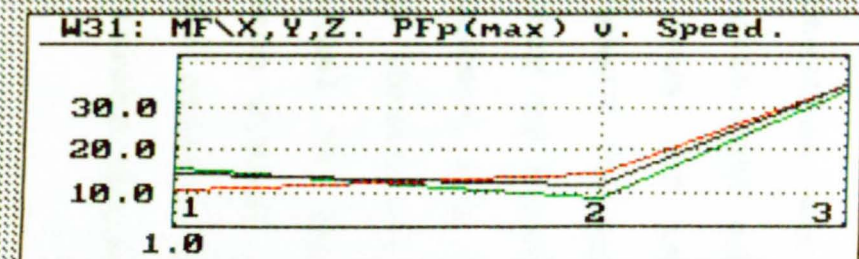
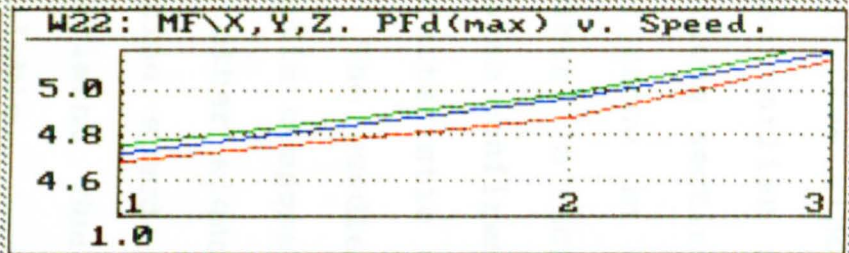
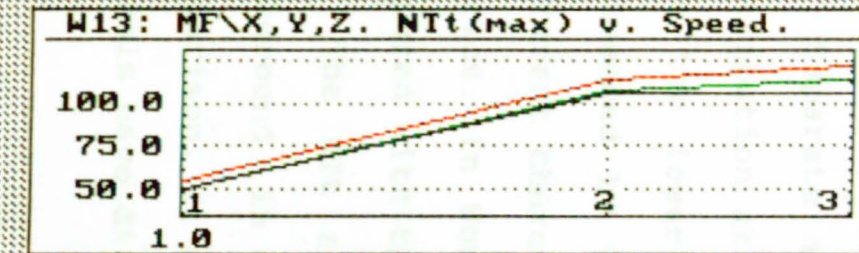


Fig. 5.6.02. The Peak Analysis of the dynamic forces in micro-fibre fabrics (X,Y,Z) at speeds of 200, 3000 and 3000rpm. X=axis(log)=Speed level:1(green),2(red),3(black).

The good linear relationship between dynamic forces, machine speed and pucker level is represented in the Fig. 5.6.02(see windows W22 and W76). This relationship was found earlier for Q and R fabrics and described in a previous section. It can also be seen in W49, where the difference in the PFp values(at Ne and at the cycle minimum) is increasing, particularly for fabric Z. It also confirms the usefulness of the measurement of this characteristic to differentiate PFp values.

The needle penetration forces (S1 signals, and an inertia component) showed a tendency similar to that of the other signals to increase in value with the sewing machine speed. The inertia was not extracted in this experiment due to the limited number of specimens available.

Separate attention was paid to the thread tension distribution at different speed levels. It was suspected that the lower level of seam pucker for fabric Z was influenced by thread tension changes, which were of a different character to those found in tests on standard fabrics. In Worksheet Fig. 5.6.03 the NTt signals are compared with the thread tension signals of fabric Q.

The NTt signal of fabric Q was inserted in the background in each window (marked in a cyan colour) for comparison. It can clearly be seen that the peaks of the signals have different shapes, altitudes and locations.

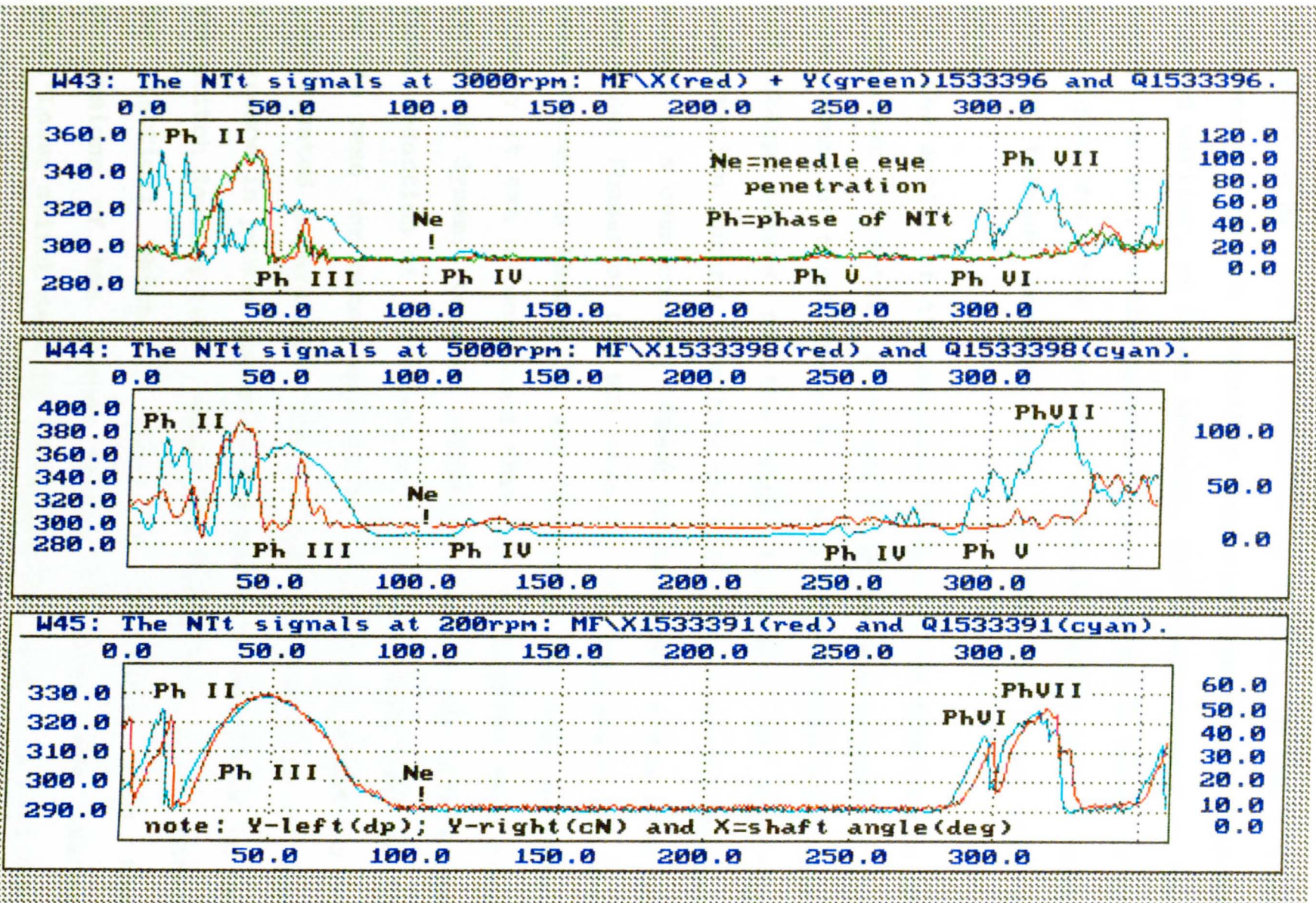


Fig. 5.6.03. An analysis of the NIt distribution in micro-fibre fabrics and standard Wool/Polyester standard fabric Q(cyan).

The distribution of the NTt1 has the same characteristics(W45). However, a difference in the shape of the peaks in MF fabrics starts to be visible in the traces obtained at 3000rpm (possibly implying that these changes started earlier, at lower speeds). The disengagement of the needle thread from the rotating bobbin hooks in Phase II of the signal does not have two separate peaks with a deep drop of tension between them, as was the case with Q fabric.

The action of the dynamic forces of MF fabrics is of a smoother character, although it lasts approximately the same amount of time. There is also a lack of the many high and sharp pulses of the high frequency of the Tup compensation spring (visible on the thread signal traces marked in a cyan colour). These differences relate also to the other Phases of the NTt signals. Significantly the max peak values in Phases II are the same for both signals. Finally it can be concluded that the MF fabrics have less stringent dynamic tensile conditions, which may affect the final reduction of strength to a lesser extent than would be the case for other apparel fabrics, which ought to be investigated separately. The possible explanation of the difference in pucker severity for fabric Z was found to be the stitch density level, which was lower than in the other two fabrics; which is also in agreement with the conclusions of the sewing thread producer, who states that:"Lower stitch density increases the risk of pucker due to thread tension caused by a reduced thread supply"(129).

5.7. Experiment Series 5. The interaction of the dynamic forces on the seam pucker for 15 types of fabrics.

This final experiment related to the testing of 23 types of fabrics at different sewing conditions, according to the experiment's testing programme. The basic assumption underlying the experiment was the hypothesis that seam pucker is correlated with the dynamic forces of the sewing process(64,66,90). This hypothesis had proved to be true during tests on a limited number of standard fabrics (Q and R), in previous experiments of this research already described. The final experiment was designed to acquire the necessary data (by RSTM and SPMS methods) and to analyse it, using the statistical and graphical packages of DADiSP 3.2 and Lotus 123.

For the final experiment the basic test results of 23 fabrics were tabulated in Lotus 123 format (an extract is shown in Appendix IX). The maximum values of the series of four main RSTM signals for 18 fabrics (others were not included due to the incomplete range of speed levels or malfunctioning of the system/operator) were recompiled in the Lotus 123W/V.4 spreadsheets and used as the basis for further statistical analysis and graphical presentation.

Over 130 basic tests were carried out at controlled atmospheric conditions. Before the start of the series of these tests, the sewing machine was re-examined by the technical support specialist from Pfaff's Hong Kong Technical Centre and its settings were approved for testing.

A sewing laboratory technician was specially trained to carry-out the sewing of test specimens, to ensure uniformity in the handling of the sewing operations over several weeks of testing, under the supervision of the author. The fabrics were cut into long strips, combined into 2-ply specimens, and properly marked. During the instrumented testing of these sewn specimens for seam pucker, some additional, simultaneous random checks for pucker grading accuracy, against AATCC-88B Standard, were carried out, according to SPMS method 1, (See Fig. 4.02.01) and no discrepancies were found.

The results obtained from these tests are analysed in the following sections with the aim of finding the correlations between individual dynamic forces and seam pucker, and how they affect the seam pucker index.

5.7.1. The distribution of the dynamic forces of the needle thread and presser-foot bar in relation to sewing machine speed increases.

The test results are presented in graphical form in two separate figures (NTt in Fig. 6.7.01 and PFp in Fig. 5.7.02).

The forces were plotted in separate colours for each fabric group (according to its mass per unit area) and each fabric type was additionally marked with separate symbols. The groups included the following fabrics:

- group A (mass < 60 g/m²): fabrics U,S,T;
- group B (mass 60-100 g/m²): fabrics V,W;
- group C (mass 100-130 g/m²): fabrics M,N,K;
- group D (mass >200 g/m²): fabrics D,F,I.

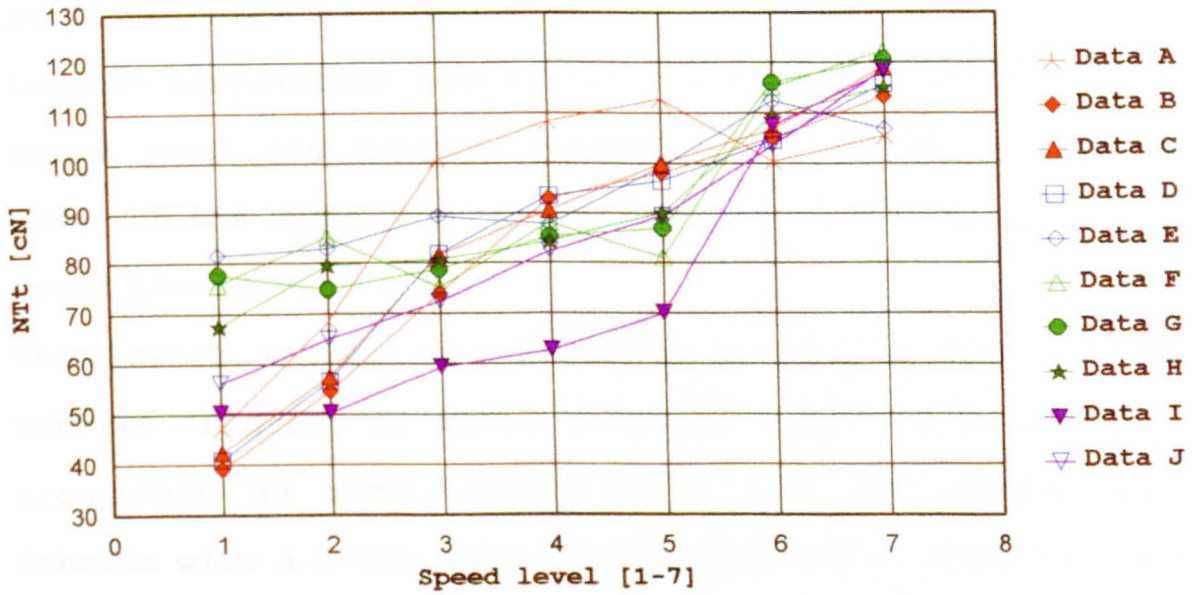
The NTt signals were plotted in line form and marked as (Data A, B, etc). Fig. 5.7.02 shows the signals in the form of symbols, with the aim of depicting the general trend of their behaviour.

5.7.1.1. An analysis of the NTt signal distribution.

The test results were divided into groups so that as many fabrics as possible could be analysed statistically together and so that the number of "missing values" could be reduced, since not all the fabrics were tested at the full range of speeds (from level 1=200rpm to level 9=5500rpm).

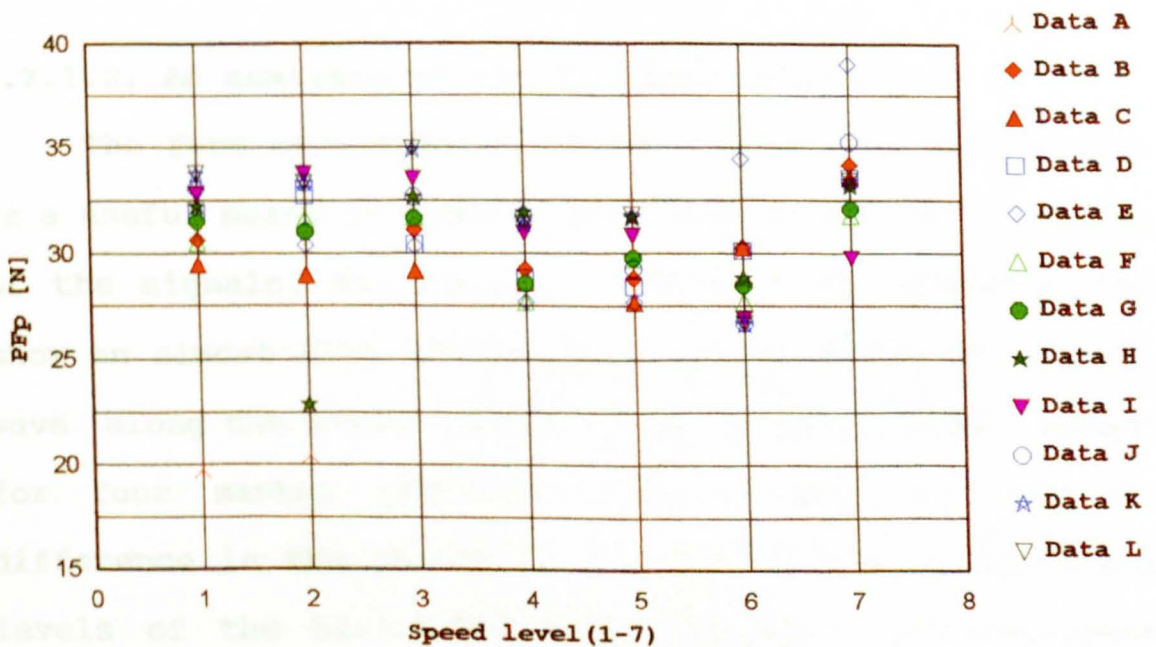
The first group contained the test results of all the fabrics tested at 7 speed levels (200-4000rpm). In the second group only 5 fabrics, on which tests had been carried out at the full range of speeds were included. For clarity the test results of these, which included data from the upper speeds(3000-5500rpm) are presented separately in Fig. 5.7.06. Tests on the three MF fabrics were discussed in the previous section of this chapter.

The general tendency of the maximum values of the sewing thread tension (max peaks from a series of 15 cycles) is to rise with an increase in speed (see Fig. 5.7.01). If the three sets of data (speeds at 3,4 and 5 level), for the two fabrics marked in red and purple, are excluded, the remaining 70% of the fabrics show an approximate linear relationship with the increase in speed of the sewing machine.



Figs 5.7.01 and 5.7.02. The distribution of the NTt(top) and PFP(bottom) signals for 12 fabric types.

Note: the signals are marked in colours(A-L), which stand for: red(group A), blue(group B), green(group C), purple (group D) and black(group E, fabric D).



This relationship was also found by Wong(132) during tests of MF fabrics at speeds of 500-3500rpm (needle thread tension correlation coefficient of 0.825). At the lowest speed level the maximum values show a wider spread (ca 40N)-see the symbols placed at level 1- which narrows with speed increase(ca 15N).

The lowest values of the tension are related to the fabrics of group A, which have the lowest mass per unit area(below 50 g/m²), which would seem to suggest that fabrics with a lower mass contribute more to sewing thread tension increases than those with a higher mass (2.5 fold for group A and 1.6 fold for fabrics of group C).

No generalisation however, is possible owing to the very small amount of data, but these findings may encourage further investigation into this area, as being of significant importance in the selection of sewing threads.

5.7.1.2. An analysis of the PFp distribution.

The form of graphical presentation that is employed is a useful means of showing the trend of the distribution of the signals. The dynamic forces of the presser-foot show an almost flat distribution in the shape of a small wave along the X-axis direction of speed increase, except for four marked off-side points. There is also no difference in the spread of the PFp values at different levels of the horizontal axis. However, a significant feature of PFp signals was found to be that they all

reached their lowest values at the sixth speed level(3000rpm). This lowest point (valley) was also found in the previous tests carried out on standard fabrics(see Fig. 5.6.01). During these tests there were no changes of the pre-set parameters of the presser-foot scale, and no equivalent responses were found in the traces of the other signals to explain the existence of the valley. One explanation for it however could be that it was caused by an occurrence of a resonance effect of the presser-foot starting to bounce in phase with other machine actions such as the movement of the feed-dog.

5.7.2. An analysis of the needle bar pressure and withdrawal forces.

The responses of the dynamic forces of the needle bar are presented in Fig. 5.7.03 for 11 fabrics, which are grouped according to their mass per unit area, as was described in the previous sections. The increase is exponential for light-weight fabrics (A,B,C groups). The heavier fabrics show maximum values that are twice as high as those of their lighter equivalents at lower speeds.

The spread of $P_{max}-P_{min}$ at relevant levels of speed narrows with the rise of their values as the sewing machine speed increases. This can be attributed to the inertia of the sewing needle bar system, which swamps the maximum NPFp peaks.

The needle bar maximum withdrawal forces rise more sharply than the needle bar pressures, and increase their

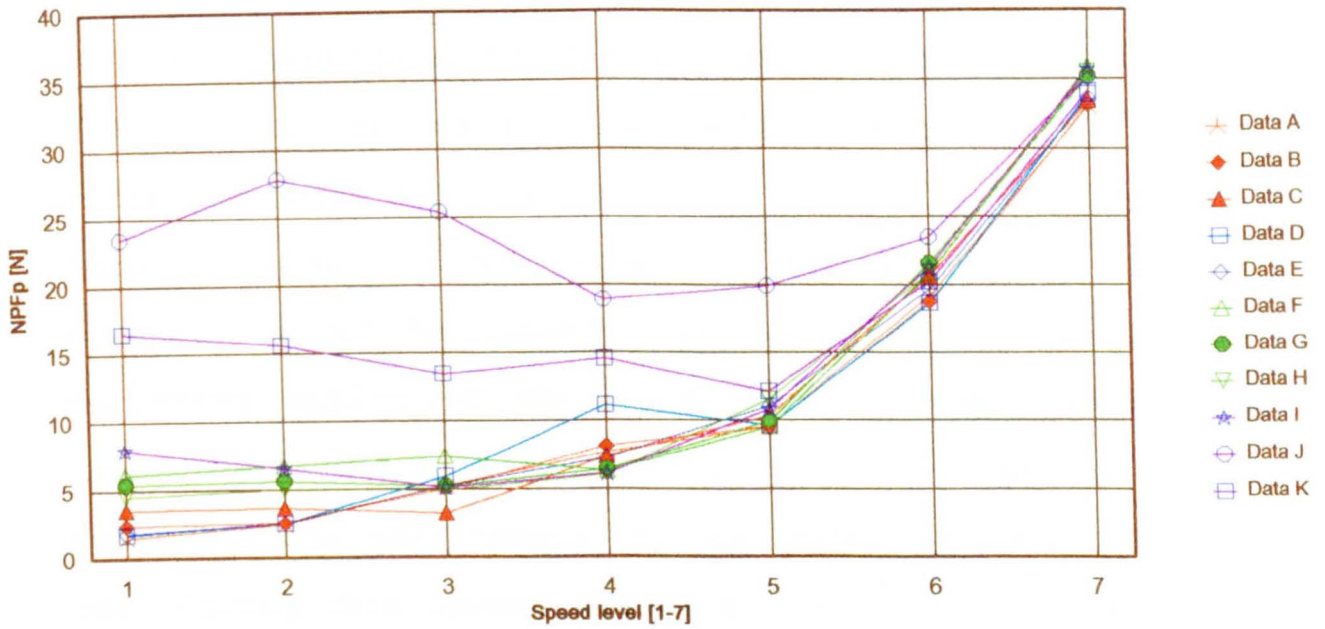


Fig. 5.7.03. The distribution of the NPFp maximum values according to the sewing machine speed level. The colour of the fabrics traces is related to the fabrics mass per unit area (groups A,B,C,D).

Note: The distribution of the signals shows only a partial linearity of the NPFp signals, starting from level 5 (2000rpm). In the bottom Fig. 5.7.04 the dependent variable was transformed into a Y-log axis, and shows an improved linearity.

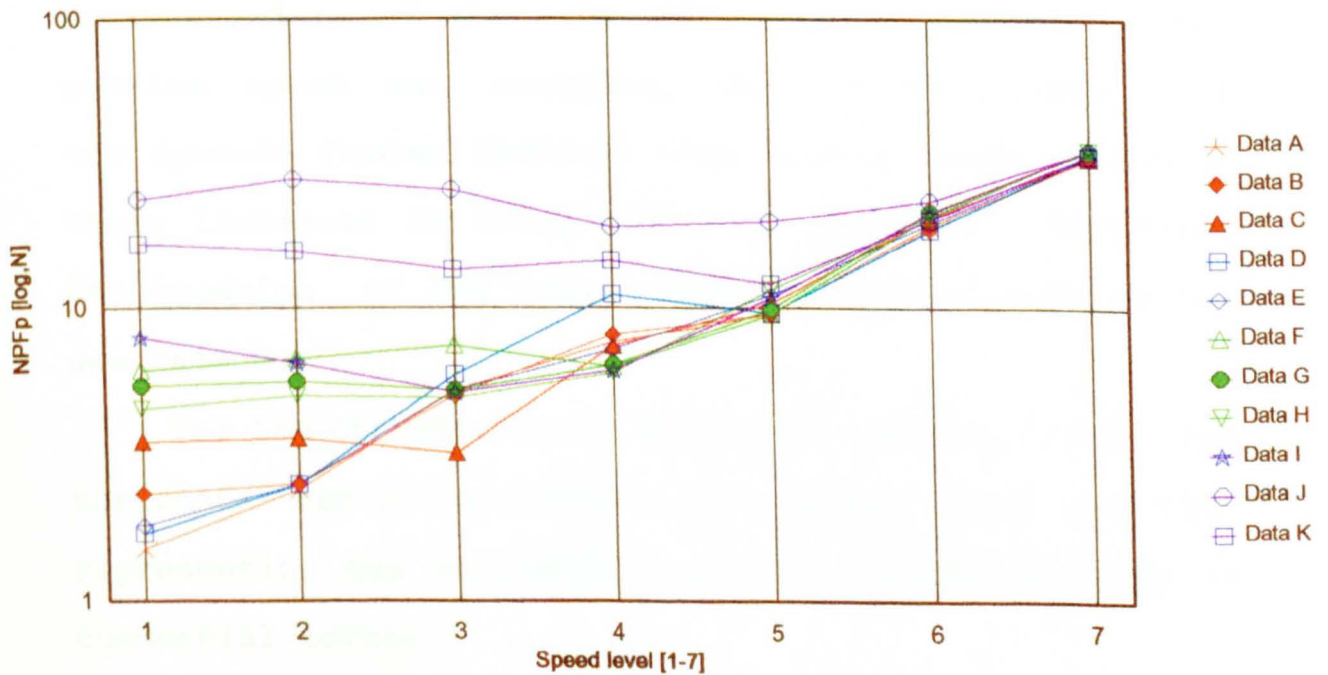


Fig. 5.7.04. The distribution of the NPFp as in the figure above but transformed into a Y-axis logarithmic scale.

values on average up to 35 fold (from a speed of 200rpm to 5500rpm) as opposed to the needle bar pressure, which increases about 2.7 fold only.

This increase in the values of the withdrawal forces however, cannot be regarded as real. It is due to the springing action of the wire loop of the needle bar transducer, which significantly affects the recorded values during measurement of the upward movement of the bar. During this upward movement the loop is compressed, increasing the values of the needle bar tension (which include the inertia of the system). These forces added together swamp the real forces at higher speeds.

5.7.3. The relationship between the maximum values of the dynamic forces of the sewing machine and seam pucker.

In previous sections the relationship between the maximum values of the main RSTM signals and the sewing machine speed was analysed, and it was found that the dynamic forces increase with sewing speed, although their increases followed different patterns. Therefore, the question of how these increases affect seam pucker was raised.

For the convenience of analysis in Figure 5.7.05 two horizontal red lines(1-lower and 2-higher) were inserted, representing the following limits of pucker severity in commercial terms:

-below Severity Line No 1 (2.75 PI) all the seam pucker results are unacceptable,

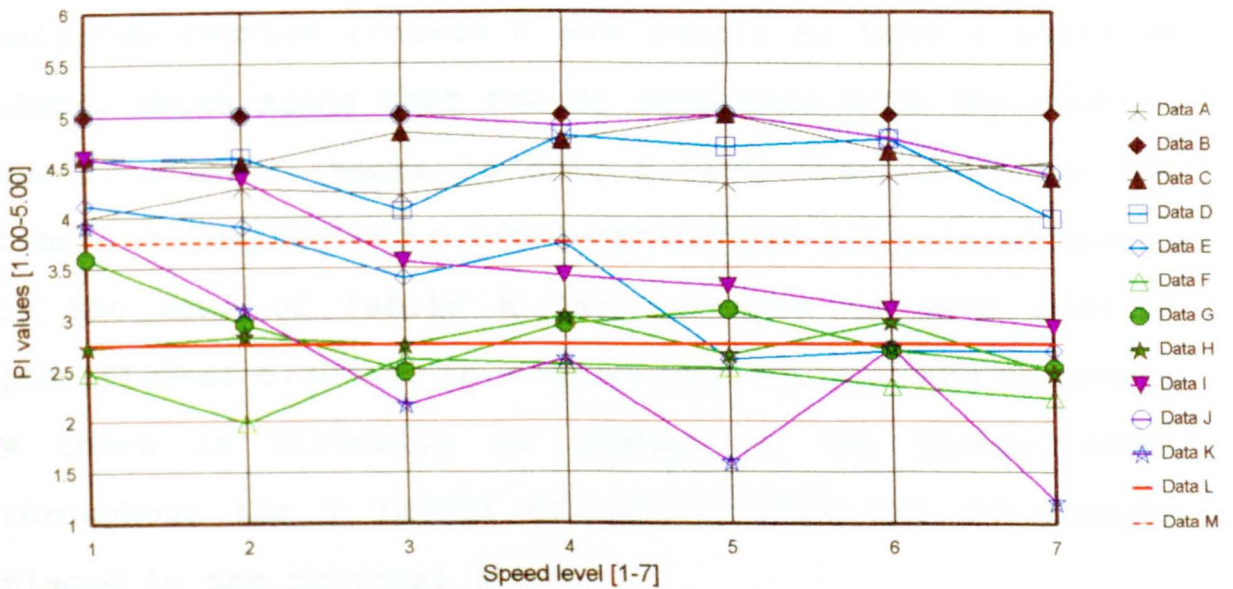


Fig. 5.7.05. The results of the Pucker Index for 11 fabrics tested at speed levels(200rpm-4000rpm).

-between Line No 1 and Line No 2 (3.75 PI) there is a critical pucker area, where the puckered seams can be acceptable provided the garments are qualified to lower quality,

-above Critical Line No 2 (all seams with the values >3.75 PI could be acceptable, unless the buyer's technical requirements stated otherwise(133).

Figure 5.7.05 includes 77 PI data points. 47.7% of the total results are located in the Acceptance area (the critical limit marked by Line No 2, 29.9% of the data points are positioned in the Severity area (between lines no 1 and 2). The remaining 22.4% are located in the Rejection area below the rejection limit marked by line No 1.

The trend of pucker values for individual fabrics is presented by the angle of the slope of relevant lines. In

Table 5.7.01 the tabulated regression equations show that only two fabrics (fabric U and fabric M) have a positive slope, which means that the PI increases with the machine speed. However, there is only a very small increase for fabric U (coefficient 0.069X) throughout 7 levels of speed. In the case of fabric M the increase is even smaller (coefficient 0.002X). This shows that in the case of fabric M there is virtually no change in the pucker level throughout the 7 levels of speed (with all PI results placed in the critical area).

Table 5.7.01.
Statistical analysis of the pucker index versus sewing machine speed for 15 fabric types tabulated in 5 groups according to mass[g/m²].

Fabr. group	RSTM Test	Win dow	Linreg. equation	Stand Error	Remark
A <60 g/m ²	U1731391-7	W63	Y1=0.069X+4.10	0.093	PI increase!
	S1731391-7		Y2= 0.0X+5.00	0.000	all PI=5.00
	T1731391-7		Y3=-0.010X+4.70	0.223	
B, 60- 100 g/m ²	V1731391-7	W71	Y4=-0.028X+4.57	0.359	
	W1731391-7		Y5=-0.270X+4.11	0.301	
C, 100- 130 g/m ²	M1732491-8	W54	Y6= 0.002X+2.38	0.223	PI increase!
	N1732491-8		Y7=-0.077X+3.15	0.325	
	K1732491-8		Y8=-0.071X+2.83	0.184	
D, 150- 200 g/m ²	P1733401-9	W45	Y9=-0.177X+4.22	0.341	
	Q1733401-9		Y10=-0.329X+5.62	0.715	
	R1733401-9		Y11=-0.069X+2.91	0.091	
E, >200 g/m ²	D1732401-	W68	Y12=-0.445X+4.78	0.301	speed 1-6-9
	F1733401-		Y13=-0.265X+5.62	0.249	speed 1-6-9
	I1733401-		Y14=-1.485X+4.95	0.154	speed 1-6-9

An example of the correlation between the dynamic forces and the pucker index and the dynamic forces and speed (for fabric Q from group D) is presented in Table 5.7.02.

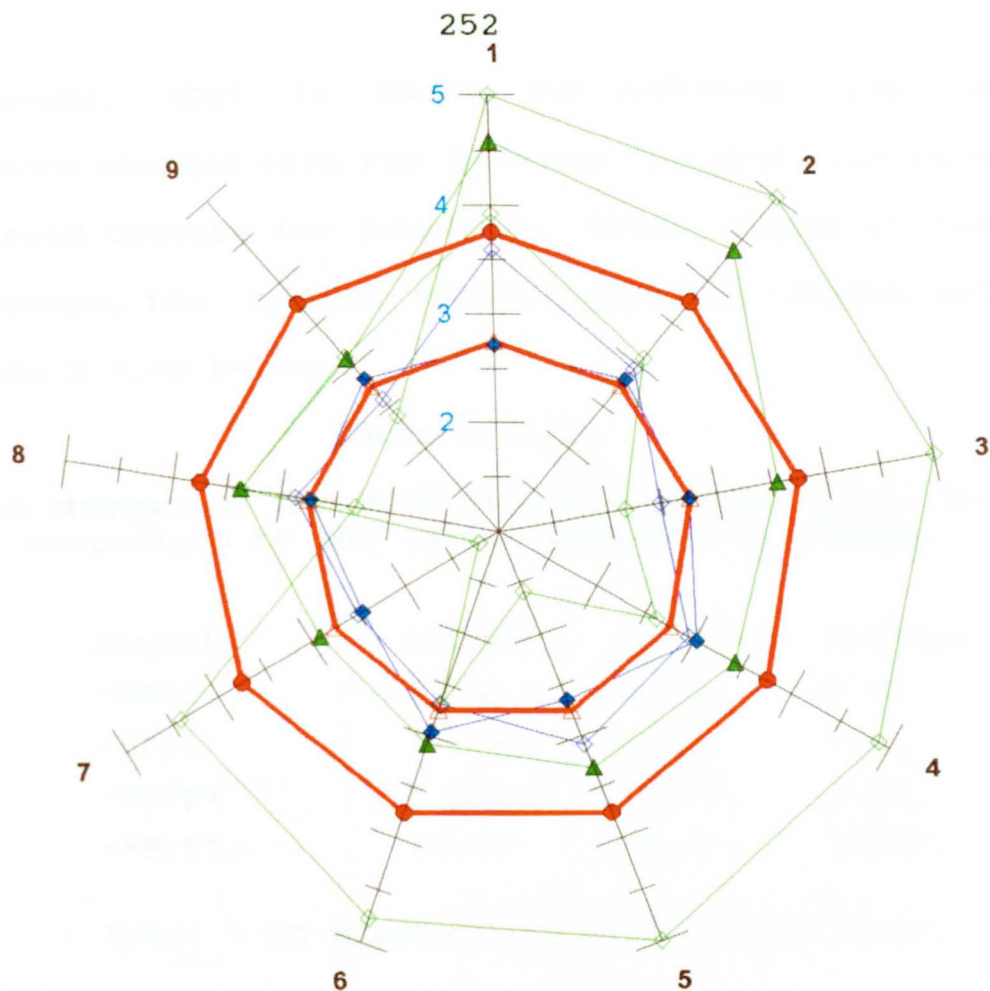


Fig. 5.7.06. The criteria for decisions on pucker level (acceptance/rejection) with the plotted results of the pucker index for 5 fabrics tested at a full range of speeds.

Note: The continuous thicker red line=Line No 2 (PI=3.75). The second continuous red line=Line No 1 (PI=2.75). The green lines present group D (the outer with square symbols=fabric Q, green triangles=fabric P and the third is fabric R. Blue lines represent group C (fabrics K, N).

The test parameters provided satisfactory results of the seam pucker level because the majority of the pucker index data is located in the Pucker Acceptance Area (see Fig. 5.7.06), throughout 7 levels of speed (200rpm-4000rpm). This range of speed is recommended as the range for commercial sewing on the Pfaff-563 lock-stitch sewing machine(126). In the "off range" of speeds used in this research, at 5000rpm and 5500rpm (levels 8 and 9 respectively) the pucker index results are located in the Pucker Rejection Area ($PI_8=2.32$ and $PI_9=2.39$ respectively).

This means, that in these circumstances the sewing conditions changed with the increase in speed. For example, with speed changes for fabric Q, from 200rpm to 3000rpm and 5500rpm, the dynamic forces increased respectively as in Table 5.7.02 below:

Table 5.7.02.

The changes of the RSTM signals' maximum peaks in comparison to the values acquired at 200rpm.

Signal	3000rpm	4000rpm	5500rpm
-NTt:	2.1x;	2.4x;	2.6x,
-PFp:	*0.8x;	1.2x;	1.2x,
-NPFp:	0.0x;	1.6x;	2.2x,
-*NPft:	12.8;	19.1x;	26.0x,

Note: * an explanation is provided later.

The increases in the dynamic forces represented by these figures seem to have a substantial influence on the increase in seam pucker. Statistical analysis performed (on Lotus 123W-V4.0) for fabric Q, as a representative fabric (due to circumstances already described above) shows the effect of dynamic forces on the seam pucker increase (Table 5.7.03).

In the case of fabric Q, in which the pucker index fell suddenly, two factors could have influenced this occurrence; firstly - the sharp increase of NPFp (from 1.6 fold at 4000rpm to 2,2 fold at 5500rpm) and secondly - the increase in NTt (2.4 fold and 2.6 fold respectively).

The values of the R²'s of NPFp, NPft and PFp are very close to each other, so that it is difficult to

differentiate their influence on seam pucker in more precise terms.

Table 5.7.03. Example of correlation between dynamic forces, speed and pucker index for fabric Q. Tests acquired at all levels of speed.

Yvar	range	unit	Xvar	range	unit	R ²	X-Co	SE-Y	SE-Co
PI	1-5	PI	Speed	1-9	rpm	0.6450	-0.32	0.71	-0.32
NTt	37-120	cN				0.9210	11.72	10.08	1.30
PFd	2-4	mm				0.8743	0.10	0.11	0.00
PFp	19-41	N				0.2719	0.90	4.34	0.56
NPFp	1-65	N				0.6016	0.35	10.44	0.11
NPFT	1-110	N				0.9397	14.68	10.88	14.68
NTt	37-120	cN	Pucker Index	1-5	PI	0.9149	-13.17	4.82	1.51
PFd	2-4	mm				0.8743	0.11	0.12	0.01
PFp	19-41	N				0.7448	-3.65	2.56	-3.65
NPFp	1-65	N				0.7395	-31.74	22.63	7.12
NPFT	1-110	N				0.7485	-3.65	2.56	0.80

X-Co=Coefficient of X(slope); SE-Y=Standard Error of Y, SE-C=Standard Error of the X- Coefficient, R²=Coefficient of Determination, commonly used model of the goodness of fit of a linear model(133); (R² ≤1, means the closer to 1 the closer the linearity); PI=Pucker index.

The ranking of the influence of the dynamic forces on seam pucker (the higher the value of R² the better the fit) is as follows: 1=NTt(0.9397), 2=QNTt(0.9210), 3=PFp(0.7448), 4=NPFp(0.7465), 5=NPFT(0.7395).

Summarising the Experiment Series No 4, it is important to point out the following factors:

1. The test results of the woven fabrics (tested in the RSTM system) in this series were analysed to explain the

following questions:

-how the speed increases of the sewing machine change the magnitudes of the dynamic forces, and

-how the increased dynamic forces affect the resultant seam pucker.

2. The woven fabrics tested had shown a common pattern of being subjected to systematic increases of the dynamic forces generated by the sewing machine speed increases (from the semi quasi-static of 200rpm to the highest level of 5500rpm).

3. It was found that increases of the dynamic forces were in the magnitude of NTt 2.6 fold, PFp 1.2 fold and NPF 2.2 times.

4. The increases of the dynamic forces were unevenly distributed throughout a full range of speeds and it was found that:

-presser-foot pressure showed the least linear pattern among the 4 main RSTM signals. There was also a systematic drop in the pressure, which occurred at 3000rpm, for all fabric types with a mass per unit area above 100g/m^2 ,

-the needle thread tension increases were very close to linear, having the coefficient of determination $R^2=0.9210$. The test results for heavyweight fabrics showed lower increases in thread tension with machine speed increases, than their lightweight equivalents, which was not unexpected, nevertheless more attention is required in

the selection of the sewing threads according to fabric mass per unit area,

-the needle penetration forces had their increase well correlated linearly with the speed increases of the sewing machine ($R^2=0.6016$). The correlation of their maximum values with the pucker index shows even higher results ($R^2=0.7395$),

-the presser-foot displacement coefficient of determination in relation to machine speed increase was $R^2=0.8743$ and in relation to pucker index $R^2=0.8749$,

4. The pucker index seemed to correlate less with the speed increase than was expected. In the majority of fabrics a slow reduction of the pucker index was observed throughout the full range of speeds. Fabric Q's coefficient of determination was found to be $R^2=0.6450$, which is confirmed in Fig 5.7.05 (where the slope is very low and of a negative direction) and in a "polar" graph Fig. 5.7.06.

5. The test results of the micro-fibre fabrics had a similar general trend of pucker increases with the increase of sewing machine speed, to the other fabrics tested. However, the traces of individual signals showed significant variation in the shapes of peaks, timing and amplitudes and confirmed the importance of the careful selection of sewing parameters on seam quality (e.g. a slight reduction in the stitch density led to a sharp increase in seam pucker).

Chapter 6.**SUMMARY.****6.1. Summary of findings.**

This research was a study of the dynamic forces generated in actual sewing conditions, in the lock-stitch type sewing machine, throughout a full range of speeds from the quasi-static conditions of 200rpm to the highest level of 5500rpm.

In order to examine the effect of dynamic forces in real time (particularly at a higher speed range) and their effect on seam pucker as a sewability factor, a special computer-based instrumentation called the RSTM, having four A/D acquisition channels was developed. This was capable of providing objective measurement of the following parameters, the sewing thread tension (NTt signal), the presser-foot pressure (presser-foot bar PFp signal) and displacement (PFd signal), the needle penetration forces (needle bar pressure NPFp) and withdrawal (needle bar tension NPft), and the seam pucker severity index (PI index).

In the first part of this research a set of five transducers was built as the first stage of the development of the RSTM. They were equipped with special sensors capable of simultaneously picking up high-frequency dynamic responses (with or without filtering), connected to the data acquisition channels of the RSTM, which could transform the analogue signals into digital data.

In order to relate the values of the acquired signals to seam pucker, a computer-based, objective evaluation system of seam pucker measurement was developed in the second part of this research.

To evaluate the reliability of the developed systems a series of preliminary tests were carried out on pre-selected standard fabrics and sewing threads. After positive results had been obtained the main series of tests with a wider range of fabrics was performed on the fully operational system (over 130 tests).

The final aim in the last part of this research (which dealt with the analysis of the distributions of the individual signals and their interactions with fabric and sewing thread) was an attempt to find the correlation between dynamic forces and seam pucker in relation to sewing machine speed increases.

6.2. Conclusions.

The conclusions are presented separately in four groups, according to the sequence of experiments.

6.2.1. The capability of the sewability testing system developed.

Throughout the range of testing carried out in this research, the capability of the RSTM system and the accuracy of data acquired (related to dynamic forces) was found to be satisfactory and to comply with the research objectives. The test results (in the form of general characteristics of the individual signals and their

timing) were found to be in close agreement with other results presented in the series of publications(7,19, 22,39,49,51,57,58,131).

6.2.2. The results of the analysis of the individual signals.

The analysis carried out on individual signals representing the main dynamic forces of the sewing process showed that:

- a. Single cycles of the signals (extracted from a series 15 cycles in length) had their own, unique, characteristic traces, and the amplitudes of their peaks in each series varied with the sewing machine speed.
- b. The magnitude of the increase of the dynamic forces was found to be lower than expected: for the NTt it was 2.6 fold; for the PFp 1.2 fold(inertia included); for the NPF 2.7(inertia included) and for the extracted ENPFp 3.2 fold(inertia excluded).
- c. The characteristics of the signals for the variety of materials tested (from woven standard fabrics of different weights, through micro-fibre fabrics of different finishes, to carbon paper which was used for comparison) showed some differences, despite their general similarity, with respect to the following features:

-the spread of values: these were influenced by the speed and pre-settings of the sewing machine, types

of threads and fabrics used, and the nature of the fabric resistance at the needle piercing point,

- the shapes of the peaks and valleys,
- location: in terms of shaft angle domain, which was found the most appropriate form for the comparison of the signals,
- timing: matching the common responses such as the T_{up} and F_d on the other signals (explained further on the phased diagram Fig. 5.5.01 and in Table 5.5.01).

d. By filtering the signals (on input) their maximum values were reduced, e.g. in the case of the NPFp signal (acquired at a speed of 5500rpm) the amplitudes of its two main peaks were reduced approximately 9.5% and 4.3%. Moreover, during the smoothing of the signals by the application of the 'Moving Average' function, some important parts of the signals were lost and this function was therefore found to be impractical. Another method of filtering by 'Adding and Averaging'(see Section 5.3), which was subsequently used to remove the noise from the acquired signals might be useful in further research in this field.

e. The test results of the main experiments carried out show that the needle thread tension maximum values of Phase III (in the stitch formation cycle), after reaching their extreme value around 3000rpm, start to decrease with the increase in the sewing machine speed (see Table

5.4.02). A similar occurrence was also found by Nowak and Wiezlak(27). However, an explanation for this finding requires further investigation.

f. It was also found that the needle thread tension for light-weight fabrics(mass around 50g/m^2) increases 2.5 fold, in comparison to the increase for heavier fabrics (mass around 200g/m^2) of only 1.6 fold, during machine speed increase from 200rpm to 5500rpm. This means that tension for heavier fabrics at lower speeds(see Fig. 5.7.01) is significantly higher than for lightweight fabrics, suggesting that thread tensile properties should be chosen with care for these conditions.

g. The presser-foot pressure (PFp signal) value was found to be at its lowest level at 3000rpm and started to rise sharply from then on(see Figs. 5.5.03 and 5.7.02).

h. The needle penetration forces (NPF) have distinctive characteristics for different fabric types. The character of the resistance to needle piercing plays an important role in the values of frictional forces opposing the needle penetration and could be clearly distinguished by the values of the P_{\max} at the needle penetration point(N_e) and the values at the shank penetration point(N_s). The signals (N_s and N_e) vary from cycle to cycle, and for example, for the extracted signals of a single cycle the difference varies between 27% (at 200rpm) to 122%(at 5500rpm). This means that the value of the needle shank

penetration force (at the shank penetration) is higher than the value of the force at the needle eye penetration, which has hitherto been regarded as the highest in the cycle(see Fig.5.4.05).

6.2.3. Changes in the interactions of the dynamic signals with sewing machine speed increases (examples).

The advantage of this system in comparison to the most advanced previous research, at NCSU in the USA(57,58), is the ability of the instrumentation of the system to acquire and to process simultaneously (in real time) four signals representing the dynamic forces of the sewing process and to relate these to the measured seam pucker index. Inclusion of a needle thread tension transducer as part of the instrumentation allows one of the main factors affecting seam pucker to be monitored. The acquired data can be presented in a graphical form, which helps in the analysis of the changes of distribution and interaction. The main findings are presented below:

a. The conditions for optimum needle penetration are known (49,128,130) to be:

- the NTt has to be at minimum,
- the presser-foot should be at its lowest position (at minimum pressure),
- the timing of the needle thread disengagement from the rotating hooks of the bobbin should be synchronised with the needle movement.

It was found in the experiments, that at the higher speeds the first two conditions were not accomplished (because the "bounce effect" had already taken place), which resulted in the reduction of the pucker index(PI), see Fig.5.4.11 and PI results for fabric Q on page 223.

The factor $PFPD = PFp_{Ne} - PFp_{cmin}$ (difference between PFp at Ne and PFp cycle minimum was found to be a good differentiating factor of the influence of the presser-foot forces on conditions at the needle penetration point (the higher the PFPD the worse the penetration conditions).

b. Another example of the interaction between dynamic forces is the 'bounce effect' of the presser-foot, which can be monitored in graphical form on the instrumentation. The mechanism was described previously (52,58,134), and in this research on page 213, and Fig. 5.4.09. It was found with respect to fabric Q that the bounce lasts about 15.3% of the full cycle at a speed of 5500rpm (when a hinged type of presser-foot is used). During the bounce the presser-foot lost contact with the feed-dog and as a result the fabrics between them were not controlled by the presser-foot pressure, which caused imbalance in the feeding of the fabric and consequently contributed to the increase in seam pucker. During its downward movement, the needle did not penetrate the fabric at the lowest level of the presser-foot position and pressure, but during its descent, which is clearly visible in Fig. 5.4.09 and

contradicts the optimum penetration conditions described in point a, above.

This finding leads to the suggestion of monitoring the bouncing during pre-production sewability evaluation, with the aim of eliminating or reducing it by applying some preventive techniques such as a special, so called "floating", presser-foot developed by Pfaff, or slowing down the bottom layer of the fabric by special sand-paper straps placed on the sewing machine table, or simply, advising the operators to reduce the sewing speed (particularly on long seam operations, which are regarded as especially suitable for highest-speed sewing).

c. The interactions between dynamic forces observed in a graphical form and the possibility of measuring their characteristic common points could help sewing machine mechanics to assess the synchronisation of the sewing machine kinematics, which is demonstrated in Fig. 5.5.01 supported by Table 5.5.01, where the common points of the single signals are marked/described with comments in the remarks column(e.g. "agreement" or "no control", etc). Having such a "technical dossier", machine mechanics and technologists could monitor and provide more detailed improved settings for the machines employed in the sewing rooms, match the needle types, feed-dogs, presser-feet, and other machine pre-settings, better. Such expertise in the form of graphical reports is an additional diagnostic "computer-based engineering tool" for technologists and

sewing machine mechanics to monitor machine characteristics.

6.2.4. Some aspects of the correlation of the individual signals of dynamic forces with sewing machine speed and the resulting pucker index.

Some attempts have been made in this research to correlate the dynamic forces under study with two factors, namely machine speed and the resultant seam pucker. The increases of sewing speed were related to the distribution of each individual signal, or all of them collectively, so that their interactions could be monitored. These distributions were therefore analysed by statistical methods to find their relationships with the seam pucker index according to the machine speed increases. Some conclusions which may contribute to the development of pucker prediction methods, as a means of achieving optimum stitching conditions, are described below:

a. It was found that, the maximum values for all signals increased with the sewing machine speed increases(global view), although these increases followed their own distinctive patterns depending on the fabric qualities(for the pre-set sewing parameters).

b. The general tendency of the needle thread tension is that its maximum values tend to rise approximately linearly with the increase in the speed of sewing, e.g. the coefficient of determination(133) of fabric type Q (of

mass 192g/m²) was very high ($R^2=0.9210$). This general trend related to woven standard fabrics of different mass per unit area and to the three types of micro-fibre fabrics tested.

However, as there is no universal single formula of linear regression available, it is suggested that individual equations should be used to measure the correlation between the needle thread tension and sewing machine speed for each type of fabric and sewing thread.

In so far as the seam pucker index is concerned there is a similar, very good correlation level ($R^2=0.9145$) with the needle thread tension rise, over the full range of sewing machine speeds from the quasi-static of 200rpm to the extreme level of 5500rpm.

c. The presser-foot pressure force showed no increases during the lower part of the speed range and its rise (up to a maximum 1.2 fold at 5500rpm) started in the upper range of speeds, see Table 5.7.02.

Therefore, in this case there was no linear correlation with speed and the coefficient of determination $R^2=0.2719$ of fabric Q was the lowest amongst all the four signals.

However, in so far as correlation with the pucker index is concerned, the presser-foot pressure correlated better with the pucker index than with speed, being more linear with $R^2=0.7395$. This is important as an example of the influence of this force on optimum sewing conditions

represented by the acceptable level of seam pucker(see criteria of acceptance/rejection on page 253, Fig. 5.7.06 and Table 5.7.03). The seam pucker factor was selected in this research as the 'determining factor' of the optimum sewing conditions.

d. The needle bar forces(pressure) were found to be well correlated with the seam pucker index($R^2=0.7395$) and less with the speed increases($R^2=0.6016$). This can be partially explained by Table 5.7.02, where the sharp increase starts from the level of 3000rpm and increases 2.2 fold at 5500rpm. In conclusion it can therefore be suggested that the influence of the needle bar penetration forces on seam pucker becomes very important at high speed ranges and close attention should be paid to this factor in the evaluation of fabric sewability.

e. At upper speed ranges the sewing conditions(well balanced at the lower range of speeds) are suddenly subjected to the combined negative influence of many factors related to the increases in the dynamic forces such as e.g. the high frequency changes in velocity of the sewing thread, an increase in frictional forces at various places in the stitch formation, the bouncing of the presser-foot, and certain difficulties in the tightening of the stitch in the stitch tightening zone.

In circumstances of such complexity it is impossible to present a universal seam pucker prediction equation in the form of one linear regression equation.

In the case of seam pucker, there is a need to study (in greater depth) the influence of other factors such as the physical and mechanical properties of fabrics and threads over a wider range of sewing machine pre-setting parameters and to collect results from a wider range of fabrics and sewing threads.

Finally, it should be noted that, due to the limited range of fabrics presented in this research, caution should be used before applying the results and conclusions to fabric types other than those tested.

6.3. Recommendations.

The recommendations presented below are listed in two groups:

A - suggestions for improvements of the existing design of the RSTM which were deduced too late to be implemented during the final stages of this research, and

B - recommendations for further development of the system.

6.3.1. Improvements of the existing set-up.

The recommendation is in the form of advice to supervisors of the system at the Institute of Textiles and Clothing of the Hong Kong Polytechnic University:

a. The strain gauges of the thread transducer should be replaced by semi-conductor types (of a higher sensitivity

and smaller size) to increase the transducer resolution, should more specialised research into finer sewing threads for new types of micro-fibre fabrics be planned. There is a possibility of acquiring data up to 750 kHz per one channel (which provide "state-of-the art" testing capability).

b. The SPMS system should be linked with the DAP programme to write automatically Pucker Index results into the RSTM hard copy report(using the available DDL macros).

c. To aid in the evaluation of the sewability of fabrics, the existing programme makes provision for up to 10 trial re-runs of tests according to the changes in those parameters which have the strongest influence on seam pucker, according to the findings of this research. The relation of the seam pucker index to sewability proved in this research to be a sufficient "determining factor" of sewing conditions.

Therefore, until new, improved prediction methods become available the RSTM "trial-and-error" method should be sufficient for the evaluation of sewability. Preliminary tests showed that, usually after 3-4 trails, satisfactory results were achieved.

6.3.2. Proposals for further improvements.

This set of proposals aims to widen the capabilities of the system to allow for more advanced experimentation.

a. It is suggested consideration be given to including the RUI¹ index in the SPMS programme, which might be helpful in subtracting the colour influence in the CCD camera readings. This solution was provided too late to be included in this research.

b. A full utilisation of the two existing D/A output channels in the DT2841-board should also be reconsidered for future research, e.g. for the automatic re-setting of the adjustment scale of the presser-foot bar (as a feedback from the DAP programme/expert system) and for automatic thread tension adjustment.

c. The lack of a 5th A/D channel can be compensated for by inserting a second DT2841-board with an additional four channels. This would allow signals such as feed-dog displacement, take-up lever displacement, pressure of the disk tensioner, to be input, widening the range of sewing process monitoring facilities.

d. The RSTM acquisition system could be used for acquiring data from other transducers installed in different types

¹ The RUI index stands for Relative Unlevelness Index. It can be measured by a CCD camera. The method was recently developed at the Institute of Textiles and Clothing of Hong Kong Polytechnic(134).

of sewing machines; this is already taking place at the HKP University (overlock machine).

e. The RSTM system could have wide ranging applications and could be used to measure the dynamic forces not only of sewing fabrics but also of leather and leather-like materials. During the course of this research for example, an experiment was carried out with carbon paper to evaluate needle penetration forces.

Chapter 7.

REFERENCES.

1. Curiskis, J.I.; Private communication. Hong Kong Polytechnic, 1989.
2. Solinger, J.; Apparel Manufacturing Handbook. Analysis, Principle and Practice. 2nd ed., Bobbin Media Corporation, 1988.
3. Uchiyama, S.; "Proposal with regard to materials". Paper presented at JIAM International Seminar, 1991.
4. Davis, W.; Journal of the Textile Institute, 24, T361, 1933.
5. Shirley Institute; a. "Some factors influencing the damage to the sewing thread. The stitching of fabrics". Part II and IV. Shirley Institute Bulletin, 12, pp.71-77, 1939.
6. Scott, L.H.; "Some problems relating to sewing". Journal of the Textile Institute, 42, pp.652-660, 1951.
7. Frederick, E.; "Development of a sewability test for cotton fabrics". Journal of the Textile Institute, 22, pp.687-692, 1952.
8. Sondhelm, W.; "Causes of seaming damage". Journal of the Textile Institute, 44, T580-585, 1953.
9. Frederick, E., and Zabieboylo, W.; "Measurement of needle heat generated during sewing of wool and wool-nylon fabrics". Textile Research Journal, 22, pp.1025-1029, 1952.
10. Dorkin, C.M., and Chamberlain, N.H.; "The causes of seaming damage and pinholing in cotton and rayon-cotton fabrics". Textile Research Journal, pp.687-692, 1952.
11. *ibid*; "The facts about needle heating". Clothing Research Journal, Technological Report No.13, 1963.
12. Khan, R.A., Hersh, S.P., and Grady, P.L.; "Simulation of needle-fabric interaction in sewing operations". Textile Research Journal, 40, (6), June 1970.
13. Howard, G.M., and Parsons, D.; "Sewing needle temperature. Part II: The effects of needle characteristics". Textile Research Journal, 40, (6), June 1970.
14. Anon; "Singerspecial nadelfabrik". J.S.N. International, pp.22-23, February 1983.

15. Baugh, C.; "Needle problems and how to avoid them".
Bobbin, January 1984.
16. Murphy, M.; "Needle problems and how to avoid them".
Bobbin, January 1984.
17. Nowak, R.; Parts I-IV, "Research into dynamic conditions
of the needle penetration in a sewing machines", [In
Polish]. Odzież, 1972.
18. Leeming, C.A., and Munden, D.L.; "Investigation into
factors affecting the penetration force of the sewing
needle in a knitted fabric and its relationship with
fabric sewability". Clothing Research Journal, 6,
No.3, pp.759-768, 1978.
19. Nestler, R., and Arnold, J.; "Technique for the study of
needle penetration forces during sewing", [In
German]. Bekleidung and Machenware, No.3, pp.132-136,
May/June 1979.
20. Gersak, J., and Knez, B.; "Determination of the needle
penetration force in a garment sewing process". [In
Slovene], Tekstil 34(10), pp.759-768, 1985.
21. Galuszynski, S.; "Effect of fabric structure on fabric
resistance to needle piercing". A letter to the
Editor of Journal of the Textile Research Institute,
No.7, 1985.
22. Stylios, G.; "A study of problems associated with fabric
sewing in commercial garment manufacture". Phd
thesis, Leeds University, 1988.
23. Jones, R.J.R. "Review of previous work on the factors
affecting the thread dynamics characteristics of the
lock-stitch". Clothing Research Journal, 3(2), 1975.
24. Kolesnikow, P.A., Pankowa, L.N., Alexeev, L.G.; "Metodika
izmerenya natyazhenya niti na sheveinoi mashine w
protsese raboty z pomoshchyu provolochnykh datezNIKOW
soprotivleniya", [In Russian],[Method of a thread
tension measurement using strain-gauges]. Naucznye
Trudy, CNiSzP, Vol.2, 1952.
25. Rusakow, S.J.; "Provedenenitki cherez tkani
priobrazowani stezka", [In Russian], [Needle thread
passage in a stitch forming process]. Naucznye
Trudy, CNiSzP, Vol.41, No.8, 1957.
26. Tomanec, L., and Sramec, L.; "Mereni dynamicesko napeti
niti pri siti"[In Slovak],[Measurement of the thread
dynamic tension during sewing process]. Textil 14,
No.3,4, pp.107-108 and 151, 1962.

27. Nowak, R., and Wiezlak, W.; "Measuring the static and dynamic stresses in the sewing thread during the sewing process", [In Polish]. *Zeszyty Naukowe Politechniki Lodzkiej*, No.93, *Wlokiennictwo*, z.16, 1967.
28. Miyashita, R.; "Measuring needle thread tension and detecting skip stitches during sewing process", [In Japanese]. *Journal of Textile Machinery Society of Japan*, 27, No.1, pp.55-62, No.2, pp.111-116, 1974.
29. Gersak, J., and Knez, B.; "Reduction in thread strength as a cause of loading in the sewing process". *International Journal of Clothing Science and Technology*, Vol.3, No.4, 1991.
30. Chmielowiec, R.; "Optimum stitching conditions". SABS Project No.441/500040, 1985.
31. Wiezlak, W., and Siejka, K.; "Downtime resulting from thread breakages on the sewing machine", [In Polish]. *Przeglad Wlokienniczy*, No.44, (11/12), pp.331-350, 1990.
32. O'Dwyer, U., and Munden, D.L.; "A study of a lock-stitch seam". *Clothing Research Journal*, Vol.3, pp.33-40, 1975.
33. Horino, T., and Kawaniski, S.; "Biaxial tensile behavior of woven fabrics sewn with open lock-stitches to form a cylinder", [English edition]. *Journal of Textile Machinery Society of Japan*, No.21(1), 1975.
34. Anon; "Thread tension analysis breakthrough". *Manufacturing Clothier*, April 1977.
35. Pilaczynski, A.; "Influence of the sewing thread quality on the stitch-forming process", [In Polish]. *Odzież*, No.28(7), 1977.
36. Frank, T.F.P.; "Study of thread feed-mechanism in commercial high-speed sewing machine. Phd thesis, Leeds University, 1979.
37. Horino, T.; "Simultaneous measurement of the tension and feed length of the needle-thread during the operation of a home sewing machine", [in Japanese]. *Journal of Textile Machinery Society of Japan*, 33, No.2, T7-13, 1980.
38. Jones, R.J.R., and Munden, D.L.; "The study of the mechanics and geometry of the 2-thread chain stitch. Part 1: An instrument for measuring static needle and looper thread tension". *Clothing Research Journal*, Vol.8, No.3, pp.107-114, 1980.

39. Catchpole, J.L., and Saradi, M.; "Stitch quality monitoring in sewing operations". Bradford Conference, July 1990.
40. Sandoz Ltd; "Avoiding sewing damage". Bobbin, 23, pp.280-286, 1981.
41. Russel, A.R.T.; "Adjusting tension overcomes problems. Sewing with difficult fabrics". Apparel World, pp.20-23, 1984.
42. Anon; "Sew right with the aid of a new thread tension service" British Clothing Manufacturer, December 1975.
43. J.&P.Coats Ltd; a. "A new meter and why". Knitting International, 82, pp.86-87, 1975 and b. "Coats Tension/Pressure Meter Mk2; Operating Instruction".
44. Greenberg, N.A.; "An instrument for measurement of the thread dynamic tension characteristics on sewing operation". Part 2. Clothing Research Journal, No.3(2), 1975.
45. Munden, D.L., and Leeming, C.A.; "US Patent 3979951-1976, and UK Patent 1483189-1977.
46. Tyler, D.J.; "The Hatra Sewability Tester". HATRANOTE, No.40, 1976.
47. Anon; "Thread tension analysis breakthrough". Manufacturing Clothier, April 1977.
48. Deery, F.C.; "Continuous measurement of thread tension". MSc Thesis, Leeds University, 1984.
49. Kamata, Y., Kinoshita, R., Ishikawa, S., and Fujisaki, K.; "The needle thread disengagement from the rotating hook, effects from its timing on the tightening tension - in the industrial sewing machines". Journal of Textile Machinery Society of Japan, Vol.30, 1984.
50. Gersak, J.; "Analysis of several parameters affecting sewing, especially in the needle-thread sector", [In Slovene]. Textil, 35, No.7, pp.447-489, 1986.
51. Ferriera, F.B.N.; "A study of thread tensions on a lock-stitch sewing machine". Phd thesis, Leeds University, 1990.
52. Price, C.D.; "Development in sewing machines". Textiles, No.15, Vol.3, pp.67-71, 1986.
53. Disher, M.; "High technology in the clothing industry". Textile Outlook International, pp.52-55, September 1986.

54. Spickerman, R.; Private communication at IMB'93 in Cologne. Pfaff's GmbH "New Technology Corner", 1991.
55. Doughty, P.J.; "Advancing thread tension understanding". Apparel International, June 1991.
56. Bodenschatz, S.; "Verbesserung der Vernachbarkeit von Textilien", [In German], [Improvement of sewability in textiles]. Institut von Textiltechnik. Textil Praxis International, pp.30-34, July 1985.
57. Matthews, B.A., and Little, T.J.; "Measuring sewing machine forces at high speeds". Textile Research Institute, July 1988.
58. Clapp, T.G., Little, T.J., Thiel, T.M., and Vass, D.J.; "Sewing dynamics. Objective measurement of fabric/machine interaction". International Journal of Clothing Science and Technology, Vol.4, No.2/3, 1992.
59. Stylios, G., Fan, J., Sotomi, J.O., and Deacon, R.; "Introducing new concept in garment manufacture. The Sewability Integrated Environment, incorporating automated objective measurement systems". Paper presented during the 2nd Bradford Conference. Bradford, UK, 1992.
60. Stylios, G., and Sotomi, J.O.; "Automatic setting of optimum sewing machine conditions for the manufacture of high quality garments made of lightweight synthetic fibre fabric". Paper presented at the Conference organised by Kyoto University, Japan, 7-9 of August 1992.
61. Data Translation, Inc.; "Data Acquisition moves into the realm of PCs". Data Acquisition Bulletin. Documentary Stories, 1991.
62. Cram, R.J.; "Fabric Joining Methods" (Survey of over 500 published references). Shirley Institute, 1984.
63. Taylor, G.; Private communication. Fashion Editor of Textile Asia. Hong Kong 1990.
64. Galuszynski, S.; "Seam pucker". Survey of 56 publications. SAWTRI Special Publication, Vol.76, May 1986.
65. Stylios, G. and Lloyd, D.W.; "A technique for identification of seam pucker due to fabric structural jamming". International Journal of Clothing Science and Technology, Vol.1, No.2, 1991.
66. Zorowski, C.F. and Patel, G.C.; "Seam pucker as a mechanical instability phenomenon"; Journal of Engineering for Industry. February, No.17-22. 1970.

67. Anon; "Seam pucker-why blame the thread?". Organisation & Methods. Manufacturing Clothier. July 1978.
68. Stolhman, D.; "A statistical quality control program for the sewn products industry". 'Sewn Product Engineering and Reference Manual' from Bobbin Publications Inc., 1984.
69. Galuszynski, S., and Robinson, G.A.; "Production profile and problems encountered in the S.A. Clothing Industry. Results of a recent survey". SAWTRI Report of 1984.
70. American Apparel Manufacturers Association (AAMA); "Elements of apparel quality program". 1984.
71. The British Standard 6476:1984; "British standard guide to garment quality and relevant british standards". 1984.
72. Hong Kong Polytechnic; "Standard Specification for men's woven dress shirts". Standard accepted by Hong Kong 'Q-Mark' Council. Prepared by Institute of Textiles and Clothing in 1987.
73. Scholes, C.F.; "The quality of stitched seams", Shirley Institute lecture 1907. February 1951.
74. Dorkin, C.M.C., and Chamberlain, N.H.; "Seam pucker its causes and prevention". Clothing Institute Journal, Technological Report, No.10, June 1961.
75. Townsend, T., and Chamberlain, N.H.; "More light on structural seam pucker in light-weight fabrics". Clothing Institute Technological Report. No.16, September 1984.
76. Taylor, J.L., and Clarke, F.C.; "Physics of seam pucker". Textile Industries, April 1967.
77. Schwartz, P.; "Effect of jamming on seam pucker in plain woven fabrics". Textile Research Journal, January 1984.
78. Stylios, G. and Lloyd, D.W.; "A technique for identification of seam pucker due to fabric structural jamming". International Journal of Clothing Science and Technology, Vol.1, No.2, 1989.
79. American Association of Textile Chemists and Colorists (AATCC); Test method 88B, (first version published in 1962 and later subsequently modified). 1981.
80. Shiloh, M.; "The evaluation of seam puckering". Journal of the Textile Institute, No.62, 176, 1971.

81. Garnindustrie GmbH; "New aid to reduce puckering risks". Readywear, No.3, pp.10-11, 1978.
82. Rosenblad-Wallin, E., and Cednas, M.; "Pressing of seams and creases". Clothing Research Journal, 2, No.3, pp.115-121, 1974.
83. Cednas, M.; "Shrinkage characteristics of fabrics and their effect on garment pucker". Clothing Research Journal, 2, No.3, pp.122-132, 1974.
84. Belser, R.B., Kwon, C.T., and Meaders, J.C.; "Instrument for grading seam pucker". Clothing Research Journal, No.38, 1985.
85. Bertoldi, A.M., and Munden, D.L.; "The effects of sewing variables on fabric pucker". Clothing Research Journal, 2, No.2, pp.68-80, 1974.
86. WIRA; Information Sheet, Pukka Tester.
87. Collins, J.; "Investigation into the objective evaluation of seam pucker". M.Phil thesis, School of Textiles, Galashields, UK. 1990.
88. Galuszynki, S.; "Measurement of seam pucker J.S.N. International, November 1986.
89. Lo Sau-wan; "An introductory investigational project on seam pucker measurement by comparative evaluation". HDip.Project, Hong Kong Polytechnic, 1989.
90. Stylios, G. and Lloyd D.W.; "Prediction of seam pucker in garments by measuring fabric mechanical properties and geometric relationships". IJCST, Vol.2, No.1, 1990.
91. Sorensen, T.; "Prediction of seam puckering by objective measurements on fabrics". Melliand Textilberichte, No. 72, 1991.
92. *ibid*; "Possibilities of predicting the seam puckering propensity of textile fabrics". Paper presented during the 2nd International Clothing Conference. Bradford, U.K., July 1992.
93. Lam, A., Chan, A., and Black, D.; "The effect of fabric properties on twin-needle lap-seam pucker of commercial shirting fabrics". Paper presented during 2nd International Clothing Conference in Bradford, U.K., July 1992.
94. Shimazaki, K.; "Study of machine sewing. An analysis of seam puckering by studying profile of the seam". Journal of Japan Research Association for Textile End-uses, No.20, p.234, 1979, and personal

- communication/ interpretation at Leeds University in 1988.
95. Inui, S., Shibuya, A.; "Objective evaluation of seam pucker using automated contactless measurement technology". Paper presented during the 2nd International Clothing Conference in Bradford, U.K., July 1992.
 96. Gupta, B.S., Leek, F.J., Barker, R.L, and Little, T.J.; "Directional variations in fabric properties and seam quality". International Journal of Clothing Science and Technology, Vo.4, No.2/3, pp.71-78, 1992.
 97. Lloyd, D.; Private communication. Hong Kong Polytechnic, 1989-1992.
 98. Pfaff GmbH Co.; "Operation Manual of the Pfaff-56 lock-stitch machine. Keiserslautern, No. 2. Germany. 1988.
 99. Kistler Instrumente AG; "Operating and Service instructions". Quartz Load Washers. Switzerland, 1989.
 100. Data Translation Inc.; Operation Manual of 2841-L. Technical Specification, USA, MA. 1988.
 101. Data Translation, Inc.; "The MACH™ DSP Subroutine Library". Technical Manual. USA, 1989.
 102. Harlock, S.C.; Private communication. Hong Kong Polytechnic, September 1991.
 103. Wieszlak, W.; Private communication. Hong Kong Polytechnic. March 1992.
 104. Lloyd, D.W.; Private Communication. Kong Kong Polytechnic, February 1992.
 105. Postle, R.; "Fabric objective measurement technology: present status and future potential". Bradford Conference 1990.
 106. Roberts, F.; "Decorative top stitch effects on poplin garments possibilities and limits of a styling method by sewing". J.S.N. International, Bobbin Show issue, 1986.
 107. Mahar, T.J., Dhingra, R.C., and Postle, R.; "Fabric mechanical and physical properties relevant to clothing manufacture"; Part I and Part II. International Journal of Clothing Science and Technology, Vol.1, No.1 and No.2, 1989.
 108. Kawabata, S., and Niwa, M.; "Application of objective measurement to clothing manufacture". International

Journal of Clothing Science and Technology. Volume 2,
No. 3/4, 1990.

109. Kawabata, S., and Niwa, M.; "Objective measurement of fabric mechanical property and quality". International Journal of Clothing Science and Technology. Vol. 3, No. 1, 1991.
110. Dingra, R.C, and Postle, R.; "Application of FOM to wool fabric finishing". Department of Textile Technology, University of New South Wales, 1990.
111. Amirbayat, J. and McLaren Miller, J.; "Order of Magnitude of compressive energy of seams and its effect on seam pucker". International Journal of Clothing Science and Technology. Vol.3, No.3, 1991.
112. Kwong, M.Y; Private communication. Hong Kong Polytechnic, 1992.
113. Off, W.A.; "MITi's new sewing concept". Apparel Industry Magazine, pp. 26-31, May 1991.
114. Jähler, H.D.; "Research and Development in Industrial Technologies in Europe". J.S.N. International, July, 1990.
115. ASTM Standard Test Method D3939-80; Snagging Resistance of fabrics (Mace Test Method).
116. Data Translation Co.; "The Image Processing. Glossary" Annual Publication, 1991.
117. Lloyd, D.W.; Private communication at the Hong Kong Polytechnic, September 1990.
118. The Cambridge Instruments Company, UK; Quantimet 520 Manual, 1988.
119. Data Translation Inc.; Image Processing Handbook, "Image processing operations", 1991.
120. Data Translation Inc.; Image Processing Handbook, Tutorial, "Choosing image processing boards and software", 1991.
121. Data Translation Inc.; 1992 Product Handbook. Part III, Tutorial: "Image processing operations". 1992.
122. Travis, M.; "True colour image processing, processing on the desktop". Product Technology Application Notes. Data Translation Inc, 1992.
123. Chong, T.F.; "Quick response in colour communication". Textile Asia, March/May 1990.

124. MacAlpine, J.K.M., and Kwan, P.F.; "Preliminary results in quantifying textile crease-resistance using a digital approach". HK Engineer Journal. November 1991.
125. Chong, T.F.; "Quick response in colour communication". Textile Asia, March/May 1990.
126. Pfaff GmbH; Service Manual. Sewing machine 563. Kaiserslautern, Germany. 1989.
127. Doughty, P.J.; "Advancing thread tension understanding". Apparel International, June 1991.
128. Wiezlak, W.; Private correspondence. Technical University, Lodz, Poland. June 1993.
129. Heckner, R.; "Making up of microfibre fabrics. Seam engineering information from Gütermann". Apparel International, July/August 1993.
130. Galuszynski, S.; "Some aspects of the seam pucker caused by the drop-feed mechanism". J.S.N. International, February 1987.
131. Wong, M.K.; "An investigation of some sewability factors affecting the seam performance of micro-fibre fabrics". BA Project, Hong Kong Polytechnic. 1992.
132. Moore, F.; Private communication. Merchandise Testing Laboratory of the "John Lewis Partnership" Ltd, London, U.K., January 1995.
133. SPSS for Windows; "Base System User's Guide". Release 5.0, 1992.
134. Johnson, E.M.; "Some factors affecting the performance of high-speed sewing machine". Clothing Research Journal, Vol.1, pp. 3-35, 1973.
135. Chong, C.L., Li, S.Q. and Yeung, K.W.; "An objective method for the assessment of levelness of dyed materials". Journal of Dyeists and Colourists. Vol.108, December 1992.

Appendices I and II. The RSTM programme.

Appendix I. The RSTM numerical data file (extract).

This DATASET example, shows the numerical data of the "RSTM/ Q1743309.dat" test. The file name is the meaningful string with information about the test setting, according to RSTM File Coding System, described in the chapter 3 and included in the Appendix IIIa.

The preceding part of the four-column data is the DADiSP Reference Header incorporated into DAP programme, to be always linked automatically to a programme buffer with ASCII data acquired with 10^{-6} precision. The INTERVAL is the threshold of the data acquisition. The COMMENT line allows the inclusion of additional information about the specifics of the test, which can not be included in the 8-digit file code, but are very useful in case of the test retrieval eg.:

-real speed marked as "5488" (noticed by the person carrying out testing), at the point of the manual initialisation of the acquisition, which differed from the pre-set level of "5500".

- "500" means pre-set number of data points per cycle,
 - "afoff"; stands for all filters off,
 - "ts2"; means the use of NTt thread transducer scale number 2 (out of 6),
 - "2p" means the NTt transducer. The C2Ph version of thread passage type was used, and
 - "cfg02", important note about file configuration used during acquisition.

"DATASET Q1743309:

```

VERSION 1
DATE 10/30/92
TIME 00:27:39
NUM_SERIES 4
STORAGE_MODE interlaced
SERIES Thread_tension,PF_disp,PF_pressure,Needle_pressure
INTERVAL 0.000005
VERT_UNITS (cN),(mm)/100,(N)/100,(N)/10
HORZ_UNITS Secs
COMMENT 5488/500/afoff/ts2/2p/cfg02
DATA:
  
```

Beginning-as row 1,2,3...,End 8192:

Thread_tension,	PF_disp,	PF_pressure,	Needle_pressure
269.274902	162.199997	2081.339844	1668.367920
269.132202	162.199997	2053.364990	1651.091919
268.846802	162.300003	2018.675903	1616.539917

268.846802	162.400009	2008.604980	1591.859985
269.132202	162.400009	2005.247925	1579.520020
268.846802	162.400009	1980.629883	1569.647949
268.846802	162.400009	1957.130981	1579.520020
.....
272.842407	158.000000	2430.468018	824.311951
271.986206	157.900009	2409.207031	886.011963."

(The 89192-th row, and the end of the File).

Appendix II. RSTM DAP.C Data Acquisition Programme.

The DAP.C programme is the main signal acquisition and processing programme. The main FUNCTIONS and COMMANDS are from MACH DSP Subroutines Library of Data Translation Co, USA. Programme also uses the GraphiC, graphics software subroutines. The programme runs on the Data Translation hardware. The integral part of the system programme is also DAP.CFG file.

Extract (only) from DAP.C Programme (because the full text is 50 pages long):

=====

"This example program acquires up to 640K data samples from the four channels of a DT2841-series board. The samples are stored in a large array onboard the DT7020.

When the specified amount of data has been transferred, the large array of A/D values is sorted by channel and scaled to calibrated values.

Compiler include files defining i/o operations

```
#include <stdio.h>
#include <stdlib.h>
#include <string.h>
#include <time.h>
#include <malloc.h>
#include <conio.h>
#include <dos.h>
#include <math.h>
#include <setjmp.h>
#include <stdarg.h>
#include <process.h>
#include <errno.h>
#include <ctype.h>
#include "bstrings.h"
#include "bfiles.h"
#include "km.h"
#include "wn.h"
#include "lm.h"
#include "mm.h"
#include "graphic.h"
```

Constant select no looping operation in apmac/apendm sequence. Constants to select the burst or continuous AP I/O modes.

```

|
| #define NOLOOP 0
| #define LOOP 1
|
| #define BURST_MODE 1.0
| #define CONT_MODE 2.0
|
| Clock signal to be used
|
| #define CLOCK 0L
| bytes of RAM) onboard the AP.
| Because of this restriction imposed by the
| system microcode,
| 2*(input buffer length + output buffer length)
| should be less
| than 24K.
| If this limit is exceeded, the input and output
| buffers will overlap.
|-----
| #define IBLEN 32768L
| #define OBLLEN 0L
| #define VBUFSIZ 655360L
|-----
| *
| Define a DT7020 signal code that will be used
| to flag a buffer full condition.
| This signal will allow us to count the
| number of 64K data blocks transferred to the
| AP by the DT2841.
|-----
| ... ..break!
| /*-----
| AP memory allocation and handshake function
| extern long ipaloc();
| extern long aptest();
| Data type declarations
|-----
| Global variable declarations
|-----
| AP base address of the array used to hold all of
| the data samples.
| channels 0-3.
| ..break!
| AP scalars used to point to the next full input
| buffer (addr_input),
| select the asynchronous I/O mode (addr_mode) and
| point to the next
| empty location in the temporary array (addr_ptr)
|-----
| ..break!
|
| AP scalars used as strides.
| AP scalars used to hold signal values that will tell us
| when a 32K block has been read into AP memory. Using
| these signals we can count the number of blocks that have
| been transferred.

```

```
-----
| Reference numbers for use in READ_HEADER and
| WRITE_HEADER
```

```
..... , b r e a k !
-----
```

```
| Seperate the contents of the large array
| (addr_vbuf) by channel.
| Since we acquired data from 4 channels, the
| contents of the array starting at (addr_vbuf)
| will contain data in the following order:
| ch0 ch1 ch2 ch3 ch0 ch1 ch2 ch3...ch0 ch1 ch2 ch3
| ch0 ch1 ch2 ch3...
```

```
| To extract all of the data for a particuliar
| channel, we must use a move instruction with
| strides.
| Once the data has been separated, we can scale
| it to required values.
```

```
.....break!
-----
```

```
Note: The above RSTM test results are avaiable in hard
      copies:\n
      a.partial report with the numerical results only;\n\
      b.full report including numerical and graphical
         results.\n\n\
```

```
°) SPMS stands for: Seam Pucker Measuring System.
   Developed at \n\ HK Polytechnic in 1991, modified June
   1992.\n\n%s\n", section);
```

```
.....break!
-----
```

```
| Stop the AP
```

```
          apstop();
          unlink("dap.sum");
          unlink("dap.tkf");
          printf("BYE!\n");
        } /* end of main */
```

```
End of the file.
```

Appendix III. THE RSTM CONFIGURATION AND CODE FILES.

Appendix IIIa. RSTM-DAP/CODE.SYS file. Coding system and calibration-maintenance procedure.

```
-----
File onsisits of two parts. The purpose of this coding
system is described in the Chapter 3.2.3.).
=====
```

Beginning:

"PART I. CODING SYSTEM for the RSTM TESTING METHOD.

Note:

a. The system was developed in the first experimental research into sewability at the Hong Kong Polytechnic.

b. Last modification to a calibration file was carried out on 30.10.1992 and denoted as DAP03.CFG.

CONTENTS:

1. File coding. Based on 8 digit length, compatible with other processing software such as: Lotus 123.Version R3.1; SPSS PC.Advanced Statistics,Ver.4.0; DADiSP, Ver.2.0B and later; DAP_RSTM; Statistical package MATLAB; SP; etc.

SYSTEM DIGIT NUMBERS (1-8):

-digit 1 = fabric type (CAPITAL letters: A,B,C,...X,Y,Z + ASCII's),

-digit 2 = experiment type (on the fabric described by digit 1),

e.g. A=additional special test..., I=inertia type as:

version [1-full load(needle+thread); 2-no thread; 3-pure inertia (no needle, no thread); 4-...?; F=only top part of the fabric feeder (useful for the thin slippery fabrics..;R= retest against problem occurred/discovered at the later stage.

-digit 3 = stitch density scale:

RSTM scale:

Pfaff designation:

1 -- 60	0,
2 -- 54	1/2,
3 -- 50	1,
4 -- 44	1 1/2,
5 -- 40	2,
6 -- 36	2 1/2,
7 -- 32	3,
8 -- 28	3 1/2,
9 -- 26	4,

-digit 4 = presser-foot pressure. The number of turns of the correction screw adjusting pressure.

1-- lowest pressure (no of treads from the screw head leveled with the surface of M/C body),

2--

3-- turning it clock-wise every 360 degrees

4-- changes the code number).

5-- < the last setting(September 1992).

6--

7--

8--

9-- highest pressure. Screw head at the lowest level inside the hole of the screw adjusting pressure of the presser foot.

-digit 5 = types of the sewing thread. Digits 1-9. Scale used in research as follows:

- 0--No thread used.
- 1--Art. N569/36/White. Big cone.
- 2--Art. N216/120/White.
- 3--Art. 3655/120/Blue.
- 4--Art. 3566/100/Navy.
- 5--Art. Rasant/75/75/. Navy.
- 6--Art. 3655/70/White.
- 9--...

-digit 6 = thread tension. Designation according to the thread tensioner's number of turns, upon which transducer was calibrated. The more details described in Andy Wong (BACS Project 1992).

- 0-- No thread used!
- 1-- lowest tension.(Plastic screw at the beginning of the tensioner's treaded core).
- 2--
- 3-- the most frequent!
- 4-- "
- 5-- "
- 6--
- 7--
- 8--
- 9-- Highest tension. (Impractical level, all tested threads were broken during trials).

-digit 7 = needle type. Digits 1-9. For easy use simplified as follows:

- X--No needle used.
- 0--No 100;
- 1--No 110;
- 2--No 120;
- ...
- 7--No 70;
- 8--No 80;
- 9--No 90;

-digit 8 = sewing speed: in [rpm]. Speed is presett by "Quick"'s control box.Details in the Pfaff-563 Operational Manual. In this test experiments, the following range was used:

- 0-- quasi-static. Moving wheel by hand.
- 1-- 200 rpm(lowest speed is 180rpm-M/C Manual),
- 2-- 500
- 3-- 1000
- 4-- 1500
- 5-- 2000
- 6-- 3000 (at this level and above the real speed
- 7-- 4000 can differ about +/-0.6% from the pre-set),
- 8-- 5000
- 9-- 5500

Note:

a. QR's control box accepts speed increases of 100 rpm. (Code G2-202 function). Adjust number of the pre-set stitches by G-201 function, up to 255 stitches in one run. Speeds over 3000 rpm need the lengths in the range of 200-255 stithes to enable the system to acquire a sufficient amount of data.

b. In cases of having the parameters outside the range of this 8-digit coding system - there is possibility to describe them in the eg: DAP pre-setting comments and /or in RSTM file: .DAT header. Important for retrieval.
End of Part I/.

Part II. Calibration-maintenance procedure.

1. Calibration methods used in the design of the RSTM are described in a separate appendix of the RSTM manual.

2. The following procedures should be adopted for the periodical instrumentation maintenance:

Notice:

Before the start of the maintenance, check the room atmospheric conditions and if no difference is found continue the work by checking the C/M settings. If after adjusting M/C, the "paper results" show an "out-of calibration" state; there is a need to assess individual transducers and/or to subject them to recalibration or replacement.

a. Due to the exceptional fatigue of the Needle Bar transducer subjected to 5500 rpm and stroke in the region of 3.00cm the wire may change its rigidity after a certain number of running hours.

From author's experience failure occurs around 50-100 running hours. The higher figure relates to testing on the slower speeds. Therefore it is advisable to have a spare transducer wire.

b. A spare calibrated wire (see correspondence with Shmidt Co Ltd, Hong Kong) was installed on 26.09.92, together with a specially inserted rubber sleeve (stren-ghtening the wire side. This resulted in re-calibration of the NBtransducer and shortenning loop length

c. Carry out maintenance check.

d. AFTER ending sewing - leave needle bar in the BDC (near Bottom Dead Centre) to rduce bending strain of the wire.

3. Maintenance Procedure.

a. Needle Bar transducer [NBT].

Sensor used: Kistler Quartz Load Washer type 9001, inserted into needle bar via precision machining. This transducer is very sensitive to bending, due to relatively short life span of the Kistler's wire (KIAG 10-32 pos:1823A-1631C3 3 m long) subjected to high frequency bending during sewing. Service Department of Kistler agent in Hong Kong provides help.

Run RSTM calibration test on an A-3 format double layer of xero-copy paper without a thread. Allow only a perforation of this paper. Stitch density 32 st/10 cm. Use a new 100Rhein-Nadel needle.

Name the file as: CAL04.001, CAL05.001 etc.

Keep them in DAP\CAL subdirectory. CAL04.002 means a second periodical maintenance procedure and mark if this procedure resulted in re-calibration and renaming configuration file as a next version of DAPxx.CFG.

Remember to add calibration version during each new RSTM test in a fileDAT Reference Header comments.

Compare the dynamical results of the channel 3 (Needle pressure /Needle tension):

-if the difference is bigger than 1.5% comparing the previous test - do modify DAP.CFG file for the channel 3. Use the "Q" Editor or any other available software editor.

Keep records of all back-up archival copies of the original (DAP00.CFG) and next versions of the calibration configurations.

It is important to keep the same calibration paper in an archives and in sufficient amount. The paper should be kept at the same ambient conditions of the RSTM testing station.

P.S.:

after testing change needle position to "down" on QR's control box). This allows the wire to relax from bending moment (higher at the needle TDC!). Before testing switch to "top" position again.

b. Presser Bar transducer [PBT].

No modification to sensor applied during precision machining. It was originally calibrated by the Manufacturer.

Type: Quartz Force Link 8301A.

Note:

The Pressure Foot transducer does not need any special maintenance like the Needle Bar transducer. It has relatively small stroke.

Due to a specially added in the RSTM set-up rubber end-sleeve to the wire - its fatigue is not foreseen as a operational risk in the near future.

Follow the advice of maintenance included in Kistler transducer's Manual.

c. Sewing Thread transducer [TT].

This transducer was tailor-built with the use of two strain gauges, temperature self-compensation type KFG-2-120-C1----11L300, and was half-bridged through Kyowa Bridge. Signal is amplified by the dynamical Kyowa amplifier DMA-602A.

Calibration procedure is described in the thesis mentioned in point 3.1.3.2.

Periodical calibration could be carried out according to a specially designed calibration procedure and included in RSTM Manual.

At this stage (on 10.09.1992) it is not envisaged as an urgent matter. Provided, that this operation will be carried out in an cautious way, not overstraining the transducer cantilever /strain gauge and protecting against physical damage.

d. Presser Foot Displacement LDVT type transducer [PFdT]. Follow procedures outlined in the RSD Operation Manual. During the operation do not lift presser foot by using sudden strong force aiming to lift rear cantilever.

The stroke of lifting the presser foot bar is smaller and limited by the insertion / modification of the bar. In case of the suspected state "off-calibration" - do use the procedure outlined in the thesis and borrow calibration slide-gauges from MME Metrology Laboratory/."

END of the PART II of RSTM\CODE.SYS file/.

Appendix IIIb. RSTM-DAP.CFG: System configuration file (extract).

 The DAP.CFG file is an integral part of RSTM sewability system. The flexibility of the system lies in an ability of an easy DAP modification (e.g. due to changes in the transducer signal characteristics) by ammending configuration file, without a major overhauling of the DAP.EXE file (main part of Data Acquisition Programme).
 =====

Beginning of DAP.CFG:

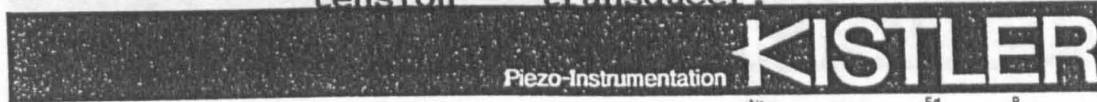
```
!-----
!" This file contains a lot of default values for the DAP
! system initialization.
! Two kinds of values are allowed: numeral and a symbolic
! values. Numerial default begins with a (#) sign, while
! a symbolic (!) is treated as a comment.
!-----
! Default window size for transferring sample values from AP
! buffer into AT buffer <= 16384
!-----
```

```

!   #window_size=8192
!-----
!   Default machine speed in rmp
!-----
!   #machine_speed=3000
!-----
!   Default number of samples per revolution
!-----
!   #samples_per_rev=500
!-----
!   Default number of 64k data blocks acquired (1-10)
!-----
!   #num_64k_blks=2
!-----
!   ADC's max. sampling frequency
!-----
!   #max_sample_freq=200000
!-----
!   Actual value = (AD value) * chX_scale + chX_offset in [dp], !
!   where dp stands for data point(-s). It relates to the original !
!   calibration of DAP00.CFG in dp. After calibration of the !
!   transducers, the channels' scale and offset values of X will be !
!   replaced and designated in a relevant units.
!-----
!   #ch0_scale=1
!   #ch0_offset=0
!   #ch1_scale=1
!   #ch1_offset=0
!   #ch2_scale=1
!   #ch2_offset=0
!   #ch3_scale=1
!   #ch3_offset=0
!-----
!   $y0_label= Thread (cN) or PF.Displ.(mm)
!   $y1_label=Newtons: PF.Pres.(N) or Needle Pres./Ten.(N)
!-----
!   END of the DAP\CFG file." End of Appendix III.
!-----

```

Appendix IV. The technical data of the Kistler force load washer type sensor used for the needle thread tension transducer.



Quarkristall-Messunterlagscheiben
Rondelles de charge à quartz
Quartz Load Washers

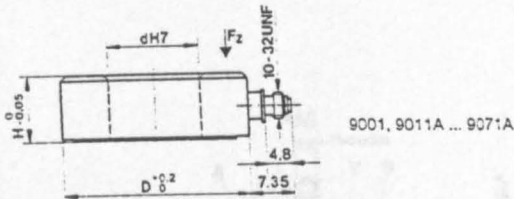
Nr. 6.011 Ed. 3.89 P. 1...4
Type

9001, 9011A ... 9091A

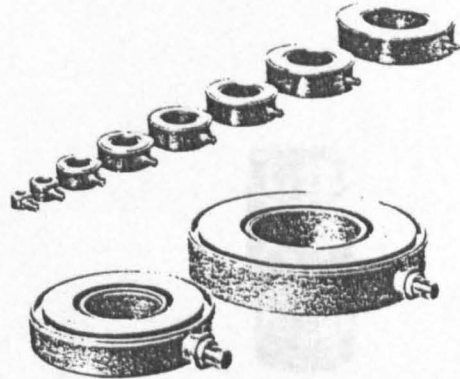
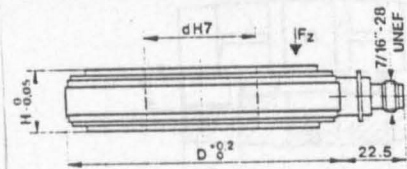
Quarkristall-Kraftaufnehmer für die Messung dynamischer und quasistatischer Kräfte von einigen N bis 1,2 MN. Höchstes Auflösungsvermögen bis zu 0,01 N bei beliebiger Vorlast. Dank sehr grosser Steifheit wird eine hohe Eigenfrequenz des Messaufbaues erreicht. Dicht verschweisste Ausführung. Geringe Abmessungen, grosser Temperaturbereich, weitgehende Temperaturkompensation.

Captteur de force à cristal de quartz pour mesurer des forces dynamiques et quasi-statiques de quelques N à 1,2 MN. Résolution très élevée jusqu'à 0,01 N, quelle que soit la précontrainte. Sa très grande rigidité confère une fréquence propre importante à l'installation de mesure. Exécution soudée hermétique. Encombrement réduit, gamme de température étendue, compensation thermique importante.

Quartz force transducers for measuring dynamic and quasistatic forces from a few N up to 1.2 MN. Very high resolution down to 0.01 N under any preload. Very high rigidity assures high resonant frequency in the measuring rig. Tightly welded assembly. Small dimensions, wide temperature range, temperature compensation over substantial range.



9001, 9011A ... 9071A



Technische Daten

Données techniques

Technical Data

TYPE	Bereich kN	Genauigkeit kN	Kalibrierbereich kN	Gain part. étalonné pC/N	Überlast N	Empfindlichkeit pC/N	Empfindlichkeit N	Ansprechschwelle Nm	Max. Biegemoment Nm	Steifheit kN/μm	Temperaturbereich °C	Kapazität pF	Dimensionen d(mm)	Dimensionen D(mm)	Dimensionen H(mm)	Gewicht g
9001	7.5	0.75	9	±1.3	0.01	5	±1	5	±1	-196...200	±8	4.1	10	6.5	3	
9011A	15	1.5	18	±1.3	0.01	15	±1.8	15	±1.8	-196...200	±23	6.5	14.5	8	8	
9021A	35	3.5	42	±1.3	0.01	60	±3.5	60	±3.5	-196...200	±37	10.5	22.5	10	21	
9031A	60	6	72	±1.3	0.01	130	±6	130	±6	-196...200	±54	13	28.5	11	38	
9041A	90	9	108	±1.3	0.01	240	±7.5	240	±7.5	-196...200	±55	17	34.5	12	57	
9051A	120	12	144	±1.3	0.01	370	±9	370	±9	-196...200	±54	21	40.5	13	80	
9061A	200	20	240	±1.3	0.01	830	±14	830	±14	-196...200	±148	26.5	52.5	15	157	
9071A	400	40	480	±1.3	0.01	2500	±26	2500	±26	-196...200	±203	40.5	75.5	17	370	
9081A	650	65	780	±2.2	0.02	2000	±30	2000	±30	-50...100	±1100	40.5	100	22	840	
9091A	1200	120	1300	±2.2	0.02	7000	±65	7000	±65	-50...100	±2200	66	145	28	2350	

Allgemeine Daten

Données générales

General Data

Linearität	Linéarité	Linearity	% FSO	≤±1
Hysterese	Hystérésis	Hysteresis	% FSO	<0.5
Isolationswiderstand	Résistance d'isolement	Insulation resistance	Ω	≥10 ¹⁴
Temperatur-Koeffizient	Coefficient de température	Temperature coefficient	%/°C	-0.02
Schubempfindlichkeit xy → z	von Einbau abhängig	Eigenfrequenz	von Zusatzmasse abhängig	
Sensibilité au cisaillement xy → z	dépendant du montage	Fréquence propre	dépendant de la masse additionnelle	
Shear sensitivity xy → z	depends on mounting	Natural frequency	depends on additional mass	

1 N = 1 kg · m · s⁻² = 0.1019...kp = 0.2248...lbf

Appendix V. The technical data of the Kistler force load sensor used in the presser-foot bar transducer.



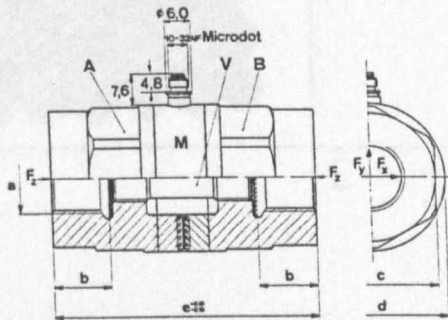
QUARZKRISTALL-KRAFTMESSELEMENTE
ELEMENTS DE MESURE DE FORCE A QUARTZ
QUARTZ FORCE LINKS

Type	Nr.	Ed.	Fol.
9301	6.013	7.80	1
9371			

Quarkristall-Kraftaufnehmer für die Messung dynamischer und quasistatischer Zug- und Druckkräfte von einigen N bis 120 kN. Höchstes Auflösungsvermögen bis zu 0,01 N bei beliebiger Vorlast. Dank sehr grosser Steifheit wird eine hohe Eigenfrequenz des Messaufbaues erreicht. Dicht verschweisste Ausführung. Geringe Abmessungen, grosser Temperaturbereich, weitgehende Temperaturkompensation.

Capteur de force à quartz pour la mesure de forces de traction/compression dynamiques et quasi-statiques de quelques N à 120 kN. Résolution très élevée jusqu'à 0,01 N, quelle que soit la précontrainte. Sa très grande rigidité confère une fréquence propre importante à l'installation de mesure. Exécution soudée hermétique. Encombrement réduit, gamme de température étendue, compensation thermique importante.

Quartz force transducers for measuring dynamic and quasistatic tension and compression forces from a few N up to 120 kN. Very high resolution down to 0,01 N under any preload. Very high rigidity assures high resonant frequency in the measuring rig. Tightly welded assembly. Small dimensions, wide temperature range, temperature compensation over substantial range.



Type 9351A, 1:2

TECHNISCHE DATEN

DONNEES TECHNIQUES

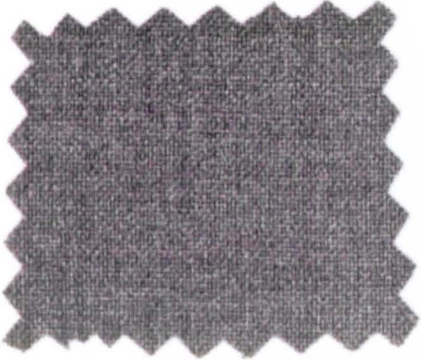
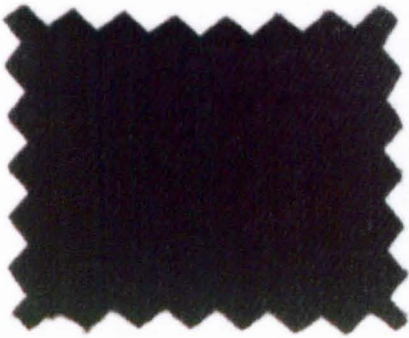
TECHNICAL DATA

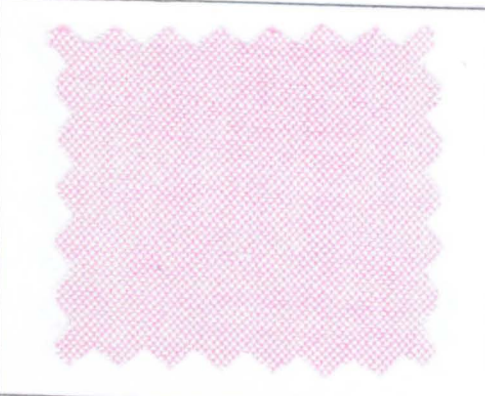
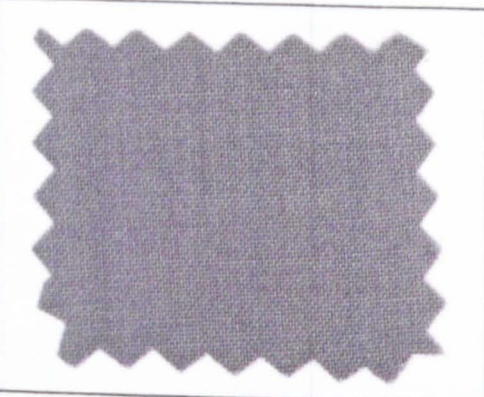
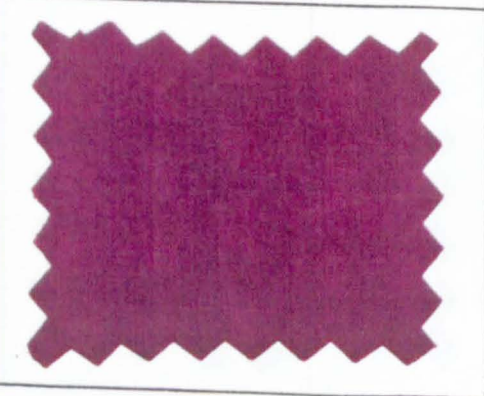
TYPE	Bereich Gamme Range F _z F _z F _z	Kalibrierter Teilbereich Gamme partielle étalonnée Calibrated partial range	Überlast Surcharge Overload	Steifheit Rigidité Rigidity	Eigenfrequenz Fréquence propre Natural frequency	Kapazität Capacité Capacitance	Max. Drehmoment (F _{xy} , F _z = 0) Max. couple de rotation Max. torsional moment	Max. Biegemoment (F _z = 0) Max. couple de flexion Max. bending moment	Max. Schubkraft (F _z = 0) Max. force de cisaillement Max. shear force	Dimensionen Dimensions Dimensions	a	b	c	d	e	Gewicht Poids Weight
9301A	± 2,5	25	± 2,75	≈ 300	≈ 90	≈ 8	1,3	5	0,38	M5 x 0,8	5	9	10	25	12	
9311A	± 5	50	± 5,5	≈ 600	≈ 70	≈ 23	3,8	15	0,75	M6 x 1	5	13	14	30	28	
9321A	± 10	100	± 11	≈ 900	≈ 55	≈ 37	12	60	1,5	M10x1,5	9,5	19	22	45	90	
9331A	± 20	200	± 22	≈ 1400	≈ 45	≈ 55	30	120	3	M12x1,75	10,5	24	28	52	170	
9341A	± 30	300	± 33	≈ 1800	≈ 40	≈ 65	55	240	4,5	M16x2	14	32	34	62	330	
9351A	± 40	400	± 44	≈ 2000	≈ 33	≈ 65	90	370	6	M20x2,5	17,5	36	40	72	480	
9361A	± 60	600	± 66	≈ 2800	≈ 28	≈ 150	180	800	9	M24x3	21,5	46	52	88	1020	
9371A	±120	1200	±132	≈ 5000	≈ 22	≈ 200	520	2300	18	M30x3,5	27,5	65	75	108	2500	

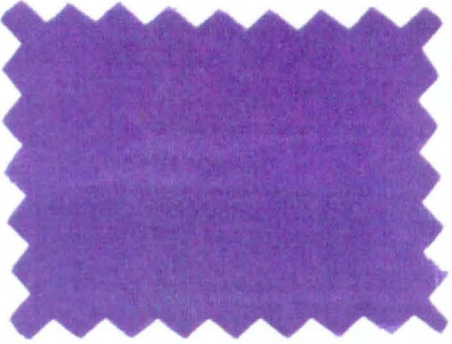
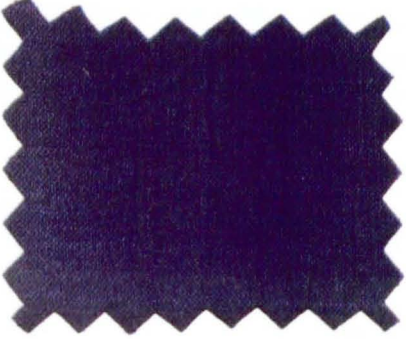
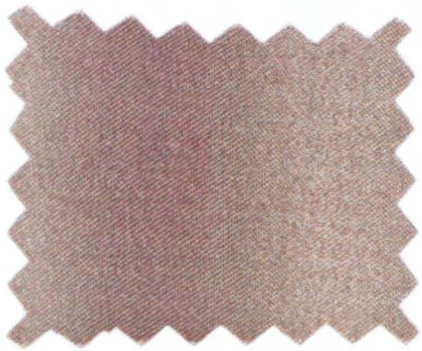
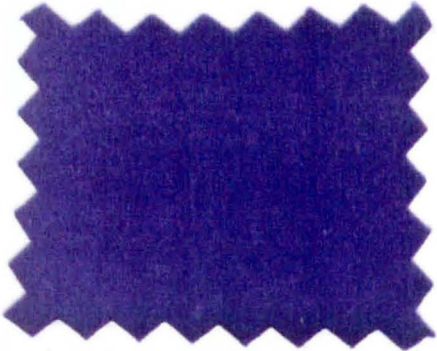
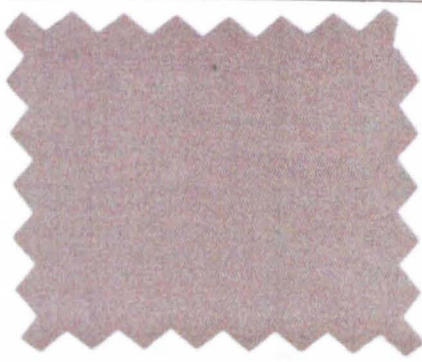
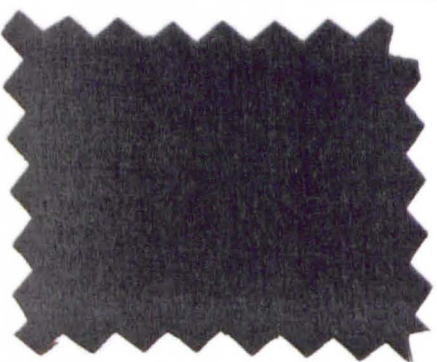
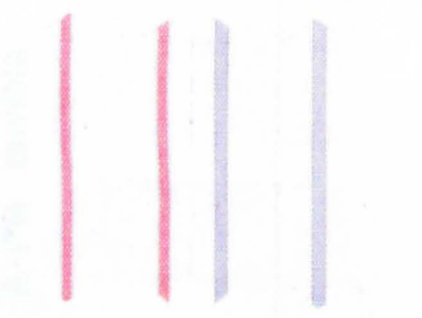
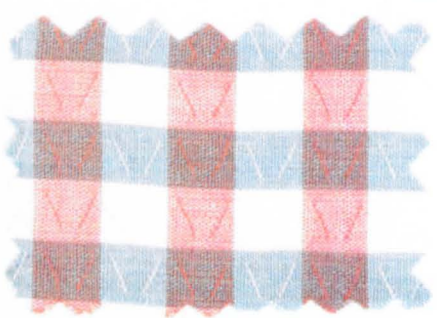
Allgemeine Daten	Données générales	General data
Empfindlichkeit	Sensibilité	Sensitivity
Ansprechschwelle	Seuil de réponse	Threshold
Linearität	Linéarité	Linearity
Isolationswiderstand	Résistance d'isolement	Insulation resistance
Temperatur-Koeffizient	Coefficient de température	Temperature coefficient
Betriebstemperatur-Bereich	Température d'utilisation	Operating temperature range

1 N = 1 kg · m · s⁻² = 0,1019... kp = 0,2248... lbf; 1 T Ω = 10¹² Ω

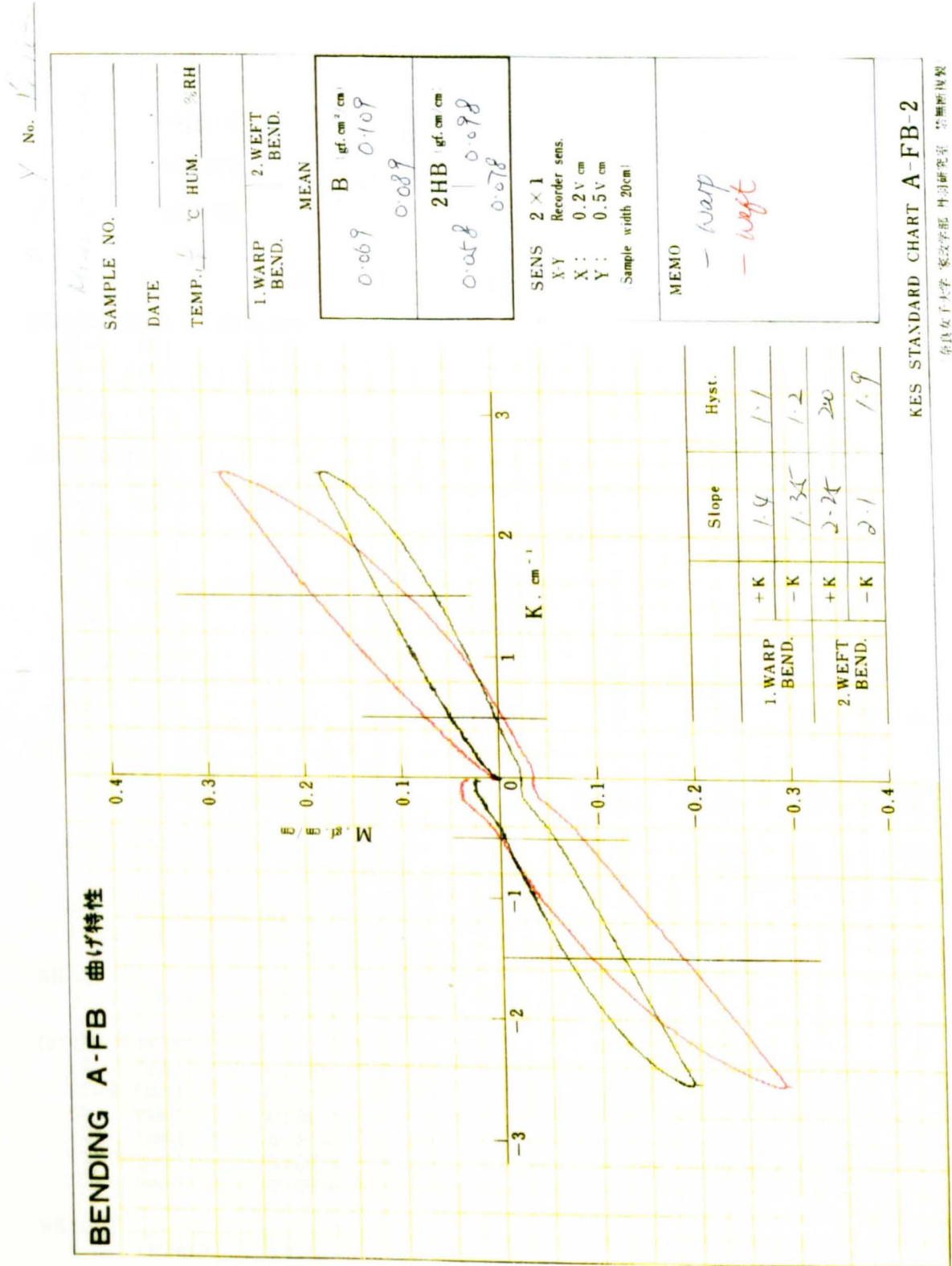
APPENDIX VI The swatches of the fabrics selected for experiments.

<p>e c a b d</p> 	<p>A</p>	<p>B</p>
	<p>C</p>	 <p>D</p>
<p>E</p>	<p>F</p>	
	<p>G</p>	<p>H</p>
	<p>I</p>	 <p>J</p>

	K	
	M	
	O	
	Q	
	S	
	L	
	N	
	P	
	R	
	T	

	U	
	W	
	Y	
	E4	
	E3	
	E5	E7
	A2-4	

Appendix VII. An example of the test result of KES Bending Test of the micro-fibre fabric type Y (one of 5 specimen tested at the HKP Textile Testing Laboratory).



Note: Graph is not of original size.

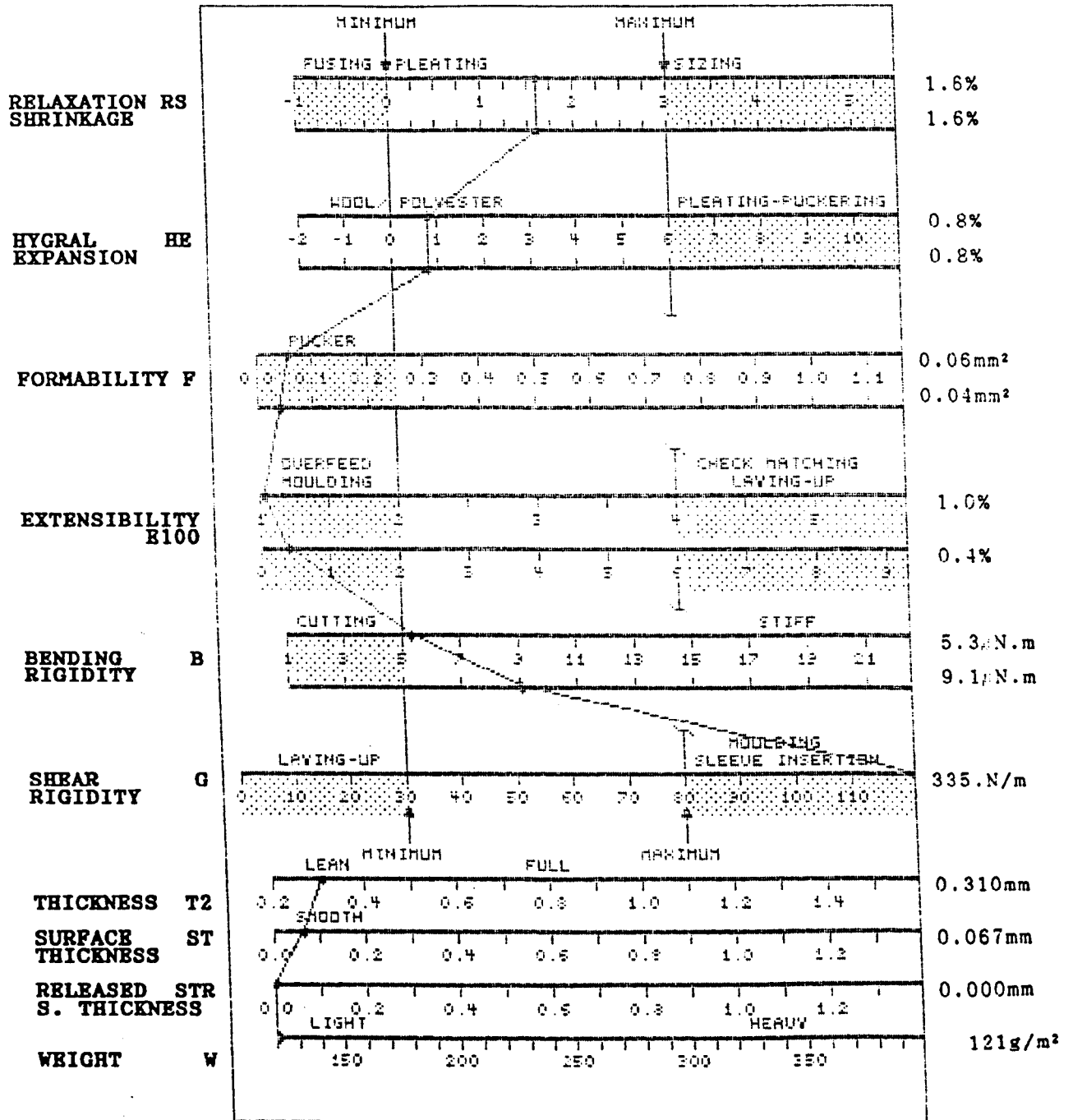
The test graphical results of the micro-fibre fabric type Y, tested on the FAST instrumentation.

FAST CONTROL CHART FOR TAILORABILITY

FAB.ID : brown
 END USE:
 REMARK :

Y

SOURCE:
 DATE :



Appendix IX. The RSM and SPMs test final results of the Experiment Series 4. Extract from the special cumulative data spreadsheet.

A	B	C	D	E	F	G	H	I	J	K	L	M	N	O	P	Q	R	S	T	U	V	W	X	Y	Z	AA	AB	
1	FILE NAMES										EXPERIMENTAL RESULTS																	
2	Next	No	reading	system	(Height	1-8)	Mean	Pucker	Sewing	Thread	Insertion (T)	In (C)	PF rise	Pressure-foot	bar	pressure	Needle	bar	pressure	Needle	bar	Insertion	(N)					
3	fabric	2	3	4	5	6	7	8	9	10	11	12	13	14	15	16	17	18	19	20	21	22	23	24	25	26	27	
4	1	2	3	4	5	6	7	8	9	10	11	12	13	14	15	16	17	18	19	20	21	22	23	24	25	26	27	
5	1	2	3	4	5	6	7	8	9	10	11	12	13	14	15	16	17	18	19	20	21	22	23	24	25	26	27	
175	U	1	7	3	1	3	1	52.3	3.99	37.56	7.13	13.24	53.79	0.78	19.73	9.28	1.22	2.66	21.11	1.5	0.16	0.25	160	1.1	0.43	0.16	37.65	
176	U	1	7	3	1	3	2	52.3	4.29	53.46	5.02	13.26	56.32	0.6	20.4	9.63	12.66	2.66	20.65	2.4	0.05	0.18	325.71	2.3	0.53	0.32	59.47	
177	U	1	7	3	1	3	3	52.3	4.22	75.43	1.05	12.67	66.3	0.85	29.24	19.77	22.27	2.15	9.66	5.2	0.67	0.46	52.94	3.6	1.9	0.81	43.71	
178	U	1	7	3	1	3	4	52.3	4.42	86.66	5.55	13	77.44	0.67	26.68	19.61	22.18	1.87	8.43	7.6	2.55	1.19	46.62	2.2	4.24	1.64	43.48	
179	U	1	7	3	1	3	5	52.3	4.33	97.4	0.76	13.43	85	0.99	28.08	18.9	22.19	1.73	7.78	9.5	5.07	2.14	42.24	12.5	7.35	3.53	47.97	
180	U	1	7	3	1	3	6	52.3	4.4	100.57	4.22	16.85	81.49	1.14	30.07	16.8	22.2	2.29	10.31	19.1	11.67	4.95	41.71	26.7	16.96	8.04	47.38	
181	U	1	7	3	1	3	7	52.3	4.53	113.28	0.78	17.45	71.63	1.28	34.5	17.78	22.19	3.75	16.91	33	22.52	6.46	37.95	50.6	28.03	15.29	54.56	
182	U	1	7	3	1	3	8																					
183	U	1	7	3	1	3	9																					
184																												
185	V	1	7	3	1	3	1	95.7	4.57	42.34	7.66	13.38	51.16	0.8	31.92	19.22	22.22	2.73	12.29	1.7	0.23	0.33	142.55	1.3	0.43	0.16	40.94	
186	V	1	7	3	1	3	2	95.7	4.59	57.43	7.66	14.66	53.85	0.81	32.74	18.67	22.23	2.69	13	2.5	0.08	0.25	297.18	2.9	0.61	0.38	56.44	
187	V	1	7	3	1	3	3	95.7	4.06	61.52	2.9	14.91	63.9	0.87	30.39	19.63	22.24	1.9	6.56	5.9	0.94	0.44	46.67	3.7	1.6	0.65	47.14	
188	V	1	7	3	1	3	4	95.7	4.8	90.52	2.63	15.07	66.06	0.95	28.81	19.02	22.25	1.72	7.74	11.1	2.61	1.17	44.97	7.3	4.14	1.62	44.08	
189	V	1	7	3	1	3	5	95.7	4.69	99.78	6.67	15.37	65.14	1.04	28.41	18.68	22.09	1.66	7.51	9.6	5	2.21	44.28	12.7	7.41	3.29	44.41	
190	V	1	7	3	1	3	6	95.7	4.76	106.66	7.66	16.2	90.9	1.13	30.1	18.82	22.2	2.12	9.53	16.6	11.22	4.62	41.14	26.4	15.93	7.34	46.1	
191	V	1	7	3	1	3	7	95.7	3.96	119.1	7.4	19.64	76.35	1.38	33.56	10.51	22.23	3.58	16.09	33.9	22.33	8.53	38.19	50	28.25	15.01	53.13	
192	V	1	7	3	1	3	8																					
193	V	1	7	3	1	3	9																					
194																												
195	W	1	7	3	1	3	1	94.6	4.12	41.02	6.46	13.82	46.41	0.93	33.06	19.21	22.22	2.35	10.57	1.6	0.23	0.34	146.56	1.5	0.39	0.19	48.19	
196	W	1	7	3	1	3	2	94.6	3.9	56.63	7.66	14.49	53.19	0.87	30.36	19.67	22.21	2.02	9.09	2.5	0.09	0.24	278.76	1.7	0.62	0.35	55.43	
197	W	1	7	3	1	3	3	94.6	3.4	81.78	5.81	15.19	63.3	0.96	30.35	19.35	22.2	1.53	6.69	5.2	0.66	0.47	47.85	3.9	1.81	0.66	47.87	
198	W	1	7	3	1	3	4	94.6	3.74	93.43	3.89	15.07	63.24	1.03	27.66	18.64	22.21	1.43	6.43	7.2	2.64	1.17	44.38	7.7	4.13	1.62	44.17	
199	W	1	7	3	1	3	5	94.6	2.6	96.34	0.25	15.48	64.55	1.13	27.68	18.71	22.17	1.26	5.76	11	5.1	2.21	43.45	12.8	7.42	3.35	45.17	
200	W	1	7	3	1	3	6	94.6	2.66	104.54	5.26	16.05	67.02	1.28	34.45	14.68	22.22	2.31	10.39	19.6	11.99	4.95	40.43	26.8	16.81	8.65	47.92	
201	W	1	7	3	1	3	7	94.6	2.68	115.68	7.66	19.63	79.46	1.45	36.68	10.23				33.6	22.73	8.41	36.99	50.6	27.66	15.32	54.99	
202	W	1	7	3	1	3	8																					
203	W	1	7	3	1	3	9																					
204																												
205	X	1	5	3	3	3	1	160	5	59.26	5.81	17.85	60.63	0.75	34.75	19.08	22.22	2.94	13.23	7	0.56	1.06	182.26	3.4	0.79	0.6	75.72	
206	X	1	5	3	3	3	2																					
207	X	1	5	3	3	3	3																					
208	X	1	5	3	3	3	4																					
209	X	1	5	3	3	3	5																					
210	X	1	5	3	3	3	6	160	5	117.25	3.69	17.37	96.43	1.11	26.89	17.91	22.2	1.76	7.95	21.2	11.77	4.73	40.15	26.7	17	7.58	44.56	
211	X	1	5	3	3	3	7																					
212	X	1	5	3	3	3	8	160	4.36	118.57	-2.13	16.57	73.02	1.58	44.16	9.9	22.21	6.02	27.09	50.1	32.76	14.77	45.07	68.1	47.66	22.66	47.57	
213	X	1	5	3	3	3	9																					
214																												
215	Y	1	5	3	3	3	1	129	4.79	62.99	7.13	19.57	83.74	0.84	30.2	19.11	22.21	1.96	8.92	19.7	3.99	4.38	109.88	6.9	1.45	1.26	66.9	
216	Y	1	5	3	3	3	2																					
217	Y	1	5	3	3	3	3																					
218	Y	1	5	3	3	3	4																					
219	Y	1	5	3	3	3	5																					
220	Y	1	5	3	3	3	6	129	4.74	122.81	4.75	16.29	96.46	1.13	31.24	16.73	22.2	2.15	9.69	19.6	11.73	4.3	36.65	33.3	16.68	7.57	45.4	
221	Y	1	5	3	3	3	7																					
222	Y	1	5	3	3	3	8	129	3.96	126.1	0.25	21.56	76.51	1.52	44.6	9.25	22.16	6.94	31.3	49.9	32.79	14.22	43.36	61.2	46.09	22.2	48.16	
223	Y	1	5	3	3	3	9																					
224																												
225	Z	1	7																									

Appendix X. The technical data of the QUANTIMET Image Analysis System. The system was used in the preliminary testing of the Pucker Standard in the process of development of the SPMS system.

The Quantimet 520 is a complete, ready to use system, providing all the hardware, software and documentation required to obtain results immediately. The basic system is an optimised combination of high speed analogue and digital image processing electronics and dual microprocessors comprising:

- Image analysis processor
- High resolution video camera
- IBM PC/XTS with mouse
- Image and text colour display
- Software

All that is required to complete the package is an input peripheral suited to the application. This may be selected from the range of Cambridge/Reichert light microscopes, Stereoscans, or, if larger specimens are to be examined, a Macroviewer.

IMAGE ANALYSIS PROCESSOR

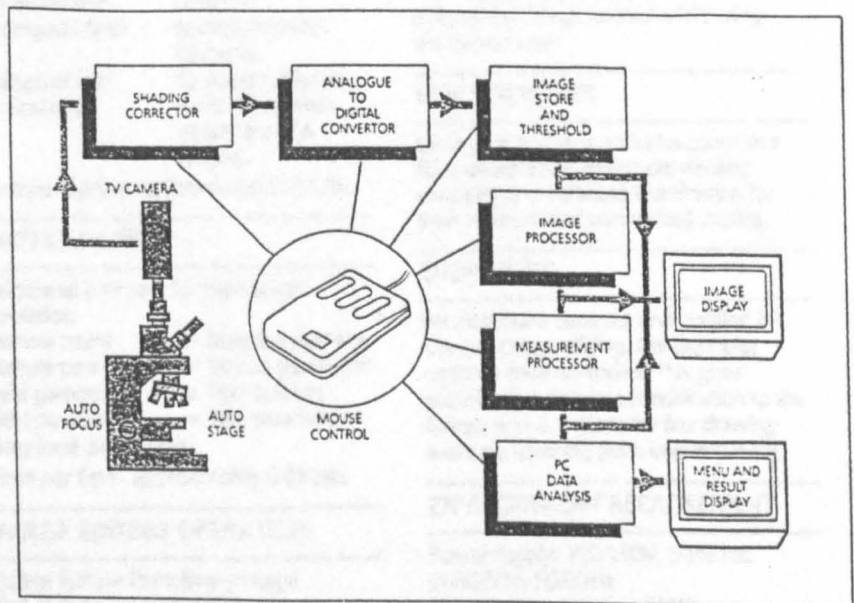
Conveniently packaged in a floor-standing tower style cabinet, this unit contains all the system's image analysis electronics, with free space and power to accommodate any options. It includes:

- Video rate analogue shading corrector
- Video rate analogue-to-digital convertor
- Dual, bit-plane image store (optionally expandable to eight bit-planes)
- Video rate, dual, independent, grey level detectors
- Colour look-up tables for pseudo-colour image display
- High speed measurement electronics
- 16/32 bit, 68000 type measurement microprocessor
- Interface to IBM PC/XTS
- Mouse
- Cables and connectors

A detailed list of image processing and analysis facilities is given opposite.

HIGH RESOLUTION VIDEO CAMERA

The scanning format used gives an image with 512 (or 480) lines, each divided into 512 picture elements (pixels), providing 262144 or (245760) pixels per image at 25 (or 30) scans per



second. Each pixel is nominally square. The camera connects to the range of Cambridge/Reichert optical microscopes via a 'C' mount TV camera adaptor, and is suitable for use with all optical techniques and other manufacturers' microscopes.

The standard camera supplied with the system has a 2/3 inch Vidicon-type tube. This provides a good depth of modulation and low noise level. Optionally a high sensitivity, long-life 1 inch Chalnicon camera can be supplied for more demanding applications.

IBM PC/XTS

The computer hardware supplied in the basic system comprises:

- IBM PC/XTS system unit
- Keyboard
- IBM colour monitor (12 inch diagonal)
- Colour/graphics adaptor
- 640K byte RAM
- One 5½ inch diskette drive and one fixed disc drive (20 Mbytes)
- Parallel printer port
- Serial RS232 port

The IBM PC/XTS may also be used off-line, in standard computer mode.

IMAGE AND TEXT COLOUR DISPLAYS

All operator messages, control information and results are displayed on the IBM colour monitor.

The video camera image is displayed on a separate high resolution colour display, and can be overlaid with binary images in different colours for easy identification. The two independent image and measurement frames are also displayed in colour. The grey level image can be pseudo coloured.

Image display size is 14 inches on a tilt and swivel base.

SOFTWARE

The software packages supplied in the standard system provide both immediate image analysis results from mouse-driven menus and the ability to program the system in Basic. Optional application specific programs are also available.

Results may be further processed and statistically evaluated, utilising optional software packages such as Lotus Symphony.t

IMAGE ANALYSIS FACILITIES

SHADING CORRECTION

Operating at video rate, the matrix type shading corrector removes the effect of uneven illumination from the image by making a multiplicative correction to the analogue video signal, based on a previously stored reference image.
Time of shading correction operation - immediate.

BINARY IMAGE OPERATIONS

Logical comparisons between stored images, i.e. AND, OR, XOR, INVERT.
Filling of holes and/or limbs in a binary image.
Modification of the stored image according to programmable chord size.
Pixel offset of image planes in X and Y.
Time per binary operation - approximately 0.05 seconds.
Rotation through 90° or 180°.
Propagation of overlapping image within a boundary determined by a second image.
Erosion Dilation Opening Closing
Remove single points producing a modified/cleaned binary image.
Variable image and measurement frames specified by X and Y position, width and height.

MEASUREMENTS

All measurements are subject to guard frame correction as appropriate and are expressed in the units by which the system is calibrated.

FIELD

All measurements made simultaneously. Normalised and accumulated values are also immediately available.

Area	Area fraction
Perimeter	Anisotropy
Horizontal intercept	Area fill ratio
Vertical intercept	Mean chord length
Feature count	Frame area

Time per field measurement - approximately 0.05 seconds.

FEATURE

The measurement of individual features in the field, providing multiple values for each. Any value can be used as the criterion for acceptance of a feature for further processing.

Area	Feret's at multiple angles
Perimeter	Convex perimeter
Co-ordinate position	Roundness
Length - maximum feret	Orientation of length
Breadth - minimum feret	Orientation of breadth
Orthogonal feret	Equivalent circle diameter
Horizontal proj.	Equivalent volume
Vertical proj.	X and Y max/min excursions of a feature

Time per feature - approximately 0.01 sec.

DISTRIBUTION

Calculated internally for high speed operation.

Feature count	v feature parameter
Feature parameter	v feature parameter
Field parameter	v field number
Field parameter	v field parameter

Grey level distribution
Time per field - approximately 0.05 sec.

IMAGE EDITING OPERATION

Delete feature from binary image
Flag feature for acceptance
Draw lines and regions into the binary image
Remove lines and regions from the binary image.

GREY IMAGE PROCESSING (OPTION)

Storage of grey level image, image arithmetic
Image transforms via look-up tables, including inversion, log square
Image filtering by matrix element, including Laplacian, gradient
Printing images, copying images.

ACCESSORIES

MICROSCOPE PACKAGE OPTIONS:

packages of three basic types are available - full details from your local Cambridge Instruments' representative.

- Basic light microscope
- Light microscope with stage automation
- Stereoscan with digital image store.

MOTORISED STAGE

and X/Y drive electronics for a light microscope include a joystick for independent stage control while using the microscope.

MACROVIEWER

for large specimens. Includes zoom lens for greatest possible sample viewing versatility and stabilised illumination for both incident and transmitted modes.

DIGITABLET

for maximum accuracy and comfort in manual image editing, the digitablet option is recommended. This gives picture point accurate modification to the image, with functions for line drawing and area covering (with immediate fill).

ENVIRONMENT REQUIREMENT

Power supply: 100-130V, 50/60Hz;
200-250V, 50/60Hz
Power consumption: 1.5kVA
Operating temperature: 18-25°C

CABINET SIZES

	Size (cm)	Weight(kg)
Tower	70 x 40 x 30	37.0
IBM PCXTS	40 x 40 x 40	14.5
IBM Monitor	30 x 40 x 37	12.0
Colour monitor	35 x 35 x 35	16.0
Printer option	8 x 40 x 30	5.2

† Lotus Symphony is a registered trademark of Lotus Development Corporation.

Appendix XI. The SPMS seam pucker index quantification programme (extract).

The SPMS stands for Seam Pucker Measurement System. The programme is based on the subroutines provided in "AURORA" Image Processing Library of the Data Translations Co., (USA). The hardware of this system is described in the Chapter 4. The following programme is integrated with the RSTM system and the measured Pucker Index(PI) is recorded in the RSTM Report.

Beginning...

```

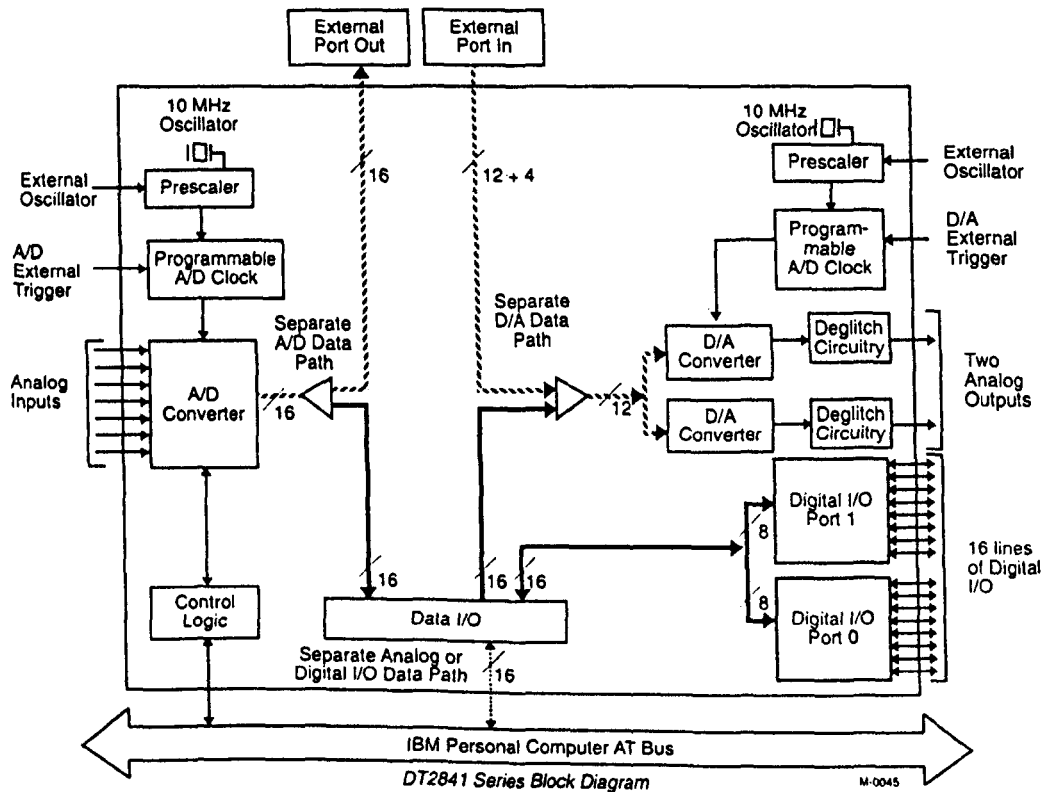
#include "auerrs.h"
#include "audefs.h"
#include <bwindow.h>
#include "graphic.h"
int class(void)
(
char *title = " Classification ";
int i;
float total, totweight, mean, meandevtot, stdtot, stddev,
meandev;
float buck_lev, std_cv, var_cv;
float *x,*y;
long data;
FILE *fp1;
FILE *fp2;
char *name;
char ch;
x = (float *) calloc(256,sizeof(float));
y = (float *) calloc(256,sizeof(float));
if(x==NULL || y==NULL) exit(0);
/
c u t -
off.....break!
k!/. .. /* calculate CV */

total=totweight=mean=meandevtot=stdtot=stddev=meandev=0;
name = "var";
fp2 = fopen(name,"rt");
for (i=0;i<256;i++) {
x[i]=i;
fscanf(fp2,"%ld",&data);
y[i]=(float) data;
total += y[i];
totweight += x[i] * y[i];}
/cut-off.....break!
/* Calculate Buckling Level */.....break!
buck_lev = 2.5369 - (0.227 * var_cv) + (0.2991 *
std_cv);) " /cut-
off.....break!.....
.....end!

```

Appendix XII. The technical data of the hardware of the SPMS and RSTM systems (DT2871, DT7020 and DT2869 boards—5 pages).

<p>Specifications All specifications are typical at 25°C and rated voltage, unless otherwise specified.</p> <p>DIGITAL I/O Number of Lines 16, organized as two 8-line ports that can be set for input or output Fanout 30 LSTTL loads Input Load 1 LSTTL load</p> <p>PACER CLOCK Function Independent A/D and D/A pacer clocks initiate A/D, D/A, or simultaneous A/D and D/A conversions; clocks are started by software trigger or separate external A/D or D/A trigger. Usable Range From 1.4µs (714kHz) to 838ms (1.19Hz) Description Pacer clock consists of a 10 MHz oscillator (.1µs increments) or an external oscillator, a prescaler (divides oscillator by powers of two from 2⁰ to</p>	<p>2¹⁵), and an 8-bit divider (divides output of prescaler by integers from 1 to 256).</p> <p>OPERATING MODES A/D Channel/Gain Selection—16-location channel-gain list Operation—single channel (one conversion on first location in channel-gain list); single scan (once through channel-gain list); continuous scan (continuous through channel-gain list) Data Transfer—programmed I/O; block or continuous transfer to DT-Connect™ processor board D/A Channel Selection—either channel singly, alternating channels, or both channels simultaneously Data Transfer—programmed I/O; block or continuous transfer from DT-Connect™ processor board</p> <p>DT-Connect™ PORTS 16-bit input and output ports; 26-pin connectors; 0–750kHz unidirectional transfer; 0–260kHz bidirectional transfer; master</p>	<p>GENERAL Interface IBM PC AT bus or EISA bus; I/O mapped, 10-bit I/O address; 16-bit data path Interrupt—one line, jumper-selected level; source: A/D, D/A error; A/D done; D/A ready; scan done; A/D, D/A transfer done Power Requirements +5V @ 2.2A max; low noise ±15V generated by onboard DC/DC converter Physical/Environmental Dimensions—full size PC AT board mechanically compatible with ISA system slots only; 11.4 x 33.6 x 1.9 cm (4.5" x 13.25" x .75") Temperature—operating: (DT2841, DT2841-F, DT2848) 0 to 70°C, (DT2847) 0–60°C, (DT2841-G, DT2841-L) 0–50°C; storage: –25 to 85°C Relative Humidity—to 95%, non-condensing</p>
---	---	--



DT2841 Series Block Diagram

M-0045

DT2871

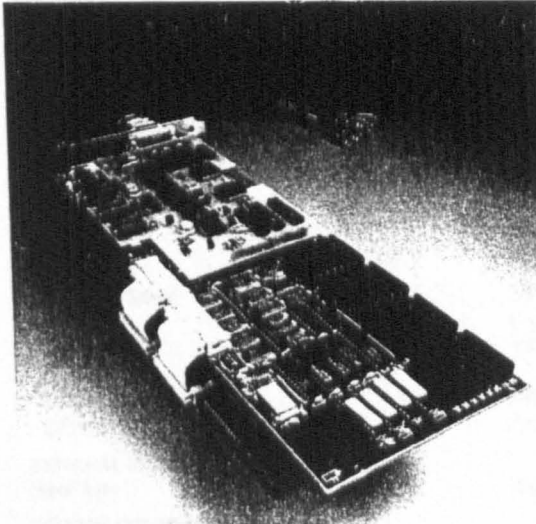


Figure 2. DT2871 (HSI)Color™ Frame Grabber (top) and DT7020 Floating-Point Array Processor (bottom)

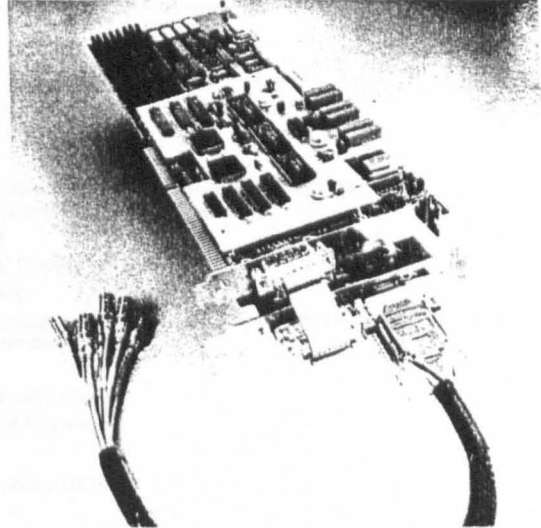


Figure 3. DT2869 Video Decoder/Encoder Board (bottom) and DT2871 (HSI)Color™ Frame Grabber (top)

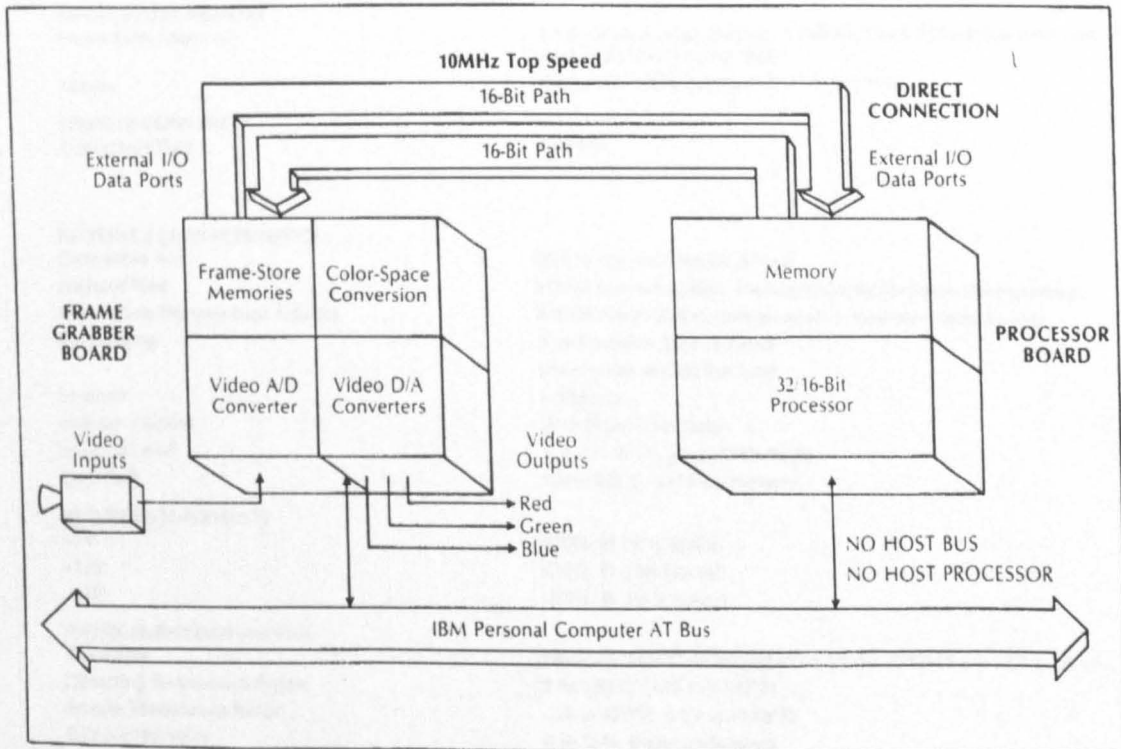


Figure 7. DT-Connect™ Image Processing Overview Block Diagram

M-0052

DT2871**SPECIFICATIONS**

Typical at +25°C and rated voltage unless otherwise specified

STANDARD RGB VIDEO INPUT

Input Signal	RS-170 RGB or RS330 RGB; ac-coupled with dc-restoration CCIR RGB; ac-coupled with dc-restoration
DT2871-60Hz	
DT2871-50Hz	
Format	Interlaced
A/D	(3) 8-bit at 10 MHz
Frame Grab Speed	1/30 second
Sync Signal	Composite from external input, or internal with sync output (for inputs without composite sync)
Resolution	
DT2871-60Hz	480 lines x 512 pixels
DT2871-50Hz	512 lines x 512 pixels

EXTERNAL TRIGGER

Input Type Edge sensitive; TTL levels

RGB/HSI CONVERTER

Conversion Rate 10 MHz

STANDARD RGB VIDEO OUTPUT

Output Signal	RS-170 RGB, dc-coupled CCIR RGB; dc-coupled
DT2871-60Hz	
DT2871-50Hz	
Format	Interlaced
D/A	(3) 8-bit D/As
Sync Signal Outputs	Composite, embedded in the green output Composite alone
Pixel Aspect Ratio	4:3

FRAME-STORE MEMORYFrame-Store Memory 1 Mbyte total, organized into 4 buffers, 512 x 512 x 8 bits each (256 Kt total each); memory-mapped
Transparent from bus; read or write any time

Access

HSI/RGB CONVERTER

Conversion Rate 10 MHz

INTERFACE CHARACTERISTICS

Compatible Bus	IBM Personal Computer AT bus
Interface Type	I/O for control registers; memory-mapped for frame-store memory
Frame-Store Memory Base Address	A00000 (hex) factory configuration; jumper-selectable by user
Bus Loading	Board presents 1 ac bus load Board presents 1 dc bus load 1 interrupt Vertical sync, not busy 3, 5, 10, or 15, jumper-selectable 16-bit I/O, 8- or 16-bit memory
Interrupt	
Interrupt Sources	
Interrupt Level	
Data Path	

POWER REQUIREMENTS

+5V	±10%, Ⓞ 3.0A typical
+12V	±10%, Ⓞ .10A typical
-12V	±10%, Ⓞ .10 A typical

PHYSICAL/ENVIRONMENTAL

Board Size	Standard IBM PC AT board 14"H x 5"W x .75"D (35.6 x 12.7 x 1.9 cm)
Operating Temperature Range	0 to +50°C (+32 to +122°F)
Storage Temperature Range	-25 to +70°C (-13 to +158°F)
Relative Humidity	0 to 95% (non-condensing)

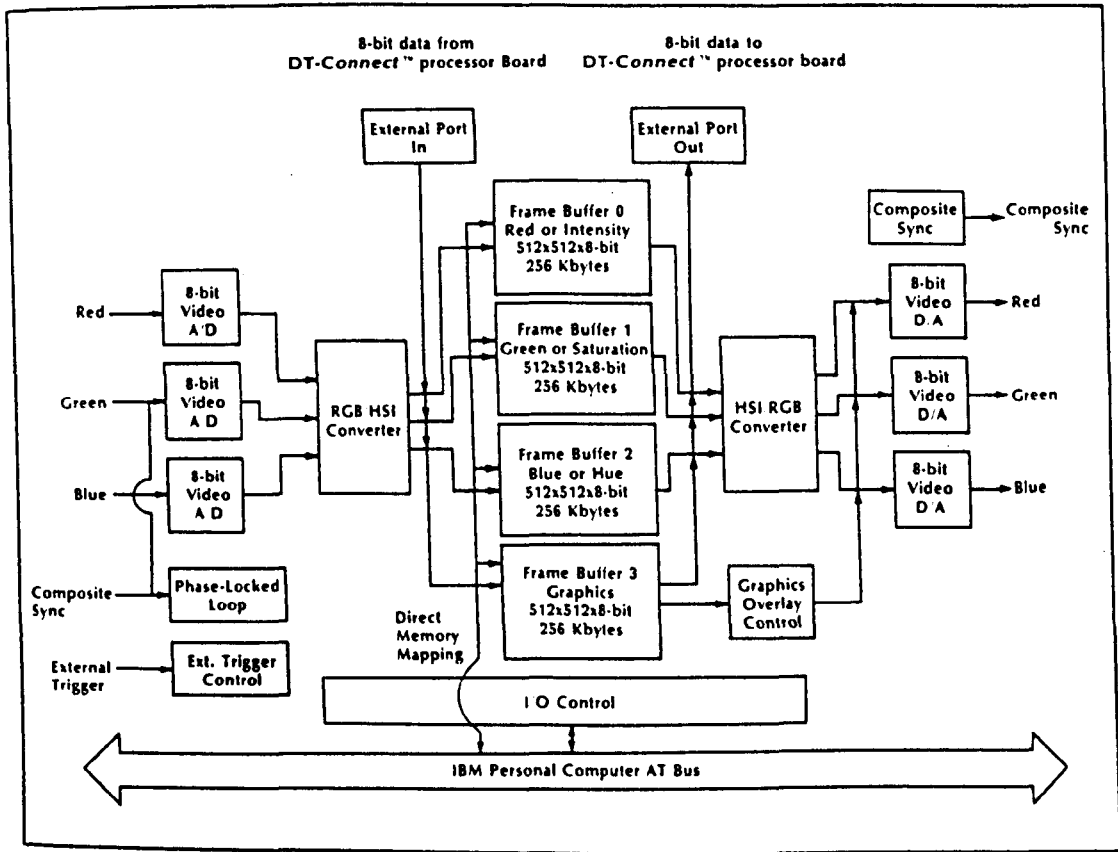


Figure 4. DT2871 (HSI)Color™ Frame Grabber Block Diagram

M-0049

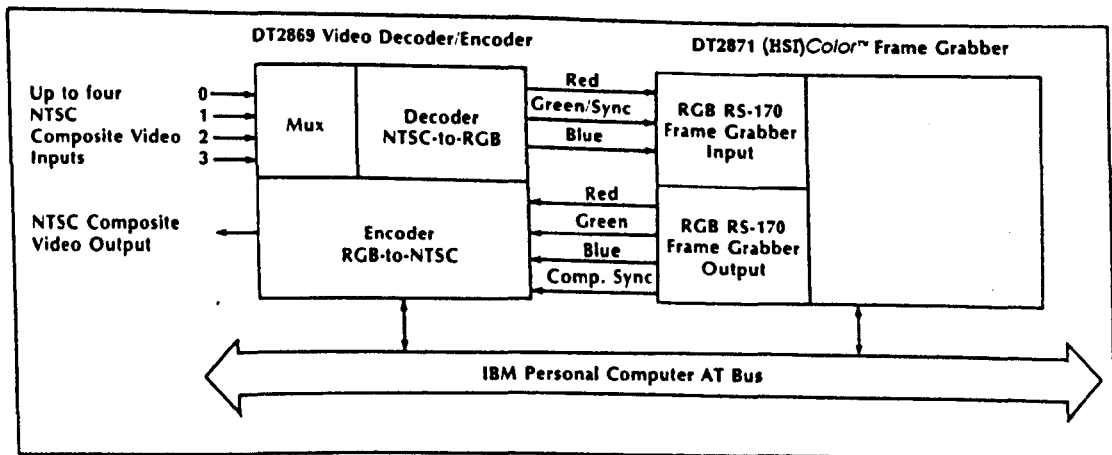


Figure 5. DT2871 (HSI)Color™ Frame Grabber and DT2869 Video Decoder/Encoder Overview Block Diagram

M-0030

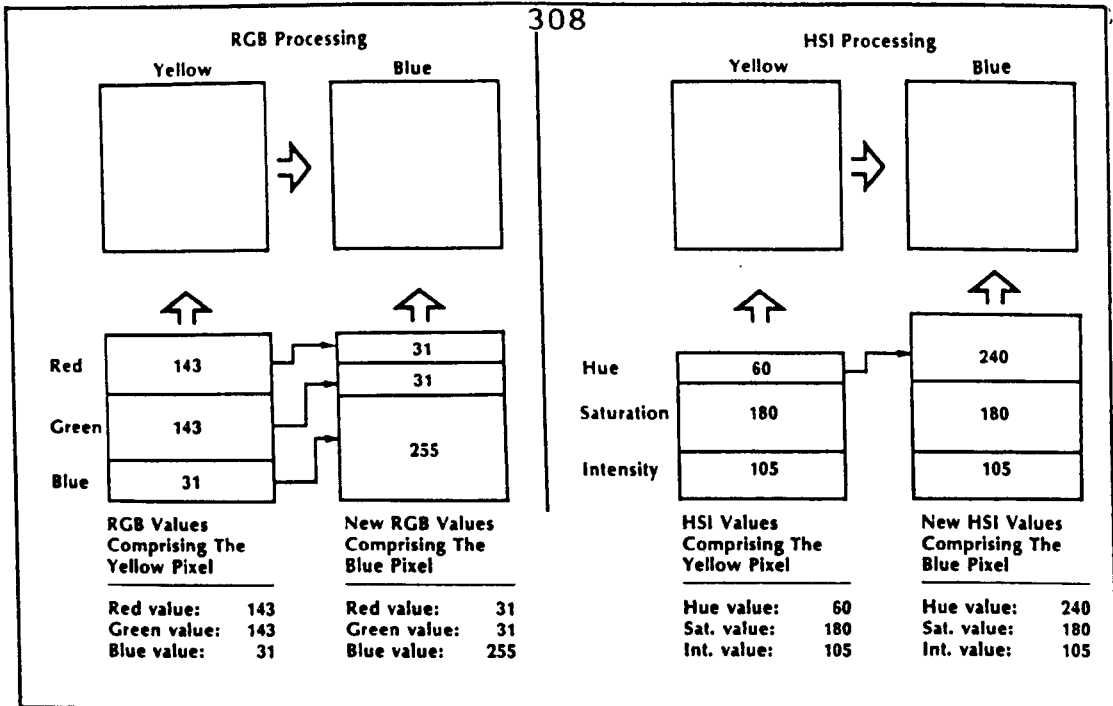


Figure 9. Color image processing can be conceptually easier, and three times faster, if performed in the HSI domain instead of the RGB domain. Above, in the RGB domain, color processing to change the color yellow to a new color, blue, requires manipulating three values (R, G, and B). In the HSI color space, color processing to change the same yellow to the same blue requires manipulating only one value: hue.

